VU Research Portal

Dancing with dendritic cells

Duinkerken, Sanne

2021

document version
Publisher's PDF, also known as Version of record

Link to publication in VU Research Portal

citation for published version (APA)
Duinkerken, S. (2021). *Dancing with dendritic cells: Targeting human skin dendritic cells for anti-tumor immunity*.

Dancing with Dendritic Cells

Targeting human skin dendritic cells
for anti-tumor immunity

Sanne Duinkerken

Dancing with Dendritic Cells

Targeting human skin dendritic cells for anti-tumor immunity

Sanne Duinkerken

VRIJE UNIVERSITEIT

DANCING WITH DENDRITIC CELLS

TARGETING HUMAN SKIN DENDRITIC CELLS FOR ANTI-TUMOR IMMUNITY

ACADEMISCH PROEFSCHRIFT

ter verkrijging van de graad Doctor aan
de Vrije Universiteit Amsterdam,
op gezag van de rector magnificus
prof.dr. V. Subramaniam,
in het openbaar te verdedigen
ten overstaan van de promotiecommissie
van de Faculteit der Geneeskunde
op donderdag 21 januari 2021 om 15.45 uur
in de aula van de universiteit,
De Boelelaan 1105

door

Sanne Duinkerken

geboren te Dronten

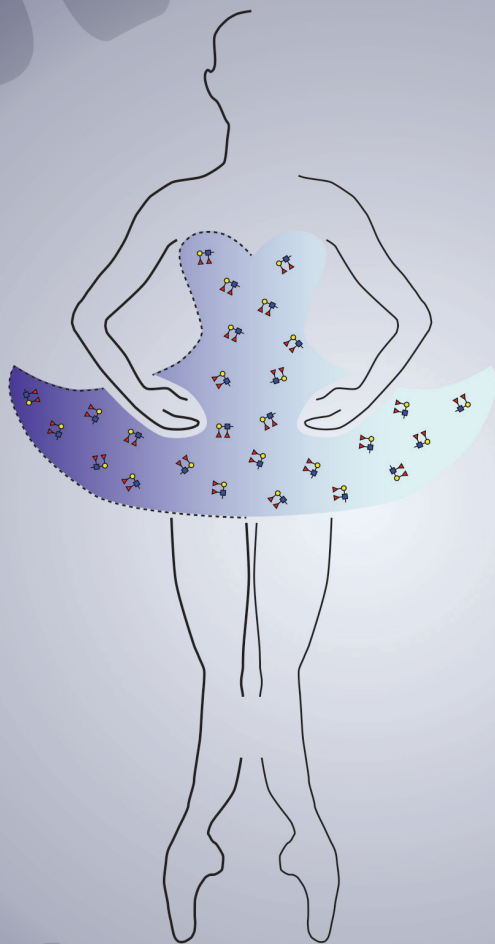# Table of contents

CHAPTER 1

GENERAL INTRODUCTION

Sanne Duinkerken, R.J. Eveline Li, Floor J. van Haften, Jesper van Eck van der Sluijs, Tanja D. de Gruijl, Fabrizio Chiodo, Sjoerd T.T. Schetters, Juan J. Garcia-Vallejo and Yvette van Kooyk

The Immune System & Anti-Cancer Vaccination

The immune system

The immune system is a powerful system that protects us against dangers from outside encompassing pathogens such as bacteria and viruses, but also from danger coming from within like tumor cells. It comprises the rapidly responding non-specific innate immune response and the slower responding but antigen-specific adaptive immune response. Both the innate and adaptive immune response have unique properties but can only induce full-blown immunity when working together [1].

Innate immune cells are the first responders to invading pathogens by recognition of pathogen-associated molecular patterns (**PAMPs**) which bind pattern recognition receptors (**PRRs**) (*Table 1*) [1, 2]. Innate immune cells include macrophages, natural killer (**NK**) cells and granulocytes which react to pathogen invasion within minutes and can either engulf the pathogens for clearance or secrete soluble factors thereby inducing killing or neutralization. However, without involvement of the adaptive immune response this reaction remains antigen non-specific, and no long-term memory will be generated. In order to enable specific clearance of danger both from outside (pathogens) and within (tumor cells), the adaptive immune response is activated via a specialized innate antigen-presenting cell (**APC**), the dendritic cell (**DC**) [1, 3]. DC reside in blood and tissues such as the skin and mucosa and, upon exposure to pathogens and activation, are able to activate T lymphocytes (T cells).

Table 1. Human innate pattern recognition receptors and their ligands

Pattern recognition receptor	*Ligands (PAMP)*
Toll-like receptor (TLR)	Bacterial lipopeptides and flagellin, LPS, single- and double-stranded RNA, hypomethylated DNA
NOD	Peptidoglycans
NOD-like receptor (NLR)	MDP, peptidoglycans, bacterial flagellin and secretion factors, double-stranded RNA
C-type lectin receptor (CLR)	Carbohydrates/glycans
RIG-like receptors (RLR)	Viral RNA, cGAS/STING, DNA resulting from double-stranded breaks, cyclic dinucleotides

T cells mediate the specific defense of the adaptive immune system. Naïve T cells recirculate through blood and secondary lymphoid organs, until they are activated by recognition of specific antigen-derived peptides presented by DC in the paracortical areas of lymph nodes (**LN**). T cell activation can lead to both a type-1 cellular response and a type-2 humoral response by subsequent activation of B cells. An important feature of the adaptive immune response is the induction of immunological memory. This property of the adaptive immune system enables antigen-specific T or B cells to rapidly respond to previously encountered antigens (e.g. microbe derived), thereby diverting disease. This feature is of great importance for the efficacy of vaccines.

Vaccination

Classic vaccines induce adaptive immunity against infectious agents. Altered parts of infectious agents are added within the vaccine to elicit antigen-specific adaptive immune responses, without causing disease. Important for the working mechanism of vaccines is recognition by DC via PRR, which elicits vaccine uptake and some phenotypic changes. Amongst these phenotypic changes is the migration of DC to draining lymph nodes (**LN**) and the reprogramming of DC towards antigen-specific T cell activation. T cells can subsequently help inducing cellular and humoral responses via activation of B cells for antibody production. Here, immunological memory is built to ensure continued protection.

DC are key players in the initiation of immunity and hence vaccine efficacy and there are various DC subsets. Main subsets comprise plasmacytoid DC (pDC) and myeloid/conventional DC 1 (cDC1), and DC 2 (cDC2) [4]. They are present throughout the body in the blood, lymphoid and non-lymphoid tissues such as mucosal tissues and the skin (**Figure 1**). pDC are migratory and reside in secondary lymphoid organs which they home to via the blood circulation. cDC are often residential and remain within tissues until activation, followed by migration to the LN for priming of naïve T cells. Of note, dedicated blood-derived cDC1/cDC2 subsets also reside in the LN [5, 6]. The different DC subsets are specialized in the induction of tailored adaptive immune responses [4, 7].

The site of vaccination can dictate vaccine efficacy and should be selected carefully. Furthermore, vaccine application should be relatively easy to ensure proper delivery of the vaccine and applicability for large cohorts. Although vaccines are often applied intramuscularly there are no resident DC in the muscle, relying on DC influx and

vaccine drainage. In contrast, the skin is easily accessible and harbors different DC subsets making it a potent vaccination site. Four main subtypes of DC have been characterized [8]. In the dermis, three DC subsets are distinguished based on the expression of the membrane markers CD1a, CD14 and CD141, while Langerhans cells (**LC**) reside in the upper layer, the epidermis (**Figure 1**) [8]. Interestingly, studies show intradermal vaccination of the flu vaccine decreases the necessary dose, while inducing similar levels of immunity as compared to intramuscular vaccination [9]. This shows the potential of the skin as prime vaccination site.
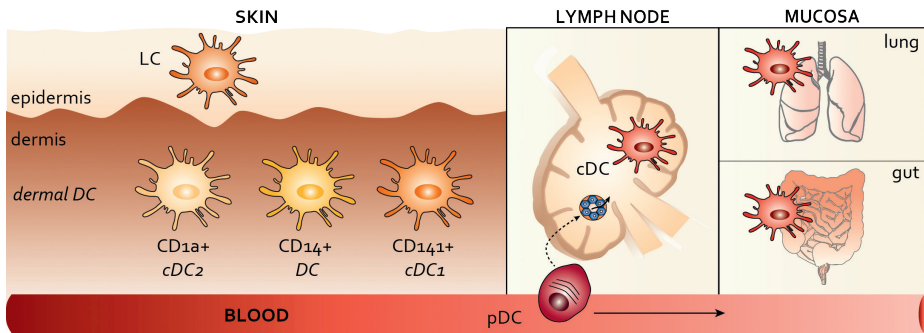
Figure 1. Human DC subsets and their localization DC are classified in the three main categories pDC, cDC1 and cDC2. pDC are migratory and circulate the lymphatics through the blood circulation. cDC are tissue resident and present within the LNs and non-lymphoid tissues such as the skin, gut and lung. Within the human skin four different DC subsets are described with the LC in the epidermis and three dermal DC subsets distinguished based on expression of the membrane molecules CD1a, CD14 and CD141

Cancer immunotherapy

Over the past decade modulation of the immune system to fight cancer, also known as cancer immunotherapy, has become a promising treatment modality for patients. Among different strategies is the design of cancer vaccines that are aimed to instruct DC to induce long-lasting immunity towards tumors. Its principle is to achieve anti-tumor immunity by facilitating processing and presentation of tumor specific antigens by DC to enhance anti-tumor immunity [10]. DC can be activated either *ex vivo* or targeted *in vivo* in their natural environment. The latter is preferable as it can, amongst others, considerably lower the costs and labor intensiveness by providing an off-the-shelf product [11].

For cancer immunotherapy *in vivo* DC targeting strategies can instruct antigen uptake by skin resident DC that present tumor antigens to T cells [8, 12, 13], using the skin as prime vaccination site. For vaccination purposes tumor-associated antigens (TAA) or neoantigens [10], in the form of peptides, can be synthesized to provide the vaccine with "tumor specificity" for T cell responses to attack or help attack the tumor [12]. Efficient induction of CD8+ cytotoxic T lymphocytes (**CTL**) with an ability to home to the tumor effector site is essential for antitumor efficacy.

To develop anti-tumor intradermal vaccination strategies, multiple aspects need to be taken into consideration. The presence of different DC subsets which vary in phenotype and function to take up tumor antigens, process and present these when migrating to the draining LNs. The vaccine can be designed to specifically target to one DC subset, but also to target more subsets simultaneously. Furthermore, DC play an important role in programming effector T cells, since the signals DC give will determine whether T cells become pro-inflammatory effector cells, or so-called regulatory T cells (**Tregs**), or will even become anergic. Moreover, the skin is highly vascularized, which facilitates the recruitment of other immune cells to the vaccination site to further reinforce and amplify the immune response. In addition, besides vaccine delivery to LN by migrating skin DC, the vaccine itself may drain to LNs where LN resident DC can respond (**Figure 2**).

Vaccine development for DC induced adaptive immunity

T cell activation signals
 For proper activation of naïve T cells three signals given by APC are necessary: (1) T cell receptor (**TCR**) triggering by recognition of major histocompatibility complex (**MHC**) bound epitopes (i.e. processed peptide derived from antigens), (2) co-stimulatory molecule signals for proliferation and (3) cytokine induced phenotypic skewing [14].

In their resting state DC have an immature phenotype and are well equipped to capture antigens while receptive for activation signals through PRR stimulation. As such, upon interaction with pathogens via PRRs, DC not only engulf them for antigen processing and retrieval, but also become activated and change their transcriptional profile to become mature DC. In the mature state, DC upregulate the expression of co-stimulatory molecules and chemokine receptors which will guide their migration

towards the LNs and mediate the subsequent induction of effector T cells. Once arrived here they are now fully equipped to activate naïve T cells to become effector cells by giving the three necessary stimulatory signals.

DC antigen processing for T cell activation

DC are professional APC capable to process and present antigens on their cell surface in a MHC dependent fashion. Recognition of the epitope-MHC complex is essential for triggering of the TCR. T cells can be divided into two main subclasses, namely CD4+ helper T cells and cytotoxic CD8+ T cells. There are multiple CD4+ T helper subsets and depending on the type of infection specific helper T cells will be activated to induce effector cell types for efficient pathogen clearance [15]. In contrast to CD4+ T helper cells, CD8+ T cells, or cytotoxic T lymphocytes (**CTL**), have cytotoxic capacities and can effectively kill virus-infected or tumor cells. Triggering of the TCR differs between the two subsets as they recognize different MHC molecules loaded with epitopes of different lengths. CD4+ T cells are activated by recognition of 12-17mer epitopes loaded in MHC class II, whereas CD8+ T cells recognize 8-11mer epitopes in an MHC class I dependent manner.

Before antigens can be presented on the respective MHC molecules they must be processed for which DC use two classical routes. Endogenous proteins are degraded to peptides by the proteasome and transported via the transporter associated with antigen processing (**TAP**) to the endoplasmic reticulum (**ER**). In the ER peptides are loaded on MHC class I molecules and the peptide-loaded complex is then transported and presented on the cell surface. When DC encounter exogenous antigens, they are taken up and degraded in the endosomal compartment followed by loading on MHC class II molecules and transported to the cell surface of the DC for presentation [16, 17]. However, two shuttle routes allow for the alternative presentation of exogenous and endogenous antigens on MHC-I and - II molecules, respectively. Autophagy induces presentation of endogenous antigens by MHC II [18] and DC use cross-presentation for the loading of exogenous antigen-derived epitopes in MHC I [19]. The latter mechanism is used by DC for the activation of cytotoxic CD8+ T cells following vaccination with whole protein antigens or long peptides.

DC antigen cross-presentation

There are two cross-presentation routes known that shuttle exogenous antigens for MHC I loading: the vacuolar and the cytosolic pathway [20]. Antigens that enter the

vacuolar pathway stay within their endocytic compartment (endosomes), followed by lysosomal degradation and subsequent loading on MHC I molecules present within endosomes. In contrast, antigens entering the cytosolic pathway are translocated from the endosome into the cytosol and degraded by the proteasome prior to loading on MHC I according to the classical process for endogenous antigens. Different DC subsets have varying cross-presenting efficiency and the migratory CD141^{+} cDC1 is described to be the prime cross-presenting DC present in human tissues [21] [22]. Interestingly, there are ways to influence cross-presentation ability and tweak vaccines to enhance cross-presentation via specific DC receptor stimulation and targeting [23]. This can enhance cross-presentation by DC subsets which are not described to be as efficient, but are interesting targets for vaccination.

DC targeting for antigen uptake

For vaccination purposes we rely on the capacity of DC to take up exogenous antigens followed by activation of both CD4^{+} and CD8^{+} T cells via regular- and cross-presentation, respectively. For active engulfment of molecules DC use endocytosis, a process which induces membrane invaginations and intracellular cleaving from the membrane for further intracellular trafficking and processing. Endocytosis can occur in various ways and depends on cell type, size and possible binding of molecules to membrane expressed receptors. Uptake of large particles (>0,5µm) or even cells is known as phagocytosis, whereas smaller particles are taken up via pinocytosis [24].

A form of endocytosis relevant for vaccination strategies is receptor-mediated endocytosis, in which membrane expressed receptors bind (pathogen) specific ligands for internalization. Making use of this property allows for the specific targeting of DC subsets via receptors by coupling their respective ligands to tumor specific particles. Furthermore, a diversity of receptors induce differential antigen processing and routing, thereby giving the ability to skew processing towards the cross-presentation route for subsequent CTL activation. The prime cross-presenting CD141^{+} DC are also located in the human skin [21]. Though, they represent a small minority of the total dermal DC pool and targeting other DC subsets might benefit vaccine efficacy. Using specific targeting can facilitate cross-presentation by DC subsets with inherent lower cross-presentation capacity, such as the CD1a^{+} and CD14^{+} dermal DC [25]. Therefore these targeting strategies hold promise for anti-tumor immunotherapies.

C-type lectin receptors for specific DC targeting

The most used DC receptors for targeting are C-type lectin receptors (**CLR**), which mediate antigen uptake and routing to facilitate antigen (cross)-presentation for DC (signal 1) [26]. CLR are a family of calcium-dependent receptors each having a highly conserved carbohydrate recognition domain (**CRD**) [27]. The CRD is able to recognize glycans thereby allowing binding of DC to pathogens or induction of cell-cell interactions. Two types of CLR can be distinguished; type I CLR contain 8 to 10 CRDs each able to recognize a multitude of glycans, whereas type II CLR only have one CRD and bind fewer glycan conformations [26, 28]. There are two strategies for CLR targeting: (1) targeting via antibodies directed against the receptor or (2) using their natural glycan ligand to bind to the receptor [28].

Although antibodies are a useful tool for specific, single receptor targeting and elucidating e.g. CLR routing, glycans may serve as a more versatile approach. Glycans are naturally occurring entities with both cellular and immunological properties, such as cell-cell interaction and pathogen recognition and uptake [29]. The use of glycans for targeting purposes instead of antibodies has several advantages. Glycans are relatively small and can be conjugated to a diversity of tumor specific peptide constructs without interfering with the conformation. In contrast, antibodies are large and have a maximum in efficient peptide coupling. Furthermore, glycans offer multiple possibilities for functionalization of vaccines through changing their density, amount and spatial orientation [30, 31]. This allows for the specific design of CLR targeting compounds, in contrast to the rigid conformation of antibodies. Production of glycans is easier on a large scale, which can considerably lower costs. Besides the conformational ease of glycans as targeting tool, also the possibility to use a single glycan for multiple CLR targeting make glycans a more versatile targeting moiety compared to antibodies (**Figure 2,** *step 1*).

Many different CLR are used for *in vivo* vaccination approaches including Langerin, DEC-205, DC-SIGN, macrophage galactose lectin (**MGL**), CLEC9A, macrophage mannose receptor (**MMR**) and dectin-1, as reviewed by van Dinther *et al* [27]. There are some interesting CLR candidates of which the glycan ligands are known. MMR, Langerin and DC-SIGN recognize high mannose containing glycans. Furthermore, Langerin and DC-SIGN bind (part of) the fucose containing Lewis type antigens [32]. This enables development of glycan-modified vaccines for specific targeting to these CLR. The conformation in which the glycans are presented can dictate CLR binding efficiency and facilitation of DC antigen cross-presentation [32].
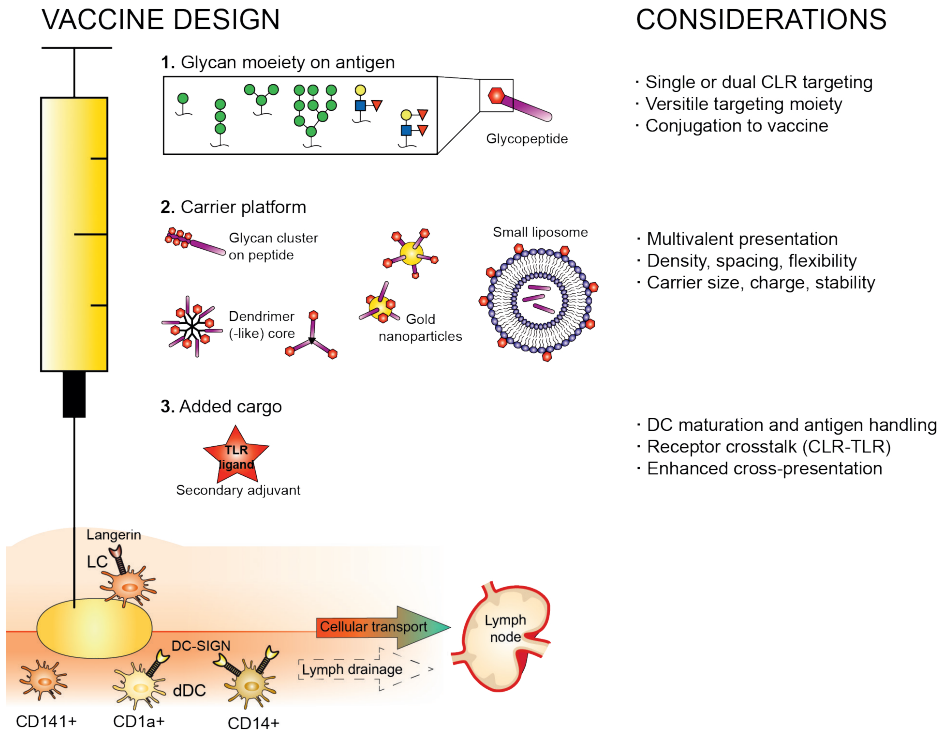
Figure 2. Schematic overview of (considerations in) vaccine design for immunotherapy. The design of a novel glycan-based immunotherapeutic vaccine consists of multiple steps. First, the carbohydrate moiety must be selected (1), taking the CLR to target into mind and its affinity to the receptor (or receptors). Covalent binding to the peptide antigen or conjugation as separate moieties to the carrier is also dependent on the carrier platform (2). Compliant to the targeted receptor, multivalent presentation with optimal density, spacing, and flexibility of the carbohydrates must be sought out. The overall carrier size, charge, and stability on incorporation of the glycopeptides must additionally be considered. Supplemental cargo can be added to boost the immunization process through DC maturation and enhanced antigen (cross)-presentation (3), provided there are no negative CLR-binding effects or alterations in processing via receptor cross talk. DC-SIGN, dendritic cell specific ICAM grabbing non-integrin; CLR, C-type lectin receptor; dDC, dermal dendritic cell; LC, Langerhans cell; TLR, Toll-like receptor.

Multivalent delivery systems

When aiming for CLR targeting, the design of the tumor antigen containing particle is very important [31]. Glycan-mediated interactions are generally weak and this low affinity is compensated through avidity [31]. Avidity ensures that the frail binding between individual ligand and receptor accumulates, thereby strengthening the interaction. In contrast to glycans, antibodies generally rely on their high binding affinity. Where an antibody or a glycan monomer can only bind one CRD with set

affinity, a glycan polymer can bind multiple CRD and CLR molecules thereby inducing receptor multimerization which enhances glycan-receptor avidity [31].

Binding of glycans by the CRD of CLR is influenced by their spatial orientation and conformation within the cellular membrane [33]. The most straightforward manner of introducing a CLR-targeting moiety is the covalent attachment of a specific glycan onto a specific amino acid in an antigenic peptide [32]. However, effective CLR receptor-glycan interactions require both affinity and avidity, through multimerization of the receptors.

The (multi)valency of a glyco-peptide can be increased by incorporation into carrier systems (**Figure 2,** *step 2*). Gold nanoparticles (AuNP) are widely used as carrier system due to their easy changeability in size, shape, surface- and other chemical properties. The simultaneous functionalization of AuNP with thiol-containing antigenic peptides and with thiol-functionalized carbohydrates has been described with successful immunizing applications *in vitro* and *in vivo* [34]. Naturally occurring carrier systems in the nano-range are the outer membrane vesicles from pathogens [35], or small liposomes including glycans in the lipid bilayer, with antigen entrapped at the core [32]. Another effective system for glyco-peptide multimerization are poly aminoamide (PAMAM)-dendrimers, which have been applied successfully for DC targeting and immunization [30]. These defined nanostructures are repetitively and uniformly branched molecules, available in a large array of sizes and terminal groups, which double with each generation [36]. Next to the glycan moiety, the density, spacing and flexibility of the carrier system can contribute to the CLR targeting. This makes PAMAM-dendrimers an interesting carrier to develop and test multiple conformations of multivalent glyco-peptide systems for optimal CLR targeting. However, not always can high affinity CLR binding be directly translated to enhanced antigen presentation and T cell responses [21].

Adjuvants for DC maturation and antigen processing
Important for anti-tumor vaccines, besides the inclusion of tumor specific antigens, is the addition of adjuvants that enhance vaccine efficacy by inducing DC maturation. DC maturation entails the expression of co-stimulatory molecules which provide T cell stimulation (signal 2) and cytokine production for T cell skewing (signal 3). Furthermore, adjuvants can improve vaccine uptake and processing. Since PRR are naturally used by DC to sense pathogens for uptake and maturation, efforts have

been made to find agonists, either naturally occurring or synthetic, to complement vaccines [37]. TLR, NOD-like receptors (NLR) and RIG-I-like receptors are PRR inducing DC maturation for T cell stimulation and skewing (signal 2 and 3).

The TLR family is commonly used for adjuvant purposes [38] and many agonists for the different TLR molecules have been described. Interestingly, cross-talk amongst TLR and CLR illustrate that the choice of adjuvant to be combined with CLR targeting may matter. Multiple CLR can react to concomitant TLR activation as described for DC immunoreceptor (**DCIR**) and TLR7/8 [39, 40], DC-specific ICAM-grabbing non-integrin (**DC-SIGN**) and TLR3/4/5 [41], BDCA-2 and TLR9 [42] and Langerin and TLR3 [43]. This can prompt immunomodulation of DC induced T cell responses, such as enhanced cross-presentation [40]. Interestingly, combinations of adjuvants for TLR and NLR stimulation can influence NLR induced signaling cascades and subsequent immunological processes including antigen uptake through autophagy [44] and presentation [45, 46]. Overall, the use of adjuvants is not only interesting for the proper induction of DC maturation to provide T cells with signal 2 and 3. Combining CLR targeting with TLR and/or NLR agonists may also enhance cross-presentation thereby further facilitating signal 1 (**Figure 2,** *step 3*).

Designing intradermal vaccine formulations for DC induced anti-tumor immunity

DC comprise a heterogeneous cell population that can be distinguished on many aspects. The classification of the different subsets is based on expression of cell surface molecules and localization throughout the body. Furthermore, transcription factor expression, transcriptional regulation and whether they are able to migrate or reside in tissue specific locations can distinguish these subsets from each other. All DC subsets can mediate peptide processing and presentation, but have varying ability in the type of T cells which are subsequently activated. [47] Moreover, the four different DC subsets in human skin may respond differently to vaccines as they express different CLR for glycan uptake of antigens, and different TLR for maturation purposes. Thus careful vaccine design is required (**Figure 2**) [48].

Langerhans cells
LC are distinguished from other DC subsets by the high expression of cell surface makers CD1a and the CLR Langerin that is specifically expressed on LC [49, 50]. Upon stimulation, they become potent APCs that preferentially induce CD4$^+$ T$_H$2 like and

CD8^{+} T-cell responses [51, 52]. Their cross-presenting capacity is largely dependent on the internalization pathway involved and the environmental cues they receive. Specific intracellular pathogens and viruses are able to elicit LC activation under inflammatory conditions, while LC are also able to distinguish between pathogens and commensals, inducing commensal tolerance [47]. Targeting LC for vaccination purposes is therefore dependent on signals that provide LC activation that tilts the balance toward anti-tumor inflammation rather than tolerance. The use of TLR agonists is a viable option to induce anti-tumor immunity. Since LC do not express TLR4, use of the clinically approved LPS derivative MPLA is not possible. However, they do express TLR3 and TLR7/8 providing opportunities to use Poly I:C [53] or imiquimod [54], respectively.

Dermal DC
Three other skin DC subsets are present in the dermal layer of the skin. These subsets are distinguished from each other based on cell surface molecules and the specific expression of CLRs.

CD1a^{+} dermal DC form the most abundant dermal DC subset. They specifically express the CLR MGL [55] and are the most mature dermal DC under steady state conditions. They have the capacity to activate both CD4^{+} and CD8^{+} T-cells [56] and are described to efficiently cross-present exogenous antigens. Expression of C-C motif receptor 7 (**CCR7**) on CD1a^{+} dermal DC involved in DC migration suggests a high migratory potential to draining LN, making them interesting targets for DC vaccination therapies aiming to activate naïve T cells [56, 57].

CD14^{+} dermal DC are distinguished based on expression of the CLR DC-SIGN [55], though, also CD1a^{+} dermal DC express DC-SIGN albeit at lower levels [57]. Steady-state, unstimulated CD14^{+} dermal DC have a more immature phenotype and induce Tregs and follicular T-helper cells (**T$_H$F**) [51, 58]. Furthermore, they have a low potential to activate allogeneic T-cell proliferation [59] and it has been shown that they are less efficient in cross-presenting antigens as compared to LC and CD1a^{+} dermal DC [51, 60]. However, recent studies showed that upon specific targeting CD14^{+} dermal DC can efficiently cross-present antigens for tumor specific T cell activation [25].

In addition to CD1a^{+} and CD14^{+} dermal DC, CD141^{+} dermal DC have been identified in the dermis of the skin and other peripheral tissues [61]. Although CD141 is highly expressed on this subset, CD141 is also expressed on all CD14^{+} dermal DC [62]. However, the CD141^{+} dermal DC can be further distinguished by the absence of CD14 and low expression of CD11c [61]. Furthermore, CD141^{+} dermal DC are characterized by the specific expression of the CLR CLEC9A [55]. This subset has been described to efficiently cross-present antigens and highly express CCR7 that correlates with the spontaneous migration seen of these cells [61].

Induction of dermal DC maturation for proper T cell stimulation can be accomplished through activation of TLR, e.g. by use of the clinically approved TLR4 agonist MPLA or the TLR7/8 agonist imiquimod. Furthermore, the combination of TLR and NLR agonists which synergize holds promise for skin DC activation.

Cross-presentation via DC-SIGN and Langerin

Although CD141^{+} dermal DC are considered the prime cross-presenting DC residing in the skin, specific CLR targeting on the other dermal DC subsets can enhance and leverage their cross-presenting capacity. Two interesting CLRs expressed by human skin DC, of which the glycan ligands are known, are DC-SIGN and Langerin. As previously described, DC-SIGN is mainly expressed on CD14^{+} dermal DC, but also found on CD1a^{+} dermal DC, whereas Langerin expression is restricted to LCs [57, 63]. Enhanced cross-presentation of melanoma specific antigens following targeting of CD14^{+} dermal DC and LCs via DC-SIGN and Langerin, respectively, confirms the potential for the targeting of these receptors for intradermal vaccination strategies [25, 43]. Interestingly, activation of DC via TLRs can alter the intracellular fate of antigens thereby favoring cross-presentation [64] and this feature can be combined with CLR targeting. Indeed, T cell activation following DC-SIGN targeting can be enhanced when combined with TLR stimulation using the TLR4 agonist MPLA [65]. Equally, Langerin targeting combined with the TLR3 agonist Poly I:C enhanced tumor specific CD8^{+} T cell activation [43]. Though, how DC-SIGN routing is affected by TLR4 signaling, and whether other TLR ligands can also affect DC-SIGN and Langerin antigen routing for enhanced cross-presentation, remains to be elucidated.

The expression of Langerin on LC and DC-SIGN on two of the dermal DC subsets and their cross-presentation induction potential, make them interesting targeted candidates for intradermal anti-tumor vaccines. To specifically target Langerin and

DC-SIGN their binding specificity to the Lewis type antigens can be used. DC-SIGN recognizes all Lewis type antigens, whereas Langerin recognizes Lewis (Le)^b and Le^Y, but not Le^a and Le^X. Interestingly, both DC-SIGN and Langerin showed highest binding affinity for Le^Y, making this a suitable glycan for dual receptor targeting. However, the conformational presentation of glycan coated tumor specific compounds influences intracellular trafficking of the antigens targeted to Langerin and DC-SIGN [32]. Hence, careful evaluation of immune responses induced by Le^Y-conjugated tumor specific particles is imperative to ensure optimal CD8$^+$ T cell activation, e.g. directed at cancer.

Intradermal delivery systems

Intradermal delivery of vaccines is often accomplished through needle injection. Though, this requires specific training and, hence, other delivery systems are being developed to simplify vaccination schemes such as delivery via microneedle-patches or upon laser skin microporation [66]. The use of (epi)dermal laser ablation is especially interesting as it can enhance vaccine immunogenicity in combination with adjuvants [67] and even work as adjuvant itself [68], thereby enhancing vaccine efficiency. These kind of technical developments prompt investigation in use for anti-tumor immunotherapy, where indeed it was shown to improve *in vivo* anti-tumor immune responses [69]. It would be very interesting to investigate the effect of laser treatment in combination with anti-tumor vaccines applied intradermally in human skin.

Future design of cancer vaccines

Tumor immunotherapy for treatment of cancer is a promising strategy as shown in the past decade. DC which bridge the non-specific innate and specific adaptive immune system can be used for induction of anti-tumor immune responses e.g. through vaccination. The human skin is easy accessible and harbors a vast number of DC subsets thereby making it a potent vaccination site. Nevertheless, vaccine design comes with several challenges. For induction of long lasting anti-tumor immunity the vaccine needs to contain both tumor specific antigens and adjuvant. Furthermore, the conformation in which the tumor specific antigens are delivered can dictate specific DC subset targeting and processing for antigen presentation. The use of glycan-induced CLR targeting by multivalent delivery systems may ensure endocytosis by multiple human skin DC subsets, and importantly, enhanced cross-presentation for CD8$^+$ T cell activation. This can be further increased by careful selection of adjuvants, such as TLR and NLR agonists, which can influence CLR induced antigen processing.

Besides, adjuvants can alter the skin microenvironment through induction of cytokine secretion thereby inducing innate immune cell influx.

Tumors develop to evade the immune system by creating an immune suppressive microenvironment [70]. This tumor microenvironment (**TME**) can use the naturally occurring brakes present on immune cells to avoid overstimulation and tissue damage, i.e. the so called immune checkpoints (**IC**). Furthermore, tumor reactive T cells cannot always penetrate into the tumor to clear tumor cells and are often "exhausted" (i.e. suppressed by coordinated expression of multiple IC) before proper tumor cell clearance. Multiple studies have shown promising results that lead to effective anti-tumor immunotherapy, either by removing the brakes through immune checkpoint inhibition [71] or by stimulating anti-tumor immunity [72-74]. Though there is still much room for vaccine improvement, ultimately combining it with IC blockade may be the way forward for effective cancer immunotherapy.

Thesis outline

In the studies described in this thesis we explored the potential of human skin DC to induce anti-tumor immunity. By the design of various vaccines we explored how the multiple human skin DC subsets responded for the induction of robust adaptive anti-tumor immunity. We used melanoma as a tumor model and synthesized a long peptide constituting both a CD4^{+} and CD8^{+} T cell specific epitope of the gp100 protein. As such, we can verify CD4^{+} T cell activation via classical antigen presentation, but also CD8^{+} T cell activation through cross-presentation.

For intradermally injected particulate vaccines, we need to ensure that the tumor antigen containing particle will reach the targeted DC subset to facilitate the induction of cytotoxic CD8^{+} T cells with tumor cell killing capacity. For this DC need to shuttle exogenously derived antigens into the endogenous presentation pathway, better known as cross-presentation. The expression of DC specific CLR gives us the opportunity to both specifically target skin DC whilst inducing cross-presentation, especially when combined with TLR stimulation. In **chapter 2** we explored the possibility to specifically target epidermal LC through either Langerin or Dectin-1 for induction of cross-presentation, using specific antibodies conjugated to the gp100 synthetic long peptide (**SLP**). We show Langerin to be superior in the activation of melanoma specific CD8^{+} T cells, compared to Dectin-1, due to differences in intracellular routing.

In order to explore whether targeting dermal DC is beneficial in facilitating cross-presentation, we used DC-SIGN as target candidate as it is expressed by CD14^{+} and CD1a^{+} DC in the dermis. In **chapter 3** we elucidated the exact intracellular routing of DC-SIGN and its cargo by using an antibody specific for the CRD and one for the neck-region of DC-SIGN. Furthermore, we elucidated whether and how concomitant TLR4 stimulation could enhance DC-SIGN induced cross-presentation. We show that simultaneous triggering of DC-SIGN using an antibody conjugated to the melanoma specific gp100 SLP and TLR4 using LPS, efficiently enhances cross-presentation. This dual stimulation ensured SLP degradation by the proteasome and antigen processing for MHC I loading.

Many targeting strategies have focused on the targeting of a single DC subset through a single CLR. We wondered whether the simultaneous targeting of multiple DC subsets in the skin would enhance adaptive immunity. We therefore aimed to target multiple human skin DC subsets through both Langerin (LC) and DC-SIGN (dermal DC) using a single Langerin-DC-SIGN targeting vaccine formulation. Earlier work showed that Langerin and DC-SIGN require different sized formulations of antigenic particles for the induction of cross-presentation. In **chapter 4,** we used the overlapping glycan binding profiles for the Lewis Y type antigens of Langerin and DC-SIGN to target both receptors. Using Lewis Y (Le[y]) as targeting glycan we aimed to generate a single glyco-vaccine targeting multiple human skin DC subsets simultaneously. As carrier system we used PAMAM-dendrimers, which are hyperbranched polymers with mirroring subunits containing reactive terminal sides to which e.g. peptides can be covalently conjugated and synthesized varied sizes, multivalent glyco-peptide vaccines. We used the generation 0 (containing 4 reactive groups) and the generation 3 (containing 32 reactive groups) PAMAM-dendrimer cores to covalently link the gp100 SLP and create two differentially sized vaccines which fall between the peptide and liposome range. For specific targeting to both Langerin and DC-SIGN, Le[y] was added to the N-terminal side of the gp100 SLP. We show the generation 3 multivalent glyco-dendrimers of approximately 50nm to efficiently target both Langerin and DC-SIGN, thereby reaching multiple human skin DC subsets when injected *in situ*. Furthermore, this enhanced activation of tumor specific CD4^{+} and CD8^{+} T cells compared to non-targeting dendrimers. Cross-presentation was further enhanced by the addition of either the TLR4 agonist MPLA (DC) or TLR3 agonist Poly I:C (LC).

In order to investigate whether we could further optimize our cancer vaccine, we investigated whether we could improve DC maturation for cytokine skewing and co-stimulation and antigen processing, by combining various PRR agonists. TLR and NOD-like receptors (**NLR**) that are expressed by different human skin DC and can synergize for DC maturation and antigen handling. In **chapter 5** we used the PAMAM-dendrimer generation 0 core, to develop a multivalent antigenic vaccine containing both the gp100 SLP and the NOD2 agonist MDP. To this end a synthetic NOD2 agonist, M-TriLYS, was covalently linked at the N-terminal side of the multivalent antigenic dendrimer. We show that the combination of the NLR agonist-antigen complex with the soluble TLR4 agonist MPLA enhances cytokine secretion within the skin micromilieu. Furthermore, it enhances cross-presentation by human skin DC for CD8+ T cell activation.

Intradermal vaccine delivery is usually achieved through injection, though efforts are made to design systems that simplify intradermal vaccine delivery. One of those systems is the use of laser devices creating small pores at set depths within the skin. These devices haven been shown to not only simplify delivery, but also induce enhanced immunity. In **chapter 6** we made use of an ablative fractional laser to verify whether it might benefit vaccination with our anti-tumor vaccine particles. We show that in our human skin explant model intradermal injection was more efficient for vaccine delivery to and uptake by skin DC, resulting in higher level CD8+ T cell activation.

This thesis aimed to develop a human skin DC targeting cancer vaccine, exploiting the expression by DC of the CLR Langerin and DC-SIGN. By the design of a multivalent glyco-vaccine incorporating melanoma specific gp100 epitopes and the targeting moiety Le^y we could efficiently target multiple human skin DC for enhanced (cross)-presentation using a single vaccine formulation. This dual targeting, multivalent vaccine can be used for inclusion of a multitude of epitopes and PRR agonists. Thereby we developed a flexible intradermal vaccine platform which has merit for clinical studies aiming to cure different types of cancer.

References

1. Delves, P.J. and I.M. Roitt, *The immune system.* New England Journal of Medicine, 2000. **343**(1): p. 37-49.

2. Mogensen, T.H., *Pathogen recognition and inflammatory signaling in innate immune defenses.* Clinical microbiology reviews, 2009. **22**(2): p. 240-273.

3. Parham, P., *The immune system.* 2014: Garland Science.

4. Collin, M. and V. Bigley, *Human dendritic cell subsets: an update.* Immunology, 2018. **154**(1): p. 3-20.

5. van de Ven, R., et al., *Characterization of four conventional dendritic cell subsets in human skin-draining lymph nodes in relation to T-cell activation.* Blood, 2011. **118**(9): p. 2502-10.

6. Segura, E., et al., *Characterization of resident and migratory dendritic cells in human lymph nodes.* J Exp Med, 2012. **209**(4): p. 653-60.

7. Haniffa, M., M. Gunawan, and L. Jardine, *Human skin dendritic cells in health and disease.* J Dermatol Sci, 2015. **77**(2): p. 85-92.

8. Kashem, S.W., M. Haniffa, and D.H. Kaplan, *Antigen-Presenting Cells in the Skin.* Annu Rev Immunol, 2017. **35**: p. 469-499.

9. Kenney, R.T., et al., *Dose Sparing with Intradermal Injection of Influenza Vaccine.* The new england journal of medicine, 2004. **351**: p. 2295-301.

10. Schumacher, T.N., W. Scheper, and P. Kvistborg, *Cancer Neoantigens.* Annu Rev Immunol, 2019. **37**: p. 173-200.

11. Tacken, P.J., et al., *Dendritic-cell immunotherapy: from ex vivo loading to in vivo targeting.* Nat Rev Immunol, 2007. **7**(10): p. 790-802.

12. Hu, Z., P.A. Ott, and C.J. Wu, *Towards personalized, tumour-specific, therapeutic vaccines for cancer.* Nat Rev Immunol, 2018. **18**(3): p. 168-182.

13. Criscuolo, E., et al., *Alternative Methods of Vaccine Delivery: An Overview of Edible and Intradermal Vaccines.* J Immunol Res, 2019. **2019**: p. 8303648.

14. Banchereau J and S. RM, *Dendritic cells and the control of immunity.* Nature, 1998. **392**(6673): p. 8.

15. Zhu, J., H. Yamane, and W.E. Paul, *Differentiation of effector CD4 T cell populations.* Annual review of immunology, 2010. **28**: p. 445.

16. Sallusto, F. and A. Lanzavecchia, *The instructive role of dendritic cells on T-cell responses.* Arthritis Research & Therapy, 2002. **4**(3): p. 1.

17. Schuck, S.D., *Mycobacterium tuberculosis-specific T-cell responses in latent infection and active disease.* 2009, Humboldt-Universität zu Berlin.

18. Crotzer, V.L. and J.S. Blum, *Autophagy and its role in MHC-mediated antigen presentation.* J Immunol, 2009. **182**(6): p. 3335-41.

19. Joffre, O.P., et al., *Cross-presentation by dendritic cells.* Nature Reviews Immunology, 2012. **12**(8): p. 557-569.

20. Joffre, O.P., et al., *Cross-presentation by dendritic cells.* Nat Rev Immunol, 2012. **12**(8): p. 557-69.

21. Haniffa, M., et al., *Human tissues contain CD141hi cross-presenting dendritic cells with functional homology to mouse CD103+ nonlymphoid dendritic cells.* Immunity, 2012. **37**(1): p. 60-73.

22. Borst, J., et al., *CD4(+) T cell help in cancer immunology and immunotherapy.* Nat Rev Immunol, 2018. **18**(10): p. 635-647.

23. Compeer, E.B., et al., *Antigen processing and remodeling of the endosomal pathway: requirements for antigen cross-presentation.* Front Immunol, 2012. **3**: p. 37.

24. Sahay, G., D.Y. Alakhova, and A.V. Kabanov, *Endocytosis of nanomedicines.* J Control Release, 2010. **145**(3): p. 182-95.

25. Fehres, C.M., et al., *In situ Delivery of Antigen to DC-SIGN(⁺)CD14(⁺) Dermal Dendritic Cells Results in Enhanced CD8(⁺) T-Cell Responses.* J Invest Dermatol, 2015. **135**(9): p. 2228-2236.

26. Figdor, C.G., Y. van Kooyk, and G.J. Adema, *C-type lectin receptors on dendritic cells and Langerhans cells.* Nature Reviews Immunology, 2002. **2**(2): p. 77-84.

27. van Dinther, D., et al., *Targeting C-type lectin receptors: a high-carbohydrate diet for dendritic cells to improve cancer vaccines.* J Leukoc Biol, 2017. **102**(4): p. 1017-1034.

28. Tacken, P.J., et al., *Dendritic-cell immunotherapy: from ex vivo loading to in vivo targeting.* Nature Reviews Immunology, 2007. **7**(10): p. 790-802.

29. Fehres, C.M., et al., *In situ Delivery of Antigen to DC-SIGN+ CD14+ Dermal Dendritic Cells Results in Enhanced CD8+ T-Cell Responses.* Journal of investigative dermatology, 2015.

30. Garcia-Vallejo, J.J., et al., *Multivalent glycopeptide dendrimers for the targeted delivery of antigens to dendritic cells.* Mol Immunol, 2013. **53**(4): p. 387-97.

31. Li, R.E., S.J. van Vliet, and Y. van Kooyk, *Using the glycan toolbox for pathogenic interventions and glycan immunotherapy.* Curr Opin Biotechnol, 2018. **51**: p. 24-31.

32. Fehres, C.M., et al., *Cross-presentation through Langerin and DC-SIGN targeting requires different formulations of glycan-modified antigens.* J Control Release, 2015. **203**: p. 67-76.

33. Drickamer, K. and M.E. Taylor, *Recent insights into structures and functions of C-type lectins in the immune system.* Curr Opin Struct Biol, 2015. **34**: p. 26-34.

34. Climent, N., et al., *Loading dendritic cells with gold nanoparticles (GNPs) bearing HIV-peptides and mannosides enhance HIV-specific T cell responses.* Nanomedicine, 2018. **14**(2): p. 339-351.

35. Schetters, S.T.T., et al., *Outer membrane vesicles engineered to express membrane-bound antigen program dendritic cells for cross-presentation to CD8(⁺) T cells.* Acta Biomater, 2019. **91**: p. 248-257.

36. Fox, L.J., R.M. Richardson, and W.H. Briscoe, *PAMAM dendrimer - cell membrane interactions.* Adv Colloid Interface Sci, 2018. **257**: p. 1-18.

37. Reed, S.G., M.T. Orr, and C.B. Fox, *Key roles of adjuvants in modern vaccines.* Nat Med, 2013. **19**(12): p. 1597-608.

38. Duthie, M.S., et al., *Use of defined TLR ligands as adjuvants within human vaccines.* Immunological Reviews, 2011. **29**: p. 178-196.

39. Meyer-Wentrup, F., et al., *DCIR is endocytosed into human dendritic cells and inhibits TLR8-mediated cytokine production.* J Leukoc Biol, 2009. **85**(3): p. 518-25.

40. Klechevsky, E., et al., *Cross-priming CD8⁺ T cells by targeting antigens to human dendritic cells through DCIR.* Blood, 2010. **116**(10): p. 1685-97.

41. Gringhuis, S.I., et al., *C-type lectin DC-SIGN modulates Toll-like receptor signaling via Raf-1 kinase-dependent acetylation of transcription factor NF-kappaB.* Immunity, 2007. **26**(5): p. 605-16.

42. Jahn, P.S., et al., *BDCA-2 signaling inhibits TLR-9-agonist-induced plasmacytoid dendritic cell activation and antigen presentation.* Cell Immunol, 2010. **265**(1): p. 15-22.

43. Fehres, C.M., et al., *Langerin-mediated internalization of a modified peptide routes antigens to early endosomes and enhances cross-presentation by human Langerhans cells.* Cell Mol Immunol, 2017. **14**(4): p. 360-370.

44. Cooney, R., et al., *NOD2 stimulation induces autophagy in dendritic cells influencing bacterial handling and antigen presentation.* Nat Med, 2010. **16**(1): p. 90-7.

45. van Beelen, A.J., et al., *Stimulation of the intracellular bacterial sensor NOD2 programs dendritic cells to promote interleukin-17 production in human memory T cells.* Immunity, 2007. **27**(4): p. 660-9.

46. Tukhvatulin, A.I., et al., *Powerful Complex Immunoadjuvant Based on Synergistic Effect of Combined TLR4 and NOD2 Activation Significantly Enhances Magnitude of Humoral and Cellular Adaptive Immune Responses.* PLoS One, 2016. **11**(5): p. e0155650.

47. Collin, M., N. McGovern, and M. Haniffa, *Human dendritic cell subsets.* Immunology, 2013. **140**(1): p. 22-30.

48. Alcantara-Hernandez, M., et al., *High-Dimensional Phenotypic Mapping of Human Dendritic Cells Reveals Interindividual Variation and Tissue Specialization.* Immunity, 2017. **47**(6): p. 1037-1050 e6.

49. Valladeau, J., et al., *Langerin, a novel C-type lectin specific to Langerhans cells, is an endocytic receptor that induces the formation of Birbeck granules.* Immunity, 2000. **12**(1): p. 71-81.

50. Hunger, R.E., et al., *Langerhans cells utilize CD1a and Langerin to efficiently present nonpeptide antigens to T cells.* The Journal of clinical investigation, 2004. **113**(5): p. 701-708.

51. Klechevsky, E., et al., *Functional specializations of human epidermal Langerhans cells and CD14⁺ dermal dendritic cells.* Immunity, 2008. **29**(3): p. 497-510.

52. Yagi, H., et al., *Induction of therapeutically relevant cytotoxic T lymphocytes in humans by percutaneous peptide immunization.* Cancer research, 2006. **66**(20): p. 10136-10144.

53. Oosterhoff, D., et al., *Intradermal delivery of TLR agonists in a human explant skin model: preferential activation of migratory dendritic cells by polyribosinic-polyribocytidylic acid and peptidoglycans.* J Immunol, 2013. **190**(7): p. 3338-45.

54. Fehres, C.M., et al., *Topical rather than intradermal application of the TLR7 ligand imiquimod leads to human dermal dendritic cell maturation and CD8⁺ T-cell cross-priming.* Eur J Immunol, 2014. **44**(8): p. 2415-24.

55. Fehres, C.M., J.J. Garcia-Vallejo, and W.W.U. andYvette van Kooyk, *Skin-resident antigen-presenting cells: instruction manual for vaccine development.* Proceedings of ICI Milan 2013, 2014: p. 6.

56. Angel, C.E., et al., *Cutting edge: CD1a⁺ antigen-presenting cells in human dermis respond rapidly to CCR7 ligands.* The Journal of Immunology, 2006. **176**(10): p. 5730-5734.

57. Fehres, C.M., et al., *Phenotypic and Functional Properties of Human Steady State CD14⁺ and CD1a⁺ Antigen Presenting Cells and Epidermal Langerhans Cells.* PLoS One, 2015. **10**(11): p. e0143519.

58. Chu, C.-C., et al., *Resident CD141 (BDCA3)⁺ dendritic cells in human skin produce IL-10 and induce regulatory T cells that suppress skin inflammation.* The Journal of experimental medicine, 2012. **209**(5): p. 935-945.

59. de Gruijl, T.D., et al., *A postmigrational switch among skin-derived dendritic cells to a macrophage-like phenotype is predetermined by the intracutaneous cytokine balance.* The Journal of Immunology, 2006. **176**(12): p. 7232-7242.

60. Segura, E., et al., *Characterization of resident and migratory dendritic cells in human lymph nodes.* The Journal of experimental medicine, 2012. **209**(4): p. 653-660.

61. Haniffa, M., et al., *Human tissues contain CD141 hi cross-presenting dendritic cells with functional homology to mouse CD103⁺ nonlymphoid dendritic cells.* Immunity, 2012. **37**(1): p. 60-73.

62. Lindenberg, J.J., et al., *IL-10 conditioning of human skin affects the distribution of migratory dendritic cell subsets and functional T cell differentiation.* PLoS One, 2013. **8**(7): p. e70237.

63. Bigley, V., et al., *Langerin-expressing dendritic cells in human tissues are related to CD1c+ dendritic cells and distinct from Langerhans cells and CD141high XCR1+ dendritic cells.* J Leukoc Biol, 2015. **97**(4): p. 627-34.

64. Alloatti, A., et al., *Toll-like Receptor 4 Engagement on Dendritic Cells Restrains Phago-Lysosome Fusion and Promotes Cross-Presentation of Antigens.* Immunity, 2015. **43**(6): p. 1087-100.

65. Boks, M.A., et al., *MPLA incorporation into DC-targeting glycoliposomes favours anti-tumour T cell responses.* J Control Release, 2015. **216**: p. 37-46.

66. Weniger, B.G. and G.M. Glenn, *Cutaneous vaccination: antigen delivery into or onto the skin.* Vaccine, 2013. **31**(34): p. 3389-91.

67. Weiss, R., et al., *Transcutaneous vaccination via laser microporation.* J Control Release, 2012. **162**(2): p. 391-9.

68. Scheiblhofer, S., et al., *Skin vaccination via fractional infrared laser ablation - Optimization of laser-parameters and adjuvantation.* Vaccine, 2017. **35**(14): p. 1802-1809.

69. Terhorst, D., et al., *Laser-assisted intradermal delivery of adjuvant-free vaccines targeting XCR1+ dendritic cells induces potent antitumoral responses.* J Immunol, 2015. **194**(12): p. 5895-902.

70. Hanahan, D. and L.M. Coussens, *Accessories to the crime: functions of cells recruited to the tumor microenvironment.* Cancer Cell, 2012. **21**(3): p. 309-22.

71. Massarelli, E., et al., *Combining Immune Checkpoint Blockade and Tumor-Specific Vaccine for Patients With Incurable Human Papillomavirus 16-Related Cancer: A Phase 2 Clinical Trial.* JAMA Oncol, 2019. **5**(1): p. 67-73.

72. Farkona, S., E.P. Diamandis, and I.M. Blasutig, *Cancer immunotherapy: the beginning of the end of cancer?* BMC Med, 2016. **14**: p. 73.

73. Finn, O.J., *The dawn of vaccines for cancer prevention.* Nat Rev Immunol, 2018. **18**(3): p. 183-194.

74. van der Burg, S.H., et al., *Vaccines for established cancer: overcoming the challenges posed by immune evasion.* Nat Rev Cancer, 2016. **16**(4): p. 219-33.
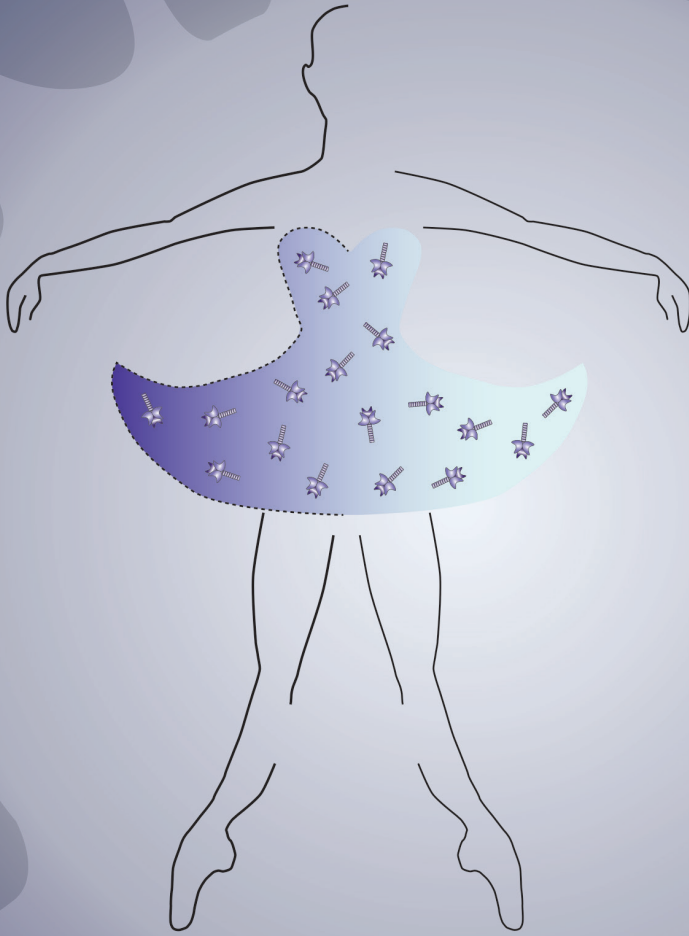
CHAPTER 2

LANGERIN-MEDIATED INTERNALIZATION OF MODIFIED PEPTIDES ROUTES ANTIGENS TO EARLY ENDOSOMES AND ENHANCES CROSS-PRESENTATION BY HUMAN LANGERHANS CELLS

Cynthia M. Fehres, Sanne Duinkerken, Sven C.M. Bruijns, Hakan Kalay, Sandra J. van Vliet, Martino Ambrosini, Tanja D. de Gruijl, Wendy W.J. Unger, Juan J. García-Vallejo and Yvette van Kooyk

Abstract

The potential of the skin immune system to generate immune responses is well established and the skin is actively exploited as vaccination site. Human skin contains several antigen-presenting cell (APC) subsets with specialized functions. Especially the capacity to cross-present exogenous delivered antigens to CD8^{+} T cells is of interest for the design of effective immunotherapies against viruses or cancer. Here, we show that primary human LCs are able to cross-present synthetic long peptides (SLPs) to CD8^{+} T cells. In addition, modification of those SLPs using antibodies against the receptor Langerin, but not dectin-1, further enhanced the cross-presenting capacity of LCs through routing of internalized antigens to less proteolytic EEA-1+ early endosomes compared to dectin-1. The potency of LCs to enhance CD8^{+} T cell responses could be further increased through activation of LCs with the TLR3 ligand polyinosinic:polycytidylic acid (pI:C). Altogether, the data provide evidence that human LCs are able to cross-present antigens after Langerin-mediated internalization. Furthermore, the potential of antigen modification to target LCs specifically provides a rationale to generate effective anti-tumor or anti-viral CTL responses.

Key words: Antigen cross-presentation, dectin-1, early endosomes, human Langerhans cells, Langerin.

Introduction

Antigen presenting cells (APCs) and, in particular, dendritic cells (DCs) induce adaptive immune responses through the presentation of endogenous peptides in the context of MHC class I and exogenous peptides in the context of MHC class II molecules to CD8^{+} and CD4^{+} T cells, respectively. In addition, DCs are able of capturing and presenting exogenously derived antigens in MHC class I molecules, a process known as cross-presentation [1]. Antigen cross-presentation plays an important role in the priming of cytotoxic T cells against viruses or tumors, but is also important in maintaining self-tolerance [2]. However, not all DC subsets have identical cross-presentation capacities and some DC subsets appear better equipped for this task. Therefore, careful selection of the DC subset is of utmost importance in the design of anti-tumor or anti-viral DC targeting vaccination strategies.

Langerhans cells (LCs) are a subset of DCs present in mucosal tissues and stratified epithelium, like the epidermis of the skin. Human LCs are characterized by the expression of CD1a, the C-type lectin receptor (CLR) Langerin and the presence of Birbeck granules, which are associated with Langerin expression [3]. Langerin mediates recognition through the interaction with glycoconjugates such as high-mannose structures, mannan or β-glucans expressed on the surface of pathogens [4]. Langerin mediates ligand internalization for antigen processing and presentation and, therefore, it has a potential to be used to specifically deliver antigens conjugated to glycans or α-Langerin antibodies to LCs. Although capture of exogenous antigens by human LCs resulted in the induction of CD4^{+} T cell responses [5, 6] it still remains under debate whether human LCs are able to cross-present exogenous antigens. *In vitro* derived LCs cultured from CD34^{+} progenitor cells efficiently promoted CD8^{+} T cell proliferation after internalization of soluble peptides [7]. Also, LCs pulsed with a short EBV peptide or a 39 amino-acid long peptide containing the EBV minimal epitope, were more efficient than pulsed dermal DCs in the cross-presentation of the EBV antigen to memory CD8^{+} T cells [8]. This enhanced CD8^{+} T cell activation by LCs was dependent on the interaction between CD70 and CD27 [8], but did not rely on specific, receptor-mediated uptake of antigens. On the other hand, others reported that isolated human LCs were unable to cross-present heat-inactivated measles virus, which was specifically recognized and internalized by Langerin [9]. In addition, studies performed in mice also suggest that LCs may have lower cross-presenting capacity [10]. Using a murine model of *Candida albicans* skin infection, the authors showed that LCs were dispensable in the generation of cytotoxic T cells [10].

Instead, Langerin[+] dermal DCs (dDCs) were required for the generation of antigen specific CTL and Th1 cells against *C. albicans*. Other studies have recently suggested that cross-presentation is mainly an attribute of the Langerin[+] dDC subpopulation and not of LCs in murine skin [11, 12]. However, the existence of an equivalent of this Langerin[+] dDC subpopulation in human skin has been questioned [13], although very recently, a Langerin[+] APC subpopulation has also been detected in the human dermis [14].

Because of their APC-restricted expression pattern and their function as antigen-uptake receptors for processing and presentation, CLRs have often been studied as targeting receptors for vaccination [15, 16]. Antigen targeting to DEC-205, DCIR, CLEC9a, dectin-1 and DC-SIGN on DCs resulted in receptor internalization and enhanced antigen-specific CD4^{+} and CD8^{+} T cell responses [17-20]. Since CLRs are expressed by specific DC subsets, the choice of a CLR for targeting does not only determine the antigen internalization pathway, but also to which DC subset the antigen is targeted. Various pathways involved in cross-presentation after CLR-mediated antigen internalization of antigens have been proposed. One mechanism involved the translocation of antigen into the cytoplasm for proteosomal degradation, followed by TAP-mediated peptide transport in the endoplasmatic reticulum (ER) and loading onto MHC class I molecules [21, 22]. Antigenic peptides can also be generated in the endocytic pathway in a proteosome-independent manner and subsequently bind to recycling MHC class I molecules present within endosomal compartments [23-25]. Recently, it was shown that antigen targeting to specific intracellular compartments, either to early endosomes via CD40 and mannose receptor antibody-conjugates or to late lysosomal compartments via DEC-205, resulted in antigen cross-presentation [26]. Targeting antigens to early endosomes has been shown to result in the most efficient antigen cross-presentation, suggesting that the endocytic compartments to which antigens are delivered determine the efficiency of cross-presentation.

In this study we set out to investigate the role of human LCs in cross-presentation of synthetic long peptides (SLPs) conjugated to antibodies specific for the CLRs Langerin and dectin-1, which gave us the opportunity to study the role of each receptor in processing and shuttling of antigens to MHC class I-loading compartments. To determine whether antigen uptake via Langerin or dectin-1 by human LCs results in a different intracellular routing and antigen cross-presentation, we analyzed

co-localization of both receptors with the early endosomes marker EEA-1 and the lysosomal marker LAMP-1 in pulse-chase experiments. Here, we report that targeting Langerin either with antibodies, but not dectin-1, resulted in enhanced cross presentation. Altogether, these results support the rationale to develop vaccines that specifically target Langerin on human LCs to induce anti-tumor CD8^{+} T cell responses.

Materials and methods

Cells

Primary, human LCs were isolated from abdominal resections from healthy donors undergoing cosmetic surgery (Bergman Clinics, Bilthoven, The Netherlands) and were obtained with informed consent within 24 h after surgery as previously described [27]. Shortly, 5 mm thick slices of skin, containing the epidermis and dermis, were cut using a dermatome. The slices were incubated in dispase II (1 mg/ml, Roche Diagnostics) in IMDM (Invitrogen) supplemented with 10% FCS (BioWhittaker), 50 U/ml penicillin (Lonza), 50 µg/ml streptomycin (Lonza) and 10 µg/ml gentamycin (Lonza) overnight at 4°C followed by mechanical separation of dermis and epidermis using tweezers. The epidermis was washed in PBS, cut into small pieces and incubated in PBS containing DNase I (200 U/ml, Roche Diagnostics) and trypsin (0.05%, Invitrogen) for 30 minutes at 37°C. After incubation, a single cell suspension was generated using 100 µm nylon cell strainers (BD Falcon) and cells were layered on a Ficoll gradient. An average of $1x10^4$ LCs per cm^2 of tissue with a purity higher than 90% were obtained and characterized as CD1a^{+} Langerin^{+} cells by flow cytometry as described below. LCs were cultured in IMDM supplemented with 10% FCS, 50 U/ml penicillin, 50 µg/ml streptomycin and 10 µg/ml gentamycin. When indicated, $5x10^4$ LCs were cultured for 24 h in 200 ul medium supplemented with 20 µg/ml pI:C (Invivogen), 20 ng/ml LPS (derived from *E. coli*, Sigma), 5 µg/ml R837 (Invivogen) or 5 µg/ml R848 (Invivogen) to induce maturation. In indicated experiments, LCs were obtained by spontaneous migration. Shortly, epidermis and dermis were separated as described above. The epidermis was washed in PBS and cultured for 2 days in a 25 cm^2 culture dish (Greiner) containing 40 ml of IMDM supplemented with 10% FCS, 50 U/ml penicillin, 50 µg/ml streptomycin and 10 µg/ml gentamycin to allow spontaneous migration of LCs. After 2 days, cells present in the supernatant were harvested and layered on a Ficoll gradient and further cultured as described above.

Tap-deficient T2 cell line

The TAP-negative BxT hybrid cell line 1.74xCEM (referred to as T2) was used for peptide stabilization assays [28]. T2 cells ($1x10^5$) were incubated overnight with peptides in RPMI at 37°C, washed twice in PBS and surface MHC class I expression assayed by flow cytometry (FACSCalibur, Becton Dickinson) using an HLA-A2 specific monoclonal antibody (Becton Dickinson).

Flow cytometry

Phenotypical analysis of isolated LCs was performed by flow cytometry. Cells were washed in PBS supplemented with 1% bovine serum albumin (BSA) and 0.02% NaN3 and incubated for 30 min at 4°C in the presence of appropriate dilutions of fluorescent-conjugated mAbs to CD1a (APC, clone HI149, Becton Dickinson), CD14 (FITC, clone MoP9, Becton Dickinson), CD70 (PE, clone Ki-24, Becton Dickinson), CD86 (PE, clone 2331, Becton Dickinson), HLA-DR (PerCP, clone L203, Becton Dickinson), HLA-ABC (FITC, clone W6/32, ImmunoTools) or CD83 (PE, clone HB15e, Beckman Coulter Immunotech), or corresponding isotype-matched control mAbs (Becton Dickinson). HLA-A2 status of the cells was determined using a specific mAb (Becton Dickinson). The cells were subsequently analyzed using the FACSCalibur and FlowJo software (Tree Star).

Imaging flow cytometry

Approximately $0.1x10$ primary human LCs, which were migrated spontaneously from human skin, were incubated for 3 hours at 37°C in culture medium with or without 20 μg/ml pI:C to induce maturation. Cells were then washed twice and incubated in ice-cold culture medium. As indicated, AF647-labeled anti-dectin-1 (AbD Serotec) and PE-labeled anti-Langerin (R&D Systems) were added and incubated for 15 min at 37°C in order to allow binding to cell surface expressed Langerin and dectin-1. Cells were then washed in ice-cold medium, transferred to a 37°C incubator and samples were obtained at the indicated time points. Cells were then washed in ice-cold PBS and fixated in ice-cold 4% PFA in PBS for 20 minutes. To prevent cell loss during the staining procedure, LCs were mixed with monocyte-derived dendritic cells. Cells were then permeabilized in 0.1% saponin (Sigma) in PBS for 30 minutes at room temperature and subsequently blocked using PBS containing 0.1% saponin and 2% BSA for 30 minutes at room temperature. Stainings were performed at room temperature in PBS supplemented with 0.1% saponin and 2% BSA. After staining, cells were washed twice in PBS, resuspended in PBS containing 1% BSA and 0.02% NaN3

and kept at 4°C until analysis. Cells were acquired on the ImageStream X (Amnis) imaging flow cytometer. A minimum of 15000 cells was acquired per sample at a flow rate ranging between 50 and 100 cells/second at 60x magnification. At least 2000 cells were acquired from single stained samples to allow for compensation (Supporting **Figure 1**). Analysis was performed using the IDEAS v6.1 software (Amnis). Cells were gated based on the Gradient RMS (brightfield) feature, which was used to select for cells in focus (Supporting **Figure 2A**) and Langerin expression (Supporting **Figure 2B**). Co-localization (Supporting **Figure 3**) was calculated using the features bright detail similarity R3 (for 2-color co-localization) or bright detail co-localization 3 (for 3-color co-localization).

Antibody degradation assay WB

LC were incubated in serum free IMDM for 30 minutes, incubated with 50µg/ml anti-Langerin (10E2) or anti-Dectin-1 (AbD Serotec) for 45 minutes on ice to ensure binding. Cells were washed twice in ice cold medium to remove unbound antibody and internalization was assessed after 0, 15 and 45 minutes incubation at 37˚C. Following indicated incubation times cells were lysed in NP40-lysisbuffer for 30 minutes on ice. Nuclei were removed by spinning cells at 14000rpm for 10 minutes and supernatant containing cell lysate was used for WB. Cell lysates were denatured in SDS-sample buffer (Bio-rad) and reducing agent and boiled for 5 minutes. Samples were loaded and separated on a 10% SDS polyacrylamide gel in electrophoresis buffer (3g Tris, 14,4g Glycine, 1L MQ, 0,1% SDS) before transfer to a nitrocellulose membrane (Bio-rad) for 2 hours at 250mV for immunoblotting. The blot was blocked in blocking solution (Roht) for 1 hour at RT, followed by incubation with a polyclonal goat anti-mouse Ig HRP conjugate (Dako)for 1 hour at RT. After extensive washing with PBS plus 0,05% Tween antibody binding was visualized using ECL (Bio-rad). Antibody staining was removed by incubating the blot in stripping buffer for 1 hour at 60˚C, followed by blocking for 1 hour at RT. Actin was stained using an goat polyclonal anti-actin IgG (Santa Cruz) and corresponding HRP-coupled secondary antibody.

Immunofluorescence microscopy

Human tissue sections (7 µm) were fixed in acetone and blocked with goat serum prior to staining. Antibodies directed against CD14, CD1a or Langerin were added at 10 µg/ml in PBS containing 1% BSA for 60 min. at 37°C followed by secondary Alexa 488-conjugated rabbit anti-mouse IgG2A, Alexa 546-conjugated rabbit anti-mouse IgG2B or Alexa 647-conjugated rabbit anti-mouse IgG1 specific antibodies

(Molecular Probes) for 30 min. at room temperature. Sections were counterstained using hoechst and analyzed by fluorescence microscopy (Leica microsystems).

Modification of MART-1 peptides with glycans and antibodies

The synthetic long peptides MART-1 (CYTTAEELAGIGILTV) were produced by solid phase peptide synthesis using Fmoc-chemistry with a Symphony peptide synthesizer (Protein Tecnologies Inc., USA). Peptides were coniugated to glycans and antibodies on the N-terminal cysteine through a tiol-maleimide reaction. To this end, glycans were activated with the use of the bifunctional crosslinker MPBH (4-N-Maleimidophenyl butyric acid hydrazide, Thermo Scientific) and antibodies through reaction with SMCC (Succinimidyl 4-(N-maleimidomethyl)cyclohexane-1-carboxylate, Thermo Scientific).

First, the hydrazide moiety of MPBH was covalently linked to the reducing end of the glycan via reductive amination. Shortly, a mixture of MPBH (3 eq.), glycan (1 eq.) and picoline-borane (10 eq.) dissolved in Dimethyl-sulfoxide/Acetic acid (7:3, anhydrous and glacial respectively, Sigma) reacted for 2 h at 65°C. After cooling down to room temperature, 4 volumes of dichloromethane (Biosolve) were added and the mixture was vortexed thoroughly. Subsequently, 4 volumes of diethyl ether (Biosolve) were added and incubated until glycan-MPBH had completely precipitated. MPBH-glycans were pelleted by centrifugation (2 min at 14000g), then the supernatant was discarded and the pelleted carbohydrate-MPBH was washed with cold diethyl ether 3 times. The obtained glycan-MPBH pellet was resuspended in aqueous 0.1% TFA (trifluoroacetic acid, Sigma) and lyophilized, followed by purification over a 22 x 250 mm Vydac MS214 prep C18 column (Grace Alltech, elution water/acetonitrile, gradient 3% to 50% of acetonitrile in 40 min) on a Dionex prep 3000 HPLC system. The fractions containing the glycan-MPBH were pooled and lyophilized.

Peptides were glycosylated on their terminal cysteines with the activated glycan through a thiol-ene reaction. Briefly, the peptides (3 eq.) were dissolved in 0,05M phosphate buffer (pH 6.5) and added to the carbohydrate-MPBH (1 eq.). After 2 h of reaction at room temperature, the glycosylated peptides were purified using and Vydac MS214 prep C18 columns 10 x 250 mm (Grace Alltech, elution water/acetonitrile, gradient 10% to 50% of acetonitrile in 40 min). The fractions containing the glycopeptide were pooled and lyophilized. The derivatization and purity of the glycosylated peptides was confirmed by HPLC (Vydac 218MS C18 5um 4.6 x 250 mm,

Grace Alltech) and MS spectrometry (LCQ-Deca XP Iontrap Thermo Finnigan mass spectrometer in positive mode using nanospray capillary needle). Conjugation of the glycans to the glycopeptides was also confirmed by ELISA using antibodies specific for Leb, LeX and LeY, as previously described [18].

Peptides were conjugated to antibodies using the bifunctional crosslinker Succinimidyl-4-(N-maleimidomethyl) cyclohexane-1-carboxylate (SMCC, Thermo Scientific). Briefly, antibodies were activated with SMCC (8 eq.) in phosphate buffer pH 8.2 for 30 min at room temperature. After desalting over a G-25 10X100 mm single use desalting gel filtration column (Amersham), peptides were dissolved in DMSO and added to the vial containing the antibody. After performing the coupling reaction at room temperature for 2 h, the un-conjugated peptide was removed through size-exclusion chromatography using a superdex 75 column (30 x 100 mm, Amersham Biotech) eluting with 50 mM ammonium formate buffer, pH 6.8. The fractions containing the antibody-peptide constructs were pooled and lyophilized.

Generation of Langerin-Fc constructs

The binding capacity of Langerin to various Lewis-type glycans was determined using Langerin-Fc molecules. Langerin-Fc was generated by amplifying the extracellular domains of Langerin (aa 63–328) on RNA of LCs by PCR. The product was confirmed by sequence analysis and fused at the C-terminus to human IgG1-Fc in the Sig-pIgG1-Fc vector. Langerin-Fc was produced by stable transfection of CHO cells and Langerin-Fc concentrations were determined by ELISA.

ELISA-based Langerin binding assay

The conjugation of the Le[b], Le[X] and Le[Y] glycans to the MART-1 peptides was confirmed by ELISA using anti-Le[b], -Le[X] and -Le[Y] antibodies (Calbiochem) [18]. Briefly, glycopeptides were dissolved in PBS containing 0.05% BSA and coated onto NUNC maxisorb plates (Roskilde) and incubated overnight at 4°C. Plates were blocked with 1% BSA in PBS to avoid non-specific binding. After extensive washing, the glycopeptides were incubated with Langerin-Fc for 90 min at RT. Binding was detected using a peroxidase-labeled F(ab')2 goat anti-human IgG/Fcγ specific antibody. Signal detection was achieved by incubation with 1.3 mM H_2O_2 in the presence of TMB (3,3',5,5'-tetramethylbenzidine) in 0.1M sodium acetate-citrate buffer until the development of the reaction. The reaction is then stopped using 1 M H_2SO_4 and absorbance is measured at 450 nm using a colorimeter (BioRad). As a

positive control, biotin-labeled Le^b, Le^X and Le^Y conjugated to polyacrylamide (PAA; Lectinity) were used.

Quantitative real-time RT-PCR

Cells were lysed and mRNA was isolated using an mRNA Capture kit (Roche). cDNA was synthesized using the Reverse Transcription System kit (Promega) following manufacturer's guidelines. Each experiment contained cells isolated from at least 5 skin donors to obtain sufficient cells numbers for analysis. Oligonucleotides were designed using the Primer Express 2.0 software (Applied Biosystems) and synthesized by Invitrogen Life Technologies. Real-Time PCR analysis was performed as previously described using the SYBR Green method in an ABI 7900HT sequence detection system (Applied Biosystems) [29]. GAPDH was used as an endogenous reference gene.

Antigen presentation to human CD8$^+$ T cell clones specific for MART-1

A CD8$^+$ T cell clone specific for MART-1$_{26-35}$ was generated and cultured as described previously [30]. The modified 16 aa long MART-1$_{21-35}$ peptides (C-YTTAEELAGIGILTV) were added to 20 000 HLA-A2$^+$ LCs, obtained after migration from the skin, per well at indicated concentrations together with poly I:C (20µg/ml) for 3 h at 37°C. After extensive washing, HLA-A2$^+$ MART-1 specific CD8$^+$ T cells (100 000/well) were added to the wells. After 24 h, supernatants were taken and IFN-γ levels were measured by sandwich ELISA using specific antibody pairs from Biosource and according to the manufacturer's guidelines.

Statistical analysis

Results were analyzed using either a one-way ANOVA followed by Bonferrroni Multiple Comparison test or a two-way ANOVA followed by Bonferroni Multiple Comparison test using GraphPad Prism software (GraphPad Software, San Diego, CA). Results were considered to be statistically significant when $p < 0.05$.

Results

LCs are the main Langerin$^+$ cells in human skin

Although Langerin has been classically reported to be exclusively expressed on epidermal LCs in human skin [31, 32], recent publications have challenged this knowledge by reporting the existence of a Langerin$^+$ CD1a$^+$ dDC in human dermis, lung, liver and lymphoid tissue [14]. In order to analyze whether Langerin expression is restricted to epidermal LCs, human

skin sections were stained for CD14, CD1a and Langerin. As shown in **Figure 1A**, the great majority of Langerin staining was observed in epidermal LCs, which were also positive for CD1a and only rare CD1a^{+} Langerin^{+} cells could be observed in the dermis in close proximity with the dermoepidermal junction (**Figure 1A**). These cells could simply represent activated LCs that migrate through the dermis to the lymph nodes [14]. In addition, it was recently demonstrated that these cells could also be dermal DCs that have been in contact with TGF-β leaked from the epidermis, resulting in upregulation of Langerin [33]. Nevertheless, the frequency of these cells is extremely low and it is questionable whether their presence in the dermis might have any functional relevance. Indeed, most of the dermal CD1a^{+} DCs observed were devoid of Langerin expression (**Figure 1**).
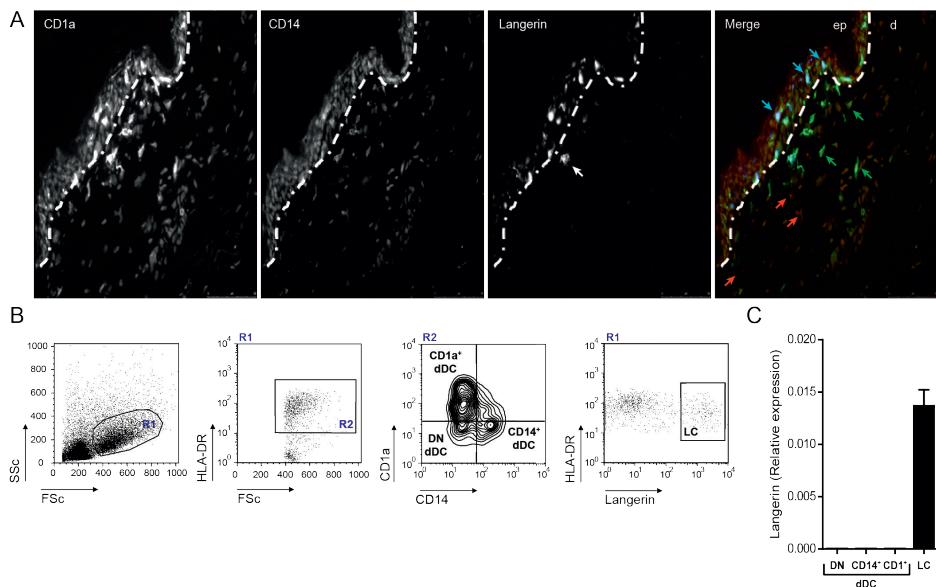

Figure 1. Langerin is exclusively expressed by human LCs. A. Staining of a section of steady-state human skin for Langerin (blue), CD1a (green), CD14 (red) and Hoechst (yellow) and analyzed by fluorescence microscopy. B. Gating strategy of FACS-sorted LCs, CD14^{+}, CD1a^{+} and double negative dermal DCs. C. Langerin mRNA is exclusively expressed in primary, FACS-sorted LCs and not by the other skin DC subsets. N=3, each experiment contains sorted cells of at least 5 skin donors. mRNA values are normalized to GAPDH levels.

Additionally, we confirmed the data by quantitative RT-PCR analysis for Langerin on FACS-sorted HLA-DR[+] APCs isolated from the dermis and epidermis (**Figure 1B**). **Figure 1C** confirms that Langerin is exclusively expressed by LCs and not by the dermal CD1a^{+} DCs, CD14^{+} DCs or the HLA-DR^{+}CD1a^{-}CD14^{-} dermal DC subset, which may be constituted,

among others, by macrophages and BDCA3^{+} skin DCs. Thus, LCs are the main Langerin^{+} cells in the human skin.
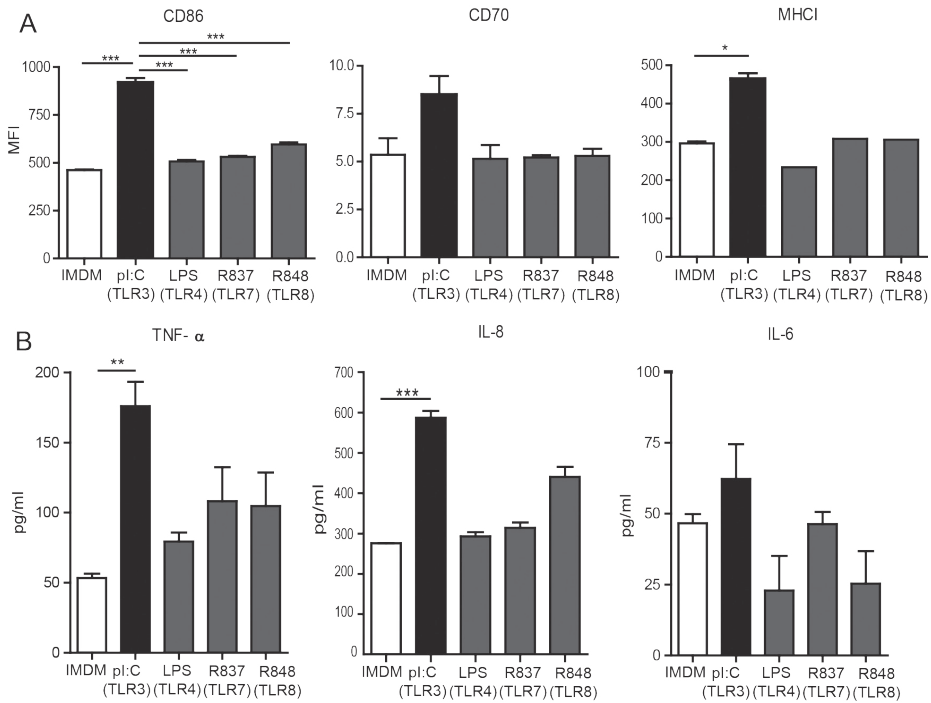

Figure 2. Maturation of LCs *in vitro* upon stimulation with the TLR3 ligand pI:C A. Phenotypical characterization of human LCs after 16 h of culture in the presence of the indicated TLR ligands. The mean fluorescent intensity is depicted for MHC class I, CD86 and CD70. Data represent average ± SEM of 3 independent skin donors. B. Cytokines produced by human LCs cultured for 16 h in the presence or absence of indicated TLR ligands. Data represent average ± SEM of 3 independent skin donors.

Human LCs mature in vitro upon stimulation with pI:C, but are not affected upon stimulation with other TLR ligands

We wanted to investigate whether human LCs are able to cross-present antigens and induce CD8^{+} T cell responses. Since cross-presentation has been described to be dependent on the maturation status of DCs [34, 35], we investigated the effects of various TLR-specific compounds on the maturation of LCs and their cytokine responses. As shown in **Figure 2A**, only the TLR3 ligand pI:C induced an upregulation of the co-stimulatory molecules CD86 and CD70 and MHC class I, while the TLR4 ligand LPS and the TLR7/8 ligands R837 and R848 had no effects (**Figure 2A**). In

addition, only pI:C induced an enhanced production of the pro-inflammatory cytokines TNF-α, IL-6 and IL-8 (**Figure 2B**). LCs did not secrete the anti-inflammatory cytokine IL-10 either in the presence or absence of pI:C, LPS, R837 or R848 (levels below 10 pg/ml; data not shown). So, human LCs mature upon stimulation with the TLR3 ligand pI:C, which can be explained by the abundant expression of TLR3 by LCs as described in the literature [36, 37]

pI:C treatment enhances the cross-presentation capacity of LCs

In order to investigate the capacity of LCs to cross-present SLPs, we pulsed human LCs with a titration of a 16 aa long MART-1 peptide (C-YTTAE*ELAGIGILTV*) containing an HLA-A2-restricted epitope (in italics) recognized by a MART-1 specific CD8^{+} T cell clone, in the presence of various TLR ligands. This clone responds to specific peptide-MHC-I complexes by the production of IFN-γ. To verify that the 16 aa SLP requires antigen processing before loading on MHC class I molecules, a T2 assay was performed. The data presented in **Figure 3A** excludes the possibility of direct external loading since the SLP did not stabilize HLA-A2 molecules on the surface of the TAP-deficient T2 cell line (**Figure 3A**). As a positive control, T2 cells were incubated with the minimal MART-1 epitope that can directly bind and stabilize HLA-A2 on the surface of the T2 cells (**Figure 3A**). In addition, HLA-A2[+] human LCs were loaded with the 16 aa MART-1 SLP or the 10 aa minimal MART-1 epitope for 30 minutes, washed and co-cultured with the MART-1 specific CD8^{+} T cell clone. Only when the LCs were loaded with the minimal epitope, the CD8^{+} T cells responded by secreting IFN-γ (**Figure 3B**). No T cell activation was observed when the LCs were incubated with the 16 aa SLP, indicating that this peptide requires processing before it can be presented on HLA-A2 molecules (**Figure 3B**).

As demonstrated in **Figure 3C**, human LCs were able to cross-present after 3 h of antigen internalization to the MART-1 specific CD8^{+} T cell clone as measured by the secretion of IFN-γ. Moreover, simultaneous administration of MART-1 peptide with pI:C resulted in a significant increased activation of the CD8^{+} T cells, whereas addition of LPS, R837 or R848 did not enhance cross-presentation (**Figure 3C**). Thus, human LCs are able to cross present soluble SLPs, which could be further enhanced in the presence of pI:C.
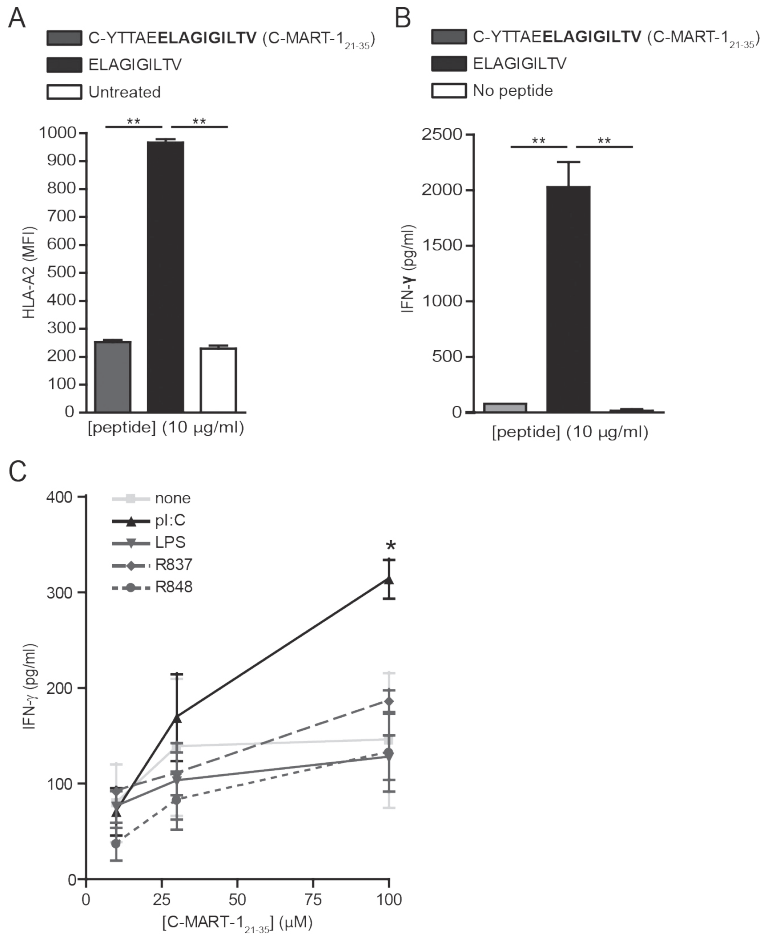
Figure 3. pI:C stimulation of LCs results in superior antigen cross-presentation A. 1x10^5 T2 cells were incubated with a 16 aa long MART-1 peptide, the minimal CD8 epitope or no peptide, where after the cells were analyzed for the expression of surface HLA-A2 by flow cytometry. Data represent average of three ± SD. **p <0.01. B. 2x10^4 HLA-A2$^+$ LCs were incubated with a 16 aa long MART-1 peptide, the minimal CD8 epitope or no peptide for 30 min, washed and co-cultured with 1x10^5 MART-1 specific CD8$^+$ T cells. After 24 h of co-culture, T cell activation was measured by IFN-γ ELISA on the supernatants. Data represent average of two experiments ± SD. **p <0.01. C. Human LCs were incubated with the synthetic long MART-1 peptide for 3 h and indicated TLR ligands, washed and co-cultured with a MART-1 specific CD8$^+$ T cell clone. After 24 h of co-culture, T cell activation was measured by IFN-γ ELISA on the supernatants. Data of one representative experiment measured in triplicate is shown, n=3. *p<0.05.

Targeting Langerin, but not dectin-1, using SLP-antibody conjugates enhanced antigen cross-presentation in LCs

Since human LCs have the capacity to cross-present MART-1 SLPs, which were presumably internalized by pinocytosis, we next investigated whether receptor-mediated internalization would enhance cross-presentation by altering the endocytic routing of the antigens. To investigate this, anti-Langerin or anti-dectin-1 mouse monoclonal antibodies were conjugated to the MART-1 SLP via maleimide-thiol coupling through the N-terminal Cys on the SLP. Both Langerin and dectin-1 are expressed on human LCs (**Figure 4A**) and, as shown in **Figure 1**, Langerin is a specific marker of human LCs, making this receptor a suitable target for LC-targeting immunotherapy. Conjugation of the SLPs to anti-Langerin antibodies resulted in significantly higher activation of the CD8$^+$ T cell clone (**Figure 4B**) as compared to the SLP alone or conjugated to the anti-dectin-1 antibody or an isotype control, indicating that Langerin-targeting enhances cross-presentation by human LCs. Furthermore, Langerin-specific responses were further increased when LCs were simultaneously exposed to pI:C (**Figure 4C**). Interestingly, although both dectin-1 and Langerin were expressed on LCs (**Figure 4A**), we could not detect any dectin-1-specific enhancement on cross-presentation as compared to the isotype control (**Figure 4b** and **C**), suggesting that antigens endocytosed via dectin-1 follow an intracellular routing that did not result in proper processing and/or loading to MHC class I. In addition, the effect of pI:C is not related to enhanced co-stimulation, as can be deduced from **Figure 4D**, where the no additional effect on IFNg production could be observed when MART-1 loaded LCs were stimulated with pI:C. Seemingly, dectin-1 or Langerin targeting did not have any co-stimulation-related effects on IFNg production (**Figure 4D**). Together, these data show that only Langerin targeting of MART-1 SLPs allowed antigen routing to a cross-presentation compartment, which could be enhanced by simultaneous triggering of TLR3.
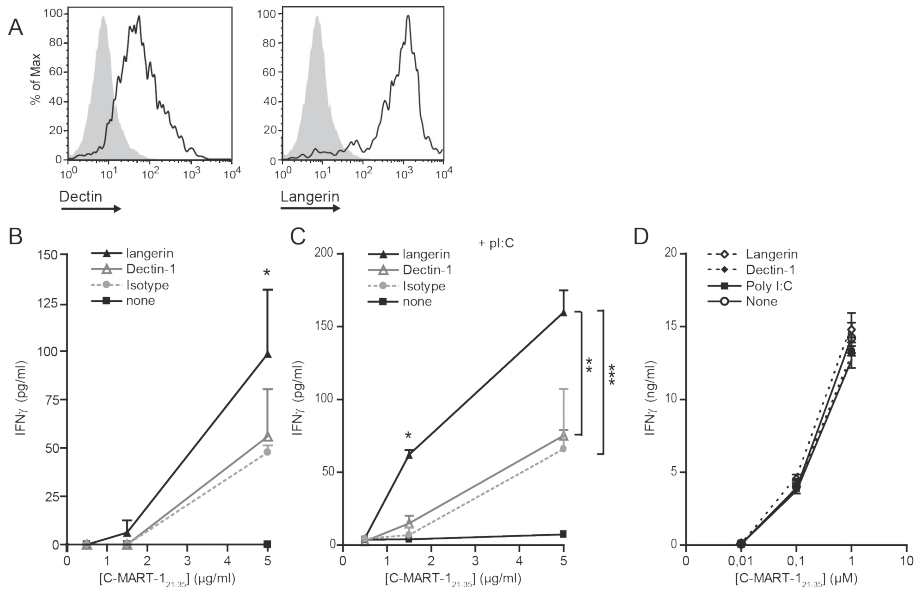
Figure 4. SLPs conjugated to Langerin result in enhanced cross-presentation to antigen-specific CD8+ T cells. A. Dectin-1 and Langerin are highly expressed by human LCs as measured by flow cytometry. Open histograms: specific antibody; filled histograms: isotype control. Data are representative for 3 donors. B+C. MART-1 (CYTTAEELAGIGILTV) peptides were conjugated to anti-Langerin and anti-dectin-1 or mIgG1 isotype control mAbs and incubated with human LCs for 3 h in the presence (C) or absence (B) of 20 µg/ml pI:C, and co-cultured with a MART-1 specific CD8+ T cell clone. Activation of the T cells was measured by IFN-γ ELISA on the supernatants taken after 24 h of co-culture. Data are representative of two independent experiments and depict average ± SEM of triplicates. D. Human LCs were incubated with the MART-1 (CYTTAEELAGIGILTV) peptide in the presence or absence of anti-Langerin, anti-dectin-1 or 20 µg/ml pI:C for 3h, washed, and co-cultured with a MART-1 specific CD8+ T cell clone. Activation of the T cells was measured by IFN-γ ELISA on the supernatants taken after 24 h of co-culture.

Langerin routes antigens to specific early endosomes

To investigate the differences in antigen cross-presentation after Langerin and dectin-1 targeting, we pulsed LCs using fluorescently-labeled antibodies and followed their intracellular localization using the early endosomal marker EEA-1 and the lysosomal marker LAMP-1 by imaging flow cytometry. The fluorescence associated to the anti-Langerin antibody hardly decreased over time (**Figure 5A**), while that of the anti-dectin-1 antibody rapidly decreased (**Figure 5B**), suggesting that Langerin routes antigens to a less degradative compartment as compared to dectin-1. To further confirm this point, we investigated antibody degradation by western blot in LC lysates obtained at the abovementioned time-points. Data indeed confirmed a

faster degradation of anti-dectin antibodies as compared to anti-Langerin (**Figure 5C**).

We then investigated the co-localization of each of the CLR-specific antibodies with EEA-1^{+} compartments and observed that dectin-1 had a longer and stronger association with EEA-1^{+} compartments compared to Langerin based on the co-localization score being close to 1 (**Figure 5E** and **G**). The co-localization between Langerin and LAMP-1^{+} compartments or dectin-1 and LAMP-1^{+} compartments was poor and did not differ in time and intensity (**Figure 5E** and **G**). Since there was a divergence in the degradation of the fluorescence signal and the localization to early endosomes, we speculated that dectin-1 and Langerin routed to different types of early endosomes with differing degradative capacities. To investigate this, we used a 3-color co-localization feature and addressed the co-localization of either EEA1 or LAMP1 with dectin-1 and Langerin simultaneously. In resting LCs, both dectin-1 and Langerin are expressed on the membrane of LCs, as shown in **Figure 4A**. However, there was a significant proportion of both receptors localized in an intracellular compartment, which appeared to be EEA1^{+} (**Figure 5F** and **Supplementary Figure 4**). Presumably, this compartment serves as an intracellular depot for quick up regulation of both receptors on the membrane of LCs. Interestingly, upon triggering of dectin-1 and Langerin 3-color co-localization with EEA1 dramatically decreases, suggesting that although both receptors are internalized and routed to early endosomes (as shown in **Figure 5E**), they do not coincide in the same endosomes (**Figure 5F** and **Supplementary Figure 4**). These data indicate that Langerin routes to specific EEA-1^{+} early endosomes that, presumably, are better equipped to facilitate cross-presentation than the early endosomes where dectin-1 routes to.

Discussion

Within the human skin, at least three main and distinct populations of DCs can be identified, namely LCs and CD14^{+} and CD1a^{+} dermal DCs. After activation, it has been shown that the Langerin^{+} LCs and dDC subsets are able to migrate to the skin-draining lymph nodes, where they activate CD4^{+} and CD8^{+} T cell responses [38, 39]. The precise function of each subset is still under debate, especially with regard to antigen cross-presentation. Recently, a minor population of BDCA3^{+} myeloid DCs has been described as homologues of mouse CD8^{+} DCs and has shown to have superior cross-presentation capacity [40-42]. Antigen targeting to CLEC9a, a CLR expressed on BDCA3^{+} DCs, resulted in antigen uptake and (cross-)presentation [43]. However, it has

also been shown that human skin resident BDCA3^{+} DCs can produce IL-10 and induce regulatory T cells (Tregs) [44]. In addition, the low numbers of these cells also make them less favorable to target for the induction of anti-tumor immune responses.

In this study, we have investigated the cross-presentation capacity of human LCs when SLPs were targeted to distinct CLRs. Specific targeting of SLPs to the LC-specific receptor Langerin, using either antibody- or glycan-modification, resulted in enhanced activation of effector CD8^{+} T cells. These results imply that human LCs are a suitable candidate for *in vivo* targeting of vaccines. Although LCs are located in the epidermis of the human skin, administration of a LC-targeting vaccine can also be applied intradermally, since intradermally deposited DEC-205 or Langerin antibodies have been shown to be rapidly captured by LCs [45].

In our studies, the targeting peptides to Langerin, as well as the targeting of proteins to Langerin [46], using monoclonal antibodies resulted in efficient antigen cross-presentation. In contrast, antigens internalized via the CLR dectin-1 did not allow enhanced cross-presentation, showing that the intracellular routing of antigens internalized via dectin-1 is different from that of Langerin in LCs. This is supported by our imaging flow cytometry data, which demonstrates that dectin-1 routes to more degradative intracellular compartments which also did not co-localize with Langerin[+]EEA-1^{+} compartments. However, it has been shown for *in vitro* generated moDCs that dectin-1 allowed binding and internalization of CMV pp65 expressing apoptotic cells and this interaction resulted in cross-presentation to CMV pp65 specific CD8^{+} T cells [19], showing the potential of dectin-1, when expressed on DC, to facilitate routing of antigen to MHC class I loading compartments. The discrepancy between these results and the findings presented in this paper concerning cross-presentation after dectin-1 targeting, might be explained by the difference in cell types, primary LCs versus *in vitro* generated DCs. Alternatively, it may also be attributed to the mode of antigen delivery. In the experiments described here, dectin-1 was targeted using monoclonal antibodies conjugated to soluble MART-1 peptides, whereas in the study of Weck *et al.* dectin-1 facilitated the uptake of total apoptotic cells [19].
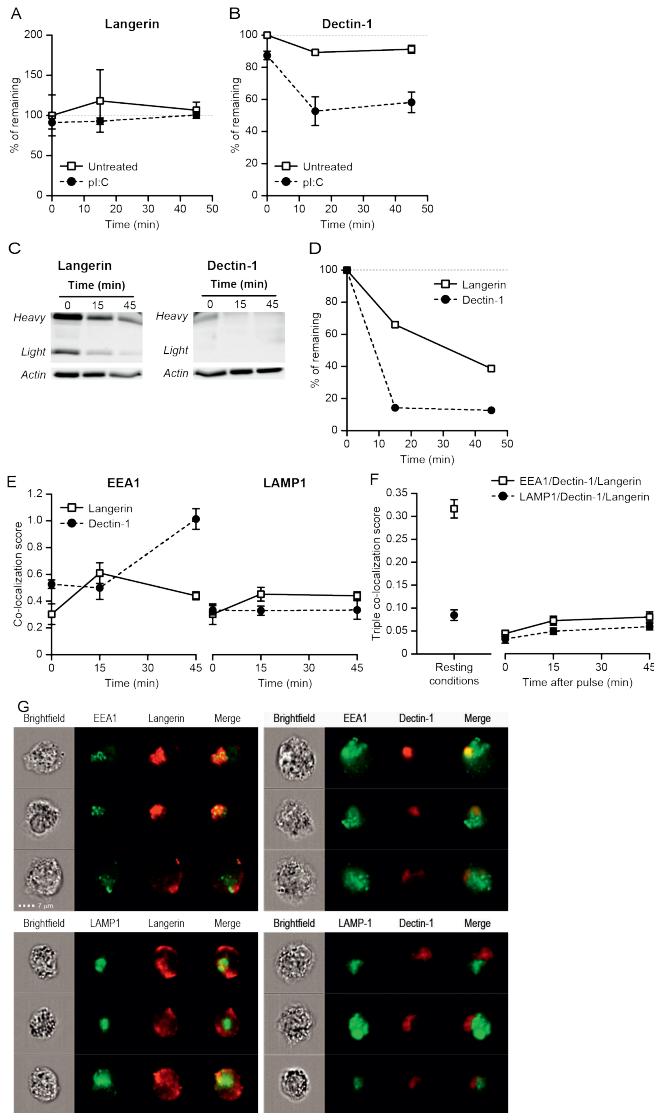
Figure 5. Langerin routes to less degradative endosomal compartments in LCs after antigenic pulse compared to dectin-1 A+B. Remaining fluorescence of anti-Langerin (A) and anti-dectin-1 antibodies (B) in a pulse-chase in the presence or absence of pI:C. C+D. Pulse-chase of anti-Langerin and anti-dectin-1 antibody degradation in LCs by western blotting using an anti-mouse Fc peroxidase-labeled antibody. Staining is shown in C, and band intensity quantification in D. E. Co-localization of Langerin and dectin-1 with the intracellular compartments EEA-1 and LAMP-1 after receptor binding and internalization at the cell surface. F. Three color co-localization score of Langerin, dectin-1 and EEA-1 or LAMP-1 in resting conditions (left panel) or after receptor triggering at the cell surface (right panel) measured by imaging flow cytometry (representative images are shown in **Supplementary Figure 4**). G. Randomly selected LCs representing data depicted in E (time-point 15m).

Dectin-1 is not the only CLR in which the capacity to cross-present is in part determined by the mode of antigen delivery. Van der Vlist *et al.* reported that human LCs were not able to cross-present antigens derived from whole measles virus (MV) or MV-infected apoptotic cells taken up via Langerin [9]. We have recently demonstrated that differences in size of the antigen influences Langerin-mediated antigen internalization and cross-presentation in LCs [47]. Bigger nanoparticles were less well internalized and cross-presented by LCs compared to small, soluble peptides [29]. These findings might explain the discrepancy found between the Van der Vlist study and the data presented here: in their study the authors used relatively big MV particles and MV-infected cells which were not cross-presented in a Langerin-dependent fashion, whereas we do show Langerin-mediated internalization and cross-presentation of small SLPs in our studies.

This study also showed that cross-presentation by human LCs was enhanced in the presence of the TLR3 agonist pI:C. The combined administration of antigens and TLR agonists is reported to be necessary to prevent the induction of T cell tolerance. Recently the requirement of a potent activator to overcome the tolerogenic state of LCs to selectively and specifically induced the activation and proliferation of skin resident Tregs has been described [48]. Similar as DCs, in the presence of danger signal derived from pathogens, LCs become activated and induced the proliferation of effector memory T cells present in the skin and reduced the activity of Tregs [48]. It seems likely that the precise function of LCs *in vivo* might be determined by danger stimuli derived from the microenvironment [49].

Altogether, we have shown the capacity of human primary LCs to cross-present soluble synthetic long MART-1 peptides. Additionally, cross-presentation by LCs was enhanced when cells were concomitantly matured using the TLR3 agonist pI:C. Targeting of MART-1 SLPs to anti-Langerin antibodies resulted in further enhancement of the activation of MART-1 specific CD8^{+} T cells through the Langerin-mediated routing of antigens to less proteolytic early endosomes compared to dectin-1-mediated antigen internalization. These results provide a rationale for the development of new *in-vivo* vaccines that target human LCs via Langerin for the induction of effective anti-tumor or anti-viral CTL responses.

Acknowledgements

References

1. Heath, W.R., et al., *Cross-presentation, dendritic cell subsets, and the generation of immunity to cellular antigens.* Immunol. Rev, 2004. **199**: p. 9-26.
2. Joffre, O.P., et al., *Cross-presentation by dendritic cells.* Nat. Rev. Immunol, 2012. **12**(8): p. 557-569.
3. Valladeau, J., C. zutter-Dambuyant, and S. Saeland, *Langerin/CD207 sheds light on formation of birbeck granules and their possible function in Langerhans cells.* Immunol. Res, 2003. **28**(2): p. 93-107.
4. Feinberg, H., et al., *Structural basis for Langerin recognition of diverse pathogen and mammalian glycans through a single binding site.* J. Mol. Biol, 2011. **405**(4): p. 1027-1039.
5. Furio, L., et al., *Human langerhans cells are more efficient than CD14(-)CD1c(+) dermal dendritic cells at priming naive CD4(+) T cells.* J. Invest Dermatol, 2010. **130**(5): p. 1345-1354.
6. Furio, L., et al., *Poly(I:C)-Treated human langerhans cells promote the differentiation of CD4+ T cells producing IFN-gamma and IL-10.* J. Invest Dermatol, 2009. **129**(8): p. 1963-1971.
7. Klechevsky, E., et al., *Functional specializations of human epidermal Langerhans cells and CD14+ dermal dendritic cells.* Immunity, 2008. **29**(3): p. 497-510.
8. Polak, M.E., et al., *CD70-CD27 interaction augments CD8+ T-cell activation by human epidermal Langerhans cells.* J. Invest Dermatol, 2012. **132**(6): p. 1636-1644.
9. van, d., V, et al., *Human Langerhans cells capture measles virus through Langerin and present viral antigens to CD4(+) T cells but are incapable of cross-presentation.* Eur. J. Immunol, 2011. **41**(9): p. 2619-2631.
10. Igyarto, B.Z., et al., *Skin-resident murine dendritic cell subsets promote distinct and opposing antigen-specific T helper cell responses.* Immunity, 2011. **35**(2): p. 260-272.
11. Bedoui, S., et al., *Cross-presentation of viral and self antigens by skin-derived CD103+ dendritic cells.* Nat. Immunol, 2009. **10**(5): p. 488-495.
12. Henri, S., et al., *CD207+ CD103+ dermal dendritic cells cross-present keratinocyte-derived antigens irrespective of the presence of Langerhans cells.* J. Exp. Med, 2010. **207**(1): p. 189-206.
13. Igyarto, B.Z. and D.H. Kaplan, *Antigen presentation by Langerhans cells.* Curr. Opin. Immunol, 2013. **25**(1): p. 115-119.
14. Bigley, V., et al., *Langerin-expressing dendritic cells in human tissues are related to CD1c+ dendritic cells and distinct from Langerhans cells and CD141high XCR1+ dendritic cells.* J Leukoc Biol, 2015. **97**(4): p. 627-34.
15. Robinson, M.J., et al., *Myeloid C-type lectins in innate immunity.* Nat. Immunol, 2006. **7**(12): p. 1258-1265.

16. Tacken, P.J., et al., *Dendritic-cell immunotherapy: from ex vivo loading to in vivo targeting.* Nat. Rev. Immunol, 2007. **7**(10): p. 790-802.
17. Tel, J., et al., *Targeting uptake receptors on human plasmacytoid dendritic cells triggers antigen cross-presentation and robust type I IFN secretion.* J. Immunol, 2013. **191**(10): p. 5005-5012.
18. Unger, W.W., et al., *Glycan-modified liposomes boost CD4+ and CD8+ T-cell responses by targeting DC-SIGN on dendritic cells.* J. Control Release, 2012. **160**(1): p. 88-95.
19. Weck, M.M., et al., *hDectin-1 is involved in uptake and cross-presentation of cellular antigens.* Blood, 2008. **111**(8): p. 4264-4272.
20. Bonifaz, L.C., et al., *In vivo targeting of antigens to maturing dendritic cells via the DEC-205 receptor improves T cell vaccination.* J. Exp. Med, 2004. **199**(6): p. 815-824.
21. Kovacsovics-Bankowski, M. and K.L. Rock, *A phagosome-to-cytosol pathway for exogenous antigens presented on MHC class I molecules.* Science, 1995. **267**(5195): p. 243-246.
22. Rodriguez, A., et al., *Selective transport of internalized antigens to the cytosol for MHC class I presentation in dendritic cells.* Nat. Cell Biol, 1999. **1**(6): p. 362-368.
23. Shen, L., et al., *Important role of cathepsin S in generating peptides for TAP-independent MHC class I crosspresentation in vivo.* Immunity, 2004. **21**(2): p. 155-165.
24. Di, P.T., et al., *Direct proteasome-independent cross-presentation of viral antigen by plasmacytoid dendritic cells on major histocompatibility complex class I.* Nat. Immunol, 2008. **9**(5): p. 551-557.
25. Gromme, M., et al., *Recycling MHC class I molecules and endosomal peptide loading.* Proc. Natl. Acad. Sci. U. S. A, 1999. **96**(18): p. 10326-10331.
26. Chatterjee, B., et al., *Internalization and endosomal degradation of receptor-bound antigens regulate the efficiency of cross presentation by human dendritic cells.* Blood, 2012. **120**(10): p. 2011-2020.
27. de, W.L., et al., *Langerin is a natural barrier to HIV-1 transmission by Langerhans cells.* Nat. Med, 2007. **13**(3): p. 367-371.
28. Salter, R.D. and P. Cresswell, *Impaired assembly and transport of HLA-A and -B antigens in a mutant TxB cell hybrid.* EMBO J, 1986. **5**(5): p. 943-949.
29. Fehres, C.M., et al., *Topical rather than intradermal application of the TLR7 ligand imiquimod leads to human dermal dendritic cell maturation and CD8+ T-cell cross-priming.* Eur. J. Immunol, 2014. **44**(8): p. 2415-2424.
30. Hooijberg, E., et al., *Immortalization of human CD8+ T cell clones by ectopic expression of telomerase reverse transcriptase.* J. Immunol, 2000. **165**(8): p. 4239-4245.
31. Angel, C.E., et al., *CD14+ antigen-presenting cells in human dermis are less mature than their CD1a+ counterparts.* Int. Immunol, 2007. **19**(11): p. 1271-1279.
32. Eisenwort, G., et al., *Identification of TROP2 (TACSTD2), an EpCAM-like molecule, as a specific marker for TGF-beta1-dependent human epidermal Langerhans cells.* J. Invest Dermatol, 2011. **131**(10): p. 2049-2057.
33. Bigley, V., et al., *Langerin-expressing dendritic cells in human tissues are related to CD1c+ dendritic cells and distinct from Langerhans cells and CD141high XCR1+ dendritic cells.* J. Leukoc. Biol, 2014.
34. Crespo, M.I., et al., *TLR7 triggering with polyuridylic acid promotes cross-presentation in CD8alpha+ conventional dendritic cells by enhancing antigen preservation and MHC class I antigen permanence on the dendritic cell surface.* J Immunol, 2013. **190**(3): p. 948-60.

35. Bonifaz, L., et al., *Efficient targeting of protein antigen to the dendritic cell receptor DEC-205 in the steady state leads to antigen presentation on major histocompatibility complex class I products and peripheral CD8+ T cell tolerance.* J Exp Med, 2002. **196**(12): p. 1627-38.

36. Flacher, V., et al., *Human Langerhans cells express a specific TLR profile and differentially respond to viruses and Gram-positive bacteria.* J. Immunol, 2006. **177**(11): p. 7959-7967.

37. van der Aar, A.M., et al., *Loss of TLR2, TLR4, and TLR5 on Langerhans cells abolishes bacterial recognition.* J. Immunol, 2007. **178**(4): p. 1986-1990.

38. Segura, E., et al., *Characterization of resident and migratory dendritic cells in human lymph nodes.* J. Exp. Med, 2012. **209**(4): p. 653-660.

39. van, d., V, et al., *Characterization of four conventional dendritic cell subsets in human skin-draining lymph nodes in relation to T-cell activation.* Blood, 2011. **118**(9): p. 2502-2510.

40. Bachem, A., et al., *Superior antigen cross-presentation and XCR1 expression define human CD11c+CD141+ cells as homologues of mouse CD8+ dendritic cells.* J Exp Med, 2010. **207**(6): p. 1273-81.

41. Jongbloed, S.L., et al., *Human CD141+ (BDCA-3)+ dendritic cells (DCs) represent a unique myeloid DC subset that cross-presents necrotic cell antigens.* J. Exp. Med, 2010. **207**(6): p. 1247-1260.

42. Poulin, L.F., et al., *Characterization of human DNGR-1+ BDCA3+ leukocytes as putative equivalents of mouse CD8alpha+ dendritic cells.* J Exp Med, 2010. **207**(6): p. 1261-71.

43. Schreibelt, G., et al., *The C-type lectin receptor CLEC9A mediates antigen uptake and (cross-)presentation by human blood BDCA3+ myeloid dendritic cells.* Blood, 2012. **119**(10): p. 2284-92.

44. Chu, C.C., et al., *Resident CD141 (BDCA3)+ dendritic cells in human skin produce IL-10 and induce regulatory T cells that suppress skin inflammation.* J. Exp. Med, 2012. **209**(5): p. 935-945.

45. Flacher, V., et al., *Epidermal Langerhans cells rapidly capture and present antigens from C-type lectin-targeting antibodies deposited in the dermis.* J. Invest Dermatol, 2010. **130**(3): p. 755-762.

46. Klechevsky, E., et al., *Cross-priming CD8+ T cells by targeting antigens to human dendritic cells through DCIR.* Blood, 2010. **116**(10): p. 1685-97.

47. Fehres, C.M., et al., *Cross-presentation through Langerin and DC-SIGN targeting requires different formulations of glycan-modified antigens.* Journal of Controlled Release, 2015. **203**: p. 67-76.

48. Seneschal, J., et al., *Human epidermal Langerhans cells maintain immune homeostasis in skin by activating skin resident regulatory T cells.* Immunity, 2012. **36**(5): p. 873-884.

49. Romani, N., P.M. Brunner, and G. Stingl, *Changing views of the role of Langerhans cells.* J. Invest Dermatol, 2012. **132**(3 Pt 2): p. 872-881.
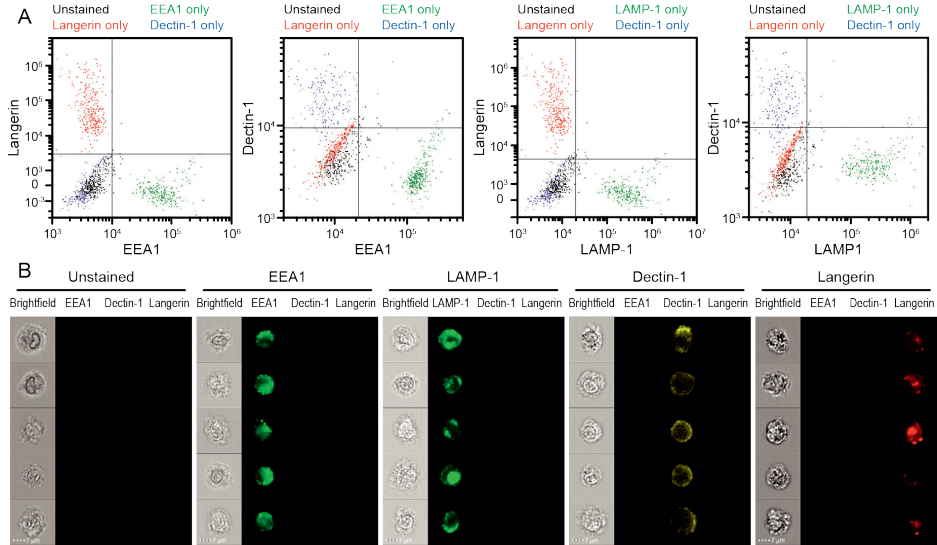
Supplementary data

Figure S1. Compensation in imaging flow cytometry experiments. A critical step in the analysis of imaging flow cytometry data consists of the elimination of fluorescence leakage in neighbouring channels. This process is identical to compensation in classical flow cytometry and involves the acquisition of single stained samples and the processing of the data with a compensation wizard present in the software package IDEAS (Amnis-Millipore). Once a compensation table has been generated, it can be applied to the raw data to process images without spectral overlap. In order to control that the compensation table has been generated flawlessly, it is applied to the single staining controls and proper separation of individual channels is verified, as shown in (**A**). (**B**) Images were randomly selected from single stained populations to verify that, indeed, only the expected channel contained fluorescence.
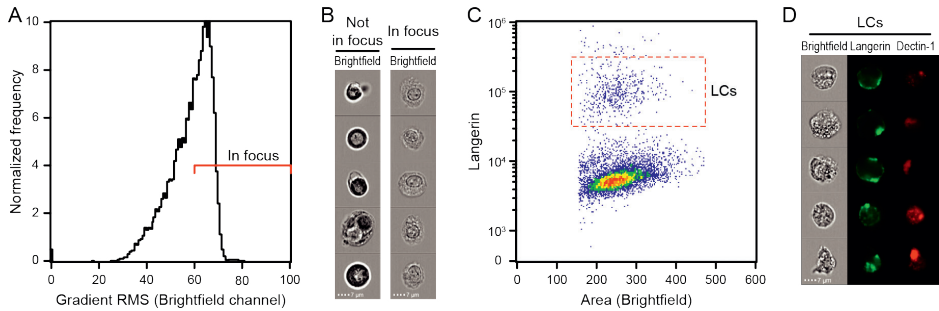
Figure S2. Imaging flow cytometry analysis strategy. In imaging flow cytometry, images are taken from cells as they pass by the detector in a flow system. The objective is calibrated such that images are taken at the center of the flow. At the magnification used in the experiments reported in this manuscript (60X), the lateral resolution corresponds to approximatey 300 nm, whilst the depth of focus is 2.5 μm. Therefore, cells that are slightly off the center of the flow may appear out of focus. In order to gate the cells that are properly focused, a necessary condition for further analysis, the *Gradient RMS* feature applied to the *Brightfield channel* was used, as depicted in (**A**). Gradient RMS measures the sharpness quality of images by detecting large changes (average gradient of a pixel normalized for variations in intensity levels) of pixel values in the image. (**B**) Examples of events according to their gradient RMS value. Only those events with values higher than 60, were further selected for analysis. (**C**) Since the amount of LCs was low and a minimum cell/rate is needed for proper acquisition, samples were spiked with fixed monocyte-derived dendritic cells. LCs could be gated by their high Langerin expression. (**D**) Randomly selected LCs showing expression of Langerin and Dectin-1
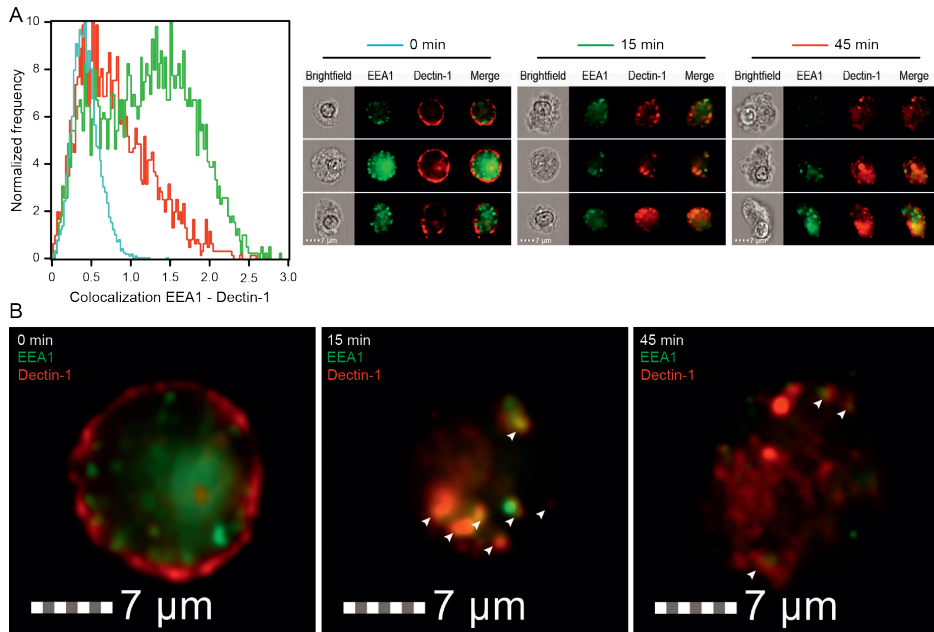
Chapter 2

Figure S3. Analysis of co-localization by imaging flow cytometry. *Bright Detail Similarity R3* is a feature designed to compare the small bright image detail of two images (pixel by pixel). Mathematically, *Bright Detail Similarity R3* is defined as the log transformed Pearson's correlation coefficient of the localized bright spots with a radius of 3 pixels or less within the masked area in the two input images. In practice, values higher than 3 are hardly ever obtained. To illustrate the range of values that can be obtained using this feature and their biological significance, the example of dectin-1 and EEA1 co-localization in monocyte-derived dendritic cells is provided. (**A**) Monocyte-derived dendritic cells were incubated with an anti-dectin-1 antibody (AF647-labeled) at 4 ºC for 30 min, washed, and chased for 0, 15, and 45 min at 37 ºC. Cells were then washed in ice-cold PBS, fixed in 4 % paraformaldehyde, and further stained as described in the *Materials and Methods* section using the anti-EEA antibody (FITC-labeled). Cells were acquired by imaging flow cytometry as described in the *Materials and Methods* section and analyzed for EEA1 and dectin-1 co-localization using the feature *Bright Detail Similarity R3* applied to the EEA1 and the dectin-1 channels. Results clearly indicate a low co-localization at 0 min (approx. 0.5 ± 0.1), which increases dramatically after 15 min (approx. 1.2 ± 0.4), to then moderately decrease at time-point 45 min (approx. 0.8 ± 0.2). Randomly selected images from each of the different time-points demonstrate the absence of co-localization at start (with dectin-1 still clearly present at the cell membrane, while EEA1 shows its typical intracellular spotted distribution), a dramatic increase in fluorescence overlap after 15 min, which decreases at the last time-point. (**B**) High resolution images were selected to depict dectin-1[+] endosomes in the merged images (white arrows). The number of endosomes is clearly superior at 15 min, correlating with the values obtained using the *Bright Detail Similarity R3* feature. 3-color co-localization can be interpreted in a similar way and is calculated using the *Bright Detail Co-localization 3* feature. Its typical values differ dramatically from 2-color co-localization and have a much lower range, hardly ever higher than 0.5.
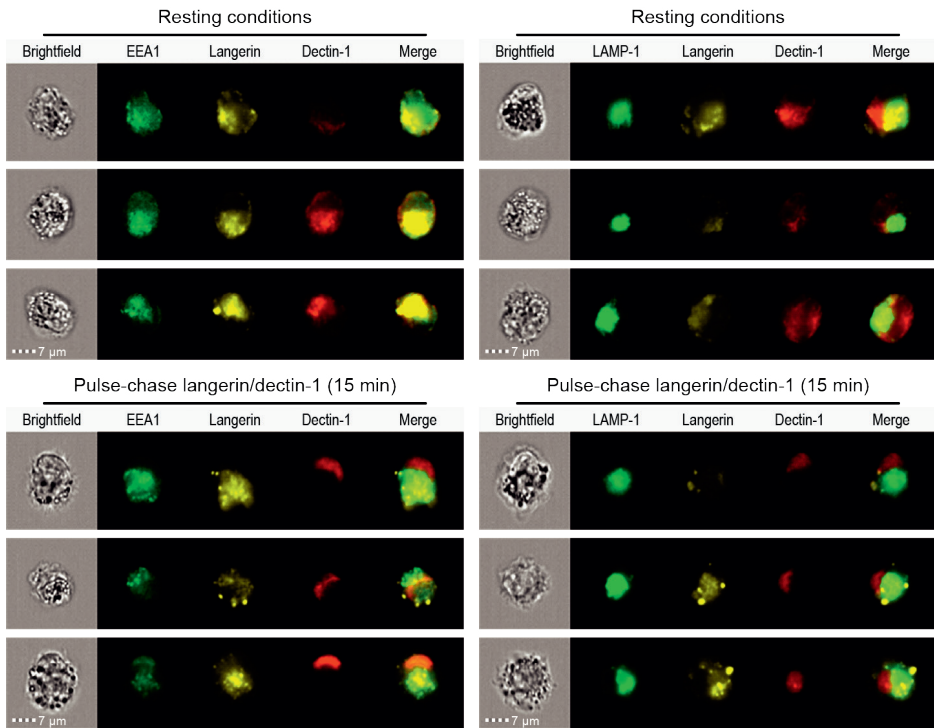
Figure S4. Representative images depicting 3-color co-localization Images were randomly selected from the experiment as described in **Figure 5F**.
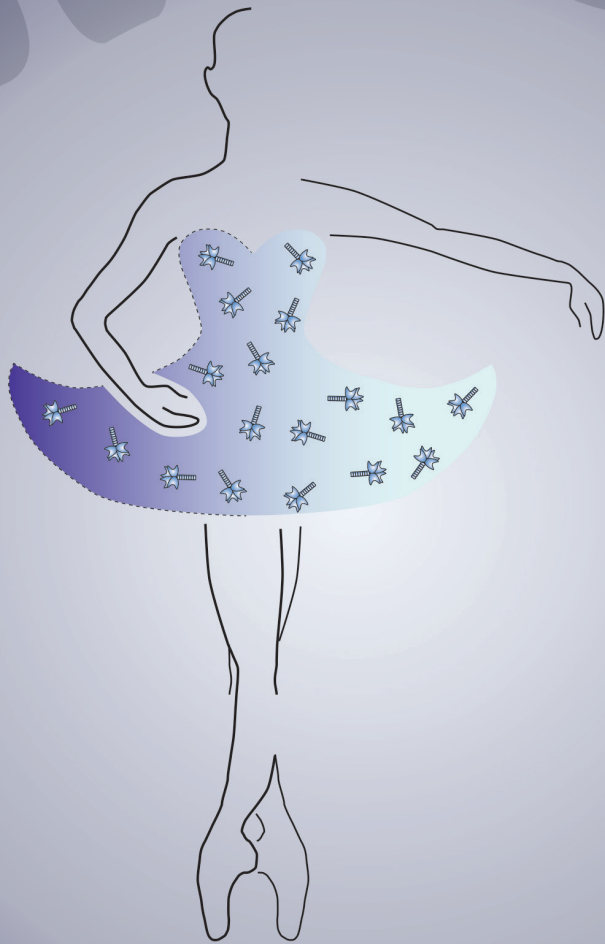
CHAPTER 3

TLR4 TRIGGERING PROMOTES CYTOSOLIC ROUTING OF DC-SIGN-TARGETED ANTIGENS FOR PRESENTATION ON MHC CLASS I

Sophie K. Horrevorts, Sanne Duinkerken, Karien Bloem, Pablo Secades, Hakan Kalay, René J. Musters, Sandra J. van Vliet, Juan J. García-Vallejo and Yvette van Kooyk

Abstract

DC-SIGN is an antigen uptake receptor expressed on dendritic cells (DCs) with specificity for glycans present on a broad variety of pathogens and is capable of directing its cargo to MHC-I and MHC-II pathways for the induction of CD8^{+} and CD4^{+} T cell responses, respectively. Therefore, DC-SIGN is a very promising target for the delivery of antigen for anti-cancer vaccination. Although the endocytic route leading to MHC-II presentation is characterized to a large extent, the mechanisms controlling DC-SIGN targeted cross-presentation of exogenous peptides on MHC-I, are not completely resolved yet. In this paper, we used imaging flow cytometry and antigen specific CD8^{+} T cells to investigate the intracellular fate of DC-SIGN and its cargo in human dendritic cells**.** Our data demonstrates that immature DCs and Toll-like receptor (TLR4) stimulated DCs had similar internalization capacity and were both able to cross-present antigen targeted via DC-SIGN. Interestingly, simultaneous triggering of TLR4 and DC-SIGN in DCs resulted in the translocation of cargo to the cytosol, leading to proteasome-dependent processing and increased CD8^{+} T cell activation. Understanding the dynamics of DC-SIGN-mediated uptake and processing is essential for the design of optimal DC-SIGN-targeting vaccination strategies aimed at enhancing CD8^{+} T cell responses.

Keywords: Dendritic cells, DC-SIGN, cross-presentation, imaging flow cytometry, TLR, MHCI, T cell, proteasome

Introduction

DCs are antigen-presenting cells (APCs) that reside in all tissues and use germ-line encoded receptors to sample the tissue environment for pathogens. Upon pathogen recognition, DCs migrate to secondary lymphoid tissues, while they mature and process the internalized antigen, to initiate antigen-specific T cells leading to humoral and/or cellular immune responses. Amongst the different receptors used by DCs to detect pathogens are C-type lectin receptors (CLRs), a large family of receptors that recognize carbohydrates in a Ca^{2+}-dependent manner. Whereas some pattern-recognition receptors, such as TLRs, are specialized in activating intracellular signaling cascades to initiate DC maturation, CLRs primarily mediate pathogen endocytosis via internalization motifs present in their cytoplasmic domains [1, 2]. This mechanism allows the efficient processing of pathogens for loading on MHC class II and I molecules and presentation to $CD4^+$ and $CD8^+$ T cells, respectively. These capacities of CLRs make them potent targets for vaccine development, especially for the induction of cellular responses for cancer treatment. The first studies on the targeting of CLRs have been done using DEC205-specific antibodies (Abs). These studies showed that targeting antigens to DCs resulted in prolonged and increased T cell responses when administered with an adjuvant. Also the amount of antigen needed for the induction of this response *in vivo* was considerably lower than when free antigen was used [3]. The CLR DC immunoreceptor (DCIR), containing an immunoreceptor tyrosine-based inhibitory motif (ITIM) and present on a variety of blood and skin DC subsets, also mediated increased $CD8^+$ T cells responses. This effect was further enhanced by the addition of a TLR 7/8 agonist [4]. DC-SIGN is a type II membrane CLR discovered as a cell-adhesion receptor that supports primary immune responses [5] and enhances HIV infection of $CD4^+$ T cells [6]. DC-SIGN is expressed on monocyte-derived DCs (moDCs) in peripheral tissue, $CD14^+$ dermal DCs in the dermal layers of the skin [7] and mature DCs in lymphoid tissues, however DC-SIGN expression is lacking on follicular DCs and $CD1a^+$ Langerhans cells [8]. The carbohydrate recognition domain of DC-SIGN contains a Ca^{2+}-coordination site and has a dual specificity for high-mannose and Lewis-type carbohydrate structures (glycans), which gives the receptor the ability to recognize a broad variety of ligands [9], both on pathogens and self-glycoproteins [10]. Lectin-glycan interactions have classically been considered to be of low affinity [11]. As DC-SIGN is present in nano-clusters on the cell surface [12], the concept of avidity is of importance in the design of DC-SIGN-targeting compounds for *in vivo* vaccination strategies. We have explored the possibility of using DC-SIGN-targeting glycoconjugates for triggering of T cell responses [13-15] and demonstrated that

DC-SIGN not only induces potent CD4^{+} T cell responses by targeting antigen to the endo-lysosomal pathway [16], but also triggers CD8^{+} T cell responses that can be boosted by supplementing a TLR4 stimulus. Unfortunately, the mechanism by which the intracellular routing initiated by DC-SIGN results in MHC-I presentation has not been fully identified. Understanding this mechanism will help in designing DC-SIGN-targeting vaccination strategies for the induction of anti-tumor immunity.

DCs are the most potent APC subset capable of priming naïve CD8^{+} T cells with exogenous antigen, for the induction of immunity against antigens derived from tumors or pathogens that do not infect DCs [17, 18]. Although processing and presentation of endogenous proteins in MHC-II is quite well characterized, the mechanisms by which exogenous antigens are processed and loaded in MHC-I for presentation to CD8^{+} T cells (cross-presentation) are not fully understood. Cross-presentation efficiency and intracellular routing can differ depending on the mode of uptake, the antigen and maturation status of the DC [19]. To date two main routes of antigen cross-presentation have been described, namely the cytosolic and vacuolar pathway. In the vacuolar pathway the exogenous antigens are processed by proteases and reloaded on MHC-I molecules without leaving the endosome. Cross-presentation via the vacuolar pathway has shown to be independent of TAP and degradation by the proteasome. In contrast, in the cytosolic pathway the exogenous acquired antigens translocate to the cytosol and are processed by the proteasome, before they are loaded on MHC-I molecules. It remains elusive if loading of MHC-I is done by the endogenous MHC-I loading mechanism in the ER or by the recruitment of these MHC-I peptide loading complexes to phagosomes and endosomes. [18,19].

Here we used imaging flow cytometry to track DC-SIGN and its ligand in DCs and their co-localization with the different compartments involved in antigen processing and presentation. To further unravel the intracellular fate of the DC-SIGN ligand we treated moDCs with different inhibitors of antigen processing. Our results demonstrate that DC-SIGN directs its cargo to early endosomal compartments, where the receptor-cargo complex partly dissociates. Since maturation status of the DCs can influence CD4^{+} and CD8^{+} T cell priming by means of co-stimulation and cytokine secretion, TLR agonists are often used as adjuvant to induce proper T cell responses. However, TLR stimulation can also influence antigen routing within the DCs, thereby changing the cross-presentation capacity [32]. We observed that the cross-presentation capacity of DC-SIGN greatly depends on concomitant TLR4

triggering, which induces translocation of the ligand from the endosomes to the cytosol, where it can be efficiently routed for loading on MHC-I and subsequent CD8^{+} T cell presentation.

Materials and methods

Chemicals and Abs

The following reagents were used: E. coli lipopolysaccharide (LPS) (Sigma-Aldrich, MO), monophosphoryl lipid A (MPLA) from Salmonella enterica (Invivogen), Paraformaldehyde (formaldehyde) aqueous solution (Electron Microscopy Sciences), Saponin (Sigma Aldrich), BSA (Roche). Abs used include: CD83-PE (Beckman coulter), CD80-PE (clone L307.4, BD biosciences), CD86-PE (clone 2331, BD biosciences), EEA1-FITC (clone 14/EEA1, BD biosciences), HLA-DM-PE (clone MaP.DM1, BD biosciences), LAMP-FITC (clone H4A3, BD biosciences), polyclonal rabbit-α-rab 11 (Invitrogen), HLA-A2-PE (BD, biosciences) CD107a-AF488 (Biolegend), CD107b-AF488 (Biolegend) Pacific Orange-labeled goat-α-rabbit IgG (Invitrogen), AF594-labeled goat-α-mouse IgG2a (Invitrogen), AF488-labeled goat-α-mouse IgG2b (Invitrogen), biotin-labeled horse-α-mouse IgG (Vector Labs). CSRD [8], the polyclonal Ab against DC-SIGN, and AZN-D1 [5], a murine monoclonal IgG1 Ab against the carbohydrate-recognition domain of DC-SIGN, were from our own stocks. DC-28 [20], the monoclonal IgG2a Ab against the stalk region of DC-SIGN was a kind gift of R. Doms (University of Pennsylvania). AZN-D1 was labeled with AF405 (Invitrogen) according to manufacturer's instructions. AZN-D1 coated fluorescent beads were made as previously described [21]. Gp100 with a C-terminal cysteine was conjugated to AZN-D1 via thiol mediated conjugation using the bifunctional linker SMCC (succinimidyl 4-(N-maleimidomethyl)cyclohexane-1-carboxylate, Thermofisher Scientific, Breda). Briefly, 5 mg AZN-D1 was activated with 8 equivalents of SMCC in 50 mM Phosphate buffer pH 8.3 containing 10 mM EDTA and 100 mM NaCl. After desalting the activated AZN-D1 over Sephadex-25 desalting columns (GE Healthcare Life Sciences, Breda), 12 equivalents of gp100 is added and vortexed thoroughly. The reaction is incubated for 1 hour at 37ºC. Final product is purified over Superdex 75 column (10x300, GE Healthcare Life Sciences, Breda).

Cells

Monocytes were obtained from buffy coats of healthy donors, with informed consent (Sanquin, Amsterdam, reference: S03.0023-XT). Monocytes were isolated through a

sequential Ficoll/Percoll gradient centrifugation (purity, >85%) and cultured in RPMI 1640 (Invitrogen) supplemented with 10% FCS (BioWhittaker), 1000 U/ml penicillin (Lonza), 1 U/ml streptomycin (Lonza), and 2 mM glutamine (Lonza) in the presence of IL-4 (262.5 U/ml; Biosource) and GM-CSF (112.5 U/ml; Biosource) for 4-7 days [22]. Monocyte-derived DCs (moDCs) differentiation and maturation was monitored by FACS analysis (Calibur, Fortessa BD biosciences) of DC-SIGN, CD83, CD80 and CD86. Stable CHO/DC-SIGN transfectants [23] were maintained in RPMI 1640 medium containing 10% FCS, 1000 U/ml penicillin, 1000 U/ml streptomycin, 2 mM glutamine, and 1 mg/ml geneticin (Invitrogen).

Pulse-chase experiments

Approximately 10^6 DCs were incubated for 20 min in 100 µl of ice-cold culture medium. AF405-labeled AZN-D1 10 µg/ml was added and incubated for 30 min on ice. Cells were washed once with ice-cold medium and then transferred to 37ºC for indicated time points or kept on ice. At indicated time points, cells were washed with ice-cold PBS, fixed in ice-cold 4% PFA in PBS for 20 min and then washed two times with ice-cold PBS. For intracellular stainings, cells were permeabilized in 0.1% saponin in PBS for 30 min at room temperature and then blocked with a solution containing 0.1% saponin, 2% BSA and 1% goat serum in PBS. Primary and secondary antibody stainings were performed in PBS with 0.1% saponin and 2% BSA at room temperature. After staining, cells were kept at 4ºC in PBS supplemented with 0.5% BSA and 0.02% NaN_3 until analysis.

Antigen presentation to human CD8+ T-cells

Immature moDCs were seeded in 96-well plates (Greiner) at $20x10^3$ cells/well and incubated with the different antigens in the presence or absence of the TLR4 ligand MPLA (10µg/ml). After 3 hours cells were washed 3 times with RPMI and co-cultured overnight with a gp100$_{280-288}$ TCR transduced CD8+ HLA-A2 restricted T cell clone [24] (10^5 cells per well, E:T ratio 1:5). IFNγ in the supernatant was measured by sandwich ELISA according to protocol (Biosource). To determine the effect of proteasomal and endosomal inhibitors moDCs ($30x10^3$ cells/well) were incubated with chloroquine (25 µM, Sigma), MG132 (10 µM, Selleck), epoxomicin (0.25 µM, Selleck) or cathepsin S inhibitor (5 µM, calbiochem) at 37°C for 30 minutes prior to the addition of antigen and the TLR4 ligand LPS (100 ng/ml). After 3h the moDCs were washed and co-cultured with a gp100$_{280-288}$ TCR transduced CD8+ HLA-A2 restricted T cell clone ($10x10^4$ cells per well, E:T ratio 3:1) [24]. Degranulation was analyzed by

flow cytometry, via the membrane staining of CD107a and CD107b, as a measure for T cell activation.

CLSM

Stained cells were allowed to adhere to poly-L-lysine-coated glass slides and mounted with anti-bleach reagent vinol. Samples were analyzed using a 63×/1.4 HCX PL APO CS oil objective on a TCS SP2 AOBS confocal microscope (Leica Microsystems GmbH). Images were acquired using LCS 2.61 (Leica Microsystems GmbH) and processed using Adobe Photoshop CS4 or ImageJ.

Live cell imaging

CHO/DC-SIGN cells were cultured on gelatin coated glass slides. AZN-D1 coated beads were added to the cells and followed for different time points. Cells were analyzed by means of a 3I Marianas™ digital imaging microscopy workstation (Zeiss Axiovert 200M inverted microscope Carl Zeiss), equipped with a nanostepper motor (Z-axis increments 10 nm) and a cooled CCD camera (Cooke Sensicam, 1280 × 1024 pixels Cooke Co). Visualization was performed with a 40× air lens. The microscope, camera, and data viewing process were controlled by SlideBook™ software (version 4.0.8.1 Intelligent Imaging Innovations).

Imaging flow cytometry

Cells were acquired on the ImageStreamX (Amnis corp.) imaging flow-cytometer. A minimum of $15x10^3$ cells was acquired per sample at 40x magnification at a flow rate ranging between 50 and 100 cells/s. Analysis was performed using the IDEAS v6.0 software (Amnis corp.). A compensation table was generated using the compensation macro built in the software and applied to the single staining controls. Proper compensation was then verified by visualizing samples in bivariate fluorescence intensity plots (**Figure S1**). A template analysis file to gate for single optimally-focused cells (**Figure S2**) and applied to the experimental samples in order to export this population to a new compensated image file to allow merging all experimental samples within a single file for direct sample analysis. Ag/receptor internalization was investigated using a combination of a mask designed to detect the intracellular space and the internalization feature (**Figure S3**).

Co-localization was calculated using the bright detail similarity R3 feature on a whole cell mask. Co-localization is calculated as the logarithmic transformation of Pearson's

correlation coefficient of the localized bright spots with a radius of 3 pixels or less within the whole cell area in the two input images (bright detail similarity R3). Since the bright spots in the two images are either correlated (in the same spatial location) or uncorrelated (in different spatial locations), the correlation coefficient varies between 0 (uncorrelated) and 1 (perfect correlation). The logarithmic transformation of the correlation coefficient allows the use of a wider range for the co-localization score. In general, cells with a low degree of co-localization or no co-localization at all between two probes show scores below 1.

mRNA isolation, cDNA synthesis, and real-time PCR

After cell lysis, mRNA was isolated by mRNA Capture kit (Roche) and cDNA was synthesized with the Reverse Transcription System kit (Promega) following manufacturer's guidelines. cDNA was diluted 1:2 in nuclease-free water and stored at -20°C until analysis. Primers specific for human DC-SIGN (5'-aacagctgagaggccttgga-3', 5'-gggaccatggccaagaca-3'), and GAPDH [36] were designed with Primer Express 2.0 (Applied Biosystems) and synthesized at Invitrogen (Invitrogen). Primer specificity was computer-tested (BLAST, National Center for Biotechnology Information) and confirmed by dissociation curve analysis. Real time PCR reactions were performed using the SYBR Green method in an ABI 7900HT sequence detection system (Applied Biosystems) as previously described [25].

Statistics

Unless otherwise stated, data are presented as the mean ± standard deviation of at least three independent experiments. Statistical analyses were performed using the statistical package SPSS. Statistical significance was set at $p < 0.05$ and it was evaluated by the Mann-Whitney U test.

Results

DC-SIGN is exclusively localized at the cell membrane and is quickly internalized upon receptor ligation

We first tested the steady state localization of DC-SIGN on moDCs using imaging flow cytometry, a technology that allows for the quantification of morphological aspects of images acquired from large populations of cells. The localization of DC-SIGN on fixed moDCs was assessed via staining with the anti-DC-SIGN polyclonal Ab CSRD [8], which does not interfere with the carbohydrate-binding site of DC-SIGN (see **Figure 1A**).
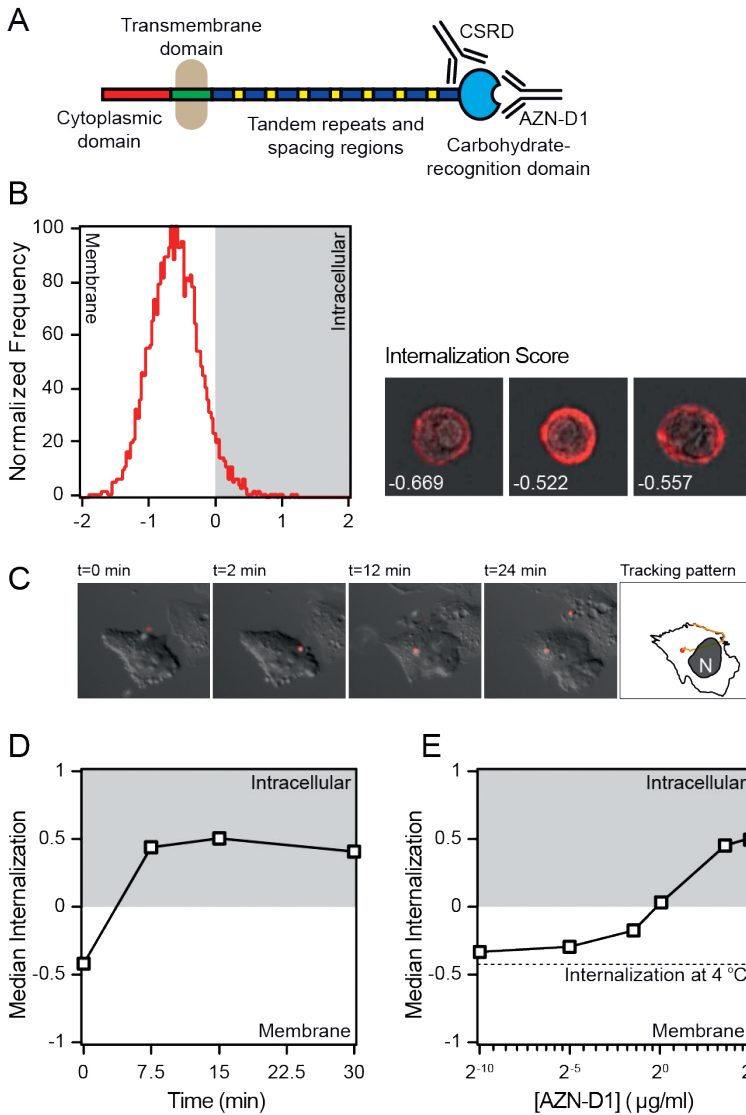
Figure 1. DC-SIGN in immature DCs is exclusively expressed on the extracellular membrane and quickly internalizes upon triggering. (A) Summary of the anti-DC-SIGN Abss used in the present study. (B) Internalization score of resting immature moDCs, after fixation, permeabilization and staining with a polyclonal antibody against DC-SIGN (n > 5000). Next to the histogram, three representative images are included with their respective internalization score. (C) Still frames of a live cell imaging experiment in which DC-SIGN-CHO cells were exposed to AZN-D1-coated fluorescent beads. The right-most frame shows the tracking pattern, representative of 8 experiments. (D) Time-course of the median internalization score of moDCs triggered with AF405-labeled-AZN-D1 (n > 5000). (E) Effect of the AF405-labeled-AZN-D1 concentration on the internalization score after 30 min at 37°C. The dotted line indicates the internalization of the highest antibody concentration after 30 min at 4 °C (n > 5000).
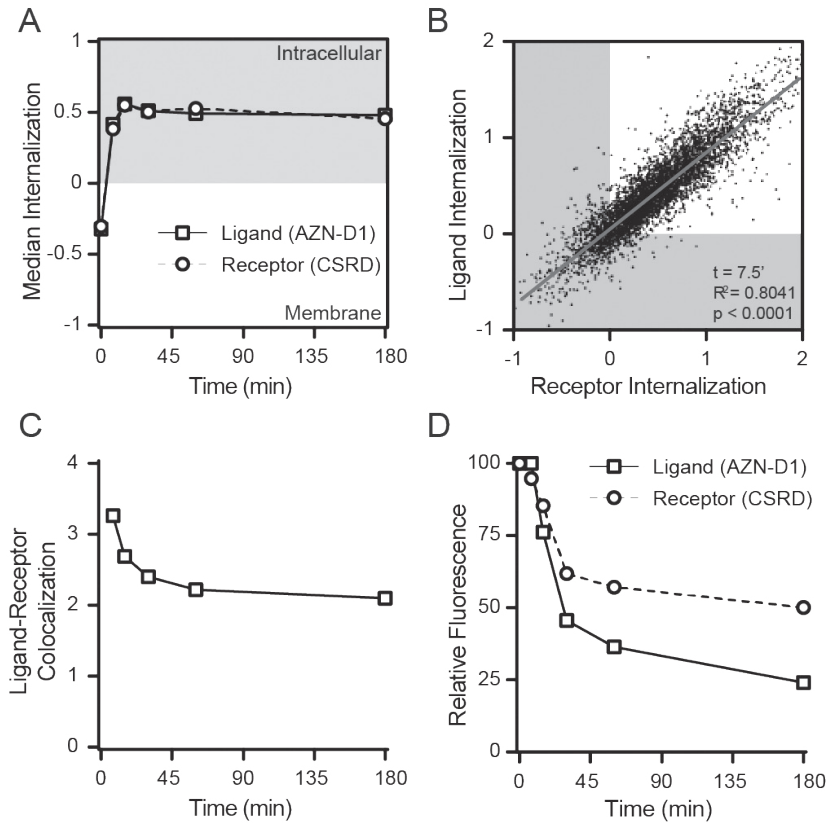
Figure 2. DC-SIGN and its cargo quickly dissociate upon internalization. (A) Time-course of the median internalization score of moDCs triggered with AF405-labeled-AZN-D1 and stained intracellular against DC-SIGN (n > 5000). (B) Scatter plot of the internalization scores of both ligand and receptor 7.5 min after triggering with AF405-labeled-AZN-D1 (n > 5000). (C) Time-course of the median co-localization of AF405-labeled-AZN-D1 and DC-SIGN (n > 5000). (D) Time-course of the fluorescence signal intensity of both AF405-labeled-AZN-D1 and DC-SIGN (n > 5000).

An internalization score higher than 0 indicates that the fluorescent signal is mainly localized inside the cell, whereas a negative internalization scores reflects exclusive membrane localization. When the intracellular and membrane localization are equal, the internalization score is set to 0. In the steady state, DC-SIGN in DCs is exclusively expressed on the cell membrane (**Figure 1.B)**, since more than 95 % of the moDCs had a negative internalization score. We confirmed the exclusive membrane localization of DC-SIGN, using the left over cells from the imaging flow cytometry for confocal laser-scanning microscopy (CLSM) imaging (**Figure S4**). To investigate the kinetics of internalization, DC-SIGN was stably transfected in CHO cells, exposed to AZN-D1-coated

fluorescent beads and followed by live cell widefield epifluorescence imaging. AZN-D1 is a monoclonal Ab against the carbohydrate-binding site of DC-SIGN and is known to trigger receptor internalization (see **Figure 1A**) [16]. The still frames in **Figure 1C**, show how a bead adheres to the surface of the cell within seconds and is quickly internalized, approximately two minutes after receptor ligation.

Because the mechanisms of internalization of particulate and soluble antigen may vary, we also investigated the internalization of AF405-labeled AZN-D1. First moDCs were incubated in the presence of AF405-labeled AZN-D1 for 30 min at 4°C. Then the cells were transferred to 37°C for the indicated time points, washed, fixed and analyzed by imaging flow cytometry. The maximum level of AZN-D1 internalization was already achieved at 7.5 min (**Figure 1D**), indicating that DC-SIGN internalization is a fast process. To investigate whether receptor internalization was dependent on the amount of antigen available, we repeated the pulse-chase experiment with a titration of AF405-labeled AZN-D1 and then fixed, permeabilized and stained the receptor with CSRD [8]. At 1 µg/ml the amount of internalized receptor equaled the amount of receptor on the surface (internalization score 0) and total internalization was achieved using 5 µg/ml of ligand (**Figure 1E**).

Subsequently, we tracked both ligand and receptor in a time-course pulse-chase experiment using the AF405-labeled AZN-D1 Ab to model the ligand and staining with CSRD after fixation and permeabilization to track the receptor. Upon DC-SIGN triggering, both ligand and receptor were quickly internalized and DC-SIGN did not return to the membrane after internalization (**Figure 2A**). At an early time-point (7.5 min), the internalization of receptor and ligand almost perfectly correlated, implying an interdependence of both processes (**Figure 2B**). When the co-localization score of the ligand and the receptor was assessed, we observed that the co-localization score was maximal at baseline (t=0 min) and decreased very quickly once both ligand and receptor were internalized (**Figure 2C**), indicating that ligand and receptor partly dissociate. We also assessed the amount of ligand and receptor at the different time points during the experiment. The signal for the ligand decayed by almost 80% during the experiment (**Figure 2D**). By blocking vesicular degradation with chloroquine we were able to significantly reduce ligand decay after 30 min (**Figure S5**), indicating that the ligand gets (partly) processed in the endosomes.

We stained for the receptor after fixation and permeabilization of the cells, allowing us to detect the total amount of intracellular and membrane associated DC-SIGN.

Chapter 3

We observed a reduction in receptor signal to approximately 50-60 % of the starting amount (**Figure 2D**). The loss of signal indicates that DC-SIGN gets degraded and does not recycle to the membrane. This is supported by previous work of Tacken et al. [26] showing that in the presence of the protein synthesis inhibitor cycloheximide barely any newly synthesized DC-SIGN molecules re-emerged on the cell surface within 3h following DC-SIGN mediated internalization. Even when DC-SIGN was targeted for a prolonged period of time (up to 2 days), the surface expression of DC-SIGN was significantly decreased. Taken into account that the recycling of receptors is a fast process that usually takes places within minutes after receptor internalization our results suggest that DC-SIGN is slowly degraded and not recycled, while the ligand of DC-SIGN quickly gets processed after internalization.

DC-SIGN directs its cargo through early endosomal compartments before dissociation

To investigate the fate of both ligand and receptor, we measured the co-localization scores of both ligand (AZN-D1) and receptor (CSRD) (see **Figure 1A**) with Abs commonly used to track endocytic compartments. Until approximately 30 min both ligand and receptor co-localized evenly with the early endosomal marker EEA1 (both scores around 1.05). Hereafter the co-localization for the receptor dramatically decreased, whereas co-localization with the ligand slowly decreased, suggesting that ligand and receptor partly dissociate in early endosomes (**Figure 3A**). This is further supported by the LAMP1 (lysosomes) co-localization scores, which show that the ligand (but not DC-SIGN receptor) reached the lysosomes before 30 min, while peaking at around 45 min (**Figure 3B**).
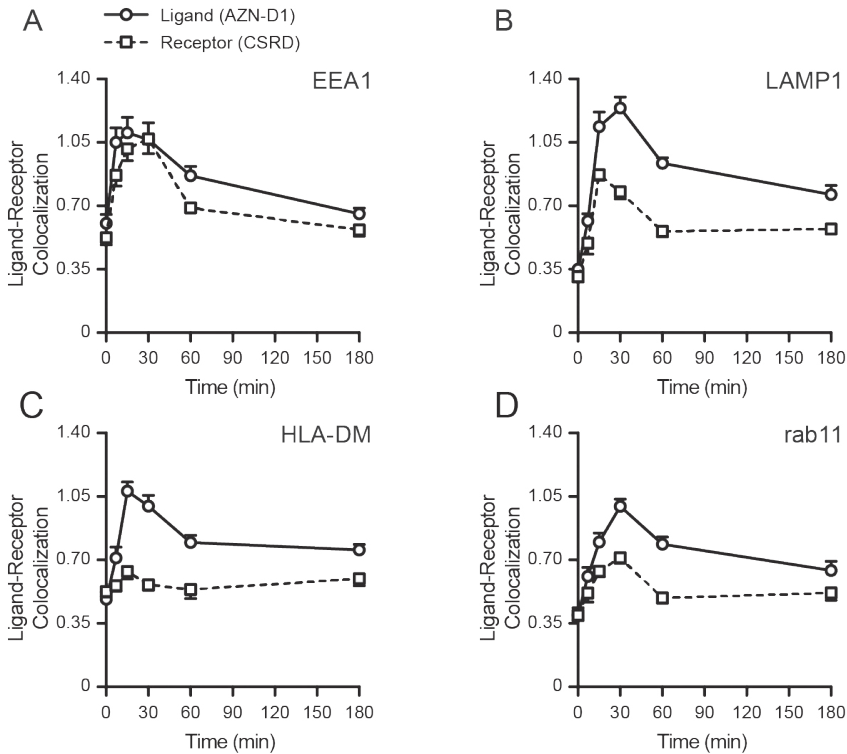
Figure 3. Intracellular routing of DC-SIGN and its ligand. MoDCs were pulsed with AF405-la-beled-AZN-D1 for 30 min on ice and transferred to 37°C. Cells were fixed at indicated time point and stained with the CSRD Ab to localize DC-SIGN. Time-course of the co-localization scores of AF405-labeled-AZN-D1 (mean ± SEM) and CSRD (DC-SIGN) with (A) EEA1, (B) LAMP1, (C) HLA-DM, and (D) Rab11 (n > 5000).

In accordance, the MHC-II compartment co-localized with the ligand (at 30 min score 1.05), but not with the receptor (30-180 min score 0.6, **Figure 3C**). Interestingly, rab11 shows a moderate co-localization with the ligand (30 min score 1.05), but a poor co-localization with the receptor (score 0.6), suggesting that routing to this compartment is receptor-independent and may follow upon a stay at the early endosomes or the lysosomes (**Figure 3D**). The decay observed for the receptor in **Figure 2D** might be explained by quick lysosomal degradation, but since there is very little co-localization of the receptor with the lysosomal marker LAMP1, degradation could also already occur in the early endosomes.Our data indicate an internalization model in which DC-SIGN mediates the internalization of its antigen ligand, which ends up in early endosomes where the receptor-ligand complex dissociates. The released cargo continues its way to lysosomes by the maturation of early endosomes, while a

fraction of receptor-ligand complexes possibly translocate to the cytosol to initiate MHC-I loading.

Simultaneous DC-SIGN and TLR4 triggering affects DC-SIGN internalization

TLR4 triggering is commonly used to address the effects of DC activation and maturation, a process that typically occurs upon pathogen recognition and that is necessary for proper antigen processing, presentation and CD8^{+} T cell priming [27]. Additionally, DC-SIGN triggering has been described to elicit a signaling cascade that modulates the TLR4-induced signaling [28, 29]. We therefore investigated the consequences of DC maturation on DC-SIGN internalization. First, we investigated the effect of TLR4-mediated moDC activation on DC-SIGN expression levels. LPS treatment of moDCs resulted in a dramatic decrease in both DC-SIGN protein (10-fold) and mRNA (100-fold) after 18h (**Figure 4A**). The decrease in DC-SIGN expression was not accompanied by an internalization of the receptor, as it was still located on the cell membrane (**Figure 4B**), indicating that DC-SIGN was lost by either shedding into the supernatant or by incorporation into exosomes, possibilities that have been previously described for DC-SIGN [30,31]. Still, simultaneous triggering of DC-SIGN and TLR4 (LPS at t=0) or triggering of DC-SIGN on mature moDCs (overnight LPS treatment) had no consequences for the overall internalization rate, which proceeded as efficiently on mature moDCs as on immature moDCs (**Figure 4C**).

Nevertheless, the fate of AZN-D1 ligand differed greatly between the simultaneous triggering of DC-SIGN and TLR4 (LPS at t=0) and the triggering of DC-SIGN on matured moDCs (o/n LPS) (**Figure 4D**). While ligand degradation was similar in immature moDCs and moDCs that received LPS at t=0, triggering of DC-SIGN on mature moDCs showed decreased ligand degradation. MoDCs less than 20% AZN-D1 degradation occurred in mature moDCs even after an extended incubation time (6h), compared to 70-80% ligand degradation in immature moDCs and moDCs receiving LPS at t=0 (**Figure 4D**). This was consistent with a reduced trafficking of AZN-D1 to the lysosomes upon overnight (o/n) treatment with LPS (**Figure 4E**).
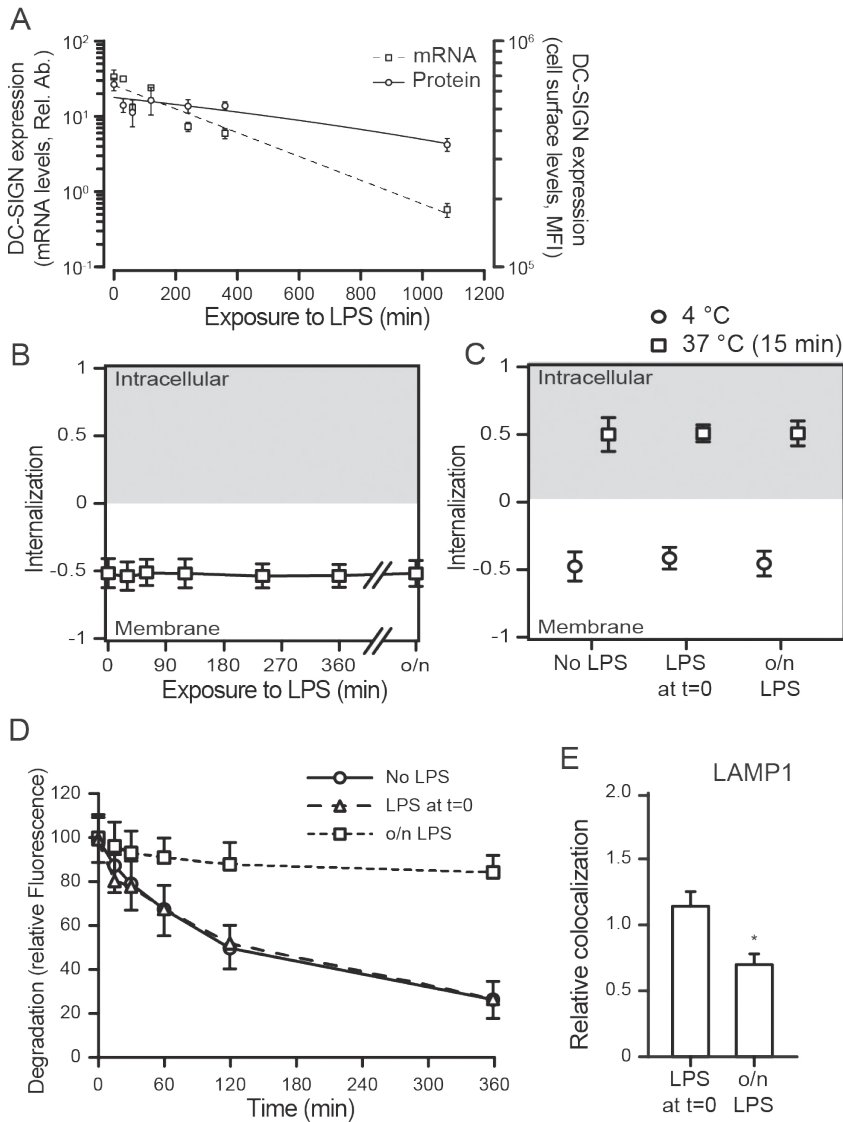
Figure 4. TLR4 triggering affects the routing of DC-SIGN and its ligand. (A) Time-course of the expression levels of DC-SIGN at both the mRNA and protein level after TLR4 (LPS) stimulation of moDCs. (B) Time-course of the internalization score of DC-SIGN after treatment with a TLR4 ligand (LPS). (C) Internalization score of AF405-labeled-AZN-D1 after a 60 min incubation at 4 °C or a 15 min incubation at 37 °C. (D) Time-course of the fluorescence signal intensity of AF405-labeled-AZN-D1. (E) Co-localization scores (relative to No LPS) of AF405-labeled-AZN-D1 with LAMP1, 60 min after triggering. Mean ± SEM (n > 5000). *, P < 0.01 compared to No LPS.

Simultaneous triggering of DC-SIGN and TLR4 affects the cross-presentation route in dendritic cells

To evaluate the effect of TLR4 triggering on cross-presentation after DC-SIGN targeting we compared the capacity of antigen pulsed immature moDCs and TLR4-stimulated moDCs (t=0), to activate CD8^{+} T cells. We excluded the DCs that were incubated o/n with a TLR4 stimulus, because of their greatly reduced DC-SIGN receptor surface expression. Therefore, pre-treatment with a TLR4 stimulus before antigen administration is not a favorable vaccine strategy when targeting DC-SIGN. As an antigen we used a gp100 synthetic long peptide (29-mer, VTHTYLEPGPVTANRQLYPEWTEAQRLDC) containing both the $gp100_{280-288}$ CD8^{+} and $gp100_{45-59}$ CD4^{+} T cell epitope conjugated to the DC-SIGN-targeting monoclonal antibody AZN-D1. A 3h antigen pulse was followed by co-culturing of moDCs o/n with $gp100_{280-288}$ specific CD8^{+} T cells, after which the released IFNγ was determined as a measure for T cell activation (**Figure 5A**). moDCs that received TLR4 stimulus at t=0 outperformed the immature moDCs in their capacity to activate CD8^{+} T cells. Next we determined the specificity of our DC-SIGN targeting Ab by pulsing immature DCs for 3h with gp100/AZN-D1 conjugates, gp100/mIgG1 isotype control conjugates, functioning as a negative control, the 29-mer gp100 synthetic long peptide (SLP) and the 9-mer minimal epitope that can directly bind to MHC-I. After a 3h antigen pulse, $gp100_{280-288}$ specific CD8^{+} T cells were added to the moDCs for 45 min and stained for degranulation markers (CD107a and CD107b). moDCs pulsed with the gp100/AZN-D1 were able to activate antigen specific CD8^{+} T cells as measured by degranulation levels. In contrast, the gp100/mIgG1 conjugate induced no CD8^{+} T cell activation. The SLP as a single non-targeted agent induced degranulation of more than 40% of the CD8^{+} T cells, confirming the robustness of this assay (**Figure 5B, Figure S6**). Therefore, the lower response induced by gp100/AZN-D1 is due to the limited amount of SLPs that can be conjugated to the antibody, rather than the sensitivity of the experiment.

The enhanced cross-presentation after TLR stimulation has been described to result from the induction of a different antigen-processing route [32-36]. To investigate if changes in DC-SIGN ligand routing after TLR4 stimulation is responsible for the observed increase in cross-presentation, we investigated the antigen-processing route by looking at CD8^{+} T cell activation after DC antigen loading in the presence of relevant inhibitors. For this experiment we incubated immature and LPS-stimulated moDCs with chloroquine for blocking of endosomal acidification, Cathepsin S inhibitors to block endosomal antigen-processing or MG132 and epoxomicin to inhibit

proteasomal degradation of antigens. Treatment with the inhibitors mentioned above showed only minor differences in viability (**Figure S7**). Interestingly, the routing of antigen in immature and LPS-treated moDCs differed substantially (**Figure 5C-D**). While the activation of CD8+ T cells by immature moDCs was not affected by the proteasome inhibitors MG132 and epoxomicin, LPS stimulated moDCs showed decreased CD8+ T cell activation in the presence of these inhibitors.
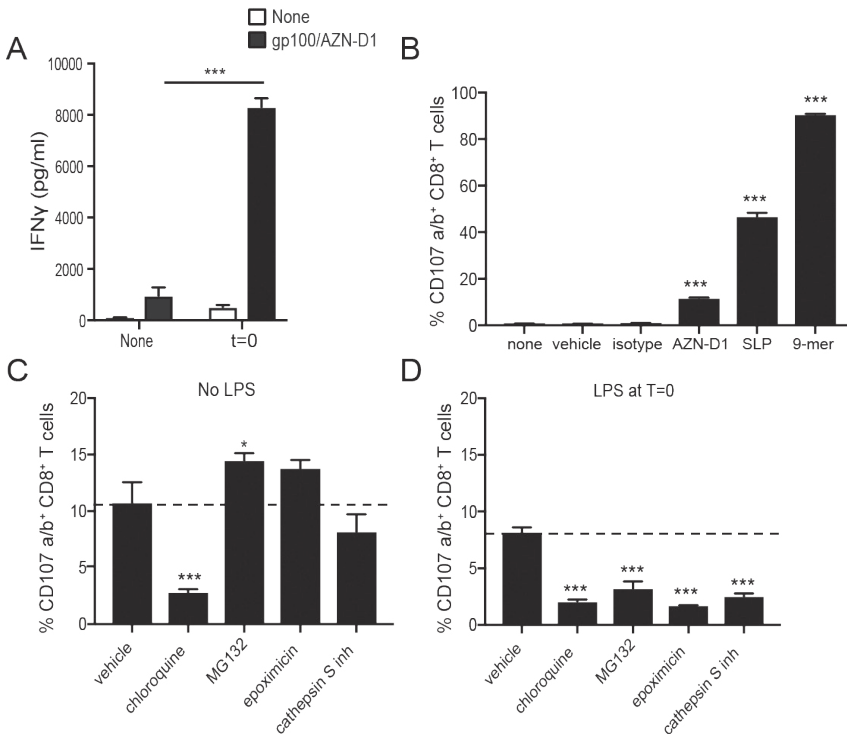

Figure 5. TLR4 triggering facilitates antigen translocation to the cytosol. (A) Immature moDCs and moDCs that received a TLR4 stimulus at t=0 (MPLA), were pulsed with gp100/AZN-D1 for 3h and subsequently co-cultured o/n with gp100$_{280-288}$ CD8+ T cells. IFN γ production was analyzed by ELISA as a measure for T cell activation. (B) Immature moDCs were incubated with 0.1% DMSO (vehicle), gp100/AZN-D1 (10 µg/ml), gp100 synthetic long peptide (SLP) (10 µM) and the gp100$_{280-288}$ 9-mer minimal epitope (1 µg/ml) for 3h. Thereafter, moDCs were co-cultured with gp100$_{280-288}$ CD8+ T for 45 min and CD107a/b expression on the cell surface was analyzed as a measure for CD8+ T cell activation. Groups are significantly different compared to none, vehicle and isotype. (C) Immature moDCs and moDCs that received a TLR4 stimulus (LPS) at t=0 (D) were incubated 30 min prior and during the 3h antigen (gp100/AZN-D1) pulse with 0.1% DMSO (vehicle), chloroquine (25 µM), MG132 (10 µM), Epoxomicin (0.25 µM) and Cathepsin S inhibitor (5 µM). Groups are significantly different compared to AZN-D1. Data represented in mean ± SD, one-way ANOVA was performed , experiments are representative of a N=2 for graph A and B and a N=3 for graph C and D (* = P < 0.05, ** = P< 0.01, *** = P< 0.001).

Also inhibition of the protease Cathepsin S reduced cross-presentation by LPS stimulated moDCs, while it did not affect cross-presentation DC-SIGN targeted antigens in immature moDCs. This indicates that DC-SIGN-mediated uptake and proteolysis of antigen in the endosomes/lysosomes of immature moDCs is not dependent on the protease Cathepsin S. In contrast, chloroquine, a drug that inhibits acidification of endosomes, significantly reduced CD8^{+} T activation by both immature and LPS stimulated moDCs. When we checked for HLA-A2 molecules on the cell surface after the inhibitor treatment we observed a decrease of HLA-A2 expression on chloroquine treated moDCs, while the other inhibitors did not affect HLA-A2 expression (**Figure S9**). However, the external loading of membrane expressed MHC-I molecules with the 9-mer minimal epitope in the presence of inhibitors did not result in a decrease in CD8^{+} T cell activation (**Figure S8**). Therefore it is difficult to say if the observed decrease in CD8^{+} T cell activation after chloroquine treatment is related to the lower expression of HLA-A2.

Surprisingly, we did not observe any enhanced cross-presentation of TLR4-stimulated moDCs within the time frame of the degranulation assay (**Figure S10**), which could possibly be explained by the short time window of antigen processing after the pulse. These results were further validated by measuring IFN-ɣ secretion after an o/n culture with the gp100 specific CD8^{+} T cells (**Figure S11**), confirming the enhanced CD8^{+} T cell activation by combining DC-SIGN targeting with a TLR4 stimulus. We observed a smaller inhibitory effect of the Cathepsin S inhibitor on CD8^{+} T cell activation. This can be explained by the different time points and assays used to analyze the amount of CD8^{+} T cell activation. The secretion of IFN- ɣ was measured in the supernatant after a co-culture of 16h. While the percentage of degranulation was analyzed after a 45 min co-culture. In both experiments the cells were treated with the inhibitors during the 3h antigen pulse. Thereafter cells were washed and co-cultured with the CD8^{+} T cells. All the inhibitors are reversible, therefore the effect can decrease overtime explaining the difference in inhibitory capacity of the Cathepsin S inhibitor (**Figure S11**).

Together our results indicate that the combination of DC-SIGN targeting and TLR4 triggering leads to the escape of antigen to the cytosol, where it is further processed via the proteasome for cross-presentation.

Discussion

In this study, we investigated the intracellular routing of the CLR DC-SIGN and its involvement in loading antigens on MHC-I through cross-presentation. While DC-SIGN targeting of antigen leads to cross-presentation by both immature and TLR4-stimulated DCs, we found a major contribution for TLR4 signaling, instigating an alternative intracellular cross-presentation route via the cytosol, which resulted in an increased capacity of moDCs to activate CD8^{+} T cells.

Targeting DC-SIGN with antigen conjugated Abs, glycan conjugated antigens or HIV virus, a natural ligand of DC-SIGN , results in efficient MHC-II and MHC-I loading and CD4^{+} T cell and CD8^{+} T cell activation, respectively [15,16,37,38, 39]. This makes DC-SIGN an attractive candidate for vaccine targeting strategies. Since vaccination strategies also rely on adjuvants inducing DC maturation, such as TLR agonists, understanding the intracellular fate of DC-SIGN and its ligand in both immature and TLR stimulated DCs is vital for vaccine development.

Previous studies have shown that pathogens and AZN-D1, both binding to the carbohydrate recognition domain (CRD), are taken up in a clathrin-dependent manner [40,41], while DC-SIGN targeting via the neck region results in clathrin-independent internalization [42]. Our data demonstrates that upon targeting the CRD with AZN-D1, DC-SIGN on immature moDCs is internalized within minutes and directed to early endosomes. At this stage, parts of the DC-SIGN-ligand complexes begin to dissociate and proceed to late endosomes and lysosomes. Co-localization of the DC-SIGN ligand with the receptor was decreased after 15-30 min, which was followed in parallel with an increase of the antigen in the lysosomes. This indicates that once DC-SIGN ligands are dissociated from the receptor in the early endosomes they are at least partly routed to maturing endosomes. Interestingly, the dissociation between the ligand and receptor occurs at the maturing endosomes, indicating that ligand and receptor follow different intracellular routes. Although DC-SIGN does not return to the membrane, we were not able to clarify its intracellular fate upon release from its ligand. Nevertheless, the clear fluorescence signal decay and previous work showing that prolonged DC-SIGN targeting with AZN-D1 significantly reduced the surface expression for up to 48h [26] suggests that DC-SIGN is targeted for destruction. Since we observed that DC-SIGN poorly co-localizes with the lysosomes, we hypothesize that it is degraded by a different mechanism, which has not yet been identified. Endocytosis via DC-SIGN is regulated by a dileucine (LL) motif in the

cytoplasmic tail of the receptor [16,43] which might function as potential targets for ubiquitination. Different modes of ubiquitination exist that regulate amongst other protein degradation [44]. Polyubiquination of the C-type lectin Mannose receptor (MR) facilitates antigen translocation from the endosomes to the cytosol [45], indicating that this process of receptor ubiquitination is a recognized mechanism, whereby C-type lectin receptors redirect their cargo to the cytosol. Possibly DC-SIGN also uses this mode of action.

Our data shows an important role for the timing of the maturation stimulus when targeting antigens via DC-SIGN for cross-presentation to CD8^{+} T cells. Triggering of TLR4 has been described to lead to an enhanced cross-presentation of soluble antigen until 16h after stimulation, while fully matured DCs (LPS for >24 h) showed a decreased ability to cross-present antigen [32,33]. Apparently, 16h or 24h of LPS stimulation can make a major difference for the ability of DCs to efficiently cross-present antigen. In our experimental setup, moDCs were stimulated with LPS o/n (16h) and therefore should still be in the enhanced cross-presentation phase. In fact, we saw decreased shuttling of the ligand to LAMP1 positive compartments in line with the findings of Alloatti *et al.*, who showed a decreased phago-lysosomal fusion after TLR triggering, resulting in a prolonged retention of the ligand in early endosomes, thereby supporting cross-presentation [33]. While LPS did not affect the uptake capacity of the DC-SIGN receptor, its expression was dramatically decreased on both mRNA and protein level, which would result in an overall decrease in antigen uptake. Based on these data, administration of the adjuvant before providing the antigen via DC-SIGN targeting would not be a favorable vaccination strategy. Multiple studies have described that the enhanced efficiency of cross-presentation after TLR triggering is due to a change in antigen routing and processing, like enhanced translocation to the cytosol and increased activity of the proteasome [33-36]. To investigate if a different route of antigen processing was responsible for the increase in cross-presentation, we blocked different molecules known to be important for MHC-I and MHC-II presentation in immature DCs and DCs that received a TLR4 stimulus at t=0. We observed a striking difference in antigen routing as early as 3h after antigen pulse. Both the immature and TLR4-stimulated moDCs were sensitive to chloroquine, a drug that inhibits endosomal acidification. Unexpectedly, chloroquine had a reducing effect on MHC-I expression, making it difficult to conclude if the observed effect on CD8^{+} T cell activation is due to the inhibition of cross-presentation or to the reduced expression of MHC-I on the cell surface. moDCs that received

a TLR4 trigger at t=0 showed a significant dependence on proteasome activity, a mechanism not observed in immature DCs. Thus, our results suggest that following TLR4 triggering antigens translocate from the endosome to the cytosol, thereby entering the cytosolic pathway of cross-presentation. This route of MHC-I loading also has been described for natural DC-SIGN ligands (HIV-1 virions) [37]. It has been described that TLR triggering can result in antigen translocation from endosomes to the cytosol. Dingjan *et al.* showed that upon LPS triggering the NOX2 complex in phagosomes produces reactive oxygen species (ROS) resulting in lipid peroxidation, thereby inducing membrane damage and the release of antigen from these 'leaky' endosomes [34]. This was a rather quick process, already observed 30 min after LPS stimulation. Also a role for sec61 in the endosomal escape after TLR triggering has been reported [35]. Our results stress the importance of appropriately timing the maturation stimulus when targeting antigens to DC-SIGN, as not only the antigen enters a more efficient route of cross-presentation, also the fate of the DC-SIGN receptor is dependent on maturation status of the DC.

The recycling endosome is characterized, amongst others, by Rab11, which allows direct recycling to the plasma membrane but also to the secretory pathway through the trans-Golgi network [46]. Our data shows that co-localization of the DC-SIGN ligand with Rab11 follows the same pattern as HLA-DM, a molecule associated with the MHC-II loading compartment. Since we cannot observe the return of DC-SIGN ligands to the plasma membrane and the MHC-II compartment originates from the trans-Golgi network, it is likely that Rab11 facilitates a connection between early endosomes and the MHC-II loading compartment without further contribution of lysosomal degradation.

The regulation of the internalization and intracellular routing of DC-SIGN on DCs is an important aspect for the rational design of antibody and glycan-based DC-SIGN-targeting vaccines [47]. Based on this study, the use of DC-SIGN ligands in combination with TLR4 ligands would serve as excellent antigen targeting platforms to enhance the antigen cross-presentation in DC-based anti-tumor vaccination strategies.

Conflict of interest

The authors declare no conflict of interest.

Authors contribution

All the authors were responsible for design of the experiments, data collection was performed by SKH, SD, KB, PS, RM and JJG, all authors participated in the data analysis and interpretation, SKH, SD, KB, SvV, JJGV and YvK drafted the article, SKH, SD, KB, SvV, JJGV and YvK critically revised the article, all authors gave their approval for publication

Funding

Acknowledgements

References

1. van Kooyk Y, Rabinovich GA. Protein-glycan interactions in the control of innate and adaptive immune responses. Nat Immunol. (2008) 9;593–601.

2. Sancho D, Reis E Sousa C. Signaling by myeloid C-type lectin receptors in immunity and homeostasis. Annu Rev Immunol. (2012) 30;491–529.

3. van Dinther D, Stolk DA, van de Ven R, van Kooyk Y, de Gruijl TD, den Haan JMM. Targeting C-type lectin receptors: a high-carbohydrate diet for dendritic cells to improve cancer vaccines. J. of Leukocyte Biology (2017) 102;1017-1034

4. Klechevsky E, Flamar AL, Cao Y, Black JP, Liu M, O'Bar A, Agouna-Deciat O, et al. Cross-priming CD8^{+} T cells by targeting antigenst o human dendritic cells through DCIR. Blood (2010) 116; 1685-1697

5. Geijtenbeek TB, Torensma R, van Vliet SJ, van Duijnhoven GC, Adema GJ, van Kooyk Y, Figdor CG. Identification of DC-SIGN, a novel dendritic cell-specific ICAM-3 receptor that supports primary immune responses. Cell. (2000) 100;575–585.

6. Geijtenbeek TB, Kwon DS, Torensma R, van Vliet SJ, van Duijnhoven GC, Middel J, Cornelissen IL, et al. DC-SIGN, a dendritic cell-specific HIV-1-binding protein that enhances trans-infection of T cells. Cell. (2000) 100;587–597.

7. Fehres CM , van Beelen AJ, Bruijns SCM, Ambrosini A, Kalay H, van Bloois L, Unger WWJ, et al. In situ Delivery of Antigen to DC-SIGN [+] CD14 [+] Dermal Dendritic Cells Results in Enhanced CD8 [+] T-Cell Responses. J. Invest. Dermatol, (2015) 135; 2228–2236.

8. Engering A, van Vliet SJ, Hebeda K, Jackson DG, Prevo R, Singh SK, Geijtenbeek TBH, et al. Dynamic populations of dendritic cell-specific ICAM-3 grabbing nonintegrin-positive immature dendritic cells and liver/lymph node-specific ICAM-3 grabbing nonintegrin-positive endothelial cells in the outer zones of the paracortex of human lymph nodes. Am J Pathol. (2004) 164;1587–1595.

9. Appelmelk BJ, van Die I, van Vliet SJ, Vandenbroucke-Grauls CMJE, Geijtenbeek TBH, van Kooyk Y. Cutting edge: carbohydrate profiling identifies new pathogens that interact with dendritic cell-specific ICAM-3-grabbing nonintegrin on dendritic cells. J Immunol. (2003) 170; 1635–1639.

10. García-Vallejo JJ, van Kooyk Y. Endogenous ligands for C-type lectin receptors: the true regulators of immune homeostasis. Immunol Rev. (2009) 230;22–37.

11. Dam TK, Gerken TA, Brewer CF. Thermodynamics of multivalent carbohydrate-lectin cross-linking interactions: importance of entropy in the bind and jump mechanism. *Biochemistry*. (2009) 48;3822–3827

12. Cambi, A & Lidke, DS. Nanoscale membrane organization: where biochemistry meets advanced microscopy. *ACS Chem. Biol.* (2012) 7;139–149.

13. Singh SK, Stephani J, Schaefer M, Kalay H, García-Vallejo JJ, Haan den J, Saeland E, et al. Targeting glycan modified OVA to murine DC-SIGN transgenic dendritic cells enhances MHC class I and II presentation. Mol Immunol. (2009) 47;164–174.

14. García-Vallejo JJ, Ambrosini M, Overbeek A, van Riel WE, Bloem K, Unger WWJ, Chiodo F, et al. Multivalent glycopeptide dendrimers for the targeted delivery of antigens to dendritic cells. Mol Immunol. (2012) 53;387–397.

15. Unger WWJ, van Beelen AJ, Bruijns SC, Joshi M, Fehres CM, van Bloois L, Verstege MI, et al. Glycan-modified liposomes boost CD4^{+} and CD8^{+} T-cell responses by targeting DC-SIGN on dendritic cells. J Control Release. (2012) 160;88–95.

16. Engering A, Geijtenbeek T, van Vliet S, Wijers M, van Liempt E, Demaurex N, Lanzavecchia A, et al. The dendritic cell-specific adhesion receptor DC-SIGN internalizes antigen for presentation to T cells. J Immunol. (2002) 168;2118–2126.

17. Haan, B. J. M. M. Den, Lehar, S. M. & Bevan, M. J. CD8 ε but Not CD8 ᾱ Dendritic Cells Cross-prime Cytotoxic T Cells In Vivo. J Exp. Med, (2000) 192;1685–1695.
18. Joffre, OP, Segura, E , Savina, A. & Amigorena S. Cross-presentation by dendritic cells. Nat. Rev. Immunol. (2012) 12;557–569.
19. Grotzke, J. E., Sengupta, D., Lu, Q. & Cresswell, P. The ongoing saga of the mechanism(s) of MHC class I-restricted cross-presentation. Curr. Opin. Immunol. (2017) 46; 89–96.
20. Baribaud F, Pöhlmann S, Sparwasser T, Kimata MT, Choi YK, Haggarty BS, Ahmad N, et al. Functional and antigenic characterization of human, rhesus macaque, pigtailed macaque, and murine DC-SIGN. J Virol. (2001) 75;10281–10289.
21. Geijtenbeek T, van Kooyk Y, van Vliet SJ, Renes MH, Raymakers R, Figdor CG. High frequency of adhesion defects in B-lineage acute lymphoblastic leukemia. Blood (1999) 94;754–764.
22. Sallusto F, Lanzavecchia A. Efficient presentation of soluble antigen by cultured human dendritic cells is maintained by GM-CSF plus IL-4 and downregulated by TNF-α. J Exp Med. (1994) 179;1109–1118.
23. van Vliet SJ, Steeghs L, Bruijns SCM, Vaezirad MM, Snijders Blok C, Arenas Busto JA, Deken M, et al. Variation of Neisseria gonorrhoeae lipooligosaccharide directs dendritic cell-induced T helper responses. PLoS Pathog. (2009) 5;e1000625–e1000625.
24. Schaft N, Willemsen RA, de Vries J et al. Peptide fine specificity of anti-glycoprotein 100 CTL is preserved following transfer of engineered TCR alpha beta genes into primary human T lymphocytes. J. Immunol (2003) 170;2186–94
25. Garcia Vallejo JJ, van Het Hof B, Robben J, van Wijk JAE, van Die I, Joziasse DH, van Dijk W. Approach for defining endogenous reference genes in gene expression experiments. Anal Biochem. (2004) 329;293–299.
26. Tacken PJ, ter Huurne M, Torensma R & Figdor CG. Antibodies and carbohydrate ligands binding to DC-SIGN differentially modulate receptor trafficking. Eur. J. Immunol. (2012) 42;1989-1998
27. Mellman I, Steinman RM. Dendritic cells: specialized and regulated antigen processing machines. Cell. (2001) 106;255–258.
28. Gringhuis SI, Dunnen den J, Litjens M, van het Hof B, van Kooyk Y, Geijtenbeek TBH. C-type lectin DC-SIGN modulates toll-like receptor signaling via Raf-1 kinase-dependent acetylation of transcription factor NF-kappa B. Immunity. (2007) 26;605–616.
29. Gringhuis SI, Dunnen den J, Litjens M, van der Vlist M, Geijtenbeek TBH. Carbohydrate-specific signaling through the DC-SIGN signalosome tailors immunity to Mycobacterium tuberculosis, HIV-1 and Helicobacter pylori. Nat Immunol. (2009) 10;1081–1088.
30. Plazolles N, Humbert JM, Vachot L, Verrier B, Hocke C, Halary F. Pivotal advance: The promotion of soluble DC-SIGN release by inflammatory signals and its enhancement of cytomegalovirus-mediated cis-infection of myeloid dendritic cells. J Leukoc Biol. (2011) 89;329–342.
31. Hao S, Bai O, Li F, Yuan J, Laferte S, Xiang J. Mature dendritic cells pulsed with exosomes stimulate efficient cytotoxic T-lymphocyte responses and antitumour immunity. Immunology. (2007) 120;90–102.
32. Kotsias, F., Magalhaes, J. G. & Amigorena, S. Dendritic cell maturation and cross-presentation: timing matters! Immunological Reviews (2016) 97–108.
33. Alloatti A, Kotsias F, Pauwels AM, Carpier JM, Jouve M, Timmerman E, Pace L. et al. Toll-like Receptor 4 Engagement on Dendritic Cells Restrains Phago-Lysosome Fusion and Promotes Cross-Presentation of Antigens. Immunity (2015) 43;1087–1100
34. Dingjan I, Verboogen DRJ, Paardekooper LM, Rvelo NH, Siitig SP, Visser LJ, Fischer von Mollard, et al. Lipid peroxidation causes endosomal antigen release for cross-presentation. Nat. Publ. Gr. 1–12 (2016) doi:10.1038/srep22064

35. Zehner M, Marschall AL, Bos E, Schloetel JG, Kreer C, Fehrenschild D, Limmer A, The Translocon Protein Sec61 Mediates Antigen Transport from Endosomes in the cytosol for Cross-Presentation to CD8^{+} T Cells. Immunity (2015) 42;850–863

36. Gil-Torregrosa BC, Lennon Duménil AM, Kessler B, Guermonprez P, Ploegh HL, Fruci D, Van Endert P, Amigorena S, Control of cross-presentation during dendritic cell maturation. Eur. J. Immunol (2004) 34;398-407

37. Moris A, Pajot A, Blanchet F, Guivel-Benhassine F, Salcedo M & Schwartz O. Dendritic cells and HIV-specific CD4^{+} T cells: HIV antigen presentation, T cell activation and viral transfer. Blood (2006) 108; 1643-1651

38. Fehres CM, Kalay H, Bruijns SCM, Musaafir SAM, Ambrosini M, van Bloois L, van Vliet SJ, et al. Cross-presentation through Langerin and DC-SIGN targeting requires different formulations of glycan modified antigens. J Control Release (2015) 203;67-76

39. Moris A, Nobile C, Buseyne F, Porrot F, Abastado JP & Swartz O. DC-SIGN promotes exogenous MHC-I-restricted HIV-1 antigen presentation. Blood (2004) 103; 2648-2654

40. Cambi A, Beeren I, Joosten B, Fransen JA, Figdor CG. The C-type lectin DC-SIGN internalizes soluble antigens and HIV-1 virions via a clathrin-dependent mechanism. Eur J Immunol. (2009) 39;1923-1928

41. Liu Y, Tai A, Joo KI, Wang P, Visualization of DC-SIGN-Mediated Entry Pathway of Engineerd Lentiviral Vectors I Target Cells. Plos one (2013) 28;8(6):e67400

42. Tacken PJ, Ginter W, Berod L, Cruz LJ, Joosten B, Sparwasser T, Figdor CG & Cambi A. Targeting DC-SIGN via its neck region leads to prolonged antigen residence in early endosomes, delayed lysosomal degradation, and cross-presentation. Blood (2011) 118;4111-4119

43. Sol-Foulon N, Moris A, Nobile C, Boccaccio C, Engering A, Albastado JP, Heard JM, et al. Immunity (2202) 16;145-155

44. Husnjak K, Dikic I. Ubiquitin-binding proteins: decoders of ubiquitin-mediated cellular functions. Annu Rev Biochem. (2012) 81;291–322.

45. Zehner M, Chasan AI, Schuette V, Embgenbrioch M, Quast T, Kolanus W and Burgdorf S. Mannose receptor polyubiquitination regulates endosomal recruitment of p97 and cytosolic antigen translocation for cross-presentation. PNAS (2011) 108 24;9933-9938

46. Li X, DiFiglia M. The recycling endosome and its role in neurological disorders. Prog. Neurobiol. (2012) 97;127–141.

47. van Kooyk Y, Unger WWJ, Fehres CM, Kalay H, García-Vallejo JJ. Glycan-based DC-SIGN targeting vaccines to enhance antigen cross-presentation. Mol Immunol. (2013) 55;143–145

48. Bloem K. (2013) C-type lectins and their role in the immune system: New insights into the characteristics of DCIR and DC-SIGN. [dissertation] [Amsterdam (Netherlands)] Free University Amsterdam.
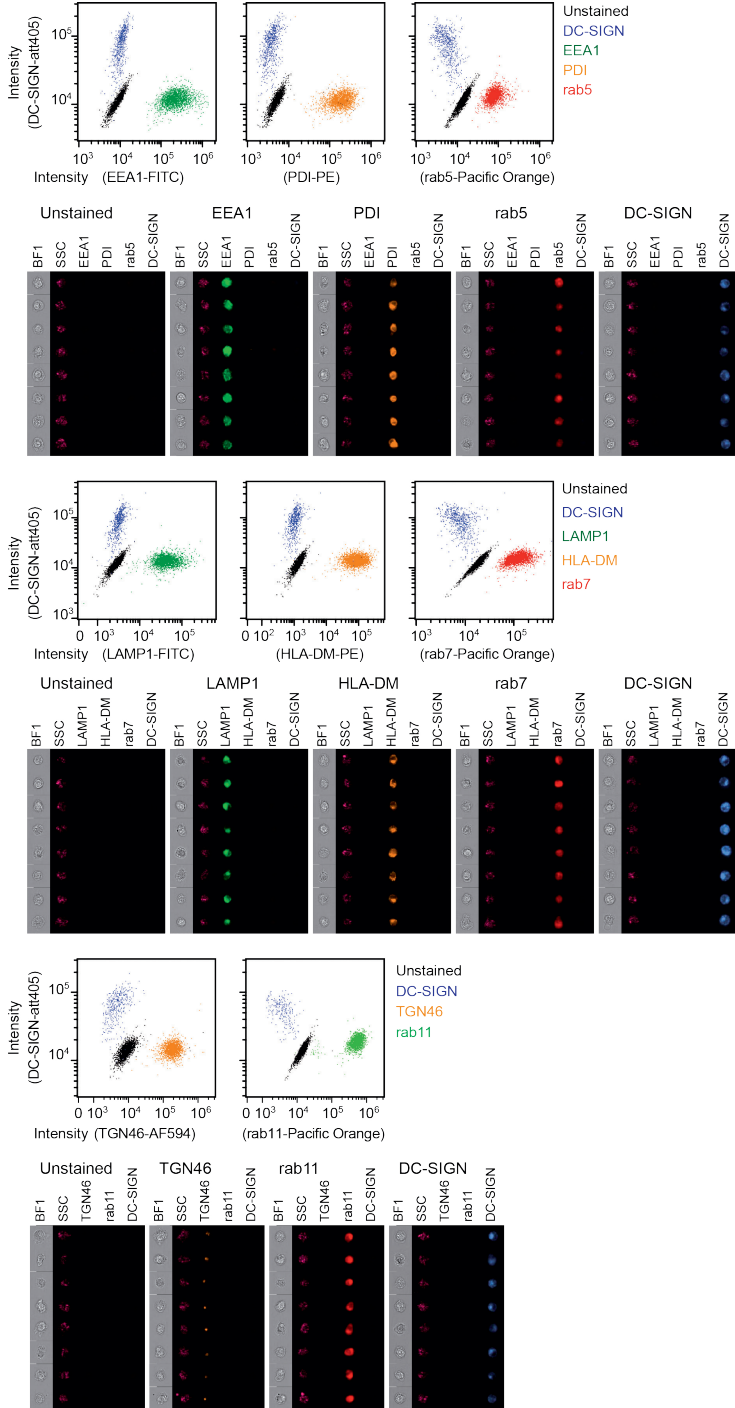
Chapter 3

Supplementary data

Figure S1. (left page) MoDCs were fixed and measured by imaging flow cytometry. Once the compensation table was calculated for each of the staining sets, it wasapplied to the single staining samples that were acquired using the same settings as experimental samples. Proper compensation was then verified by visualizing samples in bivariate fluorescence intensity plots. Representative images are displayed underneath the corresponding dotplots.
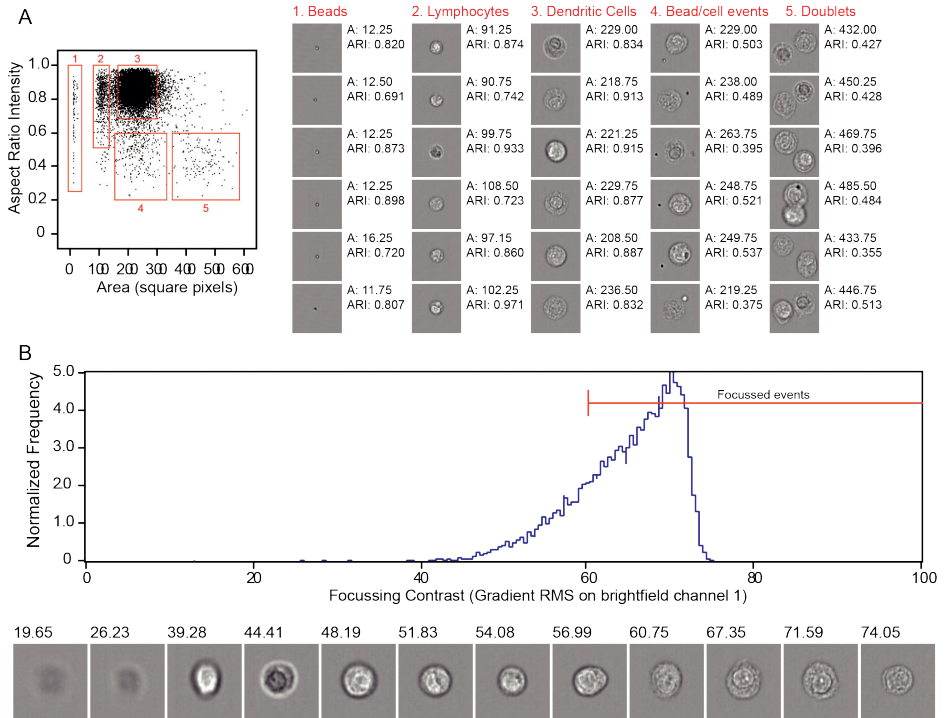

Figure S2. (A) After the application of the compensation table, cells were plotted in an area vs aspect ratio intensity bivariate scatter plot. Several populations could be identified. Population 1 was characterized by small area and high aspect ratio intensity. Images from the population 1 gate clearly show the events correspond to beads. Population 2 had an average area of approximately 100 square pixels and high aspect ratio intensity. Images from the population 2 gate show that these cells are small single cells with a large nucleus, suggesting these cells could be lymphocytes, a common contamination in Percoll-isolated monocyte-derived cell cultures. Population 3 had an area between 150 and 300 square pixels and an aspect ratio intensity higher than 0.6. These cells, the biggest population, represent dendritic cells in single cell suspension. The remaining populations (4 and 5) had a larger area and/or low aspect ratio intensity, suggestive of cell doublets and aggregates, as demonstrated in the corresponding imagery. (S2B) Gradient RMS on the brightfield channel 1 shows that the majority of the cells had a sharp contrast. Images have been selected with gradient RMS values across the whole range of gradient RMS values of the population. The threshold can then be manually set up in approximately 60.
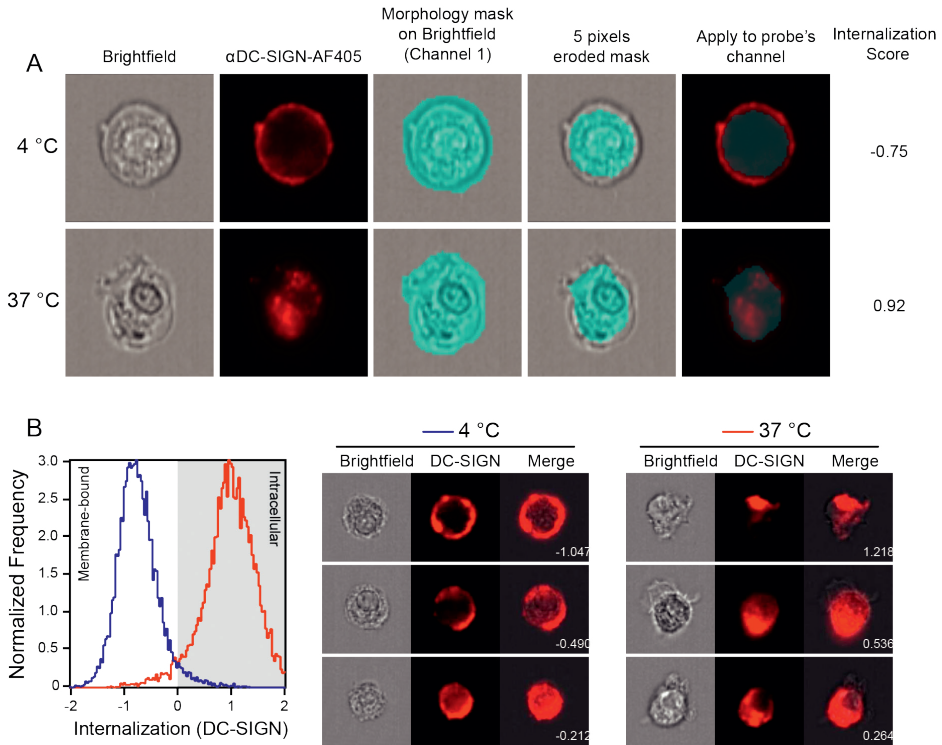
Figure S3. (A) First, a morphology mask is applied to the brightfield channel (channel 1). This mask takes the whole perimeter of the cell. Then, 5 pixels are eroded from this mask until the membrane of the cell is left out of the mask. The resulting mask is applied to the channel containing the probe of interest and a ratio of the intensity inside the mask relative to the total intensity of the cell is calculated. (B) moDCs exposed to AZN-D1 for 30 min at 4 ºC show a membrane-bound pattern of staining, with a median internalization score of -0.985. When these cells are incubated at 37 ºC for 2 h, the probe is internalized and the internalization score increases to 1.002. A selection of cells with internalization scores ranging from -1 to 1 are depicted as a merge of the brightfield (1) and the AZN-D1 (7) channels.
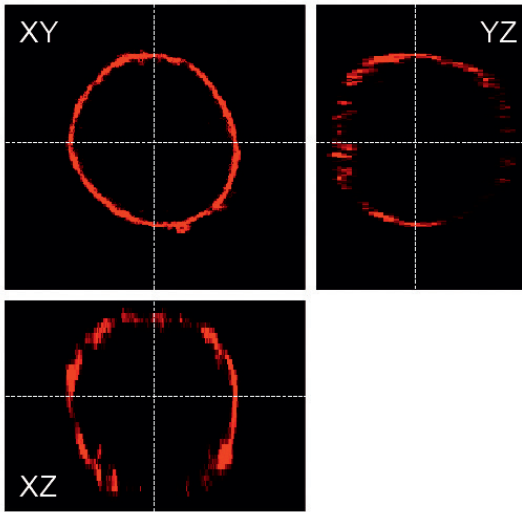
Figure S4. Cells used for Figure 1A were analyzed by CLSM. Sagital, longitudinal and transversal two-dimensional sections of a three-dimensional reconstruction are shown. Representative of 10 cells.
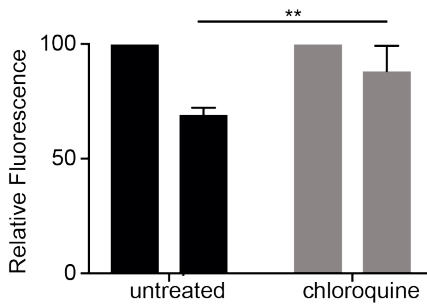
Figure S5. Immature moDCs were pre-treated with chloroquine (50-25 μM) for 30 min at 37˚ and pulsed with AF-488-labeled-AZN-D1 (10 μg/ml) for 30 min at 4˚C. Next they were washed and transferred to 37˚C for 30 min followed by fixation. Degradation of the ligand was analyzed by flow cytometry, N=3. Data is represented in mean ± SD, a two-way ANOVA was performed.
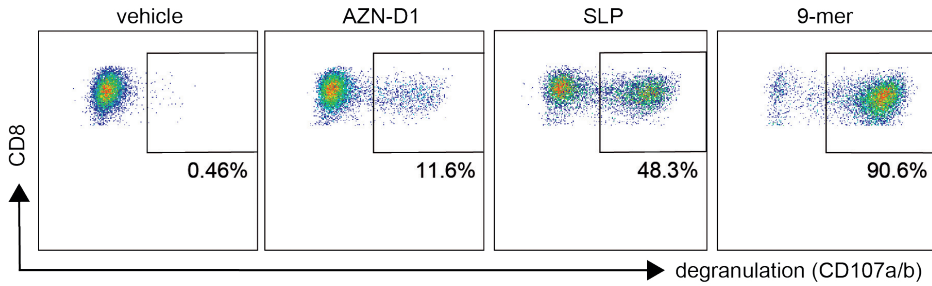
Figure S6. Representative flow cytometry dot plots of CD8+ T cell degranulation.

Figure S7. Immature and LPS stimulated (t=0) moDCs were treated with the inhibitors: chloroquine (25 µM), MG132 (10 µM), epoxomicin (0.25 µM), Cathepsin S inhibitor (5 µM) and 0.1% DMSO (vehicle) for 4h and thereafter stained with a viability dye and analyzed by flow cytometry. Representative of a N=2.
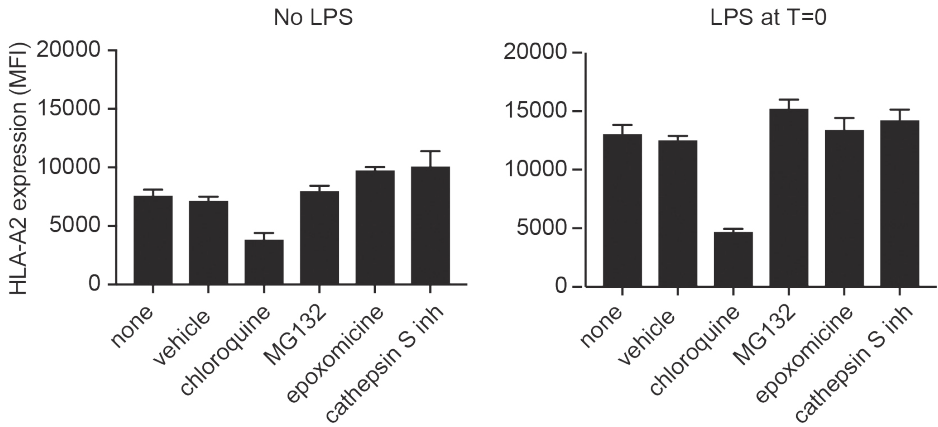
Figure S8. Immature and LPS stimulated (t=0) moDCs were treated with the inhibitors: chloroquine (25 µM), MG132 (10 µM), epoxomicin (0.25 µM), Cathepsin S inhibitor (5 µM) and 0.1% DMSO (vehicle) 30 min prior and during the 3h antigen pulse with the 9-mer minimal epitope of gp100 peptide. Followed by a co-culture with gp100$_{280-288}$ CD8$^+$ T cells for 45 min. The degranulation markers CD107$^{a/b}$ were stained as a measure of CD8$^+$ T cell activation, N=3.
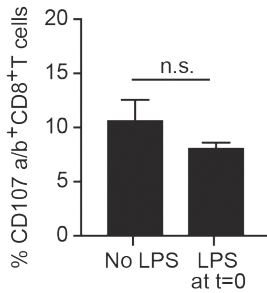
Figure S9. Immature and LPS stimulated (t=0) moDCs were incubated with chloroquine (25 µM), MG132 (10 µM), Epoxomicin (0.25 µM), Cathepsin S inhibitor (5 µM) and 0.1 % DMSO (vehicle) for 3h at 37˚C. Thereafter, cells were stained with a α-HLA-A2 Ab and the surface expression of HLA-A2 after inhibitor treatment was analyzed by flow cytometry. Representative of a N=2.

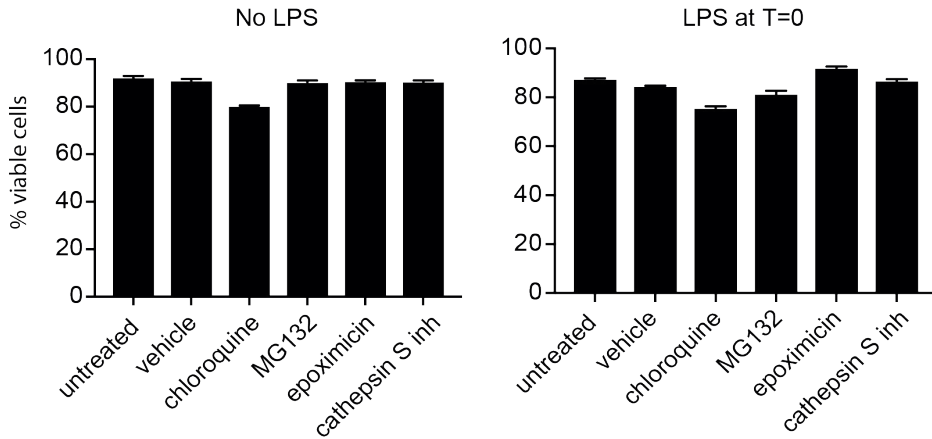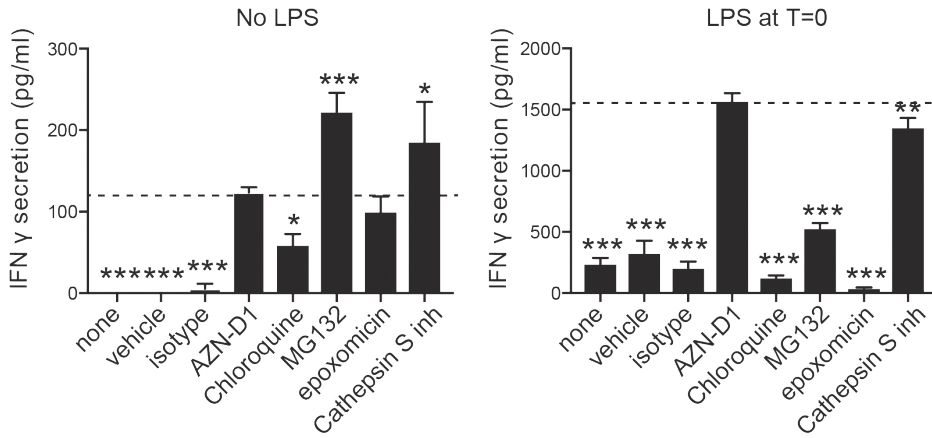**Figure S10.** Vehicle control of immature and LPS stimulated (t=0) moDCs. Representative of a N=3. (S11) Immature and LPS stimulated (t=0) moDCs were incubated 30 min prior and during the 3h antigen (gp100/AZN-D1) pulse with chloroquine (25 μM), MG132 (10 μM), Epoxomicin (0.25 μM), Cathepsin S inhibitor (5 μM) and 0.1% DMSO (vehicle). Thereafter, moDCs were co-cultured with gp100$_{280-288}$ CD8$^+$ T cells o/n, IFN γ production was analyzed by ELISA as a measure for T cell activation. Statistical analysis was performed by executing a one-way ANOVA. Groups are significantly different compared to AZN-D1.
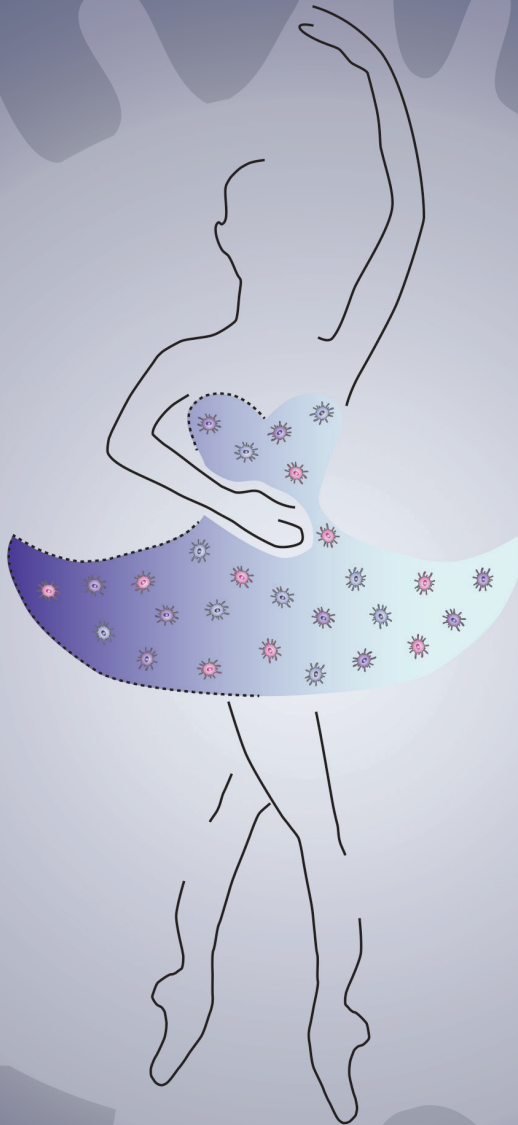
CHAPTER 4

GLYCO-DENDRIMERS AS INTRADERMAL ANTI-TUMOR VACCINE TARGETING MULTIPLE SKIN DC SUBSETS

Sanne Duinkerken, Sophie K. Horrevorts, Hakan Kalay, Martino Ambrosini, Lisa Rutte, Tanja D. de Gruijl, Juan J. Garcia-Vallejo and Yvette van Kooyk

Abstract

The human skin is an attractive anti-tumor vaccination site due to the vast network of dendritic cell (DC) subsets that carry antigens to the draining lymph nodes and stimulate tumor specific CD4^{+} and CD8^{+} T cells in. Specific vaccine delivery to skin DC can be accomplished by targeting glycan coated antigens to C-type lectin receptors (CLRs) such as DC-SIGN expressed by human dermal DCs and Langerin expressed by Langerhans cells (LCs), which facilitate endocytosis and processing for antigen presentation and T cell activation. Although there are multiple human skin DC subsets, targeting individual DC subsets and receptors has been a focus in the past. However, the simultaneous targeting of multiple human skin DC subsets that mobilize the majority of the skin antigen presenting cells (APC) is preferred to accomplish more robust and efficient T cell stimulation. Dual CLR targeting using a single tumor vaccine has been difficult, as we previously showed Langerin to favor binding and uptake of monovalent glyco-peptides whereas DC-SIGN favors binding of larger multivalent glyco-particles such as glyco-liposomes.

Methods We used branched polyamidoamine (PAMAM) dendrimers as scaffold for melanoma specific gp100 synthetic long peptides and the common DC-SIGN and Langerin ligand Lewis Y (Le[Y]), to create multivalent glyco-dendrimers with varying molecular weights for investigating dual DC-SIGN and Langerin targeting. Using DC-SIGN^{+} monocyte derived DC (moDC) and Langerin^{+} primary LC we investigated glyco-dendrimer CLR targeting properties and subsequent gp100 specific CD8^{+} T cell activation *in vitro*. *In situ* targeting ability to human dermal DC and LC through intradermal injection in a human skin explant model was elucidated.

Results Dual DC-SIGN and Langerin binding was achieved using glyco-dendrimers of approximately 100kD, thereby fulfilling our criteria to simultaneously target LCs and CD1a^{+} and CD14^{+} dermal DC *in situ*. Both DC-SIGN and Langerin targeting by glyco-dendrimers resulted in enhanced internalization and gp100 specific CD8^{+} T cell activation.

Conclusion We designed the first glyco-vaccine with dual CLR targeting properties, thereby reaching multiple human skin DC subsets *in situ* for improved anti-tumor CD8^{+} T cell responses.

Introduction

Dendritic cells (DC) have a unique capacity to endocytose antigens and to activate naïve antigen-specific T-cells in the lymph nodes and thus are considered as the initiators of adaptive immune responses [1, 2]. Hence, DCs are widely explored for targeted anti-tumor immunotherapies. Efficient tumor elimination can be accomplished by the simultaneous induction of tumor specific CD4^{+} and CD8^{+} T cells [3]. CD4^{+} T cells are activated via recognition of exogenous derived antigen loaded in major histocompatibility complex (MHC) class II, whereas CD8^{+} T cells via endogenous derived antigen loaded in MHC class I. For tumor cell killing anti-tumor immune responses rely on the induction of cytotoxic CD8^{+} T cells for which DCs need to shuttle endocytosed particles into the cross-presentation pathway to load tumor-derived epitopes into MHC class I [4]. Various DC subsets have been described to have cross-presenting capacity *in vivo*, and are attractive targets to generate robust anti-tumor T cell immunity [4].

An important requirement for intracellular trafficking of antigens is the recognition of antigen by uptake receptors such as pathogen recognition receptors (PRR). A well-known group of PRRs is the C-type lectin receptor (CLR) family. CLRs have been extensively studied for their specific expression on DC subsets, their specificity of ligands, often carbohydrates, and their intracellular routing of antigen for loading on MHC class I and II for presentation to T cells [5]. It is for this reason that CLRs have been used for vaccine delivery of (nano)particles to specific DC subsets using either antibody targeting or natural glycan ligands [5]. Multiple CLRs showed potential in DC-targeted strategies inducing DC cross-presentation, e.g. DEC205, CLEC9A, the mannose receptor (MR) and dendritic cell-specific ICAM-grabbing non-integrin (DC-SIGN) [6-8]. However, these receptors are often used to target a single DC subset, whereas targeting multiple subsets simultaneously may induce superior immune responses [9, 10].

In vivo vaccines are often applied in the human skin, since there is a high abundance of DCs and intradermal injections have shown to be dose-sparing compared to intramuscular delivery [11-13]. Multiple DC subsets reside in the skin with LCs populating the epidermis and CD1a^{+}, CD14^{+} and CD141^{+} DCs the dermis. CD1a^{+} dermal DC are inducers of cellular T cell responses, CD14^{+} dermal DC are better equipped to activate humoral responses and the CD141^{+} dermal DC subset is considered the most potent cross-presenting DC subset [14]. As such, targeting multiple skin DC subsets

simultaneously might elicit broader immune responses compared to single subset targeting. Though, it is becoming clear that the function of the different DC subsets can change depending on the vaccine format and mode of delivery [15]. Especially specific CLR targeting can alter intracellular trafficking thereby influencing choice of CLR and DC subset targeting.

Although all subsets express multiple and partly overlapping CLRs, Langerin and DC-SIGN are two well-defined CLRs expressed by LCs and dermal DCs, respectively. Their glycan binding profile is partly overlapping as both recognize the Lewis type antigens, though DC-SIGN binds Lewis (Le) A,B , Y and X, whereas Langerin only recognizes Le^B and Le^y. Interestingly, both receptors show high affinity for Le^y, making this glycan an interesting candidate for dual CLR targeting [16]. Furthermore, both receptors have been shown to efficiently deliver their cargo into the cross-presentation pathway, especially when combined with toll-like receptor (TLR) triggering [17, 18]. TLRs are PRRs expressed by DCs that induce DC-mediated T cell activation via DC maturation and modulation of intracellular antigen trafficking in DCs [19]. Combined triggering of TLR4 with DC-SIGN targeting resulted in cargo translocation to the cytosol, thus releasing it for proteasomal degradation and subsequent MHC I loading [17]. For LCs combined targeting of Langerin and TLR3 using poly I:C enhanced cross-presentation and subsequent CD8$^+$ T cell activation [18]. Both DC-SIGN and Langerin are excellent targets for *in vivo* intradermal anti-tumor vaccination strategies.

The design of an off-the-shelve vaccine targeting multiple CLRs and skin DC subsets is difficult to accomplish via antibody targeting, however natural glycan ligands might be an option especially those that are shared by Langerin and DC-SIGN and display high affinity binding such as Le^y [18, 19]. Vaccine particle formulation can influence processing by DCs and subsequent adaptive immune responses [20-22]. Spatial orientation of compounds and number of receptor ligands can change CLR binding and handling due to changes in avidity [23]. Langerin and DC-SIGN appear to require different formulations to meet the needed combination of affinity and avidity for ligand endocytosis and cross-presentation. Indeed, our previous work demonstrated that relatively small sized glyco-peptides are targeted to Langerin (~3.5kD), whereas DC-SIGN preferentially binds large size glyco-particles (200nm) [16]. This illustrates that a single glycan Le^y structure may be used for Langerin targeting, whereas DC-SIGN may require multivalent presentation of Le^y, such as glyco-liposomes (200nm) to accomplish receptor mediated uptake, and the induction of cross-presentation

[19]. This different requirement to establish receptor-mediated uptake may be linked to functional differences of LCs and DCs to mediate viral and bacterial responses, respectively [24, 25]. Moreover these DC subsets express a differential repertoire of TLR receptors to trigger maturation, such as viral TLR3 (Poly I:C) on LC and bacterial TLR4 (LPS) on dDC [26].

To meet the criteria for dual DC-SIGN and Langerin targeting, we explored different glyco-vaccine formulations which have the proper avidity for both receptors. To this end, we synthesized two multivalent Le^Y vaccines incorporating the CD4 and CD8 melanoma-specific gp100 antigen using two generations of well-defined, commercially available PAMAM dendrimer scaffolds which consist of branched subunits of amide and amine functionality [27]. By creating glyco-dendrimers with either 4 or 32 functional groups containing the gp100 synthetic long peptide and Le^Y we elucidated dual targeting capacity and subsequent induction of cross-presentation. We describe generation 3 (G3) glyco-dendrimers simultaneously targeting DC-SIGN and Langerin, thereby enhancing gp100 specific CD8$^+$ T cell activation when combined with a TLR stimulus. Furthermore, G3 glyco-dendrimers target both LCs and CD1a$^+$ and CD14$^+$ dDCs by which we have created the first glyco-vaccine targeting multiple human skin DC *in situ* for induction of anti-tumor immune responses.

Results

Multivalent Generation 3.0 glyco-dendrimers efficiently target both DC-SIGN and Langerin

To design a glyco-vaccine that simultaneously targets DC-SIGN and Langerin, we generated two multivalent glyco-dendrimers differing in molecular weight, diameter and valency using the generation 0 (G0) or generation 3 (G3) PAMAM dendrimers, that have either 4 (G0) or 32 (G3) functional groups. As antigen, we included a synthetic long peptide of the melanoma epitope gp100 containing both HLA-DR4 CD4 and HLA-A02 CD8 restricted epitopes [17]. Coupling of the gp100 peptide to the G0 or G3 dendrimers (Figure **S1A**) resulted in antigen specific multivalent dendrimers of 16.4kD (G0) (**Figure S1B**) and approximately 52nm (G3) (**Figure S1C**). Dendrimers were further modified with AF488 for tracking purposes and the targeting glycan Le^Y [16], thereby creating multivalent fluorescent glyco-dendrimers (schematic representation **Figure S1A**). Fluorescent labeling was done such that coupling

ensured equal fluorescence and epitope content of total molecules between non-glycosylated and glyco-dendrimers (schematic representation **Figure 1A**). Using DC-SIGN- and Langerin-Fc we confirmed recognition of both G0 and G3 glyco-dendrimers by the carbohydrate recognition domain (CRD) of both receptors, whereas the non-glycosylated dendrimers were not recognized by either soluble receptor in an ELISA detection system (**Figure 1B**). Further, calcium-dependent binding of the dendrimers to DC-SIGN- and Langerin-Fc was confirmed using the calcium chelator EGTA. To verify whether the membrane organization of DC-SIGN and Langerin, that cluster in tetra- and trimers in the membrane respectively, may influence the binding and internalization of the different glyco-dendrimers, we made use of an OUW cell-line transduced with DC-SIGN or Langerin. After one hour pulse the smaller G0 glyco-dendrimers did not bind DC-SIGN-expressing OUW cells, but did bind to Langerin-expressing OUW cells (**Figure 1C**, *left panel*). This is in keeping with our previous findings that in contrast to DC-SIGN, Langerin has a preference for binding smaller molecules [16]. Interestingly, the G3 glyco-dendrimers could efficiently target both DC-SIGN and Langerin after one hour incubation (**Figure 1C**, *middle panel*). Glyco-liposomes served as a positive control for DC-SIGN and, as expected, they solely bound DC-SIGN and not Langerin as previously shown (**Figure 1C**, *right panel*). Using blocking antibodies specific for either DC-SIGN or Langerin, we could confirm specific binding of G3 glyco-dendrimers to both receptors (**Figure 1D**). We therefore concluded that G3 glyco-dendrimers have all the requirements to serve as skin multi-DC subset targeting glyco-vaccine via its binding to both Langerin and DC-SIGN.

Enhanced uptake of glyco-dendrimers by moDC and primary LC mediated via DC-SIGN and Langerin

To determine whether the uptake of G3 glyco-dendrimers by moDCs and primary LCs is also mediated by Langerin and DC-SIGN, we compared uptake of glyco-dendrimers to that of non-glycosylated dendrimers. Glyco-dendrimers are efficiently taken up by moDCs as compared to non-glycosylated dendrimers within 3 hours at 37 °C, and a targeting effect is already evident at low concentrations (**Figure 2A**). To elucidate whether glyco-dendrimers show increased binding and uptake over time compared to non-glycosylated dendrimers at constant exposure, we pre-incubated moDC at 4°C with the respective dendrimers to ensure receptor binding, followed by direct incubation up to one hour at 37°C. We observed a clear increase of AF488 signal from glyco-dendrimers over-time as compared to non-glycosylated dendrimers, indicating that glyco-dendrimers are rapidly bound and internalized by moDC (**Figure 2B**).
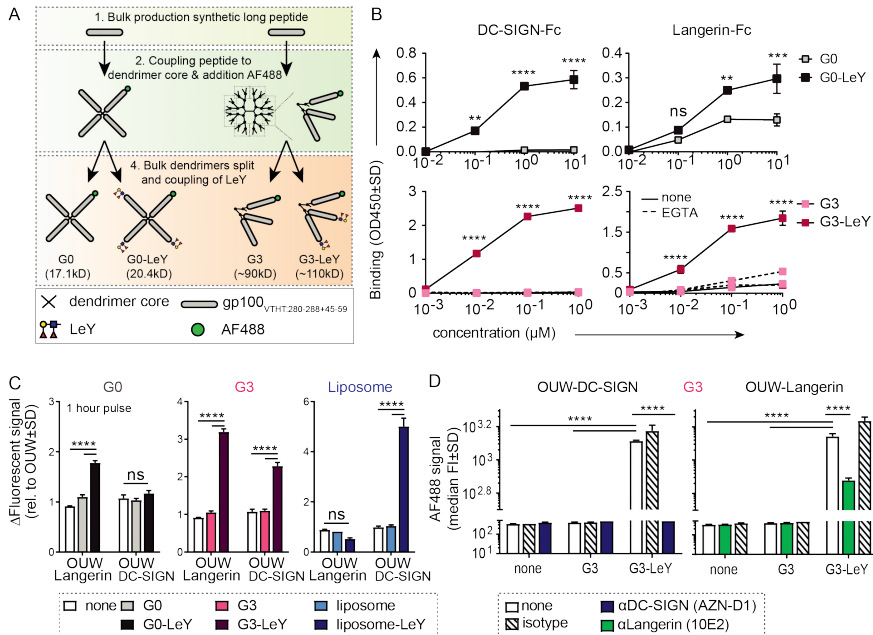
Figure 1. Generation 3.0 (G3) glyco-dendrimers efficiently target both DC-SIGN and Langerin. DC-SIGN and Langerin targeting was evaluated for different glyco-particles using CLR-Fc or a cell line transduced with DC-SIGN or Langerin **A** Schematic representation of (glyco)-dendrimer synthesis. **B** Binding of G0 (upper panels) or G3 (lower panels) (glyco)-dendrimers to human DC-SIGN-Fc (left panel) or Langerin-Fc (right panel) in the presence or absence of calcium depletion (EGTA) as measured by binding ELISA. **C** Binding to membrane DC-SIGN and Langerin of different (glyco)-particles within 1 hour at 37 degrees; G0 (grey) or G3 (pink) (glyco)-dendrimers and (glyco)-liposomes (blue). **D** DC-SIGN and Langerin specific binding by G3 glyco-dendrimers was evaluated using specific blocking antibodies for DC-SIGN and Langerin, or matched isotype control, prior to incubation. Data are representative of at least two independent experiments measured in triplicate ±SD (Statistical analysis: B two-way ANOVA Sidak's post hoc, C-D two-way ANOVA Tukey's post-hoc)

Imaging microscopy confirmed internalization of the glyco-dendrimers by moDC following 3 hours incubation at 37 °C (**Figure 2C**). Involvement of DC-SIGN in enhanced uptake by moDC was elucidated using an anti-DC-SIGN antibody known to bind the CRD and induce internalization of DC-SIGN.

Prior to incubation with dendrimers, moDC were incubated with anti-DC-SIGN at 37°C to ensure receptor occupation and partial internalization. Since DC-SIGN is a non-recycling receptor, internalized DC-SIGN will no longer be available for ligand binding. Interestingly, targeting of glyco-dendrimers to DC-SIGN appeared to be very efficient since pre-incubation with anti-DC-SIGN for 30 minutes did not affect binding and uptake, which for glyco-liposomes was sufficient (**Figure S2A**).

To demonstrate DC-SIGN-mediated internalization of glyco-dendrimers, moDC had to be pre-incubated for at least 3 hours using the blocking antibody (**Figure 2D**). Remarkably, a clear blocking effect of glyco-dendrimer uptake was seen when moDC were pre-incubated with increasing concentrations of the high affinity ligand of DC-SIGN, mannan, confirming that DC-SIGN is indeed responsible for the enhanced binding and uptake of glyco-dendrimers by moDC (**Figure 2E**).

To elucidate whether our compound also targeted Langerin on primary LCs, we used LCs obtained by two day emigration from epidermal sheets. Langerin expression is lower in emigrated LC compared to steady-state LC, nevertheless, expression levels were sufficient to elucidate Langerin targeting (**Figure S2B**). To track G3 glyco-dendrimer binding and uptake over time, primary LC were pre-incubated at 4°C for 45 minutes, followed by incubation at 37°C for multiple time-points. Similar as for moDC, we found increased signal for glyco-dendrimers compared to non-glycosylated dendrimers already at 15 minutes, indicating rapid binding and uptake by primary LCs as confirmed by imaging microscopy (**Figure 2F,H**). For primary LCs, pre-incubation with an anti-Langerin blocking antibody resulted in an almost complete abrogation of enhanced glyco-dendrimer uptake (**Figure 2G**), confirming the targeting ability of G3 glyco-dendrimers to Langerin.

Enhanced uptake of glyco-dendrimers by DC-SIGN$^+$ and Langerin$^+$ human skin DCs in situ

Since we confirmed Langerin and DC-SIGN mediated targeting and uptake specificity by G3 glyco-dendrimers, we set out to explore whether this specificity remained when injected in human skin that harbors all the different human skin DC subsets expressing DC-SIGN or Langerin. We used a human skin explant model [28] to inject the G3 (glyco)-dendrimers and verify targeting to human skin DCs expressing DC-SIGN or Langerin. This model represents a steady-state environment with the physiological localization, phenotype and ratio of the different human skin DC subsets. As such, it supplies the best possible representation of the human skin to study specific DC targeting by the glyco-vaccine upon intradermal delivery. Following injection, cells were allowed to emigrate for two days and analyzed by FACS. Skin APC subsets were defined based on HLA-DR and subset-specific markers CD1a, CD14, CD141 and EpCAM (**Figure 3A**) using manual gating and unsupervised clustering to confirm number of subsets. DC-SIGN and Langerin expression was evaluated after two day skin DC emigration for all subsets. In concordance with literature we found Langerin

on LCs and DC-SIGN expressed by CD14+ dDC and to a very small extent by CD1a+ dDC (**Figure 3B**). As expected, CD14+ dDC
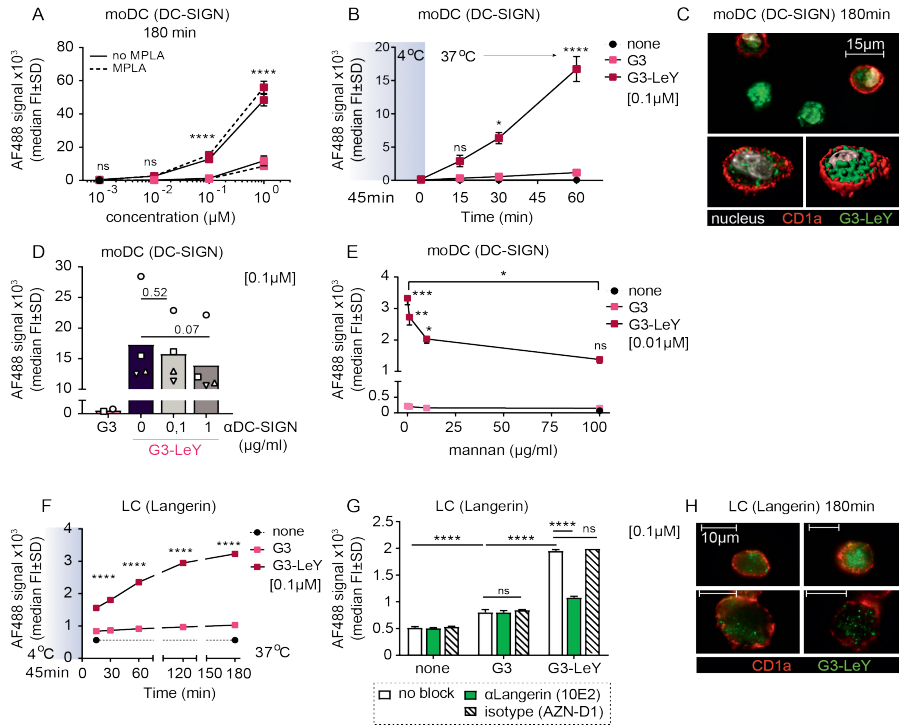

Figure 2. Enhanced glyco-dendrimer binding and uptake by moDC via DC-SIGN and primary LC via Langerin Binding and uptake of G3 (glyco)-dendrimers was evaluated for DC-SIGN+ moDC and Langerin+ primary LCs. **A** Dose-response following a 3 hour pulse, wash and 45 minutes chase of moDC with G3 (glyco)-dendrimers in the presence (dotted line) or absence (solid line) of TLR4 stimulus MPLA. Representative of n=3 measured in triplicate ±SD **B** Binding and uptake of (glyco)-dendrimers over-time by moDC following a 45 minutes pulse (no wash) at 4 °C. n=2, ±SD **C** Imaging microscopy of moDC following 3 hour incubation at 37 °C with glyco-dendrimers (green). Membrane was stained using anti-CD1a (red) and nucleus using DAPI (white) **D-E** Involvement of DC-SIGN in binding and uptake of G3 (glyco)- dendrimers was evaluated using a 3 hour pre-incubation with anti-DC-SIGN (C) or 30 minutes pre-incubation with the natural ligand mannan (D) followed by 1 hour incubation with (glyco)-dendrimers. (C) n=4, each symbol represents a donor (D) representative of n=2 measured in triplicate ±SD **F** Binding and uptake of (glyco)-dendrimers over-time by primary LC following a 45 minutes pulse (no wash) on 4 °C. Representative of n=2 measured in triplicate **G** Langerin involvement in binding and uptake of (glyco)-dendrimers by primary LCs was evaluated using 30 minutes pre-incubation an anti-Langerin blocking antibody followed by 1 hour co-incubation with (glyco)-dendrimers. Representative of n=3 measured in triplicate ±SD **H** Imaging microscopy of primary LC following 3 hours incubation at 37 °C with glyco-dendrimers (green). Membrane was stained using anti-CD1a (red) (Statistical analysis: A,E two-way ANOVA Sidak's post hoc; B,D,F two-way ANOVA Tukey's post hoc; C one-way ANOVA Dunnett's post hoc)
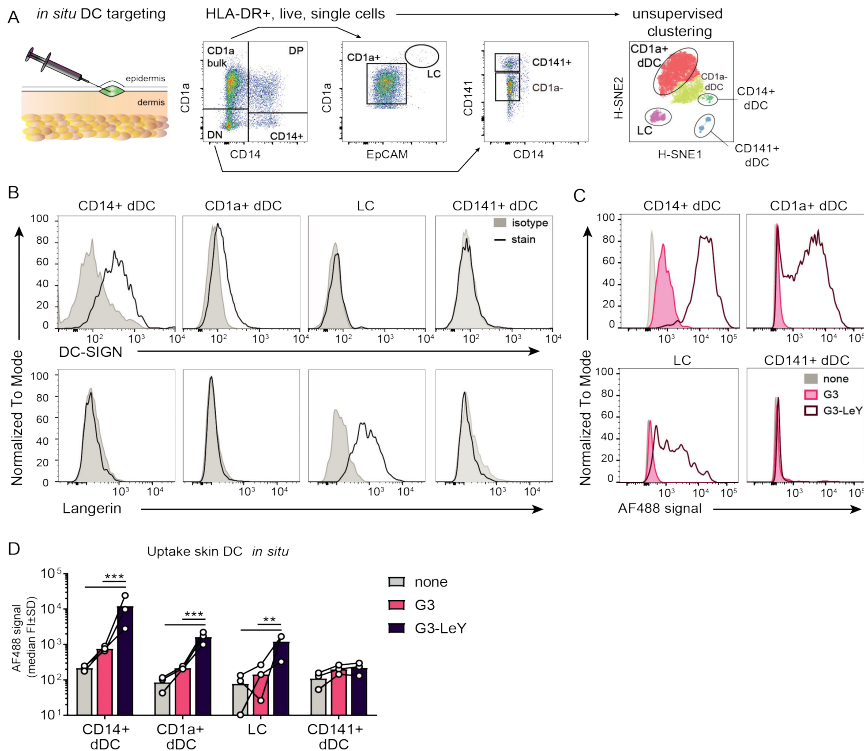
Figure 3. Glyco-dendrimers target multiple skin DC subsets for enhanced uptake A Gating strategy of human skin DC subsets following injection and two day emigration **B** DC-SIGN and Langerin surface expression on two day emigrated skin DC subsets **C-D** Binding and uptake of (glyco)-dendrimers by human skin DC subsets following in situ injection. n=3 plus representative histograms. Each dot represents a donor. (Statistical analysis: two-way ANOVA Dunnett's post hoc)

and LC showed higher uptake of G3 glyco-dendrimers compared to the non-glycosylated dendrimers. Interestingly, we found $CD1a^+$ dDC to also efficiently take up the glyco-dendrimers (**Figure 3C-D**) despite their low expression levels of DC-SIGN (**Figure 3B**), suggesting G3 glyco-dendrimers can already efficiently target DC-SIGN at lower expression levels. For the Langerin$^-$ and DC-SIGN$^-$ $CD141^+$ dDCs we did not find any enhanced uptake of the glyco-dendrimers (**Figure 3C-D**). Altogether, these data show the ability of G3 glyco-dendrimers to efficiently target multiple skin DC subsets *in situ*.

G3 glyco-dendrimers enhance cross-presentation for tumor specific $CD8^+$ T cell activation

To ensure proper delivery for $CD4^+$ and $CD8^+$ T cell activation, we used gp100 specific T cell clones recognizing either the CD4 or CD8 minimal epitope. First, we verified

activation of CD4^{+} T cells following overnight co-culture with moDC. We found gp100 specific CD4^{+} T cell activation as measured by IFNγ secretion, which increased upon glyco-dendrimer pulse both in the absence and presence of TLR4 stimulation (MPLA) (**Figure S3**). To verify whether targeting and enhanced uptake of the G3 glyco-dendrimers to both DC-SIGN and Langerin results in enhanced CD8^{+} T cell activation, we first verified cross-presentation via DC-SIGN using a DC-SIGN expressing OUW cell line and DC-SIGN^{+} moDC. Briefly, APCs exposed to (glyco)-dendrimers were co-cultured with a gp100 specific T cell clone recognizing the gp100 HLA-A2 minimal epitope and degranulation or IFNγ secretion were subsequently measured (**Figure 4A**). We observed that the G3 glyco-dendrimers induced CD8^{+} T cell activation by DC-SIGN^{+} OUW cells as measured by increased IFNγ secretion, without addition of a TLR stimulus (**Figure 4B**, *upper panel*). For moDC we have previously shown that TLR4 signaling alters routing for DC-SIGN targeted vaccines inducing enhanced CD8^{+} T cell activation compared to untargeted vaccines [17]. To elucidate the influence of TLR4 signaling on cross-presentation of the glyco-dendrimers compared to non-glycosylated dendrimers, we pulsed moDC in the presence or absence of the TLR4 stimulus MPLA followed by a direct short co-culture to avoid influence of MPLA induced moDC maturation. MoDC show enhanced degranulation of gp100 specific CD8^{+} T cells already after a short co-culture following combined triggering of TLR4 (MPLA) with G3 glyco-dendrimer targeting compared to non-glycosylated dendrimers (**Figure 4C**). In concordance, overnight co-culture of gp100 T cells with glyco-dendrimer pulsed moDC in the presence of MPLA enhanced IFNγ production compared to non-glycosylated dendrimers, but also overall IFNγ production (**Figure 4D**). This indicates DC-SIGN expressed by moDC efficiently routes antigens into the cross-presentation pathway only under the influence of TLR4 signaling, underlining the need for the presence of a potent adjuvant in the vaccine formulation.

Next, we verified whether the enhanced G3 glyco-dendrimer targeting to Langerin also resulted in antigen cross-presentation and enhanced CD8^{+} T cell activation. LC derived from MUTZ cells induced increased IFNγ production by gp100 specific CD8^{+} T cells when pulsed with glyco-dendrimers compared to non-glycosylated dendrimers (**Figure 4D**). As primary LCs are the *in vivo* target, we isolated primary LCs from human epidermal sheets to elucidate cross-presentation of G3 glyco-dendrimers in combination with the TLR3 stimulus Poly I:C, known to enhance primary LC induced CD8^{+} T cell activation [18]. There was increased IFNγ production by gp100 specific CD8^{+} T cells following o/n culture with G3 glyco-dendrimer-pulsed primary LCs compared to primary LCs pulsed with non-glycosylated dendrimers (**Figure 4E**).

A APC pulse → wash → co-culture CD8+ T cells o/n → supernatant IFNγ (secretion) → ELISA

co-culture CD8+ T cells 45 min → stain CD107a/b (degranulation) → FACS
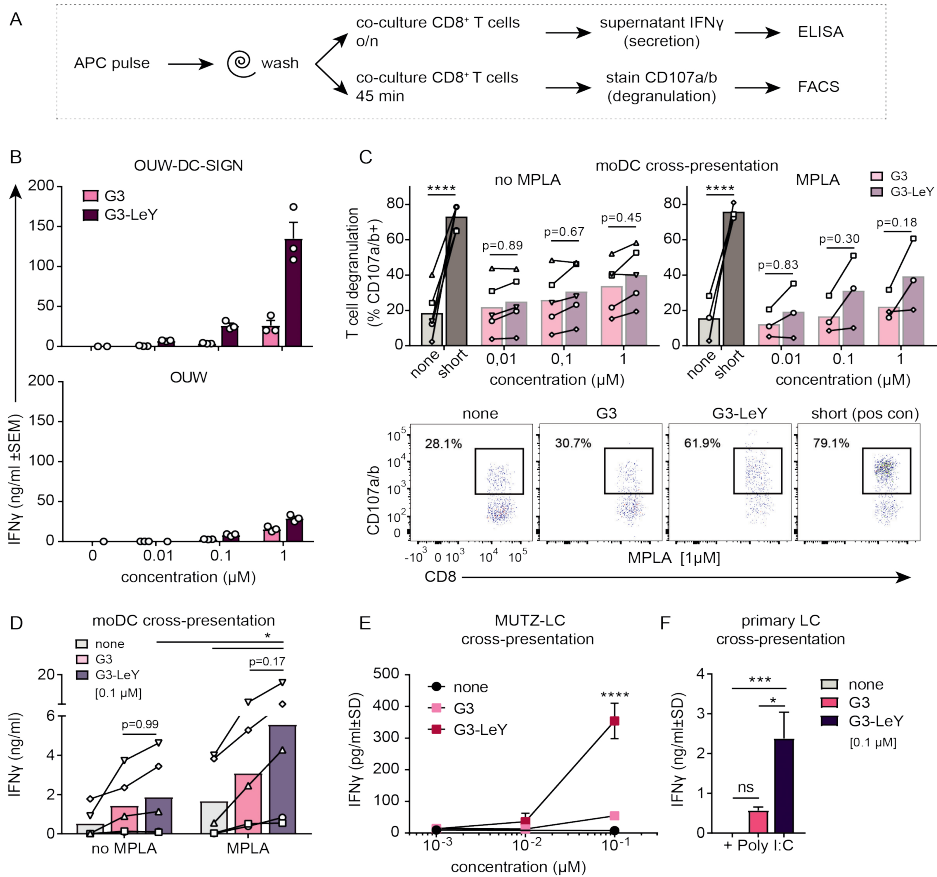
This indicates Langerin targeting by G3 glyco-dendrimers on primary LCs routes antigens into the cross-presentation pathway for enhanced CD8+ T cell activation. Overall, these data show that the enhanced binding and uptake of G3 glyco-dendrimers by DC via DC-SIGN or Langerin, combined with a TLR stimulus, induces an increase in degranulation and IFNγ production by gp100 specific CD8+ T cells.

Discussion

Here, we successfully designed a gp100 melanoma-specific vaccine that targets multiple skin DC subsets through its dual specificity for DC-SIGN and Langerin receptors. We show that the molecular architecture of the vaccine is essential in enabling efficient dual targeting, as conditions for targeting need to be met for two different receptors. Generation 3.0 glyco-dendrimers have the ability to target both DC-SIGN and Langerin through binding the Le^Y glycan, thereby reaching LC, CD1a+ and

Figure 4. Enhanced cross-presentation of glyco-dendrimers by moDC and primary LC A APC were pulsed with the (glyco)-dendrimers for 3 hours or 30 minutes, washed and co-cultured with a gp100 specific T cell clone for either 45minutes or o/n. CD8^{+} T cell activation was measured by FACS using CD107a/b staining for degranulation or by ELISA for IFNγ secretion in the supernatant **B** IFNγ production of gp100 specific T cells after o/n culture with pulsed OUW cells transduced with DC-SIGN (upper panel) or non-transduced (lower panel). Representative of n=2±SD measured in triplicate **C** Degranulation of gp100 specific T cells following 45min culture with 3 hour pulsed moDC in the absence (left) or presence (right) of the TLR4 stimulus MPLA. n=3-5, each symbol represents a donor. Representative dot plots for MPLA 1µM **D** IFNγ production by gp100 specific T cells following o/n culture with 30 minutes pulsed moDC in the absence or presence of the TLR4 stimulus MPLA. n=5, each symbol represents a donor. **E-F** IFNγ production by gp100 specific T cells following o/n co-culture with 3 hour pulsed (E) MUTZ-LC or (F) primary LC in the presence of TLR3 stimulus Poly I:C. Representative of n=2±SD measured in triplicate. (Statistical analysis: C,D two-way ANOVA Sidak's post hoc, D,E one-way ANOVA Tukey's post hoc)

CD14^{+} dDC within the human skin *in situ*. Combination of glyco-dendrimer targeting to DC-SIGN and Langerin with a TLR stimulus resulted in cross-presentation and enhanced gp100 specific CD8^{+} T cell activation, illustrating their great potential for intradermal anti-tumor vaccination strategies and shedding additional light on the requirements for glyco-vaccine formulation.

Although DC-SIGN and Langerin have overlapping glycan binding specificity, their internalization and intracellular processing differs greatly. Despite their difference in intracellular compartmentalization, different studies showed that both receptors process antigen intracellularly for cross-presentation. However, our earlier work showed induction of cross-presentation by Langerin via small glyco-peptides, whereas by DC-SIGN via large glyco-liposomes [16]. Interestingly, often viruses and bacteria use DC-SIGN to either escape the immune system or alter T helper cell responses via intracellular signaling cascades [29]. In contrast, Langerin-mediated uptake of viruses such as HIV and fungi mediates clearance [30], which might be due to the specific formation of Birbeck Granules upon Langerin-mediated internalization. Birbeck Granules are subdomains of the endosomal recycling compartment [31] that regulate antigen degradation differently from other endocytic compartments. [32, 33]. These discrepancies might explain why until now no glyco-vaccine has been

developed with the capacity to target both receptors simultaneously whilst inducing cross-presentation.

Interestingly, DC-SIGN can also be efficiently targeted for *in vivo* cross-presentation via Le[x] coupled glyco-dendrimers with increasing multivalency, a technique not yet explored for Langerin targeting [34]. In this study, we used PAMAM dendrimer scaffolds to create two formulations of melanoma-specific glyco-dendrimers that differed in molecular weight to investigate targeting properties to both DC-SIGN and Langerin. The smallest G0 glyco-dendrimers with four functional groups only showed targeting ability towards Langerin and not DC-SIGN, whereas higher multivalency G3 glyco-dendrimers harboring 32 functional groups showed binding to both receptors on the cellular membrane. Targeting with G3 glyco-dendrimers resulted in enhanced binding and uptake for both moDC and primary LC over time. Interestingly, low generation PAMAM dendrimers have high flexibility [27, 35] and efficient binding to Langerin and DC-SIGN may require membrane movement of the CLRs explaining enhanced binding at 37°C.

Membrane organization of DC-SIGN can affect glycan-coated ligand binding, as shown for synthetic hyperbranched polymers containing mannose, but also viral entry [36, 37]. Interestingly, our results show that the same targeting moiety on different formulations of cargo can alter targeting properties to a single receptor. Using previously described glyco-liposomes known to target DC-SIGN [16] we found efficient blocking when moDC were simultaneously incubated with the common blocking antibody AZN-D1. Strikingly, for G3 glyco-dendrimers the strong binding to moDC showed partial DC-SIGN blocking with the AZN-D1 antibody, whereas pre-incubation with the high affinity natural binding ligand mannan [38] efficiently blocked the binding and uptake of glyco-dendrimers by DC-SIGN[+] moDC, indicating high binding efficiency of G3 glyco-dendrimers to DC-SIGN. Although mannan can also bind to other receptors such as the mannose receptor (MR), our glycan of choice (Le[y]) is high affinity for DC-SIGN and thus binding to other receptors on DC is unlikely. [39]

Glyco-dendrimer targeting to primary LC was considerably lower compared to moDC, possibly due to lower expression levels of Langerin. MoDC have high expression of DC-SIGN, whereas primary LCs, migrated from the epidermis for two days, show decreased Langerin expression levels (**Figure S2B**). The phagocytic capacity of the

different cell types can also be important for *in situ* targeting, since DC-SIGN^{high} CD14^{+} dDC showed greater glyco-dendrimer uptake compared to DC-SIGN^{low} CD1a^{+} dDC and epidermal LCs. CD14^{+} dDC are considered to have a monocytic lineage background [40] and hence may have higher phagocytic capacity compared to other skin DCs, as represented by moDC.

Anti-tumor vaccination strategies aim to induce cross-presentation for the priming of tumor-specific CD8^{+} T cells and effective tumor cell killing. In murine models, XCR1^{+} DCs, present in lymph nodes and peripheral tissues, have been postulated as potent target candidates for induction of cytotoxic T cell responses [41] and anti-tumor immune responses [42]. The dermis of human skin contains CD141^{+} cross-presenting DCs, which are considered to be the homologue of murine CD103^{+}XCR1^{+} dermal DCs [43]. Nonetheless, we did not observe *in situ* targeting towards CD141^{+} dDCs by the G3 glyco-dendrimers, consistent with their lack of DC-SIGN or Langerin expression. Although this skin DC subset is considered a potent target candidate for induction of cytotoxic anti-tumor immune responses [44], it represents a minority of the total dermal DC pool. In contrast, we show efficient G3 glyco-dendrimer targeting towards LCs and the larger pool of CD1a^{+} and CD14^{+} dDCs. Targeting of LCs and CD14^{+} dDCs via Langerin and DC-SIGN, respectively, can induce cross-presentation when different glyco-vaccines are used [8, 18, 28]. Here we show that G3 glyco-dendrimers are cross-presented via both DC-SIGN and Langerin when combined with a TLR stimulus, thereby enhancing gp100 specific CD8^{+} T cell activation. Combining CLR targeting with TLR stimuli can induce cross-talk and alter the intracellular fate of CLR bound cargo. We previously showed that simultaneous TLR4 and DC-SIGN triggering translocated DC-SIGN cargo into the cross-presentation pathway, most likely via endosomal escape and proteasomal degradation [17]. Also combined activation of Langerin and TLR3 enhanced CD8^{+} T cell activation [18], but a direct link between Langerin and TLR3 signaling for cross-presentation has not yet been demonstrated.

Combination of glycan CLR targeting and TLR stimulation is gaining interest in the vaccination field as it can elicit superior humoral and cellular immunity when incorporated within a single vaccine particle [45, 46]. Our dual CLR targeting G3 glyco-dendrimers have the potential for adjuvant coupling, which is an interesting feature for future research into glyco-adjuvant vaccines for intradermal anti-tumor vaccination strategies. Furthermore, recent advances in anti-tumor immunotherapies show the importance of neo-antigens and CD4^{+} T cell help for induction of long

Chapter 4

lasting anti-tumor CD8^{+} T cell immunity [47, 48]. The high branched multivalent G3 glyco-dendrimers allow inclusion of multiple TAA, such as neo-antigens and combined CD4 and CD8 restricted epitopes, thereby generating a highly diverse vaccine platform. Here we already combined the melanoma specific gp100 HLA-DR4 and HLA-A2 restricted epitopes for activation of both CD4^{+} and CD8^{+} gp100 specific T cells (**Figure S3 and figure 4**).

Evaluating the therapeutic efficacy and immune responses induced upon multiple DC subset targeting of our newly designed glyco-vaccine would be of great importance. However, since we specifically designed a glyco-vaccine for dual targeting of DC-SIGN and Langerin on human skin DC, a murine model with comparable expression by similar DC subsets is imperative. Although the murine CD209a/SIGNR5, or mDC-SIGN, displays some similarities to the human counterpart [49] the glycan binding profile has not been studied. As such, a humanized DC-SIGN murine model would be needed to evaluate *in vivo* efficacy of our glyco-vaccine specifically designed to target human DC-SIGN. While a humanized DC-SIGN murine model is available, it harbors DC-SIGN expression under the CD11c promotor thereby containing multiple hDC-SIGN[+] DC subsets [50]. Unfortunately, this renders the model unsuitable for the glyco-vaccine of this study since human skin has restricted DC-SIGN expression to CD14^{+} and CD1a^{+} dermal DCs (**Figure 3B**).

In summary, we designed an intradermal glyco-vaccine simultaneously targeting multiple human skin DC subsets *in situ*. Simultaneous targeting was accomplished by the use of G3 glyco-dendrimers targeting both DC-SIGN and Langerin, which enhanced activation of gp100 specific CD8^{+} T cells in combination with TLR stimulation. These promising results pave the way for future studies investigating the *in vivo* behavior of G3 glyco-dendrimers following intradermal vaccination and induction of systemic anti-tumor immune responses via dual DC-SIGN and Langerin targeting.

Material and methods

Cells
OUW, OUW-DC-SIGN and OUW-Langerin B cell lines were cultured in RPMI (Invitrogen, USA) supplemented with 10% FCS (Lonza), 50U/ml penicillin, 50ug/ml streptomycin, 2mM glutamine (all BioWhittaker, USA) (complete RMPI).

Monocytes were isolated from buffy coats (Sanquin, The Netherlands) using serial Ficoll/Percoll gradient centrifugation and cultured in complete RPMI. For human moDC differentiation and DC-SIGN expression, rhGM-CSF plus rhIL-4 (500U/ml; Biosource, Belgium) were added for 4-6 days.

Primary LCs were isolated from human skin explants (Bergman Clinics, Bilthoven, The Netherlands) obtained within 24 hours following abdominal resection of healthy donors with informed consent. Part of the epidermal and dermal sheet (5-mm thickness) were removed using a dermatome blade (Zimmer, Germany), rinsed with PBS plus gentamycin (10μg/ml; Lonza) and incubated in serum free IMDM supplemented with 50U/ml penicillin, 50ug/ml streptomycin, 2mM glutamine, gentamycin and dispase II (1mg/ml, Roche Diagnostics) for 2 hours at 37°C. The epidermal sheet was separated from the dermis using tweezers, followed by two day culture in IMDM supplemented with 10% FCS, penicillin, streptomycin, glutamin, gentamycin (complete IMDM skin medium) and rhGM-CSF (500U/ml) for LC migration at 37°C. LCs were harvested and purified using a Ficoll gradient (>85%). For purity evaluation LCs were incubated with anti-human antibodies against HLA-DR (clone G46-6, BD Biosciences), CD1a (clone HI149, BD Biosciences) and Langerin (clone 10E2, Biolegend).

MUTZ-LC were kindly provided by Prof. dr. S. Gibbs and cultured as previously described [51]. Cells were used when >70% were CD1a and Langerin positive.

The retroviral TCRαβ transduced T cell clone specific for the $gp100_{280-288}$ HLA-A2 minimal epitope (YLEPGPVTA) [52] and HLA-DRB1*0401-restricted T cell line Bridge gp:44 B8 [53] were cultured in IMDM medium (Invitrogen), supplemented with Yssel's medium (20 μg/ml human transferrin (Boehringer), 5 μg/ml insulin (Sigma-Aldrich), 2 μg/ml linoleic acid (Calbiochem), 2 μg/ml palmitic acid (Calbiochem), 0.25% BSA (Sigma-Aldrich), and 1.8 μg/ml 20-amino ethanol (Sigma-Aldrich)), 1% human serum (Sigma-Aldrich) and penicillin, streptomycin, glutamin. Cells were expanded for 10-12 days in the presence of IL-2 (100IU/ml; Peprotech) and PHA-L (2μg/ml; Sigma) prior to storage in liquid nitrogen. For co-cultures T cells were either used at day 12 in expansion or thawed and rested for at least 6 hours before co-culture.

FACS staining, measurement and analysis

A pre-mix of surface marker antibodies diluted in PBS plus 0,5% BSA (0,5% PBA; Roche) was prepared prior to incubation for 30 minutes on ice. Unbound antibodies were washed away with PBS, followed by fixation using 4% paraformaldehyde (PFA; Electron Microscopy Science) for 20 minutes on ice. Next, cells were washed two times with PBS and resuspended in 0,5% PBA for measurement using the FACS Fortessa-X20 (BD). Analysis was performed with FlowJo 10 software (Tree Star, Ashland, OR, USA).

Peptide synthesis

Thz-VTHTYLEPGPVTANRQLYPEWTEAQRLD-(Abu)$_3$-C peptide was synthesized at the GlycO2pep unit at our lab by microwave assisted solid phase peptide synthesis using Fmoc chemistry on a peptide synthesizer (Liberty blue peptide synthesizer, CEM). The peptide was deprotected with 92.5% TFA, 2.5% MilliQ, 2.5% TIS and 2,5% EDT cleavage solution. After collection, the peptide was lyophilized and purified on a preparative Ultimate 3000 HPLC system (Thermo Fisher) over a Vydac 218MS1022 C18 25x250mm column (Grace Vydac). Mass and purity were confirmed by UHPLC-MS on a Ultimate 3000 UHPLC system (Thermo Fisher) hyphenated with a LCQ-Deca XP Iontrap ESI mass spectrometer (Thermo Finnigan) using a RSLC 120 C18 Acclaim 2.2um particle 2.1 x 250 mm column and ionizing the sample in positive mode.

Glyco-dendrimer synthesis

G0/G3-Gp100-AF488-Lewis Y constructs were synthesized via thiol-ene mediated reactions. In short, PAMAM generation 0 or 3 dendrimer (Sigma) were functionalized with maleimide or LC-SMCC bifunctional crosslinker (ThermoFisher), respectively. After purification, the dendrimer was loaded with GP100 long synthetic peptide Thz-VTHTYLEPGPVTANRQLYPEWTEAQRLD-(Abu)$_3$-C through its C- terminal cysteine. After removing the excess peptide, labelling and glycation was achieved by unmasking the N-terminal thioproline (Thz; Novabiochem) and reacting it with AF488 (Invitrogen) /Lewis Y (Elicityl) pentasaccharide maleimide. G0 dendrimer MW was determined using mass spectrometry. Particle size of G3-PAMAM-GP100, dissolved in MilliQ at 0.1 mg/ml and 0.05 mg/ml, was determent using a dynamic and static light scattering measurement (Malvern Zetasizer Nano S, Breda, Netherlands). The average of 3 measures was used to calculate the particle size. These measurements indicate that the average particle size of our peptidic dendrimer is 52.03 nm.

Binding ELISA DC-SIGN-Fc and Langerin-Fc

DC-SIGN-Fc and Langerin-Fc were obtained as previously described [54]. Dendrimers with and without LeY conjugation were coated on NUNC maxisorb plates (Roskilde) o/n at 4°C. Following removal of free dendrimers with TSM for DC-SIFN-Fc or HBSS (Invitrogen) for Langerin-Fc wash, wells were blocked using 1% BSA (Fraction V, Fatty acid free, PAA laboratories) in TSM or HBSS. Next, dendrimers were incubated with 2µg/ml DC-SIGN-Fc or Langerin-Fc diluted in TSM or HBSS plus 0,5% BSA, respectively, for 2 hours at RT. After 3 washes, binding was detected using a HRP-labeled F(ab')2 goat anti-human IgG specific antibody. HRP binding was visualized using 3,3',5,5'-tetramethylbenzidine (TMB) substrate (Sigma Aldrich) followed by measurement at 450nm.

Binding and uptake assays

Triplicates of $5x10^4$ cells were plated in a 96-U bottom plate (Greiner) and incubated with AF488 conjugated (glyco)-dendrimers or vehicle control (max. 0,2% DMSO) diluted in serum free IMDM for LCs and complete RPMI for moDCs. When indicated cells were pre-incubated for 1 hour at 4°C, followed by incubation at 37°C for indicated time-points. Next, cells were stained with a fixable viability dye eFluor780 (FVD; eBioscience), anti-human HLA-DR BV510, CD1a APC (clone HI149; BD) (moDC) and EpCAM BV421 (clone EBA-1; Biolegend) (LCs). Binding and uptake was analyzed using FACS.

For antibody blocking assays cells were pre-incubated with 20µg/ml mouse-anti-human IgG1 Langerin (10E2) or DC-SIGN (AZN-D1) for 30 minutes at 37°C, followed by addition of (glyco)-dendrimers for 1 hour at 37°C with blocking antibodies at a final concentration of 10µg/ml. For 3 hour pre-incubation cells were incubated with a 10x serial dilution starting at 10µg/ml AZN-D1, washed and cultured for 1 hour with (glyco)-dendrimers at 37°C. Liposomes with LeY were taken along as positive control for AZN-D1 blocking assays. For DC-SIGN block using mannan moDC were pre-incubated for 30 minutes with a 10x serial dilution starting at 100µg/ml, followed by co-incubation with 0,01µM (glyco)-dendrimers.

Imaging microscopy

MoDC or primary LC were pulsed for 3 hours with glyco-dendrimers at 37 °C, as described above. Cells were transferred to ice and stained with anti-human CD1a-biotin (clone HI149; Biolegend) for 30 minutes, washed and subsequently stained

using streptavidin-AF555 (Invitrogen) for 30 minutes on ice. Next, cells were washed in ice cold PBS and fixed with 4% PFA for 20 minutes on ice prior to nuclei stain using DAPI for 10 minutes at RT. Cells were mounted on slides using MoWIOL. Z-stack images were taken with the Leica DM6000 at 63x magnification and images were analyzed using Imaris Software.

Antigen presentation assay
APC were seeded in 96-wells plates at a concentration of $2x10^5$/ml and pulsed with (glyco)-dendrimers or DMSO vehicle control in complete medium for 3 hours at 37°C. MoDC were pulsed in presence or absence of 10µg/ml MPLA (Invivogen) and primary LCs of 20µg/ml Poly I:C (Invivogen). Pulsed APC were washed and co-cultured with the gp100$_{280-288}$ specific T cell clone. For T cell degranulation, moDC were washed two times at 900rpm to remove free products and co-cultured with gp100 T cells in a 3:1 effector to target ratio for 45 minutes at 37°C. To measure degranulation cells were stained with a FVD, anti-human CD8 BV421 (clone RPA-T8, BD), CD107a (clone H4A3, Biolegend) and CD107b Fitc (clone H4B4, Biolegend).

For IFNγ production by T cells, moDC were pulsed for 30 minutes and LC for 3 hours at 37°C and co-cultured in a 1:5 effector to target ratio for 16-21hours. IFNγ production was measured in supernatant using human cytokine ELISA (IFNγ Ready-Set-Go kit, eBioscience) according to manufacturer's protocol. Incubation with a short peptide containing the HLA-A2 minimal epitope was used to set maximum activation levels per experiment.

In situ human skin DC targeting
Human skin explants (obtained as described above) were prepared by cleaning with PBS supplemented with gentamycin. Products were diluted in serum free IMDM prior to injection. Insulin needles were used to inject 20µl/biopsy i.d. at 66pmol/ml so a small blister appeared. A punch biopsy (8mm; Microtec) surrounding the blister was taken and 8 biopsies per condition were cultured with the epidermis facing upwards in a 48-wells-plate with 1ml IMDM complete skin medium for 48hours. Biopsies were discarded and crawl-out cells harvested and pooled per condition prior to FACS staining. To distinguish the different emigrated skin DC subsets cells were stained using the following anti-human antibodies: HLA-DR BV510, CD1a APC, CD14 AF700 (clone M5E2, Sony), CD141 BV711 (clone 1A4, Biolegend), EpCAM BV421 and FVD. For DC-SIGN and Langerin expression levels extra biopsies were taken and emigrated

DCs stained with above cocktail plus anti-DC-SIGN AF488 (AZN-D1; own production) and anti-Langerin PE (10E2; Biolegend).

Statistical analysis

Statistical analysis were performed using Graphpad Prism version 7.02 software (San Diego, CA). Statistical significance was determined using one- or two-way ANOVA followed by Tukey's, Sidak's or Dunnett's **post hoc** analysis as indicated per graph in figure legends. Data are represented as mean ±SD or symbol per donor. *ns = not significant, *P < 0.05, **P < 0.01, ***P < 0.001, ****P < 0.0001*.

Abbreviations

APC: antigen presenting cell; CLR: c-type lectin receptor; CRD: carbohydrate recognition domain; DC: dendritic cell; DC-SIGN: dendritic cell-specific ICAM-grabbing non-integrin; G0: generation 0; G3: generation 3; LC: Langerhans cell; Le: Lewis; MHC: major histocompatibility complex; moDC: monocyte derived DC; MR: mannose receptor; PAMAM: polyamidoamine; PRR: pathogen recognition receptor; TLR: toll-like receptor

Acknowledgements

Author contributions

S.D., Y.K. designed the study. S.D., S.K.H., L.R. conducted the experiments, acquisition and analyzed the data. H.K. and M.A. were involved in compound synthesis. S.D., J.J.GV., T.D.G. and Y.K. contributed to conception and interpretation of the work. S.D. and Y.K. wrote the manuscript. All authors were involved in discussion of results and critical revisions of the manuscript.

Competing interests

The authors have declared that no competing interest exists.

References

1. Steinman RM, Banchereau J. Taking dendritic cells into medicine. Nature. 2007; 449: 419-26.
2. Banchereau J, Briere F, Caux C, Davoust J, Lebecque S, Liu YJ, et al. Immunobiology of dendritic cells. Annu Rev Immunol. 2000; 18: 767-811.
3. Melief CJ, Kast WM. Cytotoxic T lymphocyte therapy of cancer and tumor escape machanisms. Semin Cancer Biol. 1991; 2: 347-54.
4. Embgenbroich M, Burgdorf S. Current Concepts of Antigen Cross-Presentation. Front Immunol. 2018; 9: 1643.
5. van Dinther D, Stolk DA, van de Ven R, van Kooyk Y, de Gruijl TD, den Haan JMM. Targeting C-type lectin receptors: a high-carbohydrate diet for dendritic cells to improve cancer vaccines. J Leukoc Biol. 2017; 102: 1017-34.
6. Schreibelt G, Klinkenberg LJ, Cruz LJ, Tacken PJ, Tel J, Kreutz M, et al. The C-type lectin receptor CLEC9A mediates antigen uptake and (cross-)presentation by human blood BDCA3^{+} myeloid dendritic cells. Blood. 2012; 119: 2284-92.
7. Burgdorf S, Lukacs-Kornek V, Kurts C. The mannose receptor mediates uptake of soluble but not of cell-associated antigen for cross-presentation. J Immunol. 2006; 176: 6770-6.
8. van Kooyk Y, Unger WW, Fehres CM, Kalay H, Garcia-Vallejo JJ. Glycan-based DC-SIGN targeting vaccines to enhance antigen cross-presentation. Mol Immunol. 2013; 55: 143-5.
9. Dhodapkar MV, Dhodapkar KM. Recent advances and new opportunities for targeting human dendritic cells in situ. Oncoimmunology. 2014; 3: e954832.
10. Kastenmuller K, Wille-Reece U, Lindsay RW, Trager LR, Darrah PA, Flynn BJ, et al. Protective T cell immunity in mice following protein-TLR7/8 agonist-conjugate immunization requires aggregation, type I IFN, and multiple DC subsets. J Clin Invest. 2011; 121: 1782-96.
11. Haniffa M, Gunawan M, Jardine L. Human skin dendritic cells in health and disease. J Dermatol Sci. 2015; 77: 85-92.
12. Hung IFN, Yuen KY. Immunogenicity, safety and tolerability of intradermal influenza vaccines. Hum Vaccin Immunother. 2018; 14: 565-70.
13. Fehres CM, Garcia-Vallejo JJ, Unger WW, van Kooyk Y. Skin-resident antigen-presenting cells: instruction manual for vaccine development. Front Immunol. 2013; 4: 157.
14. Klechevsky E. Functional diversity of human dendritic cells. Adv Exp Med Biol. 2015; 850: 43-54.
15. Saliba H, Heurtault B, Bouharoun-Tayoun H, Flacher V, Frisch B, Fournel S, et al. Enhancing tumor specific immune responses by transcutaneous vaccination. Expert Rev Vaccines. 2017; 16: 1079-94.
16. Fehres CM, Kalay H, Bruijns SC, Musaafir SA, Ambrosini M, van Bloois L, et al. Cross-presentation through Langerin and DC-SIGN targeting requires different formulations of glycan-modified antigens. J Control Release. 2015; 203: 67-76.
17. Horrevorts SK, Duinkerken S, Bloem K, Secades P, Kalay H, Musters RJ, et al. Toll-Like receptor 4tTriggering promotes cytosolic routing of DC-SIGN-targeted antigens for presentation on MHC class I. Front Immunol. 2018; 9: 1231.
18. Fehres CM, Duinkerken S, Bruijns SC, Kalay H, van Vliet SJ, Ambrosini M, et al. Langerin-mediated internalization of a modified peptide routes antigens to early endosomes and enhances cross-presentation by human Langerhans cells. Cell Mol Immunol. 2017; 14: 360-70.

19. Alloatti A, Kotsias F, Pauwels AM, Carpier JM, Jouve M, Timmerman E, et al. Toll-like receptor 4 engagement on dendritic cells restrains phago-lysosome usion and promotes cross-presentation of antigens. Immunity. 2015; 43: 1087-100.

20. Manolova V, Flace A, Bauer M, Schwarz K, Saudan P, Bachmann MF. Nanoparticles target distinct dendritic cell populations according to their size. Eur J Immunol. 2008; 38: 1404-13.

21. Mottram PL, Leong D, Crimeen-Irwin B, Gloster S, Xiang SD, Meanger J et al. Type 1 and 2 immunity following vaccination is influenced by nanoparticle size: formulation of a model vaccine for respiratory syncytial virus. Mol Pharm. 2006; 4(1): 73-84.

22. Szeto GL, Lavik EB. Materials design at the interface of nanoparticles and innate immunity. J Mater Chem B. 2016; 4: 1610-8.

23. Iborra S, Sancho D. Signalling versatility following self and non-self sensing by myeloid C-type lectin receptors. Immunobiology. 2015; 220: 175-84.

24. van der Aar AMG, Sylva-Steenland RMR, Bos JD, Kapsenberg ML, de Jong EC, Teunissen MBM. Cutting edge: Loss of TLR2, TLR4, and TLR5 on Langerhans cells abolishes bacterial recognition. J Immunol. 2007; 178: 1986-90.

25. Renn CN, Sanchez DJ, Ochoa MT, Legaspi AJ, Oh CK, Liu PT, et al. TLR activation of Langerhans cell-like dendritic cells triggers an antiviral immune response. J Immunol. 2006; 177: 298-305.

26. Flacher V, Bouschbacher M, Verronese E, Massacrier C, Sisirak V, Berthier-Vergnes O, et al. Human Langerhans cells express a specific TLR profile and differentially respond to viruses and gram-positive bacteria. J Immunol. 2006; 177: 7959-67.

27. Fox LJ, Richardson RM, Briscoe WH. PAMAM dendrimer - cell membrane interactions. Adv Colloid Interface Sci. 2018; 257: 1-18.

28. Fehres CM, van Beelen AJ, Bruijns SCM, Ambrosini M, Kalay H, Bloois LV, et al. In situ delivery of antigen to DC-SIGN(+)CD14(+) dermal dendritic cells results in enhanced CD8(+) T-cell responses. J Invest Dermatol. 2015; 135: 2228-36.

29. Geijtenbeek TBH, van Kooyk Y. DC-SIGN functions as a pathogen receptor with broad specificity. APMIS 2003; 111: 698–714.

30. de Jong MA, Geijtenbeek TB. Langerhans cells in innate defense against pathogens. Trends Immunol. 2010; 31: 452-9.

31. Mc Dermott R, Ziylan U, Spehner D, Bausinger H, Lipsker D, Mommaas M, et al. Birbeck granules are subdomains of endosomal recycling compartment in human epidermal Langerhans cells, which form where Langerin accumulates. Mol Biol Cell. 2002; 13: 317-35.

32. Uzan-Gafsou S, Bausinger H, Proamer F, Monier S, Lipsker D, Cazenave JP, et al. Rab11A controls the biogenesis of Birbeck granules by regulating Langerin recycling and stability. Mol Biol Cell. 2007; 18: 3169-79.

33. Thépaut M, Valladeau J, Nurisso A, Fiechi F. Structural Studies of Langerin and Birbeck Granule: A Macromolecular Organization Model. Biochemistry. 2009; 48: 2684-98.

34. Garcia-Vallejo JJ, Ambrosini M, Overbeek A, van Riel WE, Bloem K, Unger WW, et al. Multivalent glycopeptide dendrimers for the targeted delivery of antigens to dendritic cells. Mol Immunol. 2013; 53: 387-97.

35. Smith PES, Brender JR, Dürr UH, Xu J, Mullen DG, Holl MMB, et al. Solid-state NMR reveals the hydrophobic-core location of poly(amidoamine) dendrimers in biomembranes. J Am Chem Soc. 2010; 132: 8087–97.

36. Tabarani G, Reina JJ, Ebel C, Vives C, Lortat-Jacob H, Rojo J, et al. Mannose hyperbranched dendritic polymers interact with clustered organization of DC-SIGN and inhibit gp120 binding. FEBS Lett. 2006; 580: 2402-8.

37. Cambi A, de Lange F, van Maarseveen NM, Nijhuis M, Joosten B, van Dijk EM, et al. Microdomains of the C-type lectin DC-SIGN are portals for virus entry into dendritic cells. J Cell Biol. 2004; 164: 145-55.

38. Zhang Y, Luo Y, Li W, Liu J, Chen M, Gu H, et al. DC-SIGN promotes allergen uptake and activation of dendritic cells in patients with atopic dermatitis. J Dermatol Sci. 2016; 84: 128-36.

39. Holla A, Skerra A. Comparative analysis reveals selective recognition of glycans by the dendritic cell receptors DC-SIGN and Langerin. Protein Eng Des Sel. 2011; 24: 659-69.

40. Bigley V, McGovern N, Milne P, Dickinson R, Pagan S, Cookson S, et al. Langerin-expressing dendritic cells in human tissues are related to CD1c^{+} dendritic cells and distinct from Langerhans cells and CD141high XCR1^{+} dendritic cells. J Leukoc Biol. 2015; 97: 627-34.

41. Kitano M, Yamazaki C, Takumi A, Ikeno T, Hemmi H, Takahashi N, et al. Imaging of the cross-presenting dendritic cell subsets in the skin-draining lymph node. Proc Natl Acad Sci U.S.A. 2016; 113: 1044-9.

42. Terhorst D, Fossum E, Baranska A, Tamoutounour S, Malosse C, Garbani M, et al. Laser-assisted intradermal delivery of adjuvant-free vaccines targeting XCR1^{+} dendritic cells induces potent antitumoral responses. J Immunol. 2015; 194: 5895-902.

43. Haniffa M, Shin A, Bigley V, McGovern N, Teo P, See P, et al. Human tissues contain CD141hi cross-presenting dendritic cells with functional homology to mouse CD103^{+} nonlymphoid dendritic cells. Immunity. 2012; 37: 60-73.

44. Haniffa M, Collin M, Ginhoux F. Identification of human tissue cross-presenting dendritic cells: A new target for cancer vaccines. Oncoimmunology. 2013; 2: e23140.

45. Wilson DS, Hirosue S, Raczy MM, Bonilla-Ramirez L, Jeanbart L, Wang R, et al. Antigens reversibly conjugated to a polymeric glyco-adjuvant induce protective humoral and cellular immunity. Nat Mater. 2019; 18: 175-85.

46. Boks MA, Ambrosini M, Bruijns SC, Kalay H, van Bloois L, Storm G, et al. MPLA incorporation into DC-targeting glycoliposomes favours anti-tumour T cell responses. J Control Release. 2015; 216: 37-46.

47. Ahrends T, Spanjaard A, Pilzecker B, Babala N, Bovens A, Xiao Y, et al. CD4([+]) T cell help confers a cytotoxic T cell effector program including coinhibitory receptor downregulation and increased tissue invasiveness. Immunity. 2017; 47: 848-61 e5.

48. Yarchoan M, Johnson BA, 3rd, Lutz ER, Laheru DA, Jaffee EM. Targeting neoantigens to augment antitumour immunity. Nat Rev Cancer. 2017; 17: 209-22.

49. Schetters STT, Kruijssen LJW, Crommentuijn MHW, Kalay H, Ochando J, den Haan JMM, et al. Mouse DC-SIGN/CD209a as target for antigen delivery and adaptive immunity. Front Immunol. 2018; 9: 990.

50. Schaefer M, Reiling N, Fessler C, Stephani J, Taniuchi I, Hatam F, et al. Decreased pathology and prolonged survival of human DC-SIGN transgenic mice during mycobacterial Infection. J Immunol. 2008; 180: 6836-45.

51. Kosten IJ, Spiekstra SW, de Gruijl TD, Gibbs S. MUTZ-3 derived Langerhans cells in human skin equivalents show differential migration and phenotypic plasticity after allergen or irritant exposure. Toxicol Appl Pharmacol. 2015; 287: 35-42.

52. Schaft N, Willemsen RA, de Vries J, Lankiewicz B, Essers BWL, Gratama JW, et al. Peptide fine specificity of anti-glycoprotein 100 CTL is preserved following transfer of engineered TCR genes into primary human T lymphocytes. J Immunol. 2003; 170: 2186-94.

53. Aarnoudse CA, Bax M, Sanchez-Hernandez M, Garcia-Vallejo JJ, van Kooyk Y. Glycan modification of the tumor antigen gp100 targets DC-SIGN to enhance dendritic cell induced antigen presentation to T cells. Int J Cancer. 2008; 122: 839-46.

Chapter 4

54. Geijtenbeek TB, van Duijnhoven GC, van Vliet SJ, Krieger E, Vriend G, Figdor CG, et al. Identification of different binding sites in the dendritic cell-specific receptor DC-SIGN for intercellular adhesion molecule 3 and HIV-1. J Biol Chem. 2002; 277: 11314-20.

Supplementary material and methods

MPBH functionalization of Lewis Y pentasaccharide - The bifunctional cross-linker (4-Nmaleimidophenyl) butyric acid hydrazide (MPBH) was covalently linked to the reducing end of the Lewis Y pentasaccharide via reductive amination. Briefly 1 equivalent of Lewis Y pentasaccharide (50 mg, 0.06 mmoles) was dissolved in 1 ml 20% acetic acid in DMSO containing 2.7 equivalents of MPBH (50 mg, 0.16 mmoles). 5.4 Equivalents of 2-Methylpyridine borane complex (34 mg, 0.32 mmoles) was added as reductant and the mixture was incubated at 65^{0}C for 2 hours. After 2 hours 3 ml DCM is added and vortexed thoroughly. 10 ml Diethyl ether is added to precipitate further the MPBH activated Lewis Y pentasaccharide. After pelleting by centrifugation and pellet was washed 2 times more with diethyl ether. The activated glycan was dissolved in 0.1% TFA-MilliQ, lyophilized and subsequently purified on a preparative Ultimate 3000 HPLC system (Thermo Fisher) over a Vydac 218MS1022 C18 25x250mm column (Grace Vydac). Mass and purity were confirmed by UHPLC-MS on a Ultimate 3000 UHPLC system (Thermo Fisher) hyphenated with a LCQ-Deca XP Iontrap ESI mass spectrometer (Thermo Finnigan) using a RSLC 120 C18 Acclaim 2.2um particle 2.1 x 250 mm column and ionizing the sample in positive mode.

G0-PAMAM-Maleimide synthesis -To a solution of ethylenediamine core PAMAM Generation 0.0 dendrimer (15.4 mg, 29.81 μmoles) in 1 ml anhydrous DMSO was added to 5 equivalents of (succinimidyl 4-(N-maleimidomethyl)cyclohexane-1-carboxylate) (50 mg, 149.05 μmoles). After thoroughly vortexing 15 uL of 2,4,6-Trimethylpyridine was added in 5 aliquots of 3 μL over 30 minutes. The reaction mixture was placed on a shaker for 1 hour at room temperature. Subsequently the reaction mixture was transferred into a 50 ml falcon tube and 20 ml DCM was added. After vortexing thoroughly 25 ml Diethyl ether mixture was added to precipitate maleimide functionalized dendrimer. G0-PAMAM-maleimide was pelleted by centrifugation and washed 3 times with diethyl ether. Final product was dissolved and purified on a preparative Ultimate 3000 HPLC system (Thermo Fisher) over a Vydac 218MS1022 C18 25x250mm column (Grace Vydac). Mass and purity were confirmed by UHPLC-MS on a Ultimate 3000 UHPLC system (Thermo Fisher) hyphenated with a LCQ-Deca XP Iontrap ESI mass spectrometer (Thermo Finnigan) using a RSLC 120 C18 Acclaim 2.2um 2.1 x 250 mm column. Mass spectrometer analysis was measured in positive mode.

G3-PAMAM-LC-SMCC synthesis - To a solution of ethylenediamine core PAMAM Generation 3.0 dendrimer (16.08 mg, 2.33 µmoles) in 1 ml anhydrous DMSO was added to 48 equivalents of (succinimidyl 4-(N-maleimidomethyl)cyclohexane-1-carboxy-(6-amidocaproate)) (50 mg, 149.05 µmoles). After thoroughly vortexing 15 uL of 2,4,6-Trimethylpyridine was added in 5 aliquots of 3 µL over 30 minutes. 100 µL of 3% TFA in MilliQ was added to the reaction mixture and product was purified on a preparative Ultimate 3000 HPLC system (Thermo Fisher) over a Vydac 218MS1022 C18 25x250mm column (Grace Vydac). Fractions containing the product were pooled and lyophilized.

G0/G3-gp100-Thz synthesis - To a solution of G0-PAMAM-maleimide (3.7 mg, 2.66 µmoles) or G3-PAMAM-maleimide (5.8 mg, 0.331 µmoles) in 1 ml anhydrous DMSO either 5 (G0) or 40 (G3) equivalents of Thz-VTHTYLEPGPVTANRQLYPEWTEAQRLD-(Abu)3-C peptide (50 mg, 13.24 µmoles) were added in a 15 ml falcon tube. After thoroughly vortexing 15 uL of 2,4,6-Trimethylpyridine was added in 5 aliquots of 3 µL over 30 minutes. The reaction mixture was placed on a shaker for 3 hours at room temperature in the dark. 100 µL of 3% TFA in MilliQ was added to the reaction mixture and product was purified on a preparative Ultimate 3000 HPLC system (Thermo Fisher) over a Vydac 218MS1022 C18 25x250mm column (Grace Vydac). G0-gp100-ThZ mass and purity were confirmed by UHPLC-MS on a Ultimate 3000 UHPLC system (Thermo Fisher) hyphenated with a LCQ-Deca XP Iontrap ESI mass spectrometer (Thermo Finnigan) using a RSLC 120 C18 Acclaim 2.2um 2.1 x 250 mm column. Mass spectrometer analysis was measured in positive mode. G3-gp100-Thz fractions containing the product were pooled and lyophilized.

G0/G3-gp100-SH - For unmasking the N-terminal thioproline lyophilized peptidic dendrimer was dissolved in 1 ml Thz-deprotection solution (NaAc buffer pH 4.5, 6M Gu.HCl, 0.1M Methoxylamine) and incubated at room temperature for 4 hours while shaking. The unmasked peptidic dendrimer G0-or G3-GP100-SH was purified over C18 500 mg SPE according to manufacturer's protocol. Deprotected peptidic dendrimer was brought to dryness by lyophilisation.

G0/G3-Gp100-AF488/LewY construct - The G0- and G3-Gp100-SH were functionalized with either 1 (G0) or 3 (G3) equivalents of AF488-maleimide in 1 ml DMSO containing 100 mM 2,4,6-Trimethylpyridine. After 10 minutes, either 4 (G0) or 42 (G3) equivalents of Lewis Y-MPBH were added to half of the mix and the reaction

was prolonged for 2 hours at room temperature on a shaker. 3 ml of DCM was added and after vortexing thoroughly 10 ml Diethyl ether was added to precipitate the labelled and glycated peptidic dendrimer. Construct was pelleted by centrifugation and washed 2 times with diethyl ether. Pellet was dissolved in MilliQ and brought to dryness by lyophilisation. Lyophilized construct was dissolved in 2 ml MilliQ-0.1% TFA and washed 6 times over 10 kD centrifugal filter to remove all excess labels and glycans. Retentate was collected and brought to dryness by lyophilisation.
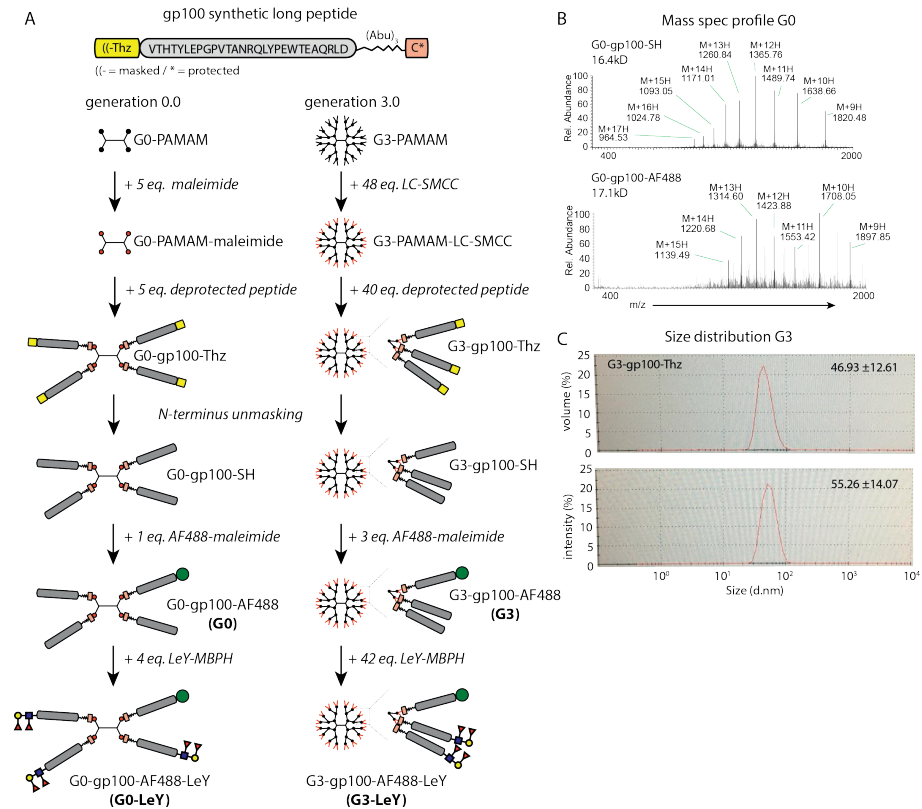
Figure S1. (Glyco)-dendrimer synthesis and characterization A Schematic representation of (glyco)-dendrimer synthesis. **B** Mass spectrometry profile of G0-gp100-dendrimers depicting their molecular weight (MW) without (upper panel) and with AF488 (lower panel). **C** Size determination of G3-gp100-dendrimers using a dynamic and static light scattering measurement. Average particle size was determined based on volume (upper panel) and intensity (lower panel).
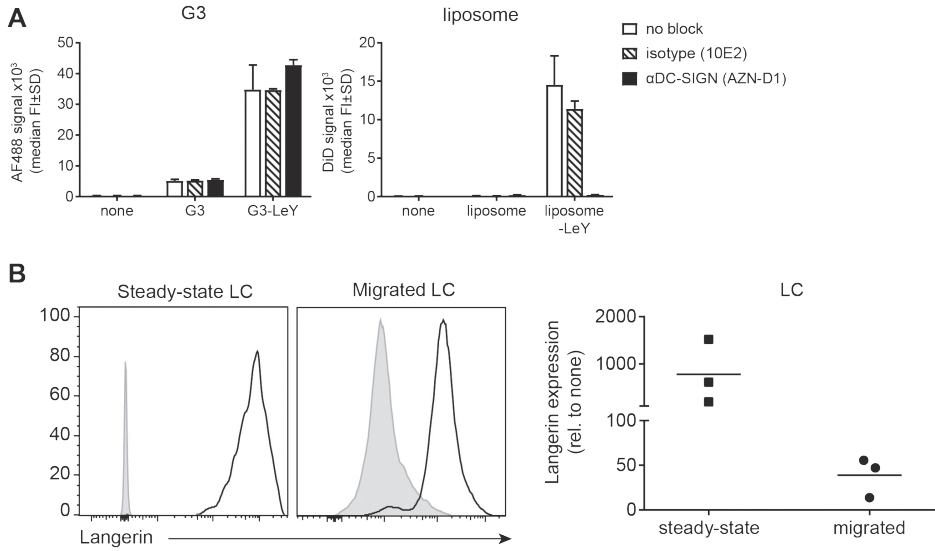
Figure S2. A Binding and uptake of (glyco)-dendrimers (left panel) or (glyco)-liposomes (right panel) by moDC following pre-incubation with an anti-DC-SIGN blocking antibody or matched isotype control. **B** Langerin expression by LC isolated from human epidermal sheets using dissociation (steady-state) or two day emigration.
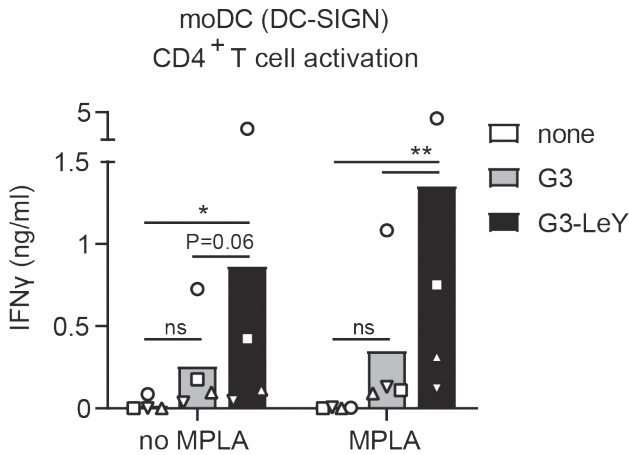
Figure S3. Enhanced activation of gp100 specific CD4+ T cells by glyco-dendrimer pulsed moDC MoDC were pulsed with (glyco)-dendrimers for 30 minutes followed by an o/n co-culture with gp100 specific CD4+ T cells. T cell activation was evaluated by IFNγ ELISA. n=4, each symbol represents a donor. (Statistical analysis: two-way ANOVA Tukey's post hoc)
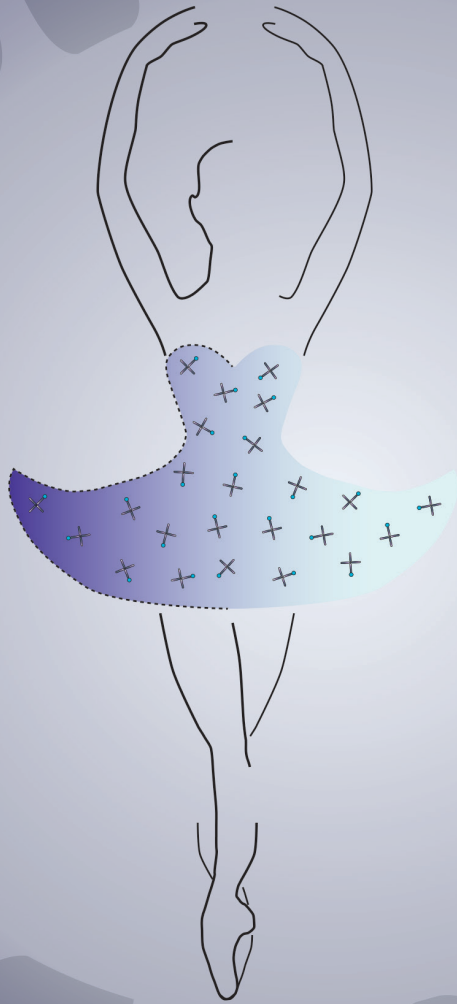
CHAPTER 5

DENDRIMERS FUNCTIONALIZED WITH NOD2-LIGANDS BOOST INTRADERMAL PEPTIDE-BASED ANTI-TUMOR VACCINATION

Sanne Duinkerken, Lisa Rutte, Sven Bruijns, Sophie K. Horrevorts, Martino Ambrosini, Hakan Kalay, Juan J. Garcia-Vallejo and Yvette van Kooyk

Abstract

The activation of adaptive immunity through vaccination can occur either prophylactic or therapeutically. The use of therapeutic anti-cancer vaccination strategies aiming to instruct DC *in vivo* are emerging, as it brings advantages compared to *ex vivo* DC instruction. Prophylactic vaccines against viruses such as the flu benefit from intradermal injection compared to the current standard of intramuscular delivery. This can be attributed to the presence of a vast network of dendritic cells (DC) within the skin. As such, developing intradermal anti-cancer vaccination strategies to specifically activate skin DC holds promise to enhance anti-tumor immune responses. Though, vaccines which only harbor tumor specific peptides have low immunogenicity and need addition of adjuvants for DC maturation to trigger T cell mediated cancer immunity. DC express a variety of pattern recognition receptors (PRR) that react to pathogen associated molecular patterns (PAMP) to induce DC maturation. The use of synthetic PRR agonists have paved the way for making vaccines more immunogenic. Within the PRR family are toll-like receptors (TLR) and NOD-like receptors (NLR), which synergize for induction of DC maturation and subsequent T cell responses. The effect of NLR stimulation on human skin DC phenotype and function following intradermal vaccine delivery has not yet been investigated. Using a PAMAM-dendrimer core we developed a multivalent tumor antigen-adjuvant complex (MAAC) harboring a NOD2 agonist. Here we tested the effects of MAAC on human skin micro-milieu, DC maturation, and its antigen processing and presentation upon intradermal vaccination. Intradermal injection of the NOD2 agonist conjugated MAAC, resulted in enhanced pro-inflammatory cytokine secretion within the skin micro-milieu and CD8^{+} T cell activation by human skin DC. This was enhanced in combination with the TLR4 stimulus MPLA. Overall, this newly developed tumor specific MAAC shows potential as vaccine adjuvant that warrants further investigation of NOD2 stimulation to induce anti-tumor immunity through intradermal vaccination.

Introduction

Dendritic cells (DC) are imperative for the working mechanism of vaccination, as they initiate adaptive immune responses by instruction of T cells. This instruction induces both effector T cell responses and, importantly, immunological memory. Initially developed for infectious diseases, now vaccination strategies are also being explored for anti-tumor immunotherapy [1]. Anti-tumor vaccines aim to induce cytotoxic T lymphocytes (CTL) due to their killing capacity and recognition of MHC I bound antigens expressed by all tumor cells. To this end, peptides holding tumor specific antigen sequences are used to give the vaccine its tumor specificity.

Intradermal vaccination shows promise due to the presence of a vast DC network and the relative easy accessibility of the skin [2]. However, skin DC have an immature phenotype and will induce immune tolerance, rather than inflammation, when only antigenic peptides are administered [1]. Hence, vaccines need adjuvants combined with the antigenic peptides to induce DC maturation and robust anti-tumor immune responses.

DC express pattern recognition receptors (PRRs), including C-type lectin receptors (CLRs), Toll-like receptors (TLRs), RIG-I-like receptors (RLRs) and NOD-like receptors (NLRs), which are the innate immune sensors for invading pathogens. Triggering of PRR on DC with pathogen associated molecular patterns (PAMP) induces DC maturation for co-stimulatory, survival and skewing signals to T cells [3]. Consequently, PRR properties are explored for the use in vaccination strategies to induce proper adaptive immunity. Synthetic antigenic peptides are combined with mainly TLR agonists to induce DC maturation and increase vaccine immunogenicity [4]. Different TLR agonists have been explored for intradermal vaccination strategies, such as agonists for TLR3 (poly I:C) [5], TLR4 (LPS, MPLA) [6] and TLR7/8 (R848, imiquimod, Aldara) [7], showing diverse responsiveness by the different skin DC subsets. Simultaneous triggering of different classes of PRR can result in synergy, such as described for TLR and NOD in DC derived from monocytes and in *in vivo* settings using mouse models [8-10]. Interestingly, NOD2 stimulation is implicated with positive effects in anti-cancer immunotherapy [11], also following intradermal administration in the skin [12]. Though, the combination of antigen and a NOD2 agonist for intradermal anti-tumor vaccination has yet to be elucidated in human skin.

The peptidoglycan (PGN) minimal bioactive motif muramyl dipeptide (MDP) is a NOD2 specific agonist [13], which has potent adjuvant activity for vaccination. MDP can be added within its soluble form in *in vitro* culture systems to investigate its effect on DC activation. However, *in vivo* it is easily cleared from the system and in tissues it may activate (immune) cells other than DC. Many different variations of the MDP derivatives have been developed to overcome these issues [11]. Interestingly, studies show that conjugation of MDP-like molecules within antigenic constructs can enhance vaccine efficacy [14]. As the skin is rich in many immune cell types, such as mast cells, T cells and APC, and strongly irrigated, the use of an antigenic construct with conjugated MDP is an attractive option to investigate skin DC specific uptake and activation.

In this study, we developed a tumor specific, multivalent antigen-adjuvant construct (MAAC) harboring a NOD2 agonist. We show conjugation of a synthetic MDP variant remained functional for induction of DC cytokine secretion, in combination with TLR4 stimulation. Furthermore, there is induction of pro-inflammatory cytokine secretion within the skin micro-milieu upon *in situ* vaccination. Upon *ex vivo* DC stimulation with the MAAC and a TLR agonist, we show enhanced tumor specific CD8+ T cell activation. Overall, our MAAC with NOD2 agonist can be used to further investigate induction of anti-tumor immunity upon intradermal vaccination.

Results and discussion

Conjugation of synthetic MDP to the tumor specific antigenic construct retains DC stimulating properties

To synthesize a tumor specific, antigenic construct containing a NOD2 agonist, we used the generation 0 PAMAM-dendrimer core (G0-PAMAM). First, we synthesized a tumor specific multivalent antigenic dendrimer (MAD), with reactive N-terminal sites for NOD2 agonist conjugation. A synthetic long peptide (SLP) containing a CD4 and CD8 specific epitope of the gp100 melanoma model peptide was synthesized and conjugated through the C-terminal end to the G0-PAMAM. Since the commonly used NOD2 agonist muramyl-di-peptide (MDP) cannot be conjugated to the MAD, we used the synthetic variant muramyl tripeptide (M-triLYS), shown to have similar activating properties [10, 15]. M-TriLYs was conjugated at the N-terminal end of the gp100 specific MAD, to create a multivalent antigen-adjuvant complex (MAAC) (schematic representation **Figure 1A**).

The conformation of MDP-like molecules which are covalently linked to antigenic constructs can influence their functionality [14]. To test whether the NOD2 MAAC retained NOD2 stimulation for DC activation, monocytes were cultured for 5 days with GM-CSF and IL4 for moDC differentiation. MoDC were subsequently stimulated for 3 hours with the MAD, MAD plus soluble MDP or the MAAC, washed and cultured overnight. Soluble MDP was added in an equal concentration as conjugated within the MAAC. Activation was measured by the release of cytokines within the supernatant. As expected, addition of MAD alone did not induce moDC activation (**Figure 1B**, *grey bars*).
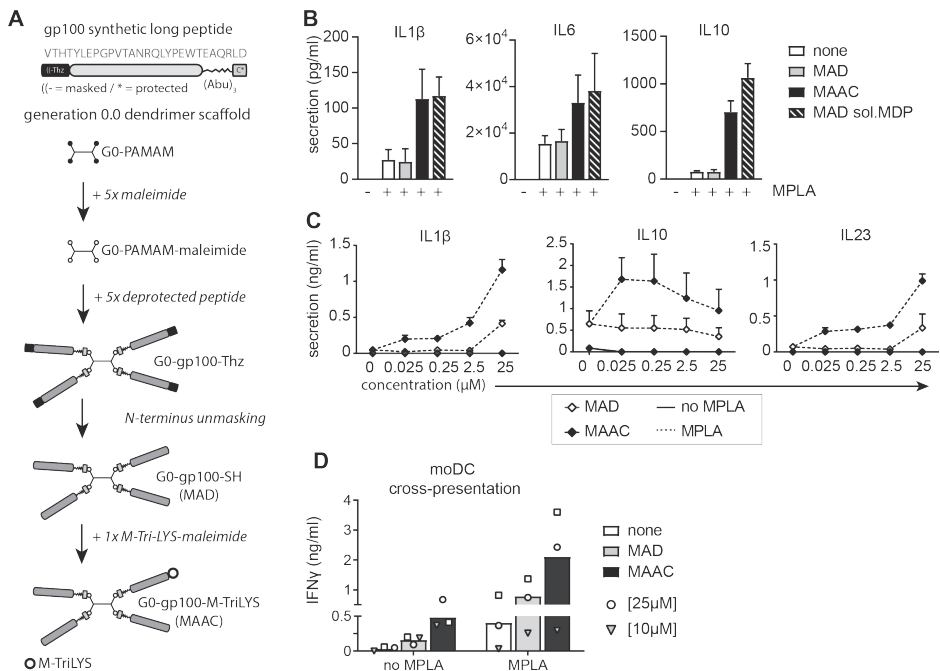
Figure 1. Antigenic dendrimer scaffold harboring a synthetic NOD2 agonist activates moDC (A) schematic representation of antigen and synthetic MDP coupling to a generation 0.0 dendrimer scaffold. (B) Cytokine secretion by moDC pulsed with MAD, MAAC and MAD plus soluble MDP (12,5μg/ml) in the presence of MPLA for 3 hours, followed by o/n culture (n=2±SD) (C) Dose dependent cytokine secretion by moDC following 3 hour pulse with dendrimers and o/n culture. (IL1β repr of n=2, IL10/23 n=2±SD). (D) gp100 specific CD8$^+$ T cell activation, as measured by IFNγ production of T cells co-cultured overnight with moDC pulsed with antigenic-dendrimers for 3 hours in the absence or presence of MPLA (n=3, each dot represents a donor).

It has been previously shown that moDC need the subsequent activation of TLRs to perceive NOD2 signaling [8], because TLR signaling induces release of NOD2 ligands from and NOD2 recruitment to the endosome [16]. We incubated moDC with the MAD and MAAC in the presence of the TLR4 agonist monophosphoryl lipid A (MPLA). We observed secretion of IL1β, IL6 and IL10 following addition of soluble MDP in combination with the TLR4 stimulus MPLA (**Figure 1B** *striped bars*), showing the need of dual PRR stimulation. Cytokine secretion by moDC was maintained with conjugation of the synthetic variant to the MAAC, with a slight decrease in IL10 secretion (**Figure 1B** *closed bars*). This indicates that NOD2 stimulation can be induced by addition of synthetic MDP (M-TriLYS) to the MAD.

Next, we elucidated the dose-response curve for cytokine secretion by moDC stimulated with the MAAC, in the presence of a constant concentration MPLA. MDP is known to activate the inflammasome through NOD2 stimulation [17]. Therefore, we measured secretion of the inflammasome induced cytokines IL1β and IL23, and the anti-inflammatory cytokine IL10. As expected, no cytokine secretion was observed following MAD and MAAC stimulation in the absence of MPLA (**Figure 1C** *solid line*). In contrast, both IL1β and IL23 secretion increased with increasing concentrations of the MAAC in the presence of MPLA (**Figure 1C** *dotted line*). Interestingly, we observed a decrease in IL10 production with increasing concentration of the MAAC and, hence, increasing concentration of the synthetic MDP. Other studies show the production of IL10 upon simultaneous TLR4 and NOD2 triggering. Though, here the concentration of both MDP and LPS remains equal, or, only a varying concentration of LPS is used. This indicates that the IL10 production is mainly driven by the TLR triggers and not NOD2 [8]. The negative effect of increasing concentrations of MDP for NOD2 stimulation on IL10 production as seen here, has not been described elsewhere. These data show the simultaneous stimulation of TLR4 and NOD2 has a delicate balance for the induction of pro-inflammatory versus anti-inflammatory responses.

Simultaneous stimulation of NOD2 and TLR was shown to affect DC antigen handling and presentation [18-20]. Thus, we verified antigen cross-presentation capacity of moDC upon endocytosis of the MAD and MAAC. To this end, moDC followed a 3 hour pulse with the respective antigenic dendrimers and were subsequently co-cultured overnight with a gp100 specific T cell clone recognizing the HLA-A2 minimal epitope build within the MAD (**Figure 1A**). We observed a significant increase in gp100 specific CD8+ T cell activation when moDC were pulsed with the MAAC, that

included the synthetic NOD2, compared to the MAD (**Figure 1D**). When moDC were pulsed simultaneously with MAD or MAAC and MPLA this further enhanced CD8^{+} T cell activation (**Figure 1D**). These data show that synthetic MDP can be used for conjugation to MAD for DC stimulation and antigen handling to induce antigen specific CD8^{+} T cell responses. This allows us to further elucidate the effect of human skin DC NOD2 stimulation following intradermal vaccination using the MAAC.

MAAC enhance pro-inflammatory cytokine secretion within skin micro-milieu

To evaluate the effect of *in situ* MAAC injection on the human skin micro-milieu, we made use of a human skin explant model [7]. The human skin explant model represents the steady-state situation of skin resident (immune) cells to investigate the effect of our vaccine following intradermal injection. The model can either be used for *in situ* vaccine injection (**Figure 2A**), or by specifically isolating the DC for *ex vivo* antigen loading (**Figure 3A**). First, we evaluated whether human skin DC endocytose the MAD following *in situ* intradermal injection. To this end, AF488 was conjugated to the N-terminal end of the MAD instead of synthetic MDP, according to a similar synthesis scheme as presented in Figure 1A [21]. Dendrimers were injected below the epidermis until a small blister appeared. Next, biopsies were directly taken and cultured for 2 days to allow skin DC emigration. DC were harvested and uptake per subset was analyzed using flow cytometry by staining of the cell surface markers CD1a, CD14, CD141 (dermal DC) and EpCAM (LC), as previously described [21] (**Figure 2A**). We observed uptake of the MAD-AF488 by all human skin DC subsets (**Figure 2B**), but not by HLA-DR negative non-APC (data not shown).

To analyze the effect of NOD2 stimulation following intradermal injection, we measured cytokine secretion within biopsy cultured supernatants. Since we observed the need for concomitant TLR stimulation in moDC (**Figure 1**), we co-injected MAD and MAAC with MPLA for TLR4 stimulation. We found increased secretion of IL1β, IL6 and IL8 in the presence of MPLA and the MAAC (**Figure 2C**). There was a minimal increase in IL10 production (**Figure 2C**), which might reflect the decrease in IL10 production with higher concentration MAAC and thus synthetic MDP, as seen in figure 1C.
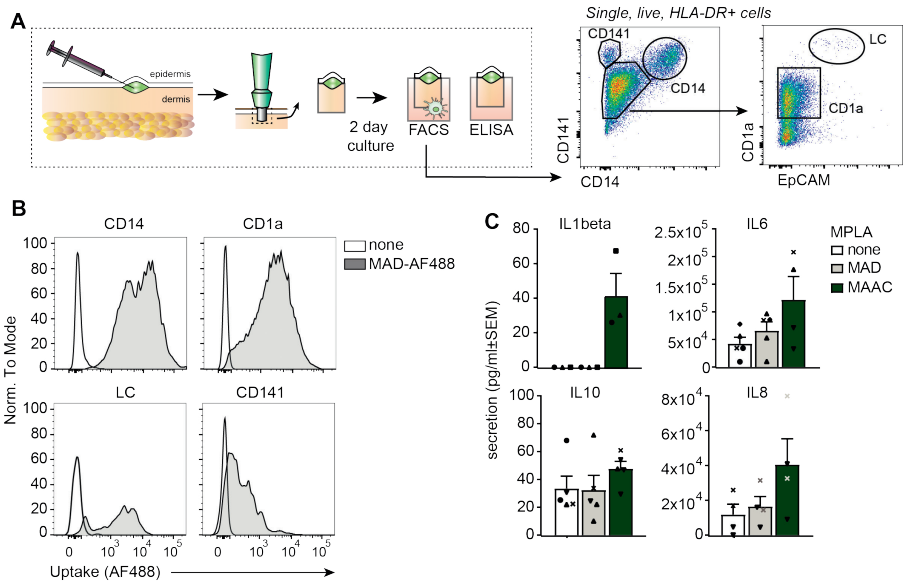
Figure 2. MDP-dendrimers enhance pro-inflammatory cytokine secretion within the skin micro-milieu (A) Schematic representation of dendrimer injection in a human skin explant model followed by 2 day culture of skin biopsies for skin DC emigration and supernatant conditioning. (B) Uptake of antigenic dendrimers with AF488 by human skin DC subsets as measured by FACS. (C) Cytokine secretion in full skin biopsy conditioned medium following injection of antigenic MAD or MAAC (33μM) in the absence or presence of MPLA (10μg/ml). n=3±SD, each symbol represents a donor

Cytokines were measured within full skin biopsy conditioned medium and, thus, we cannot discriminate whether human skin DC were responding to the MDP-dendrimer or via other skin resident cell types such as keratinocytes through immune cell cross-talk [22]. Keratinocytes also express NLRs and can potentially respond to NOD2 agonists [23]. However, the synthetic MDP is covalently linked to the MAD and we did not observe any uptake of MAD by non-APCs, which makes it is unlikely that keratinocytes will directly respond via NOD2 stimulation. Overall, these data indicate that the skin micro-milieu may be altered through the appearance of influx of innate immune cells such as neutrophils (IL8) upon NOD2 stimulation [24].

Human skin DC process MAAC for antigen retrieval and subsequent CD8+ T cell activation

To elucidate antigen presentation by human skin DC following MAD uptake, epidermal and dermal sheets from skin explants were cultured for 48 hours to allow dermal DC and LC emigration (**Figure 3A**). In moDC we observed the additive effect of

concomitant TLR4 stimulation with MAAC pulse, for cytokine secretion and CD8^{+} T cell activation (**Figure 1B-D**). However, TLR expression differs between dermal DC and LC, causing the need for differential TLR stimulation. LC express viral sensing TLR, such as TLR3, whereas dermal DC express both viral and bacterial sensors such as TLR4 [25]. As such, we used the TLR3 stimulus Poly I:C for LC activation and MPLA for dermal DC stimulation through TLR4 activation.

Emigrated skin DC were harvested and equal amount of LC and dermal DC were pulsed with the dendrimers *ex vivo* for 3 hours in the presence of Poly I:C (LC) or MPLA (dermal DC). Next, DC were washed prior to overnight co-culture with the gp100 specific T cell clone (**Figure 3A**). Interestingly, when testing two donors, we observed for dermal DC that one donor clearly responded to NOD2 stimulation leading to increased cross-presentation, whereas LC showed enhanced antigen presentation by both the MAD and MAAC (**Figure 3**). It appears that the increased CD8^{+} T cell activation was dependent on the simultaneous NOD2-TLR4 triggering.
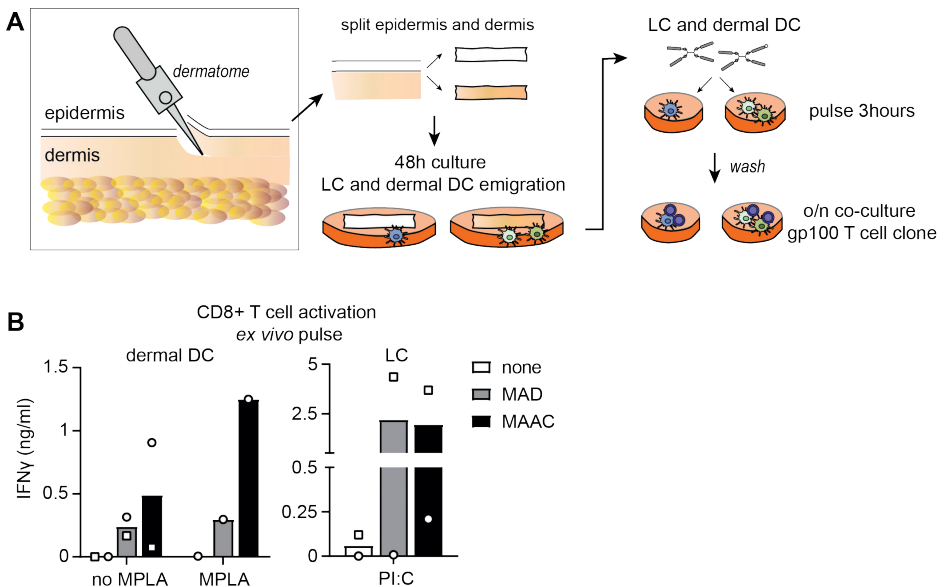
Figure 3. Gp100 specific CD8^{+} T cell activation by human skin DC following MAAC pulse (A) Human skin was shaved and epidermal and dermal sheet separated for 2 day culture and LC and dermal DC emigration. Emigrated human skin DC were harvested and pulsed for 3 hours with (gp100) MAD or MAAC in the absence or presence of a TLR stimulus prior to o/n co-culture with a gp100 specific T cell clone. (B) CD8^{+} T cell activation by dermal DC (left) pulsed in the presence or absence of MPLA and LC (right) pulsed in the presence of Poly I:CPoly I:C. CD8^{+} T cell activation was measured using IFNγ cytokine ELISA. (n=2, each symbol represents a donor)

The simultaneous NOD2-TLR3 stimulation induced MAAC cross-presentation by LC for one of the two donors (**Figure 3,** *round symbol*). Thus, further investigation is necessary to pin point what dictates donor dependent enhancement of antigen processing for CD8$^+$ T cell activation upon MAAC endocytosis and NOD2 stimulation. NOD2 comes in a variety of polymorphisms differing between individuals which may explain the variety in antigen processing following stimulation [26]. Furthermore, there is a delicate balance between the human skin microbiome and resident immune cells [27]. Changes in this symbiotic relationship may influence APC responses to PRR stimuli, such as NOD2, thereby inducing differential antigen processing upon NOD2 stimulation between human donors.

NOD2 MAAC for future intradermal vaccination strategies

In light of our findings with moDC and partly human skin DC (**Figures 1D** and **3B**), it would be interesting to further investigate the effect of simultaneous TLR and NOD2 stimulation on the processing of antigens for MHC I loading by human skin DC. NOD2 stimulation by MDP is implicated with enhanced DC autophagy for MHC II peptide loading and subsequent CD4$^+$ T cell activation [18, 28]. In this study we did not investigate the induction of gp100 specific CD4$^+$ T cell activation, however HLA-DR gp100 epitopes are included in the MAD and MAAC, indicating that this can be studied in future experiments.

Our designed MAAC harboring synthetic MDP can serve as tool for these type of studies. However, the SLP sequence can influence solubility and subsequent MAD synthesis and processing by DC. We found that substitution of the gp100 SLP with a CD8$^+$/HLA-A2 human CMV pp65 specific epitope hindered solubility. The hydrophobic nature of the CD8$^+$ specific epitope resulted in aggregation of the peptide (**Figure S1A**). Surprisingly, this aggravated when the SLP was conjugated to the G0 PAMAM-dendrimer core to synthesize the MAD (**Figure S1A**), although these are described to enhance solubility [29].

The advantage of using synthetic peptide vaccines is the possibility to chemically alter solubility. With our melanoma gp100 specific peptide we increased solubility by incorporating a CD4$^+$ T cell specific sequence, which has a more hydrophilic nature. Another approach is the addition of hydrophilic amino acids such as lysine (K). To this end, we elongated our CMVpp65 SLP with either a "CEEK-KEEK" sequence instead of the natural flanking amino acids, or added a lysine-tale (5K). Although the CEEK-

KEEK addition indeed ensured proper dissolving of the CMVpp65 SLP (**Figure S1B**), the SLP was no longer efficiently processed by DC for CD8^{+} T cell activation (**Figure S1C** *square*). In contrast, the 5K tale showed clear solution of the CMVpp65 SLP (**Figure S1B**) and processing by DC for CD8^{+} T cell activation (**Figure S1C** *triangle*). Interestingly, the 5K-tale CMVpp65 SLP showed higher CD8^{+} T cell activation by DC compared to the initial CMVpp65 SLP at lower concentration (**Figure S1C**).

An important aspect of DC induced immune responses is their migration to the draining lymph nodes for (naïve) T cell activation. Whether stimulation of NOD2 also induces enhanced DC migration has not been investigated. Though, it would be very interesting to evaluate the effect of simultaneous TLR and NOD2 stimulation on human skin DC migration. It has been described that DC CCR7 expression can increase upon TLR4 and NOD2 stimulation, however, this does not directly denote migration capacity [30]. Similarly, the spontaneous emigration of human skin DC from biopsies does not reflect lymph node homing properties. We developed an *ex vivo* human skin DC migration assay, where biopsy emigrated DC are loaded in a transwell system with the lymph node homing chemokine CCL21 (**Figure S2A**). Migration of the different human skin DC subsets can be evaluated using FACS by staining the different DC subsets as described in figure 2A. We tested the possibility to pre-inject human skin DC stimuli *in situ* prior to *ex vivo* migration using the previously described human skin DC stimuli GM-CSF and IL4 (GM/4). We found CD1a^{+} dermal DC and LC to have high migrational capacity towards CCL21 (**Figure S2B**). Interestingly, also approximately 20% of the CD14^{+} dermal DC subsets showed chemokine induced migration, which was further enhanced upon GM/4 stimulation (**Figure S2B**). It would be interesting to investigate migrational capacity of the different human skin DC subsets following intradermal delivery of the NOD2 MAAC, using this assay.

Overall, this study shows the MAAC harboring both antigen and a NOD2 agonist can be used to elucidate the effect of NOD2 stimulation via intradermal delivered vaccines.

Material and methods

Multivalent antigenic dendrimer and antigen-agonist complex synthesis
Multivalent antigenic dendrimers were synthesized as previously described [21]. In short, the gp100 SLP (Thz-VTHTYLEPGPVTANRQLYPEWTEAQRLD-(Abu)$_3$-C)

and CMVpp65 SLP (Thz-ILARNLVPMVATVQGQN / ILARNLVPMVATVQGQNKKKKK / CEEKNLVPMVATCKEEK -(Abu)$_3$-C) were synthesized using microwave assisted solid phase peptide synthesis at our GlycO2pep unit. To multimerize the SLP, a maleimide functionalized generation 0 PAMAM-dendrimer core was used. The SLP was conjugated through its C-terminal cysteine and added in 5 equivalents per dendrimer-core followed by removal of excess peptide, thereby synthesizing multivalent antigenic dendrimers (MAD). Next, the N-terminal thioproline (Thz) was unmasked and reacted with 4 equivalents maleimide-AF488 (Invitrogen) or M-TriLYS (Sigma) to synthesize MAD-AF488 or the multivalent antigen-agonist complex (MAAC) (**Figure.1A**), respectively.

Monocyte derived DC culture and stimulation

Monocytes isolated from buffycoats (Sanquin) using sequential Ficoll/Percoll gradient centrifugation, were cultured for 4-6 days in complete RPMI (10% FCS, pen/step/glut) containing rhIL4 and rhGM-CSF (500U/ml; Biosource) to generate moDC as previously described [31]. For moDC stimulation $5x10^4$cells/well were stimulated overnight with a serial dilution of either MAD or MAAC in the absence or presence of MPLA (10µg/ml). Soluble MDP (Sigma) was added in an equal concentration (12,5µg/ml) as present with addition of the MAAC. Supernatants were harvested and secretion of IL1β, IL6, IL10 and IL23 was measured using sandwich ELISA according to manufacturer's protocol (Bioscource).

Human skin explant model

Human skin explants (Bergman Clinics, Bilthoven, The Netherlands) were obtained within 24 hours following abdominal resection of healthy donors with informed consent.

In situ – Human skin explants were prepared by cleaning with PBS supplemented with gentamycin. Products were diluted in serum free IMDM prior to injection. Insulin needles were used to inject 20µl/biopsy i.d. at 66pmol/ml so a small blister appeared. A punch biopsy (8mm; Microtec) surrounding the blister was taken and 8 biopsies per condition were cultured with the epidermis facing upwards in a 48-wells-plate with 1ml IMDM complete skin medium (10% FCS, penicillin, streptomycin, glutamin, gentamycin) for 48hours. Biopsies were discarded and emigrated cells harvested and pooled per condition prior to FACS staining. To distinguish the different emigrated skin DC subsets cells were stained using the following anti-human antibodies:

HLA-DR BV510, CD1a APC, CD14 AF700 (clone M5E2, Sony), CD141 BV711 (clone 1A4, Biolegend), EpCAM BV421 and FVD.

Ex vivo – For *ex vivo* assays, primary LC and dermal DC were isolated by partially removing the epidermal and dermal sheet (5-mm thickness) using a dermatome blade (Zimmer, Germany). The skin sheet was rinsed with PBS plus gentamycin (10μg/ml; Lonza) and incubated in serum free IMDM supplemented with 50U/ml penicillin, 50ug/ml streptomycin, 2mM glutamine, gentamycin and dispase II (1mg/ml, Roche Diagnostics) for 2 hours at 37°C. The epidermal sheet was separated from the dermis using tweezers, followed by two day culture in complete IMDM skin medium supplemented with rhGM-CSF (500U/ml) for LC and dermal DC emigration at 37°C. Skin sheets were discarded and LC and dermal DC were harvested and purified using a Ficoll gradient (>85%). For purity evaluation cells were incubated with anti-human antibodies against HLA-DR (clone G46-6, BD Biosciences), CD1a (clone HI149, BD Biosciences), CD14 (clone M5E2, Sony) and Langerin (clone 10E2, Biolegend).

Antigen presentation assay

For antigen presentation assays $5x10^3$ APC were pulsed for 3 hours, washed and co-cultured with a gp100 specific T cell clone recognizing the HLA-A2 minimal epitope (YLEPGPVTA) [32] in a 1:5 T:E ratio. T cell activation was measured using IFNγ (Invivogen) sandwich EILSA according to manufacturer's protocol.

Human skin DC migration assay

Human skin DC were harvested following two day culture from biopsies as described above. Harvested DC from 8 biopsies were pooled and loaded on the top well of an 8μm pore transwell system (Corning, Sigma) with the chemokine CCL21 (250ng/ml) in the lower well. DC were incubated for 4 hours at 37°C to allow chemokine induced migration to the lower well. To evaluate human skin DC subset specific migration cells from both top and lower well were harvested and stained for HLA-DR, CD1a, CD14, CD141 and EpCAM, followed by acquisition for 1 minute per sample using FACS. Migrated cells were calculated as percentage of total cell number (top $^+$ lower well) loaded on top: % migrated = $\dfrac{\text{\#DC lower well x 100}}{\text{total \# DC}}$

Cell staining and FACS measurement

Cells were incubated with membrane markers diluted in 0,5% BSA in PBS (PBA) for 30 minutes on ice, washed and fixated in 4% paraformaldehyde (PFA;..) for 20 minutes on ice. Next, cells were stained with a fixable viability dye (FVD; Invitrogen) for 5 minutes on RT, washed and resuspended in 0,5% PBA. Cells were measured using the FACS Fortessa X-20 and analyzed with FLowJo10 software.

Acknowledgements

Funding

Competing interests

All authors have no competing interests to declare.

References

1. Palucka, K. and J. Banchereau, *Cancer immunotherapy via dendritic cells.* Nat Rev Cancer, 2012. **12**(4): p. 265-77.

2. Fehres, C.M., et al., *Skin-resident antigen-presenting cells: instruction manual for vaccine development.* Front Immunol, 2013. **4**: p. 157.

3. van Vliet, S.J., et al., *Innate signaling and regulation of Dendritic cell immunity.* Curr Opin Immunol, 2007. **19**(4): p. 435-40.

4. Duthie, M.S., et al., *Use of defined TLR ligands as adjuvants within human vaccines.* Immunological Reviews, 2011. **29**: p. 178-196.

5. Fehres, C.M., et al., *Langerin-mediated internalization of a modified peptide routes antigens to early endosomes and enhances cross-presentation by human Langerhans cells.* Cell Mol Immunol, 2017. **14**(4): p. 360-370.

6. Fehres, C.M., et al., *In situ Delivery of Antigen to DC-SIGN(+)CD14(+) Dermal Dendritic Cells Results in Enhanced CD8(+) T-Cell Responses.* J Invest Dermatol, 2015. **135**(9): p. 2228-2236.

7. Fehres, C.M., et al., *Topical rather than intradermal application of the TLR7 ligand imiquimod leads to human dermal dendritic cell maturation and CD8+ T-cell cross-priming.* Eur J Immunol, 2014. **44**(8): p. 2415-24.

8. Schwarz, H., et al., *TLR8 and NOD signaling synergistically induce the production of IL-1beta and IL-23 in monocyte-derived DCs and enhance the expression of the feedback inhibitor SOCS2.* Immunobiology, 2013. **218**(4): p. 533-42.

9. Tukhvatulin, A.I., et al., *Powerful Complex Immunoadjuvant Based on Synergistic Effect of Combined TLR4 and NOD2 Activation Significantly Enhances Magnitude of Humoral and Cellular Adaptive Immune Responses.* PLoS One, 2016. **11**(5): p. e0155650.

10. Fritz, J.H., et al., *Synergistic stimulation of human monocytes and dendritic cells by Toll-like receptor 4 and NOD1- and NOD2-activating agonists.* Eur J Immunol, 2005. **35**(8): p. 2459-70.

11. Nabergoj, S., I. Mlinaric-Rascan, and Z. Jakopin, *Harnessing the untapped potential of nucleotide-binding oligomerization domain ligands for cancer immunotherapy.* Med Res Rev, 2019. **39**(5): p. 1447-1484.

12. Puri, N., et al., *An investigation of the intradermal route as an e€ective means of immunization for microparticulate vaccine delivery systems.* Vaccine, 2000. **18**: p. 2600-2612.

13. Girardin, S.E., et al., *Nod2 is a general sensor of peptidoglycan through muramyl dipeptide (MDP) detection.* J Biol Chem, 2003. **278**(11): p. 8869-72.

14. Willems, M.M., et al., *Lipophilic Muramyl Dipeptide-Antigen Conjugates as Immunostimulating Agents.* ChemMedChem, 2016. **11**(2): p. 190-8.

15. Macho Fernandez, E., et al., *Anti-inflammatory capacity of selected lactobacilli in experimental colitis is driven by NOD2-mediated recognition of a specific peptidoglycan-derived muropeptide.* Gut, 2011. **60**(8): p. 1050-9.

16. Nakamura, N., et al., *Endosomes are specialized platforms for bacterial sensing and NOD2 signalling.* Nature, 2014. **509**(7499): p. 240-244.

17. Hsu, L.-C., et al., *A NOD2–NALP1 complex mediates caspase-1-dependent IL-1β secretion in response to Bacillus anthracis infection and muramyl dipeptide.* Proc Natl Acad Sci U S A., 2008. **105**(22): p. 7803-8.

18. Cooney, R., et al., *NOD2 stimulation induces autophagy in dendritic cells influencing bacterial handling and antigen presentation.* Nat Med, 2010. **16**(1): p. 90-7.

19. Wagner, C.S. and P. Cresswell, *TLR and nucleotide-binding oligomerization domain-like receptor signals differentially regulate exogenous antigen presentation.* J Immunol, 2012. **188**(2): p. 686-93.

20. Corridoni, D., et al., *NOD2 and TLR2 Signal via TBK1 and PI31 to Direct Crosspresentation and CD8 T Cell Responses.* bioRxiv, 2019.

21. Duinkerken, S., et al., *Glyco-Dendrimers as Intradermal Anti-Tumor Vaccine Targeting Multiple Skin DC Subsets.* Theranostics, 2019. **9**(20): p. 5797-5809.

22. Nestle, F.O., D.H. Kaplan, and J. Barker, *Psoriasis.* New England Journal of Medicine, 2009. **361**: p. 496-509.

23. Voss, E., et al., *NOD2/CARD15 mediates induction of the antimicrobial peptide human beta-defensin-2.* J Biol Chem, 2006. **281**(4): p. 2005-11.

24. Ajendra, J., et al., *NOD2 dependent neutrophil recruitment is required for early protective immune responses against infectious Litomosoides sigmodontis L3 larvae.* Sci Rep, 2016. **6**: p. 39648.

25. Oosterhoff, D., et al., *Intradermal delivery of TLR agonists in a human explant skin model: preferential activation of migratory dendritic cells by polyribosinic-polyribocytidylic acid and peptidoglycans.* J Immunol, 2013. **190**(7): p. 3338-45.

26. Dominguez-Martinez, D.A., et al., *NOD2: Activation During Bacterial and Viral Infections, Polymorphisms and Potential as Therapeutic Target.* Rev Invest Clin, 2018. **70**(1): p. 18-28.

27. Dreno, B., et al., *Microbiome in healthy skin, update for dermatologists.* J Eur Acad Dermatol Venereol, 2016. **30**(12): p. 2038-2047.

28. Khan, N., et al., *Signaling through NOD-2 and TLR-4 Bolsters the T cell Priming Capability of Dendritic cells by Inducing Autophagy.* Sci Rep, 2016. **6**: p. 19084.

29. Svenson, S. and A.S. Chauhan, *Dendrimers for enhanced drug solubilization.* Nanomedicine, 2008. **3**(5): p. 679-702.

30. Khan, N., et al., *NOD-2 and TLR-4 Signaling Reinforces the Efficacy of Dendritic Cells and Reduces the Dose of TB Drugs against Mycobacterium tuberculosis.* J Innate Immun, 2016. **8**(3): p. 228-42.

31. Sallusto, F. and A. Lanzavecchia, *Efficient Presentation of Soluble Antigen by Cultured Human Dendritic Cells Is Maintained by Granulocyte/Macrophage Colony-stimulating Factor Plus Iuterleukin 4 and Downregulated by Tumor Necrosis Factor α* Journal of Experimental Medicin, 1994. **179**: p. 1109-1118

32. Schaft, N., et al., *Peptide Fine Specificity of Anti-Glycoprotein 100 CTL Is Preserved Following Transfer of Engineered TCR Genes Into Primary Human T Lymphocytes.* The Journal of Immunology, 2003. **170**(4): p. 2186-2194.

Supplementary data
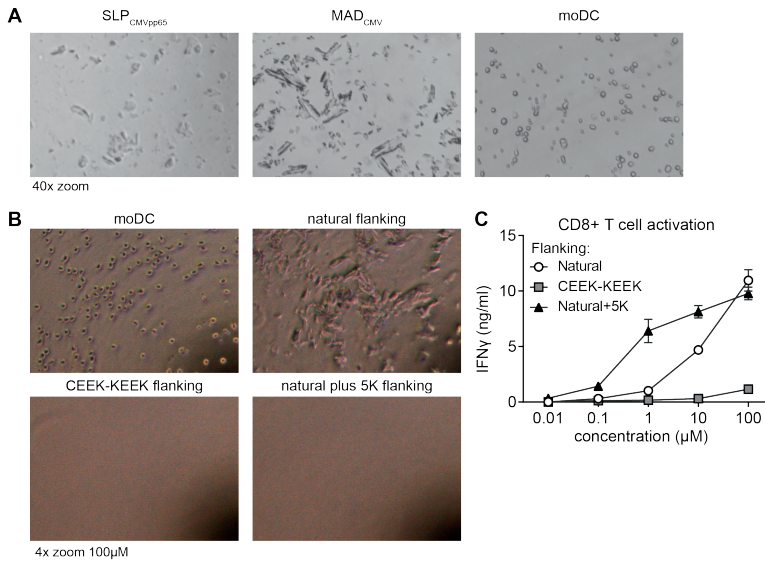
Figure S1. SLP sequence for MAD can influence solubility and processing (A) Aggregation of CMVpp65 SLP when dissolved in PBS. (B) Solubility of CMVpp65 SLP with chemically altered flanking amino acids. (C) Processing and presentation to CD8$^+$ T cells of three differential flanking sequences in the CMVpp65 SLP by moDC.
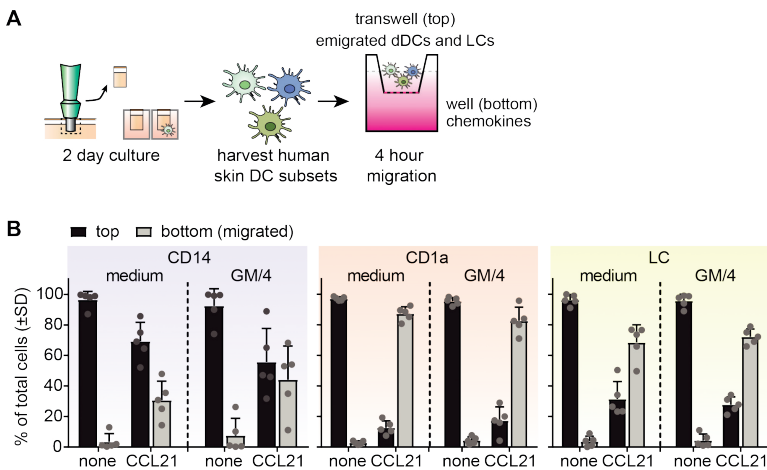
Figure S2. Human skin DC migration assay (A) schematic representation of the transwell migration assay using primary human skin DC emigrated out of human skin explants. (B) Migration towards CCL21 of the different human skin DC subsets as percentage of total cells loaded in topwell. Skin was injected prior to emigration with medium or GM-CSF and IL4 (GM/4). n=5 each dot represents a donor
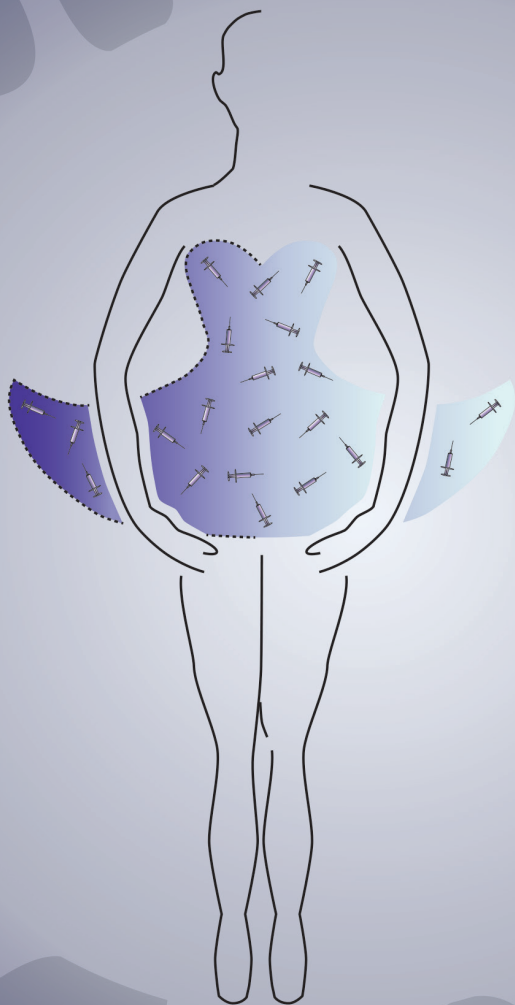
CHAPTER 6

COMPARISON OF INTRADERMAL INJECTION AND EPICUTANEOUS LASER MICROPORATION FOR ANTITUMOR VACCINE DELIVERY IN A HUMAN SKIN EXPLANT MODEL

Sanne Duinkerken, Joyce Lübbers, Dorian A Stolk, Jana Vree, Martino Ambrosini, Hakan Kalay and Yvette van Kooyk

ABSTRACT

Human skin is a prime vaccination site containing multiple antigen presenting cells (APC), including Langerhans cells (LC) and dendritic cells (DC). APC deliver antigens to lymph nodes for induction of adaptive immunity through stimulating antigen specific T- and B-cells. Since intradermal (ID) injections require specific training, easy applicable delivery systems like laser microporation are emerging. In mice, combination of laser treatment and allergen injection showed enhanced T-cell responses and skewing of B-cell responses without adjuvants. However, it remains to be elucidated whether laser microporation can alter human skin DC phenotype and function without adjuvants. In an *ex-vivo* human skin explant model, we compared ID injection and laser microporation as anti-tumor vaccination strategy. A melanoma specific synthetic long peptide and multivalent dendrimer with gp100 antigen were used as vaccine formulation to measure APC phenotype, emigration and ability to stimulate gp100 specific CD8^{+} T-cells. We show that skin APC phenotype and emigration capacity was similar after laser microporation and ID injection. However, laser microporation reduced vaccine uptake by APC, resulting in decreased induction of gp100 specific CD8^{+} T-cell activation. To conclude, in our human skin model ID injection remains the most potent strategy to deliver antigens to skin APC for T-cell induction.

INTRODUCTION

The human skin is a potent vaccination site as it contains numerous antigen presenting cells (APC), including epidermal Langerhans cells (LC), dermal dendritic cells (dDC) and monocyte derived macrophages (moMØ)[1]. APCs in the dermis can be subdivided into three distinct subsets: CD1a^{+} dDC, CD141^{+} dDC, CD14^{+} moMØ and a small population of Langerin^{+} dDC[1,2]. APC constantly scan their environment to detect changes in homeostasis, and are equipped with a plethora of pattern recognition receptors (PRR), such as toll-like receptors (TLR) that detect invading pathogens[3]. To help DC internalize antigenic content, DC express uptake receptors like C-type lectin receptors (CLR) that further process endocytosed pathogens into antigenic fragments to present on major histocompatibility complex (MHC) molecules. DC carry MHC presented antigenic peptides to draining lymph nodes for instruction of T-cell mediated adaptive immune responses[4]. LC and CD1a^{+} dDC are natural inducers of cytotoxic CD8^{+} T-cell responses, whereas the skin resident CD14^{+} moMØ can do so following specific CLR targeting and uptake[5]. CD141^{+} dDC can rapidly migrate to the skin draining lymphnodes and represent 20-40% of the DCs in the lymphnode [1,2]. Furthermore, CD141^{+} dDC can skew the CD4^{+} T cell response to a th1 phenotype. Overall, the different skin APCs are excellent targets for vaccination strategies that can induce CD8^{+} T-cell responses required in the context of pathogens or tumors.

Compared to standard vaccine administration routes, skin immunization is more potent and dose-sparing[6]. Though, as intradermal (ID) injections require specific training and handling, most vaccination strategies still use subcutaneous or intramuscular vaccine delivery. In recent years new administration techniques have paved the way for easier and even pain free ID vaccination[7]. One of these techniques uses fractional laser ablation at a wavelength of water absorption to create clean micropores without thermally damaged ridges[8]. Depending on the settings, micropores can either disrupt the stratum corneum, reach into the epidermis or deeper into the dermis[9]. Multiple studies showed vaccine deposition within the skin already at minor disruption of the epidermis, thereby likely making vaccine particles available for endocytosis by skin APC[9].

An important aspect for induction of adaptive immunity by DC, is the activation of PRRs which induces DC maturation and is often accomplished by adjuvant inclusion into the vaccine. Mature APC present antigens in MHC molecules, express co-stimulatory markers and secrete cytokines for proper T-cell activation in the lymph

nodes[10,11]. The human skin is a plastic environment also containing non-immune cells such as keratinocytes and fibroblasts which can alter the environment by secretion of inflammatory cytokines[12] and thereby activate skin resident APCs. Furthermore, dermal vasculature allows for influx of innate cells such as monocytes. Interestingly, recent murine studies showed immunomodulation upon non-destructive laser treatment in combination with ID vaccine injection. This included enhanced vaccine uptake, DC motility and increased CD4+ T-cell numbers and antigen specific antibody titers[13]. Since this technique still requires ID injection, other studies investigated the potency of destructive lasers creating micropores for vaccine delivery and enhancement of immune responses. Although laser microporation efficiently delivers vaccine particles into the dermis[14], it was not directly compared to ID injection. Furthermore, the type of antigen appears to determine Th1 or Th2 skewing of immune responses and addition of adjuvant did not further enhance antibody titers compared to single laser treatment[15]. Thus, implying that laser microporation can be used for ID vaccine delivery and triggering of immune responses without a need for adjuvants.

Since both vaccination against pathogens and cancer require the induction of antibody responses and effective CD8+ T-cell responses, laser microporation may also be beneficial for anti-tumor vaccination strategies. A direct comparison between ID injection and laser microporation with tumor specific antigenic compounds needs to be tested in a human skin setting. In this study, we used a human skin explant model to investigate laser induced effects on human skin APC subsets. Using the P.L.E.A.S.E. laser device we compared epicutaneous laser microporation to ID injection of two tumor specific antigenic vehicles without adjuvant. Since tumor specific epitopes can be included in different types of vaccines, thereby favoring APC endocytosis[16], we tested a linear synthetic long peptide (SLP) of the melanoma antigen gp100 and a larger multivalent dendrimer comprising multiple gp100-SLP bound to a scaffold. Both laser microporation and ID injection resulted in equal numbers human skin APC subset emigration with identical phenotype. Although laser microporation supplied both vaccine compounds to all human skin APC subsets, a lower amount accumulated compared to ID injection, that resulted in decreased gp100 specific CD8+ T-cell activation. Overall, our data shows that tumor specific compounds reach human skin APC more efficient through ID injection, resulting in efficient tumor specific CD8+ T-cell stimulation.

RESULTS

ID injection and laser microporation induce equal skin APC emigration

The skin consists of the epidermis covered by the stratum corneum (SC) and the dermis which are connected by a basal membrane containing tight-junctions that provide a barrier function[17]. To ensure proper vaccine delivery to APCs in the skin, both the SC and basal membrane need to be crossed. Laser microporation creates micropores in the skin with different depths depending on the laser settings. We verified that in a human skin explant model, laser ablation with 23.7J/cm², four pulses and a depth of approximately 95μm as indicated by the P.L.E.A.S.E laser (**Figure S1a**) was sufficient to penetrate through the epidermis and basal membrane, while leaving the dermis intact to allow vaccine delivery to LC, dDC and moMØ. Therefore, these settings were used for vaccine delivery in comparison to ID injection in a human skin explant model.

First, we evaluated whether laser microporation can enhance skin APC emigration compared to ID injection by analyzing subset ratio and absolute number of skin resident APC emigrated out of cultured skin biopsies (schematic representation **Figure 1a**). Using specific markers, MHC II⁺ (HLA-DR) human skin APC subsets were separated into the different epidermal and dermal subsets based on their marker expression (**Figure S1b**), as previously described[18]. No differences were observed in skin APC subset emigration after two days of biopsy culture when skin was either untreated, ID injected or treated with laser microporation (**Figure 1b,c**). This indicates that laser microporation potentiates all human skin APC subsets to emigrate from the human skin equally well as ID injection.
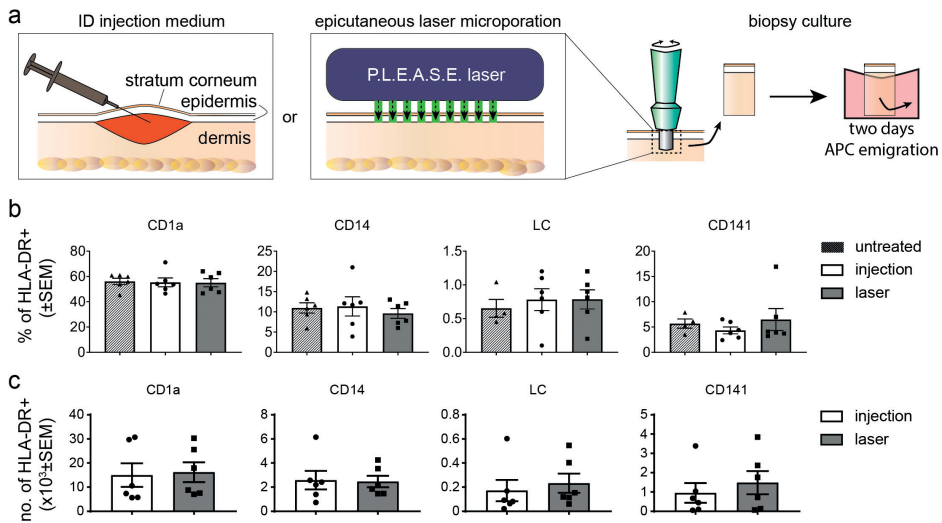
Figure 1. Equal human skin APC emigration following ID injection or laser microporation (A) Human skin explants were untreated or treated with ID injection using insulin needles or laser microporation using the P.L.E.A.S.E. Professional laser device. Biopsies were cultured for two days followed by evaluation of emigrated skin APC subset ratio (B) and absolute number for ID injection or laser poration. (C) n=6±SEM each dot represents a donor (Statistical analysis: Student's t-test showed no significant differences).

ID injection outperforms laser microporation for vaccine delivery to human skin APC

An important DC feature is their endocytic capacity for antigen or vaccine particle processing and subsequent presentation to T-cells in the lymph nodes. Antigen endocytosis by skin APC can be influenced by particle size and, as such, we used two sizes of synthetic vaccines to verify uptake by the different skin APC subsets following ID injection or laser microporation. A single SLP containing the melanoma specific gp100-epitope for presentation in MHC I, was either injected as linear peptide (~3kD) or coupled to a dendrimer with four functional groups to create a larger multivalent peptide structure (~20kD).
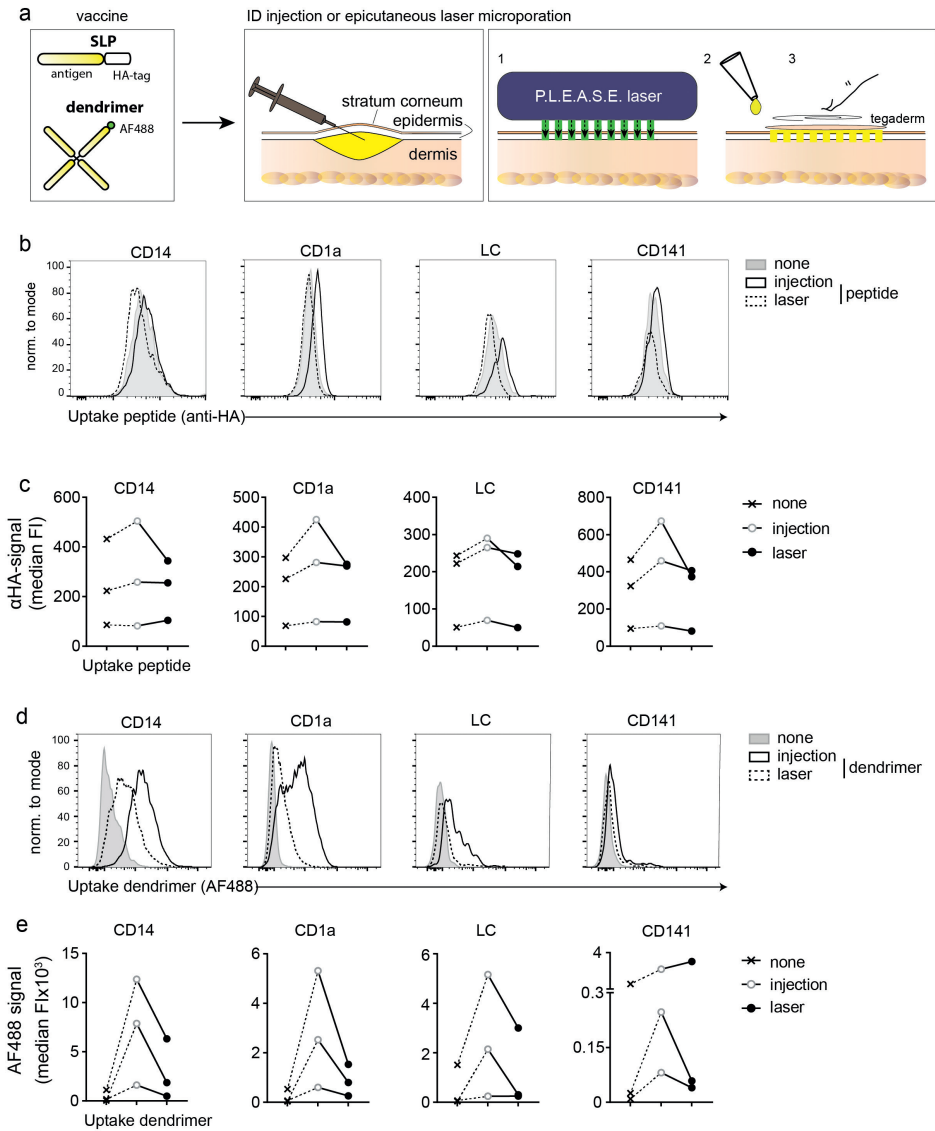
Figure 2. Superior vaccine uptake by skin APC following ID injection (A) Human skin explants were used to evaluate in situ uptake of SLP or dendrimers by the different skin APC subsets following ID injection or laser microporation. (B,C) HA-signal of gp100-peptides compared to medium ID injection with the secondary antibody against the HA-tag (none) and (D,E) AF488 signal of multivalent gp100-dendrimers taken up by the different human skin APC subsets compared to medium ID injection (none). n=3 with representative histograms, each dot represents a donor. Symbols represent different treatments.

Chapter 6

To evaluate uptake, the SLP amino acid sequence was elongated with an HA-tag and an AF488 was coupled to the dendrimer extremities (schematic representation **Figure 2a**). Using an insulin needle SLP or dendrimers were ID injected creating a small blister just under the epidermis of approximately $0.8cm^2$. For delivery following laser microporation the SLP or dendrimers were topically applied on an area of $1cm^2$. To avoid evaporation of the vaccine dissolvent, micropores were covered with Tegaderm followed by gentle massage of the applied vaccine area (schematic representation **Figure 2a**). Biopsies were cultured for two days to allow skin APC emigration. Following ID injection we could find HA-signal with FACS analysis in all APC subsets after two day emigration from skin biopsies (**Figure 2b,c**). Strikingly, application following laser microporation decreased uptake by all skin DC, moMØ and LC for both gp100-SLP (**Figure 2b,c**) and gp100-dendrimers (**Figure 2d,e**). No uptake for both gp100-SLP and gp100-dendrimers was found in the HLA-DR negative population (**Figure S2a**). These data indicate that despite similar amount of vaccine molecule application, ID injection may facilitate better vaccine uptake by skin APC compared to topical application following laser microporation.

Similar skin APC phenotype and skin micro-milieu following ID injection and laser microporation

Although skin APC subset emigration was similar following ID injection and laser microporation (**Figure 1b,c**) without an adjuvant, we wanted to verify if lowered antigen uptake by APC following laser microporation was due to phenotypical changes. Therefore, we analyzed co-stimulatory marker surface expression by the different skin APC subsets after two-day emigration. Overall, CD14+ moMØ showed lower expression levels of CD40, CD80, CD83 and CD86 compared to the other APC subsets, as previously described[19]. However, no differences in co-stimulatory marker expression after emigration were observed within the APC subsets between ID injection and laser microporation (**Figure 3**). Also, no differences were observed for CD83 and CD86 within the APC subsets between untreated and ID injected skin (**Figure S2b**) Human skin APC mature upon emigration[20], so two days of emigration from the biopsy might overrule any initial differences in co-stimulatory marker expression induced upon laser treatment. Hence, we also elucidated cytokine secretion within the whole skin micro-milieu upon ID injection and laser microporation. During skin culture, biopsy conditioned supernatant was evaluated for presence of IL-1β, IL-6, IL-10, IL-12p70 and TNF-α at multiple time-points. Measurable levels of IL-6, IL-8 and IL-10 were detected after 6, 24 and 48 hour migration, whereas IL-1β, IL-12p70 and TNF-α were not detected. Figure 4 shows a significant decreased secretion of IL-6 and

a trend for IL-8 after 48 hours when human skin was treated with laser microporation compared to ID injection (**Figure 4**). Overall, these data show that laser microporation does not induce phenotypical changes in APC marker expression and slightly alters cytokine micro milieu compared to ID injection in the absence of an adjuvant.
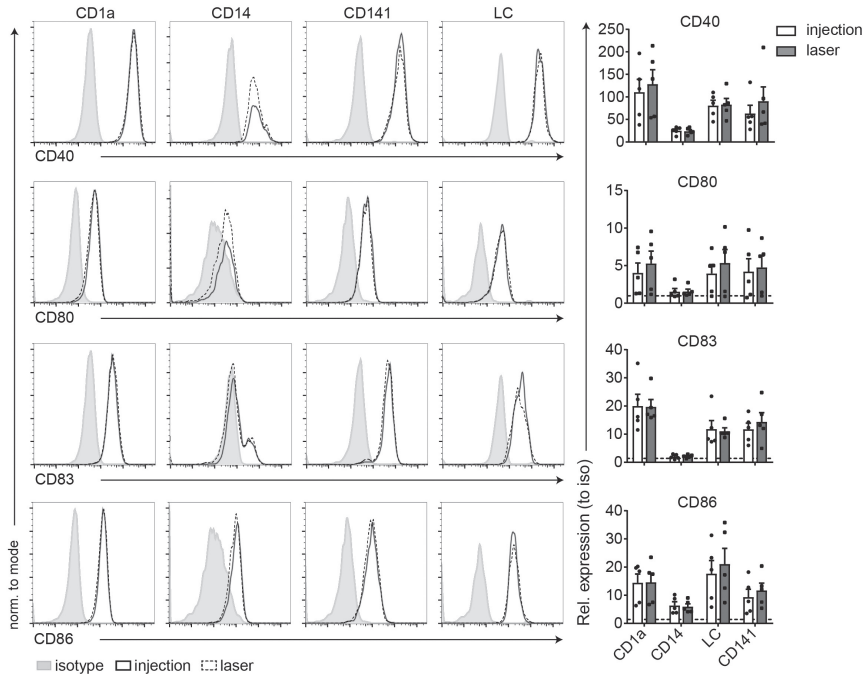
Figure 3. Similar co-stimulatory marker expression by skin APC subsets following ID injection and laser microporation Human skin explants were either ID injected with culture medium or laser micro-porated followed by two-day biopsy culture. Emigrated skin APC subsets were analyzed for expression of maturation markers CD40, CD80, CD83 and CD86 using FACS analysis. n=6±SEM, each dot represents a donor. Representative histograms of one donor.
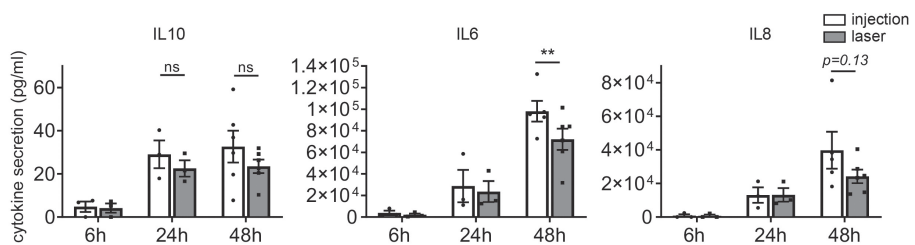
Figure 4. Skin micromilieu cytokine profile slightly changes upon laser microporation Human skin explants were either ID injected with culture medium or laser micro-porated followed by two-day biopsy culture. Next, biopsy cultured supernatant was harvested and analyzed for secretion of cytokines after 6, 24 and 48 hours. Time course samples of 6h, 24h and 48h for 3 donors, 48h samples alone for 2 (IL-6) or 3 (IL-10 and IL-8) donors and each dot represents a donor.

Higher CD8⁺ T-cell activation by skin APC following ID vaccine injection compared to laser microporation

Anti-tumor vaccination strategies rely on the induction of tumor specific CD8⁺ T-cells which requires APC to shuttle tumor antigens into the cross-presentation pathway for MHC I loading[21]. Therefore, cross-presentation of peptides and dendrimers by human skin APC was assessed following the different administration routes. We applied the gp100-SLP or the gp100-dendrimer as tumor vaccine to the human skin through injection or upon laser microporation. After two-day skin APC emigration, total skin APC were harvested and co-cultured with a gp100 specific T-cell clone recognizing the cross-presented vaccine gp100 minimal epitope in MHC I, and evaluated gp100 specific CD8⁺ T-cell activation by IFNγ secretion. Clearly, ID injected vaccines that targeted APC showed an increase in gp100 specific CD8⁺ T-cell activation for both the gp100-peptide and gp100-dendrimer vaccine (**Figure 5a,b** *open bars*). Surprisingly, but in line with the decreased uptake by skin APC following laser microporation (**Figure 2**), we observed that similar content of vaccine antigen delivered through laser microporation led to lower gp100 specific CD8⁺ T-cell activation compared to ID injection (**Figure 5a,b** *closed bars*).

To verify whether direct changes within the skin biopsy alter the capacity of skin APC to activate CD8⁺ T-cells, we first treated the skin with laser microporation followed by injection of the gp100-SLP vaccine in the skin. The capacity of the skin emigrated APC to activate CD8⁺ T-cells was restored as when the vaccine was only ID injected in the skin (**Figure 5c**). This indicates that a decreased uptake of the vaccine by human skin APC following laser microporation results in reduced gp100 specific CD8⁺ T-cell activation.
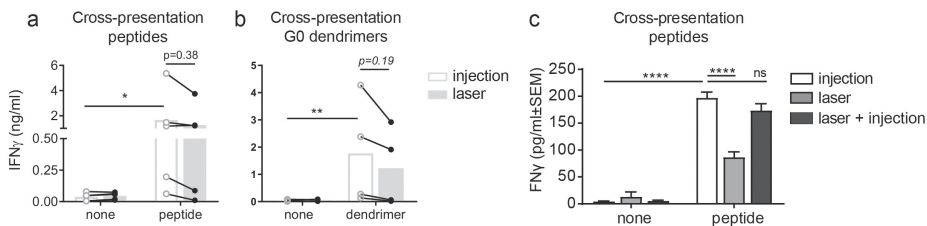
Figure 5. Higher gp100 specific CD8⁺ T-cell activation following ID vaccine injection Melanoma specific gp100-peptides (a) or gp100-dendrimers (b) compared to a medium control (none) were either ID injected, applied topically following laser microporation or ID injected following laser microporation (c). After two-day biopsy culture emigrated APC were harvested and co-cultured with a gp100 specific T-cell clone. T-cell activation was measured by IFNγ secretion in the supernatant. (a) n=5, (b) n=4, each dot represents a donor. (c) representative of n=2 measured in triplicate.

DISCUSSION

In this study we compared the use of ID anti-tumor vaccine delivery to human skin APC via injection or laser microporation without adjuvant. Laser microporation creating micropores with a depth just through the epidermis did not compromise human skin APC emigration or phenotype. However, tumor-specific vaccine particles were more efficiently delivered to the different human skin APC subsets upon ID injection compared to application following laser microporation. This resulted in higher tumor specific CD8^{+} T-cell activation following ID injection. Overall, our data show that in the ex-vivo human skin model, ID delivery of unmodified tumor-specific particles reaches human skin APC subsets best through ID injection.

For anti-tumor immune responses, the induction of cytotoxic CD8^{+} T-cells for tumor cell killing is important[22]. To achieve this, APC must shuttle exogenous derived tumor specific antigens into the cross-presentation pathway for loading on MHC I[21]. Cross-presentation by APC is influenced by mode of antigen uptake, but also signaling events occurring during antigen uptake. For example, concomitant TLR4 signaling enhances cross-presentation by retention of antigens in the endosomes through delay of endo-lysosmal fusion for antigen destruction[23]. As such, vaccines are often administered in the presence of TLR activating adjuvants to induce productive anti-tumor immune responses. However, laser microporation might induce so called adjuvanting effects e.g. by enhancing APC motility and antigen uptake. Our vaccination setting using unmodified peptidic compounds without adjuvant, did not benefit from laser microporation compared to ID injection. Leading to diminished activation of the CD8^{+} gp100 T cell clone, which appeared to be due to failure of particle uptake by the different APC subsets, although this might be underestimated due to processing of the SLP or dendrimer by the APC in the two-day culture and thereby removing the HA-tag or fluorescent label. Furthermore, there is a difference in diffusion of the products over time after laser treatment as shown by HX Nguyen et al [24] where the diffusion in vertical direction is highest in the first four hours and the horizontal diffusion in the skin after laser treatment is strongest after 8 hours. This will also impact uptake of the products by APCs over time.

The characteristics of vaccine compounds appear to dictate vaccine distribution and uptake by APC[14]. Interestingly, an important characteristic that can be altered to increase vaccine particle uptake is the size of the antigenic component[25], however, even with the multivalent dendrimers we did not see a favorable contribution of laser

microporation to uptake by skin resident APC. This is in line with previous studies where the molecular weight of particles did not influence vaccine distribution in the skin following laser microporation[14].

Alternatively, the ability to specifically target vaccine formulations to APC via CLRs, such as DC-SIGN and the mannose receptor, which recognize specific carbohydrate structures, is an option[26]. Targeting vaccines can be created by coupling of carbohydrates to antigen specific vaccine particles. Using the grass pollen Phl p 5 protein functionalized with the mannose receptor binding carbohydrate mannan, Machado *et al* showed efficient targeting of skin APC[18]. Interestingly, this study showed synergy between targeting ability of the vaccine and laser microporation, where laser microporation enhanced uptake of the targeting particles in human skin APC compared to ID injection. In contrast, our study uses unmodified SLP and dendrimers without specific targeting characteristics that might be necessary for enhanced antigen delivery to human skin APC in combination with laser microporation.

In a murine study by Terhorst *et al*, XCR1 targeting anti-tumor vaccibodies were combined with (epi) cutaneous laser microporation and showed enhanced anti-tumor immune responses and both therapeutic and prophylactic efficacy[27]. Interestingly, here laser microporation induced immunomodulatory responses, thereby bypassing the need for adjuvant application. In our study we did not observe enhanced APC maturation as measured by co-stimulatory marker expression upon laser microporation. Though, co-stimulatory marker expression is often induced upon TLR activation. The immunomodulation of laser microporation does not appear to rely on signaling through TLR, but rather be an effect of signaling cascades initiated through local cell death and immune cell influx[27]. Unfortunately, we cannot study effects of laser microporation in the context of immune cell influx in the human skin explant model. Though, local cell death of KC is most likely induced which may alter local cytokine levels in the skin thereby affecting local (immune) cells and immune cell influx[28]. Interestingly, we observed a minor decrease in secretion of IL-6, IL-8 and IL-10 within the skin biopsy micro-milieu compared to ID injection. This hints to a micro-milieu with less attraction of e.g. neutrophils (IL-8). Importantly, this secretion of cytokines were measured within the total skin biopsy, whereas conflicting data is published when looking at the cytokine secretion profile of T-cells harvested from the spleen[8,29]. Where Weiss *et al* showed that deeper microporation into the dermis

of mice increases Th1/2/17 cytokine secretion profiles by splenic T-cells[8], Chen *et al* observed an overall decrease in cytokine responses[29]. Overall, it appears either immune cell influx induced upon laser microporation, or, skin layer dependent cell death is important for immunomodulatory effects of laser microporation.

Besides ablative fractional lasers (AFL), as used in this study, also non-ablative fractional lasers (NAFL) have been developed for the disruption of skin tissue without the formation of micropores. Combination of NAFL prior to ID injection enhanced uptake of unmodified vaccine through enhanced APC motility[13]. This resulted in both increased antigen uptake and migration toward the lymphatic system within the skin. Therefore, NAFL might be a better approach for intradermal vaccinations using unmodified antigenic compounds as used in our study, since we did not observe enhanced uptake following AFL treatment. Overall, our study demonstrates that using the human skin explant model ID injection results in better antigen uptake by skin APC compared to laser microporation reflecting a superior tumor specific CD8^{+} T-cell activation.

MATERIAL AND METHODS

Human skin explant culture and DC isolation
Human skin explants were obtained within 24 hours after abdominal resection surgery (Bergman Clinics, Hilversum, The Netherlands) from healthy donors following informed consent as approved by the VUmc Medical Ethical Committee and research was performed according to the local guidelines and regulations of the Amsterdam UMC location VUmc. Obtained skin was rinsed with PBS substituted with 10µg/ml Gentamycin (Lonza) and subsequently ID injected using an insulin needle or porated using the P.L.E.A.S.E. Professional laser device (Pantec Biosolutions) with the following settings: fluency of 23.7 or 35,6 J/cm^2, 4 pulses/pore, repetition rate 200Hz, pulse duration 75µs and 10% pore density. Per condition 8-12 biopsies were taken using 8mm biopsy-punches (Microtek, Zutphen, Netherlands) and cultured for 48 hours in 1 ml IMDM supplemented with 10% FCS, 10ug/ml gentamycin, penicillin/streptomycin (Lonza), and L-glutamin (Lonza) at 37˚C and 5% CO_2. Conditioned supernatant was collected at 6, 24 and 48 hours during culture for cytokine measurements. Following culture, skin biopsies were discarded and emigrated cells were harvested and pooled per condition for further analysis.

Chapter 6

151

Human skin section staining

For pore depth evaluation following laser microporation, skin biopsies were dried shortly on a tissue followed by emersion in TissueTek (Sakura Finetek, USA) and immediate freezing under liquid nitrogen. Skin biopsies were cut in 7mm sections (CryoStar NX70, ThermoFisher scientific), placed on 1% gelatin (Merck, Darmstadt, Germany) coated slides, dried and stored at -80°C. Prior to staining, sections were dried o/n at RT. Standard Haematoxylin Eosin (H&E) staining was performed and microscopic pictures were captured using the Leica DM6000 (Leica microsystems).

Phenotypical analysis LC dDC and moMØ

Emigrated cells were washed in PBS with 1% BSA and 0.02% NaN_3 and incubated for 30 minutes on 4°C with subset markers HLA-DR BV510 (clone G46-6, BD biosciences), CD1a APC (clone HI149, BD), CD14 AF700 (clone M5E2, Antibody Chain), CD141 BV711 (clone 1A4, BD), EpCAM BV421(clone 9C4, Antibody Chain) and maturation markers CD86 FITC (clone BU63, ImmunoTools), CD80 FITC (clone 2D10, Biolegend), CD40 PE-Cy7 (clone 5C3, Biolegend), CD83 PE-Cy7 (clone HB15e, BD) and Fixable Viability Dye eFluor780 (eBioscience). Cells were measured by flow cytometry (Fortessa X-20, Beckton Dickinson, San Jose, CA, USA) and analyzed with FlowJo (V10, Tree Star, Ashland, OR, USA).

Cytokine secretion skin biopsies

Cytokine secretion was measured using sandwich ELISA according to manufacturer's protocol with specific cytokine antibody pairs for IL-1b, IL-6, IL-8 (BioSource), IL-10, IL-12p70 and TNF-a (eBioscience).

Peptide and dendrimer synthesis

In short, the gp100-SLP containing the $CD8^+$ T-cell epitope (bold) and HA-tag (underlined) (Thz-VTHT**YLEPGPVTA**NRQLYPEWTEAQRLD<u>YPYDVPDYA</u>-C) was synthesized by microwave assisted solid phase peptide synthesis using Fmoc chemistry on the Liberty blue peptide synthesizer (CEM).

A generation 0.0 PAMAM dendrimer core was functionalized with maleimide followed by coupling at the C-terminal end of the gp100-SLP containing a specific linker (Thz-VTHTYLEPGPVTANRQLYPEWTEAQRLD-**(Abu)**$_3$-C). Next, AF488-maleimide was added at the unmasked N-terminal (Thz) end for tracking. Mass and purity of all steps were confirmed by UHPLC-MS (Ultimate 3000 UHPLC, Thermo Fisher) hyphenated with a

LCQ-Deca XP Iontrap ESI mass spectrometer (Thermo Finnigan) using a RSLC 120 C18 Acclaim 2.2um 2.1 x 250 mm column. Mass spectrometer analysis was measured in positive mode (**Figure S3**).

Human skin APC in-situ vaccine uptake

HA-tagged peptides or AF488-labeled dendrimers were diluted in serum-free IMDM and 20µl was ID injected or 10µl (2x concentration) was applied topically on 10mm^2 following laser microporation and gently massaged (10seconds). Laser microporated areas were covered with Tegaderm film (Newpharma, Luik, Belgium) to avoid evaporation. Ten 8mm punch-biopsies were taken per condition and cultured as described above. For peptide uptake, APCs were fixed and permeabilized using a Cytofix/Cytoperm kit (BD) according to manufacturer's instructions and stained with an anti-HA-AF488 (clone 6E2; Cell Signaling) antibody for 30minutes at 4°C. Cells were stained for subset markers and analyzed by flow cytometry as described above.

Human skin APC antigen presentation

For antigen presentation a specific T-cell clone recognizing the gp100 HLA-A2 minimal epitope was produced and cultured as previously described[30]. HLA-A2$^+$ skin was used for vaccine injection or application after laser microporation and 8 biopsies were taken and cultured as described above. Harvested cells were co-cultured in a 96-well round bottom plate with the T-cells in a 1:5 ratio (triplicate). After 24 hours supernatants were harvested and T-cell activation measured using an IFNγ Ready-Set-Go kit (eBioscience) according to manufacturer's protocol.

Statistical analysis

GraphPad Prism (V7.02) was used for statistical analysis. Student's T-test was used to compare percentage or number of cells. For group comparison two-way ANOVA followed by Tukey multiple comparison test were used with paired analyses for multiple donors. P-values <0.05 were considered to be significant.

DATA AVAILABILITY

No datasets were generated or analyzed during the current study.

CONFLICT OF INTEREST

The authors have no conflicts of interest to declare.

AUTHOR CONTRIBUTIONS

S.D., J.L., Y.v.K. Conceptualization; Y.v.K. Funding Acquisition; S.D., J.L., D.S., J.V. Investigation; S.D., J.L. Methodology; S.D., Y.v.K. Project Administration; M.A., H.K. Resources; Y.v.K. Supervision; S.D., J.L., D.S. Validation; S.D. Visualization; S.D., Y.v.K. Writing - Original Draft Preparation; all authors Writing - Review and Editing

ACKNOWLEDGEMENTS

REFERENCES

1   Kashem, S. W., Haniffa, M. & Kaplan, D. H. Antigen-Presenting Cells in the Skin. *Annu Rev Immunol* **35**, 469-499, doi:10.1146/annurev-immunol-051116-052215 (2017).

2   Bigley, V. *et al.* Langerin-expressing dendritic cells in human tissues are related to CD1c^{+} dendritic cells and distinct from Langerhans cells and CD141high XCR1^{+} dendritic cells. *J Leukoc Biol* **97**, 627-634, doi:10.1189/jlb.1HI0714-351R (2015).

3   Kawai, T. & Akira, S. The role of pattern-recognition receptors in innate immunity: update on Toll-like receptors. *Nat Immunol* **11**, 373-384, doi:10.1038/ni.1863 (2010).

4   Guermonprez, P., Valladeau, J., Zitvogel, L., Thery, C. & Amigorena, S. Antigen presentation and T cell stimulation by dendritic cells. *Annu Rev Immunol* **20**, 621-667, doi:10.1146/annurev.immunol.20.100301.064828 (2002).

5   Klechevsky, E. Functional Diversity of Human Dendritic Cells. *Adv Exp Med Biol* **850**, 43-54, doi:10.1007/978-3-319-15774-0_4 (2015).

6   Weniger, B. G. & Glenn, G. M. Cutaneous vaccination: antigen delivery into or onto the skin. *Vaccine* **31**, 3389-3391, doi:10.1016/j.vaccine.2013.05.048 (2013).

7   Kim, Y. C., Jarrahian, C., Zehrung, D., Mitragotri, S. & Prausnitz, M. R. Delivery systems for intradermal vaccination. *Curr Top Microbiol Immunol* **351**, 77-112, doi:10.1007/82_2011_123 (2012).

8   Weiss, R. *et al.* Transcutaneous vaccination via laser microporation. *J Control Release* **162**, 391-399, doi:10.1016/j.jconrel.2012.06.031 (2012).

9   Bachhav, Y. G. *et al.* Effect of controlled laser microporation on drug transport kinetics into and across the skin. *J Control Release* **146**, 31-36, doi:10.1016/j.jconrel.2010.05.025 (2010).

10   Jaques Banchereau *et al.* Immunobiology of dendritic cells. *Annu. Rev. Immunol.* **18**, 767-811 (2000).

11   Kapsenberg, M. L. Dendritic-cell control of pathogen-driven T-cell polarization. *Nat Rev Immunol* **3**, 984-993, doi:10.1038/nri1246 (2003).

12   Gutowska-Owsiak, D. & Ogg, G. S. The Epidermis as an Adjuvant. *Journal of Investigative Dermatology* **132**, 940–948, doi:10.1038/ jid.2011.398 (2012).

13   Chen, X. *et al.* A novel laser vaccine adjuvant increases the motility of antigen presenting cells. *PLoS One* **5**, e13776, doi:10.1371/journal.pone.0013776 (2010).

14   Bachhav, Y. G., Heinrich, A. & Kalia, Y. N. Controlled intra- and transdermal protein delivery using a minimally invasive Erbium:YAG fractional laser ablation technology. *Eur J Pharm Biopharm* **84**, 355-364, doi:10.1016/j.ejpb.2012.11.018 (2013).

15   Scheiblhofer, S. *et al.* Skin vaccination via fractional infrared laser ablation - Optimization of laser-parameters and adjuvantation. *Vaccine* **35**, 1802-1809, doi:10.1016/j. vaccine.2016.11.105 (2017).

16   Sahay, G., Alakhova, D. Y. & Kabanov, A. V. Endocytosis of nanomedicines. *J Control Release* **145**, 182-195, doi:10.1016/j.jconrel.2010.01.036 (2010).

17   Kubo, A., Nagao, K., Yokouchi, M., Sasaki, H. & Amagai, M. External antigen uptake by Langerhans cells with reorganization of epidermal tight junction barriers. *J Exp Med* **206**, 2937-2946, doi:10.1084/jem.20091527 (2009).

18   Machado, Y. *et al.* Synergistic effects of dendritic cell targeting and laser-microporation on enhancing epicutaneous skin vaccination efficacy. *J Control Release* **266**, 87-99, doi:10.1016/j.jconrel.2017.09.020 (2017).

19   Tulumen, E. *et al.* Early repolarization pattern: a marker of increased risk in patients with catecholaminergic polymorphic ventricular tachycardia. *Europace*, doi:10.1093/ europace/euv357 (2015).

Chapter 6

20   Botting, R. A. *et al.* Phenotypic and functional consequences of different isolation protocols on skin mononuclear phagocytes. *J Leukoc Biol* **101**, 1393-1403, doi:10.1189/jlb.4A1116-496R (2017).

21   Embgenbroich, M. & Burgdorf, S. Current Concepts of Antigen Cross-Presentation. *Front Immunol* **9**, 1643, doi:10.3389/fimmu.2018.01643 (2018).

22   Ahrends, T. *et al.* CD4([+]) T Cell Help Confers a Cytotoxic T Cell Effector Program Including Coinhibitory Receptor Downregulation and Increased Tissue Invasiveness. *Immunity* **47**, 848-861 e845, doi:10.1016/j.immuni.2017.10.009 (2017).

23   Alloatti, A. *et al.* Toll-like Receptor 4 Engagement on Dendritic Cells Restrains Phago-Lysosome Fusion and Promotes Cross-Presentation of Antigens. *Immunity* **43**, 1087-1100, doi:10.1016/j.immuni.2015.11.006 (2015).

24   Nguyen, H. X., Puri, A., Bhattaccharjee, S. A. & Banga, A. K. Qualitative and quantitative analysis of lateral diffusion of drugs in human skin. *Int J Pharm* **544**, 62-74, doi:10.1016/j.ijpharm.2018.04.013 (2018).

25   Foged, C., Brodin, B., Frokjaer, S. & Sundblad, A. Particle size and surface charge affect particle uptake by human dendritic cells in an in vitro model. *Int J Pharm* **298**, 315-322, doi:10.1016/j.ijpharm.2005.03.035 (2005).

26   van Dinther, D. *et al.* Targeting C-type lectin receptors: a high-carbohydrate diet for dendritic cells to improve cancer vaccines. *J Leukoc Biol* **102**, 1017-1034, doi:10.1189/jlb.5MR0217-059RR (2017).

27   Terhorst, D. *et al.* Laser-assisted intradermal delivery of adjuvant-free vaccines targeting XCR1^{+} dendritic cells induces potent antitumoral responses. *J Immunol* **194**, 5895-5902, doi:10.4049/jimmunol.1500564 (2015).

28   Gröne, A. Keratinocytes and cytokines. *Veterinary Immunology and Immunopathology* **88**, 1–12 (2002).

29   Bach, D. *et al.* Transcutaneous immunotherapy via laser-generated micropores efficiently alleviates allergic asthma in Phl p 5-sensitized mice. *Allergy* **67**, 1365-1374, doi:10.1111/all.12005 (2012).

30   Schaft, N. *et al.* Peptide Fine Specificity of Anti-Glycoprotein 100 CTL Is Preserved Following Transfer of Engineered TCR Genes Into Primary Human T Lymphocytes. *The Journal of Immunology* **170**, 2186-2194, doi:10.4049/jimmunol.170.4.2186 (2003).

Supplementary data

a 23,7J/cm2, 95µm

35,6J/cm2, 142µm

b
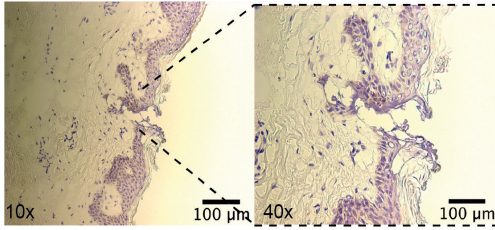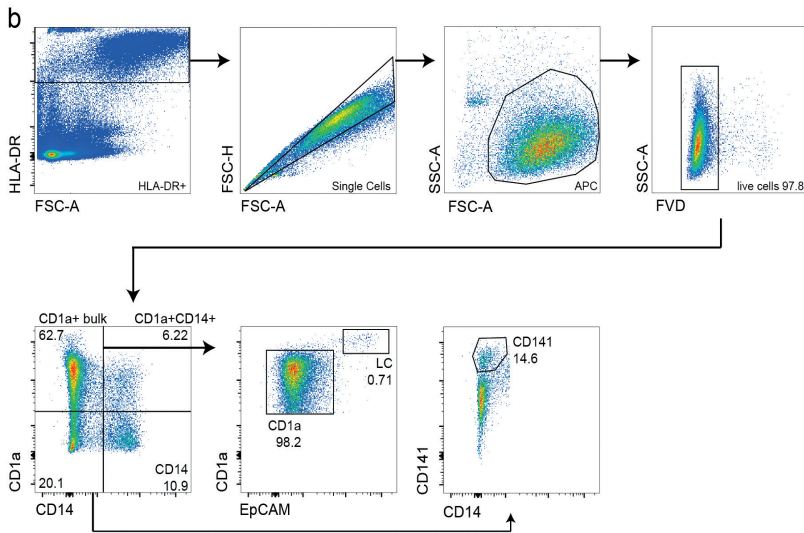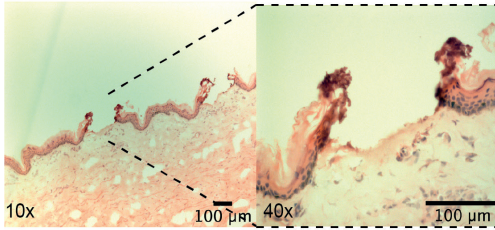
Figure S1. (A) H&E staining of laser microporated human skin using 4 pulses and 23,7J/cm2 (top) or 35,6J/cm2 (bottom). (B) Gating strategy of human skin DC subsets following two day emigration using FACS.
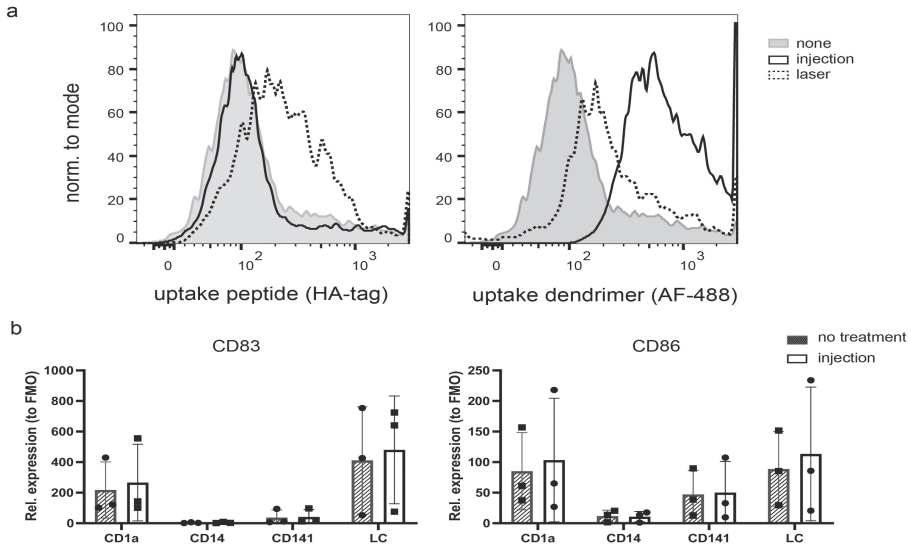
Figure S2. (A) Uptake of the SLP with HA-tag (left) and dendrimer-AF488 (right) by HLA-DR- cells following ID injection and laser poration. (B) CD83 and CD86 relative to FMO in the different skin DC subsets upon no treatment or medium injection.
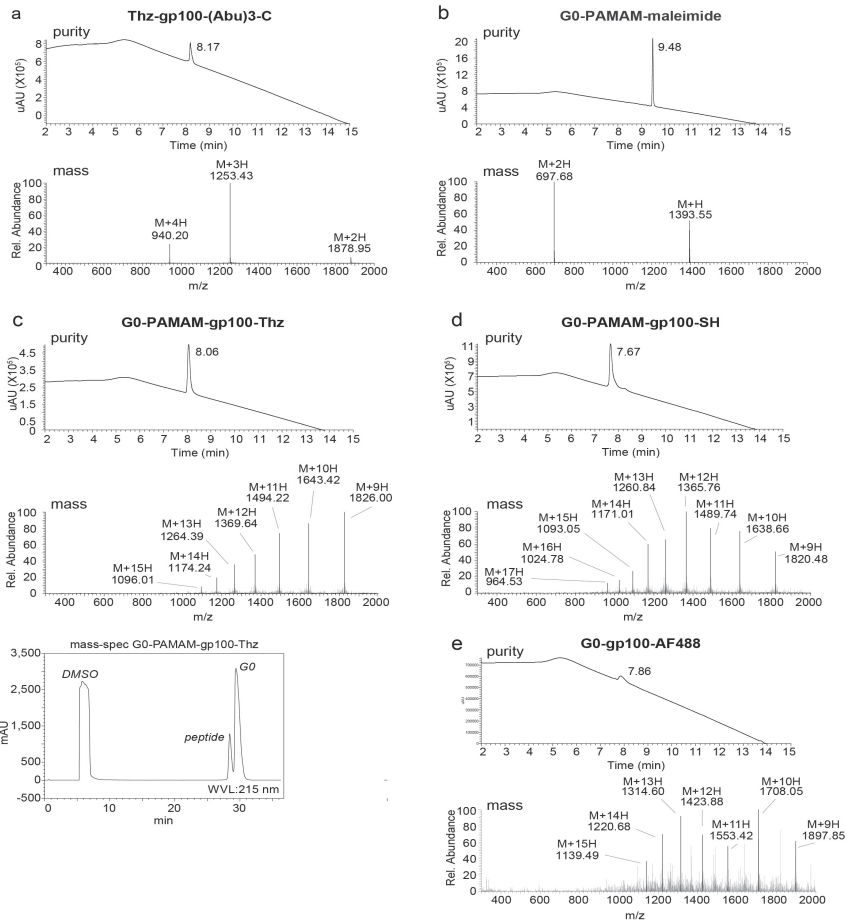
Figure S3. Purity and mass analysis of peptide and dendrimer synthesis as measured by UHPLC-MS and mass spectrometer systems. (A) SLP (B) functionalized G0-PAMAM-dendrimer (C) SLP conjugation to G0-PAMAM-dendrimer (D) Unmasking of G0-PAMAM-gp100 dendrimer (E) Conjugation of AF488 to antigenic dendrimer.

CHAPTER 7

GENERAL DISCUSSION

S. Duinkerken, R.J. E. Li, F.J. van Haften, F. Chiodo, S.T.T. Schetters,
T.D. de Gruijl, J.J. Garcia-Vallejo and Y. van Kooyk

Anti-tumor immonutherapy: exploring the human skin (DC) potential

Immunotherapy to treat cancer has gained much interest over the past two decades and strategies are rapidly developing. Approaches explored include antibody therapy (tumor-targeted, targeting TNF-R family members or immune checkpoint blockade [1]) cell-based therapy using innate immune cells (NK cells [2], neutrophils [3]), adoptive T cell transfer [4] and DC vaccines, or immune modulatory therapies (e.g. oncolytic viruses, TLR-L), or combinations of the above. Unfortunately, a treatment modality effective for a majority of patients has not yet been defined. This can have many reasons but is certainly attributed to the complex nature of cancer which comes in many types, residing in different tissues and varying in aggressiveness, immune suppression and mutational load.

It is becoming clear that anti-tumor immunotherapy benefits from the induction of tumor specific T cells resulting in systemic and long-lasting immunity against existing tumors, but also providing protection against the development of new tumors [5]. Anti-cancer immunotherapy largely relies on the induction of CD8^{+} cytotoxic T cells which have tumor killing capacity. DC play an important role in the priming and activation of these T cells. Recent insights show that CD8^{+} T cell priming by DC occurs in a two-step process. Both migratory DC and LN resident DC, which have encountered CD4^{+} helper T cells, successively present antigen to CD8^{+} T cells thereby enhancing the quality of the CD8^{+} T cell response [6, 7]. The pivotal role of DC in T cell activation has led to the development of DC based vaccination strategies for anti-tumor therapy. Initial efforts, and tested in clinical trials, included the *ex vivo* loading and activation of patient derived DC followed by injection into the patient. However, the fact that this type of vaccination is individualized, makes it ambitious due to time-management, costs and logistic issues [8]. Consequently, *in vivo* vaccination strategies are being developed to instruct DC using a single off-the-shelf vaccine applicable for a large patient cohort [8]. The use of DC specific receptors, and especially CLR, for targeting purposes and facilitating antigen cross-presentation in MHC I is a promising strategy to enhance anti-tumor immunity [9-11]. There are multiple DC subsets residing in different tissues with varying receptor expression and function [12]. Consequently, there is a major ongoing research effort to discover the optimal DC-receptor targeting combination in order to induce potent anti-tumor immunity.

In this PhD thesis we explored the potential of the human skin, as prime site for vaccination, and its richness in DC subsets for the development of an *in vivo* anti-tumor vaccination strategy, specifically targeting multiple human skin DC subsets. We used a human skin explant model to evaluate the targeting capacity *in situ* and subsequent CD8^{+} T cell activation. Multiple parameters may dictate whether our designed vaccine will show effectiveness *in vivo*, such as human skin DC migration, lymphatic drainage and local immune cell influx upon vaccination.

Human skin DC targeting for the induction of anti-tumor immunity.

Targeting anti-tumor vaccines to intradermal DC for anti-cancer immunity has shown its potential in both murine models and human skin explants [13, 14]. In **chapter 4, 5** and **6** of this thesis we used the human skin explant model to evaluate the local effect of our vaccines. First, we evaluated the targeting efficiency of our glycan-modified tumor specific (glyco-dendrimer) vaccine to multiple human skin DC subsets. We did this via dual Langerin and DC-SIGN targeting of which the intracellular routing for cross-presentation was investigated in **chapter 2** and **3**, respectively. Second, we elucidated the immune responses induced by our NOD2 multivalent tumor antigen-adjuvant complex (**MAAC**) through human skin DC activation and cross-presentation. Lastly, the feasibility of applying the vaccines with either injection or laser microporation for DC antigen uptake and presentation was evaluated.

The human skin explant model encompasses the various human skin DC subsets present in their natural 3D environment and physical state. As such, it can address targeting efficiencies and internalization by DC for processing and presentation to T cells. However, within human skin explants it remains challenging to elucidate the combination of local effects at the injection site with systemic effects inducing immunity. In **chapter 4** the hypothesis is tested that targeting to multiple DC subsets simultaneously may enhance vaccine efficiency. Although we could evaluate the targeting capacity of our glyco-dendrimers to the multiple skin DC subsets, the question remains whether this will indeed enhance anti-tumor immunity *in vivo*.

The intrinsic capacity to activate and modulate adaptive immunity is described to differ between the human skin DC subsets. Where LC and CD1a^{+} dermal DC are considered to initiate cellular responses, CD14^{+} dermal DC appear to induce humoral responses by T_{FH} differentiation [15, 16]. One can argue that stimulating different DC subsets simultaneously can hence induce broad and possibly complementary

Chapter 7

adaptive immune responses. By addition of targeting moieties, such as glycans, uptake and antigen processing by DC can be enhanced, as we show in **chapter 4**. Additionally, in this thesis we focus on augmenting cross-presentation by specific CLR targeting, particularly Langerin (**chapter 2**) and DC-SIGN (**chapter 3**), regardless of the intrinsic capacity of the different human skin DC. The discussion remains which human skin DC subset would be the prime target for cross-presentation of tumor antigens, and thus the activator of anti-tumor CD8+ T cell responses. In literature the CD141+ dermal DC (or cDC1) often wins this battle owing to its inherent capacity for cross-presentation and high MHC I expression [17, 18]. We observed uptake of our (glyco)-dendrimers by LC and both CD1a+ and CD14+ dermal DC, yet hardly by the CD141+ dermal DCs (**chapter 4**). As such it is questionable whether these so-called prime cross-presenters will take part in the induction of adaptive immunity upon intradermal vaccination with our glyco-dendrimers. Furthermore, with the right targeting strategy many different DC subsets can cross-present exogenous derived antigens for CD8+ T cell activation [11]. Indeed, both the lower (CD1a+ dermal DC) and high (CD14+ dermal DC) DC-SIGN expression levels of dermal DC can be used to efficiently target glycan-modified vaccines to these DC (**chapter 4**) for induction of cross-presentation, as previously described [14, 19]. Furthermore, while DC have always been considered the prime cross-presenting APC, a recent study showed that both monocyte derived DC (moDC) and macrophages (moMac) have cross-presenting ability [20]. However, the discrepancy lay in the activation of effector CD8+ T cells which was accomplished by moDC, but not moMac.

In this thesis we used the human skin explant model in combination with melanoma specific T cell clones. These clones do not require co-stimulation for activation and are a great tool to evaluate loading and presentation of the vaccine antigens in MHC class I. However, this also means it does not resemble naïve T cell priming in the lymph nodes (**LN**), though previous studies show the priming capacity of human skin DC [21-23]. An interesting development is the recognition that not only CD8+ T cell priming for effector CTL induction is important for anti-tumor immunity. Also (re) activation of CD8+ tissue resident memory T (T_{RM}) cells impacts the efficacy of cancer immunotherapy, as they induce superior immunity compared to effector cells [24] and potentially induce long-term protection against tumor recurrence as described for melanoma [25]. In melanoma it was shown that upon intradermal vaccination using a DEC205 targeting strategy, tumor antigen-specific T_{RM} accumulated in the skin and suppressed tumor growth *in vivo* in mice [26]. Interestingly, CD14+ dermal

DC have been reported to play a role in the maintenance/activation of skin-resident T_{RM}. It would be interesting in future studies to evaluate the specific induction of various CD8+ T cell subsets and differentiation states, including effector and memory cells, upon intradermal vaccination with our multivalent (glyco)-vaccines.

Lymphatic drainage of vaccins, implications for DC targeting

Naïve T cell activation requires antigens to arrive at the draining LN, or tumor-adjacent tertiary lymphoid structures, for presentation by DC. This can occur via two routes; namely via migratory DC which present processed antigen in MHC or transfer the antigen to LN resident DC, or by drainage of the vaccine antigens via the lymphatics and subsequent uptake and presentation by LN (resident) DC. For intradermal vaccination, targeting of numerous DC populations at their site of residence is important [7, 27]. However, lymph drainage of the vaccine itself may result in uptake by DC present in skin-draining LN. These include LN DCs which stem from blood precursors, but also DCs that have migrated from the skin via the afferent lymph vessels [12, 28]. This might enhance vaccine efficacy as LN resident DCs are capable of antigen cross-presentation upon activation and can induce strong CD8+ T cell responses [29]. Importantly, vaccine delivery-systems can promote antigen transport to lymphoid organs e.g. through size requirements. Particles of (up to) 200 nanometer sizing are preferentially trafficked into the lymphatic vessels [30]. Our tumor specific glyco-dendrimers described in **chapter 4** have a size of approximately 50nm and thus comply with the LN trafficking size requirement. As such, the glyco-dendrimers might reach the LN by drainage via the lymphatics. Interestingly, in steady state DC-SIGN+ (dermal) DCs are present in the paracortex of the LN, the site where DCs and T cells interact [28, 31]. Also Langerin+ LCs can be found in the skin draining LN [12]. Currently it is not known whether our glycan-modified DC targeting cancer vaccine will drain to the LN and subsequently instruct LN resident DC that express Langerin or DC-SIGN besides the skin DC. It would be interesting to elucidate whether vaccine trafficking to LN occurs and, if so, what the impact on vaccine efficacy could be.

Studying human skin DC migration

Intradermal vaccination strategies are designed with the rationale that DCs will take up antigens in the skin, followed by migration and presentation in the LN to T cells. However, not all skin resident DC subsets are equally well equipped to migrate from the skin to the draining LN to activate naive CD4+ and CD8+ T cells. In CCR7 deficient

Chapter 7

mice no skin DCs were present in the skin draining LN during inflammation, which highlights the importance for DCs to express CCR7 for LN trafficking [32]. Indeed, upon inflammation mature LCs and CD1a^{+} dermal DCs are able to migrate from the dermis to the LNs through CCR7 expression [33, 34]. Furthermore, these subsets have also been found in sentinel LN of melanoma patients [28], resembling steady state human skin DC migration. Interestingly, although expression of CCR7 on CD14^{+} dermal DC is controversial, it has been observed that CD14^{+} dermal DCs can emigrate spontaneously from the skin. The past years the CD14^{+} dermal DC ontogeny has been re-evaluated. It is postulated that the CD14^{+} dermal DC subset closely resembles monocyte derived macrophages [35], though they are not to be confused with the CD14^{+} resident macrophages of human skin. The CD14^{+} resident macrophages are sporadically replenished, whereas the CD14^{+} dermal DC is a transient population more rapidly replenished through monocyte influx [35]. Furthermore, the CD14^{+} dermal DC emigrate from the human skin biopsies during culture, while CD14^{+} macrophages remain situated in the skin. When imaging of steady state human skin, CD14^{+} dermal DC were not observed within the skin lymph vessels [35]. So far, the localization of CD14^{+} dermal DCs is unclear as they may lose their CD14 expression during migration, which makes it difficult to trace this subset [36].

The human skin explant model lacks dynamics such as that of chemokine induced DC migration, since all the different human skin DC subsets migrate out of skin biopsies spontaneously. As such, this does not denote chemokine induced migration upon vaccine challenge. To elucidate which human skin DC subset can migrate to LN in response to the chemokines CCL19 and CCL21, we developed an *ex vivo* human skin DC migration assay using a transwell system (**chapter 5**). The LN homing receptor CCR7 is described to be restricted to CD1a^{+} dermal DC and epidermal LC, though, also shows variable expression by CD14^{+} dermal DC [37]. Interestingly, approximately 20% of the CD14^{+} dermal DC also showed migration towards CCL21 within 4 hours (**chapter 5**), which concurs with the variable expression of CCR7 [37]. Notably, CD14^{+} dermal DC migration could be increased to ~45% when the activation stimuli GM-CSF/IL4 were injected prior to DC emigration from biopsies (**chapter 5**). The combination of GM-CSF and IL-4 injection in the skin was previously shown to prevent switching of CCR7^{+} DC to a non-migratory macrophage-like phenotype [38]. The use of GM-CSF/IL4 as adjuvant for intradermal vaccines targeting skin DC might be a viable option to enhance (CD14^{+}) dermal DC migration to draining LN.

The functional implications of the CD14^{+} dermal DC migration capacity towards draining LN for induction of tumor specific immune responses remains elusive. It is clear they are capable of cross-presentation and subsequent activation of effector CD8^{+} T cells, especially upon DC-SIGN mediated antigen uptake [14]. Interestingly, in breast cancer patients skin-emigrated CD14^{+} dermal DC were increased, though, induced a Treg phenotype rather than priming of effector T cells under the influence of IL10 [39]. However, these emigrated CD14^{+} dermal DC displayed a more immature phenotype while the mature CD1a^{+} dermal DC subset did induce efficient priming of effector T cells. The addition of adjuvants such as Aldara might overcome this issue by induction of skin DC maturation [40]. Though, no study has elucidated whether there might be a difference in the migrating versus non-migrating CD14^{+} dermal DC, for example in relation to induction of effector or memory T cell responses. In **chapter 4** we show that the CD14^{+} dermal DC subset can be efficiently targeted for antigen uptake via DC-SIGN, together with CD1a^{+} dermal DC. The next step would be to investigate whether both dermal DC subsets can migrate to draining lymph nodes, or, whether they have different immunological outcomes in regard to effector or memory T cell activation. Importantly, CD14^{+} dermal DC can be rapidly replenished via monocyte influx thereby resembling CD14^{+}, DC-SIGN^{+}, monocyte derived DC (**moDC**) [37]. These DC-SIGN^{+} moDC are important inducers of anti-tumor immune responses especially after challenge of antigen in combination with specific adjuvants, such as AddaVax, that rapidly induces local influx of monocytes and neutrophils, with moDC accumulating at 12 hours after injection. Addavax enhanced antigen specific CD4^{+} and CD8^{+} T cells while targeting moDC with DC-SIGN additionally boosted antigen specific antibody responses [41, 42]. Overall, future studies should investigate the contribution of the different resident skin DC subsets, and possibly moDC, in induction and maintenance of anti-tumor immune responses upon intradermal vaccination using our multivalent glyco-dendrimers.

Intradermal vaccination and influx of innate immune cells

Central to the efficacy of clinically approved adjuvants are DC [43]. With the design of *in vivo* intradermal vaccination strategies the main focus lies on the effect of the vaccine formulation on skin DC, since these are the cells able to initiate adaptive anti-tumor immune responses. However, with intradermal injections the vaccine comes into contact with more than just DC since the tissue also comprises supportive cell types, such as stromal cell types like keratinocytes, melanocytes and fibroblasts, which are considered to play an important role in immune responses [44]. The

vaccine is also able to accumulate various immune cells that are recruited from the blood to the dermis upon inflammatory signals provided by the vaccine (**Figure 1**).

Many vaccine adjuvants have shown to depend on local activation and recruitment of neutrophils or monocytes that may differentiate into DC [45]. Fibroblasts can play an important role in the induction of an innate immune cell influx, since they can respond to TLR agonists by cytokine secretion e.g. IL-6 and IL-8 [46] (**Figure 1**). Intradermal vaccination with influenza virus using micro-needle patches can increase multiple inflammatory cytokines in the skin, such as IL-1β, macrophage inflammatory protein 1 and 2 (**MIP-1/2**), TNF-α and monocyte chemoattractant protein 1 (**MCP-1**), thereby attracting monocytes and neutrophils [47]. Furthermore, adjuvants that stimulate DC maturation, such as the TLR4-agonist monophosphoryl lipid A (**MPLA**) and the TLR7/8 agonist imidazoquinoline (Resiquimod, R848) can recruit macrophages and affect the relative percentages of macrophages and inflammatory monocytes in the human skin, respectively [48]. Squalene-based adjuvants MF59 or AddaVax (oil-in-water nano-emulsion formulations), which is regularly used in seasonal influenza vaccines [49], are described to induce monocyte recruitment via the CCR2/CCL2-axis in mice [50]. Influx of monocytes upon intradermal vaccination may result in transport of the vaccine by monocytes or monocyte-derived DC. Indeed, addition of small amounts MF59 could increase the migration capacity of intramuscularly differentiated monocyte-derived DCs in mice [51]. In fact, MF59 may have similar effects in the murine skin, recruiting monocyte-derived DC expressing the mouse orthologue of DC-SIGN [42]. These monocyte-derived DC can take up antigen and are capable of inducing T cell activation in the draining LN [52], thereby influencing immunological outcome following intradermal vaccination. With our NOD2-MAAC vaccine described in **chapter 5** we found increased levels of IL6 and IL8, indicating that this vaccine might also induce innate immune cell influx. Furthermore, the absence of innate immune cell influx within our human model skin explant might explain why in **chapter 6** we did not find the benefits of laser microporation for intradermal vaccine delivery, as described in other studies using mouse models [53, 54]. Influx of innate immune cells such as neutrophils and monocytes may alter the skin micro-milieu and uptake of the vaccine.
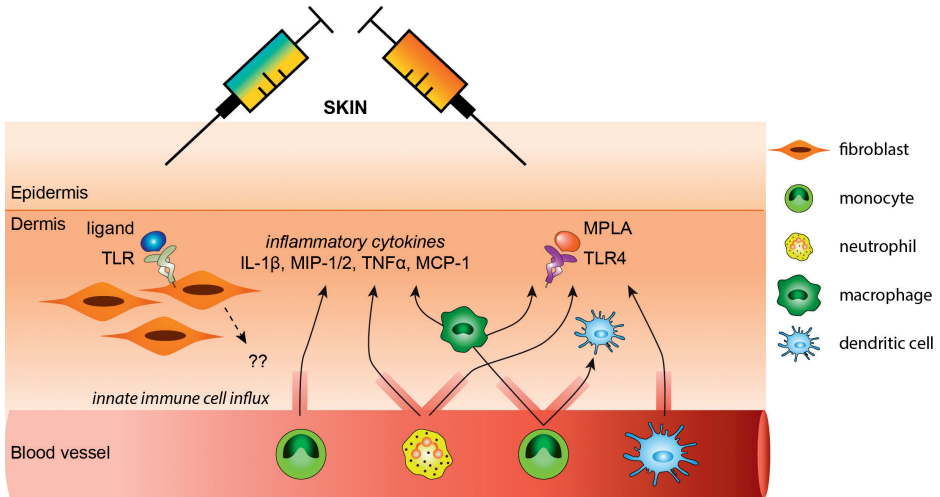
Figure 1 Influx of innate immune cells in the skin after vaccination. Upon vaccination inflammatory cytokine (IL-1b, MIP1/2, TNF-a and MCP-1) levels are increased to which monocytes, neutrophils and macrophages are attracted. Since fibroblasts express TLRs they might react to TLR ligands (blue) after which fibroblast can change the local environment of the skin thereby inducing innate immune cell influx. After injection of a MPLA-containing vaccine (red) neutrophils and monocytes/macrophages are recruited from the blood to the skin.

Modelling skin immune complexity to predict vaccine efficacy

At this time, the full complexity of how local vaccine injection can drive systemic responses can only be modeled in live organisms such as mice. However, they show many differences with humans [55] and there is an urgent need for humanized models [56]. These can be mouse models that include microbial composition [57], expression of human receptors (for example DC-SIGN [58]), humanized immune cell compositions [59, 60] and the inclusion of both sexes [61].

The potential of multivalent glycan-modified anti-tumor vaccines was shown in a mouse model with human DC-SIGN expression [STT Schetters *et al* Biomaterials, submitted]. Here vaccination with OTI-OTII specific antigen matrices (AMAX) induced tumor specific T cell activation. Though the restricted DC-SIGN expression in humans calls for the use of artificial, humanized models to test our glyco-dendrimer vaccine *in vivo*. Although a mouse model with human DC-SIGN (hSIGN) under the control of the CD11c promotor has been generated [62], this does not reflect the DC restricted DC-SIGN expression as observed in humans. Currently, a new mouse model is being developed which controls DC-SIGN expression under its own promotor region,

thereby mimicking DC-SIGN expression in man. This model would be useful for the *in vivo* testing of our glycan-modified vaccine of **chapter 4**, simultaneously targeting multiple human skin DC subsets through DC-SIGN and Langerin.

Meanwhile, there are new developments which might make the use of mouse models redundant in the future. One such an approach is the use of skin-on-chip technology [63], which aims to mimic the physiology of the human skin. This model consists of three layers, including epidermis, dermis and fat tissue, in which the dermis and fat tissue are linked to a systemic circulation system via micro-capillaries [12]. The present skin-on-chip models contain epidermal LC [64], however the incorporation of dermal DC has yet to be resolved and, therefore, these skin-on-chip systems are not yet suitable to study the effect of intradermal vaccination. However, induced pluripotent stem cells could be integrated in the skin-on-chip model to induce the presence of immune cells [12]. These induced pluripotent stem cells can differentiate into B cells, NK cells and T cells [65, 66]. Combined with a micro-capillary system for influx of innate immune cells this could be a promising strategy in the future to optimize the skin-on-chip model. Moreover, with advanced microfluidics connecting different tissue compartments like bone marrow, lymph node and tumor, one could envision studying combined local and systemic effects of vaccination like immune cell recruitment, T cell priming, trafficking and anti-tumor effector T cell efficacy. Thus, future directions should be aiming to develop these complete *ex vivo* human-on-a-chip immune networks that allow us to study the dynamics of (adjuvant-induced) anti-tumor immunity of DC targeted vaccines.

Targeted intradermal anti-tumor vaccines: one size fits all?

Besides the model systems which are important for the research encompassing targeted intradermal anti-tumor vaccination strategies, also the type of tumor to fight may determine vaccine efficacy. In this thesis we focused on designing anti-melanoma vaccines, using melanoma specific antigens (gp100) to synthesize our glycan-modified vaccines. Future research should focus on how we can use intradermal glycan-modified vaccines for other solid tumors and what other factors are of importance. One of these factors is the choice of antigen, since they may in large part determine immunogenicity [67]. Tumors which are virally induced [68] or have a high mutational load (such as melanoma or lung cancer [69]), can be targeted using highly immunogenic viral antigens or neoantigens, respectively. For the design of the glyco-modified vaccines which we generated, this should be easy

to implement, as they are built with synthetic long peptides. Synthesis of the right peptidic sequences, based on individual patient tumor sequences, together with MHC binding prediction programs, may be easily accomplished and the synthesized peptides could subsequently be coupled to the dendrimer core, in effect leading to personalized vaccines.

Viral antigens for solid tumor eradication: glioblastoma and human CMV

Viral infections can induce cancer formation, e.g. HPV infection and cervical cancer [70], which can be used to vaccinate prior to cancer development. On the other hand, viruses may also contribute to cancer progression. Although here a prophylactic vaccine will not work, it can open the door to develop therapeutic vaccines with higher immunogenicity due to the presence of viral, non-self antigens. Especially in cancers which have a low mutational load, such as glioblastoma multiforme (**GBM**) [69], and hence, hardly express immunogenic neoantigens, targeting the viral antigens might be the solution for effective anti-cancer vaccination.

GBM is the most aggressive brain tumor and median survival time with current therapies is only 14.6 months. Although multiple immunotherapeutic strategies are being explored, efficacy remains poor. Neuro-oncologists are increasingly interested in the presence and involvement of human cytomegalovirus (HCMV) in the pathogenesis of GBM and its potential use for targeted therapy. GBM comprises 80% of malignant brain tumors in adults and, owing to the highly infiltrative nature of GBM, surgical resection is unable to remove the entire tumor, therefore current standard-of-care treatment also includes chemoradiation. Unfortunately, GBM stem-like cells (SLC) are resistant to chemoradiation and often patients experience recurrence [71]. It is increasingly clear that new therapies are warranted and immunotherapeutic strategies are widely explored. Unfortunately, ongoing immunotherapeutic strategies based on vaccination against tumor antigens such as rindopepimut, a peptide-based vaccine targeting epidermal growth factor receptor variant III (EGFRvIII), have not demonstrated complete clearance [72]. Moreover, due to the relatively low mutational rate of GBM there is a lack sufficient neoantigens and new antigenic targets are necessary [69].

The fact that human cytomegalovirus (HCMV) is absent in healthy tissue, but found in 75-100% of various grade gliomas makes it an attractive target candidate for HCMV-

specific cytotoxic (CD8^{+}) T cells [73]. Interestingly, recent studies showed that HCMV has a higher infection efficiency in GBM SLC compared to other glioma cell lines and HCVM infection can even induce a SLC phenotype in GBM tumor cells [74]. As GBM is a highly heterogeneous tumor, a single antigenic target is likely insufficient. Therefore we hypothesize that the combination of endogenous and HCMV epitopes for the activation of tumor specific T cells would represent a viable alternative to enhance killing of both 'regular' tumor cells and SLC. The potential of patient-derived HCMV specific T cells to target GBM has been described. A clinical trial using HCMV pp65-RNA pulsed DCs in combination with vaccine site pre-conditioning showed effective pp65-specific immune responses for several months and highest in long-term surviving patients, confirming the potential of HCMV as target for GBM treatment [75]. The multivalent glyco-dendrimer vaccine described in **chapter 4** of this thesis can represent a viable strategy to include the different HCMV antigens and induce adaptive immunity against cancers such as GBM.

Epitope inclusion within multivalent antigenic dendrimers

Designing synthetic peptide (anti-tumor) vaccines comes with challenges, including chemical parameters such as solubility and stability, and the influence on biological activity [76]. The PAMAM-dendrimers used in this thesis (**chapter 4 and 5**) are often used as tool to enhance both aqueous solubility and stability [77]. We observed that conjugation of hydrophobic peptide sequences, such as the HLA-A2 specific HCMV epitope, appeared to overrule PAMAM-dendrimer core solubility leading to aggregates (**Chapter 5, Figure S1A**). There are ways to avoid this aggregation e.g. by addition of combined hydrophobic CD8 (MHC I) and hydrophilic CD4 (MHC II) epitopes as we used in **chapter 4** with the melanoma specific gp100 construct. Also addition of hydrophilic amino acids to the antigenic epitope could rescue solubility of the HCMV specific glyco-dendrimers (**chapter 5, Figure S1B-C**). However, when combining epitopes or including other amino acids within the natural peptide sequence, it is important to ensure that no unwanted peptide sequences appear following intracellular processing. These unwanted sequences may instruct adverse immune responses against epitopes present on other tissues than the tumor. Furthermore, we should be aware that different peptide sequences may influence 3D conformation of the glyco-dendrimers [78]. Careful evaluation of CLR targeting for enhanced uptake and (cross)-presentation is required when new peptides are conjugated to create tumor specific (glyco)-dendrimers. Nevertheless, our glycan-modified vaccine described in **chapter 4** has the potential to be used in a "one-size-

fits-multiple-tumors" format, since the multivalent nature can harbor multiple tumor specific or shared epitopes.

Concluding remarks

In summary, this thesis shows that the CLR Langerin and DC-SIGN expressed by human skin LC and dermal DC, respectively, are excellent candidates for targeted intradermal anti-tumor vaccination strategies. By designing a ''tailor-made'' multivalent glycan-modified vaccine with the glycan Le^y, a dual targeting ability arises to both receptors. This ensures endocytosis by multiple human skin DC *in situ* using one formulation of a glycan-modified vaccine. Inclusion of an SLP consisting of both a CD4$^+$ and CD8$^+$ gp100 specific antigen resulted in activation of both CD4$^+$ and CD8$^+$ T cells. Furthermore, we show that the addition of PRR agonists as adjuvant enhances tumor specific CD8$^+$ T cell activation. Importantly, future studies should focus on the use of models which combine the complexity of the human skin and adjuvant induced immune cell- and antigen trafficking. The intradermal anti-tumor vaccination strategy targeting multiple human skin DC subsets that we have generated has potential merit for use against multiple tumor types that are eradicated by tumor specific CD4$^+$ and CD8$^+$ T cells.

Chapter 7

References

1. Pardoll, D.M., *The blockade of immune checkpoints in cancer immunotherapy.* Nat Rev Cancer, 2012. **12**(4): p. 252-64.

2. Minetto, P., et al., *Harnessing NK Cells for Cancer Treatment.* Front Immunol, 2019. **10**: p. 2836.

3. Granot, Z., *Neutrophils as a Therapeutic Target in Cancer.* Front Immunol, 2019. **10**: p. 1710.

4. Restifo, N.P., M.E. Dudley, and S.A. Rosenberg, *Adoptive immunotherapy for cancer: harnessing the T cell response.* Nat Rev Immunol, 2012. **12**(4): p. 269-81.

5. Spitzer, M.H., et al., *Systemic Immunity Is Required for Effective Cancer Immunotherapy.* Cell, 2017. **168**(3): p. 487-502 e15.

6. Ahrends, T., et al., *CD4(⁺) T Cell Help Confers a Cytotoxic T Cell Effector Program Including Coinhibitory Receptor Downregulation and Increased Tissue Invasiveness.* Immunity, 2017. **47**(5): p. 848-861 e5.

7. Borst, J., et al., *CD4(⁺) T cell help in cancer immunology and immunotherapy.* Nat Rev Immunol, 2018. **18**(10): p. 635-647.

8. Gall, C.M.L., et al., *Dendritic cells in cancer immunotherapy.* Nature Materials 2018. **17**(6): p. 472-477.

9. Tacken, P.J., et al., *Dendritic-cell immunotherapy: from ex vivo loading to in vivo targeting.* Nat Rev Immunol, 2007. **7**(10): p. 790-802.

10. Hawiger, D., et al., *Dendritic Cells Induce Peripheral T Cell Unresponsiveness Under Steady State Conditions In Vivo.* Journal of Experimental Medicin, 2001. **194**(6): p. 769-779.

11. van Dinther, D., et al., *Targeting C-type lectin receptors: a high-carbohydrate diet for dendritic cells to improve cancer vaccines.* J Leukoc Biol, 2017. **102**(4): p. 1017-1034.

12. Collin, M. and V. Bigley, *Human dendritic cell subsets: an update.* Immunology, 2018. **154**(1): p. 3-20.

13. Unger, W.W., et al., *Glycan-modified liposomes boost CD4⁺ and CD8⁺ T-cell responses by targeting DC-SIGN on dendritic cells.* J Control Release, 2012. **160**(1): p. 88-95.

14. Fehres, C.M., et al., *In situ Delivery of Antigen to DC-SIGN(⁺)CD14(⁺) Dermal Dendritic Cells Results in Enhanced CD8(⁺) T-Cell Responses.* J Invest Dermatol, 2015. **135**(9): p. 2228-2236.

15. Klechevsky, E., et al., *Functional specializations of human epidermal Langerhans cells and CD14⁺ dermal dendritic cells.* Immunity, 2008. **29**(3): p. 497-510.

16. Haniffa, M., M. Gunawan, and L. Jardine, *Human skin dendritic cells in health and disease.* J Dermatol Sci, 2015. **77**(2): p. 85-92.

17. Haniffa, M., et al., *Human tissues contain CD141hi cross-presenting dendritic cells with functional homology to mouse CD103⁺ nonlymphoid dendritic cells.* Immunity, 2012. **37**(1): p. 60-73.

18. Dudziak, D., et al., *Differential Antigen Processing by Dendritic Cell Subsets in Vivo* Science, 2007. **315**(5808): p. 107-111.

19. Duinkerken, S., et al., *Glyco-Dendrimers as Intradermal Anti-Tumor Vaccine Targeting Multiple Skin DC Subsets.* Theranostics, 2019. **9**(20): p. 5797-5809.

20. Tang-Huau, T.L., et al., *Human in vivo-generated monocyte-derived dendritic cells and macrophages cross-present antigens through a vacuolar pathway.* Nat Commun, 2018. **9**(1): p. 2570.

21. Klechevsky, E., et al., *Cross-priming CD8⁺ T cells by targeting antigens to human dendritic cells through DCIR.* Blood, 2010. **116**(10): p. 1685-97.

22. Hain, T., et al., *Dermal CD207-Negative Migratory DendriticCells Are Fully Competent to Prime Protective,Skin Homing Cytotoxic T-LymphocyteResponses.* Journal of Investigative Dermatology, 2019. **139**: p. 422-429.

23. Santegoets, S.J.A.M., et al., *Inducing Antitumor T Cell Immunity: Comparative Functional Analysis of Interstitial Versus Langerhans Dendritic Cells in a Human Cell Line Model.* The Journal of Immunology, 2008. **180**(7): p. 4540-4549.

24. Mami-Chouaib, F., et al., *Resident memory T cells, critical components in tumor immunology.* J Immunother Cancer, 2018. **6**(1): p. 87.

25. Malik, B.T., et al., *Resident memory T cells in the skin mediate durable immunity to melanoma.* Sci Immunol, 2017. **2**(10).

26. Galvez-Cancino, F., et al., *Vaccination-induced skin-resident memory CD8($^+$) T cells mediate strong protection against cutaneous melanoma.* Oncoimmunology, 2018. **7**(7): p. e1442163.

27. Embgenbroich, M. and S. Burgdorf, *Current Concepts of Antigen Cross-Presentation.* Front Immunol, 2018. **9**: p. 1643.

28. van de Ven, R., et al., *Characterization of four conventional dendritic cell subsets in human skin-draining lymph nodes in relation to T-cell activation.* Blood, 2011. **118**(9): p. 2502-10.

29. Schmidt, S.T., et al., *The administration route is decisive for the ability of the vaccine adjuvant CAF09 to induce antigen-specific CD8($^+$) T-cell responses: The immunological consequences of the biodistribution profile.* J Control Release, 2016. **239**: p. 107-17.

30. Kelly, H.G., S.J. Kent, and A.K. Wheatley, *Immunological basis for enhanced immunity of nanoparticle vaccines.* Expert Rev Vaccines, 2019. **18**(3): p. 269-280.

31. Leon, B. and F.E. Lund, *Compartmentalization of dendritic cell and T-cell interactions in the lymph node: Anatomy of T-cell fate decisions.* Immunol Rev, 2019. **289**(1): p. 84-100.

32. Ohl, L., et al., *CCR7 governs skin dendritic cell migration under inflammatory and steady-state conditions.* Immunity, 2004. **21**(2): p. 279-88.

33. Segura, E., et al., *Characterization of resident and migratory dendritic cells in human lymph nodes.* J Exp Med, 2012. **209**(4): p. 653-60.

34. Stoitzner, P., et al., *Visualization and characterization of migratory Langerhans cells in murine skin and lymph nodes by antibodies against Langerin/CD207.* J Invest Dermatol, 2003. **120**(2): p. 266-74.

35. McGovern, N., et al., *Human dermal CD14($^+$) cells are a transient population of monocyte-derived macrophages.* Immunity, 2014. **41**(3): p. 465-77.

36. Klechevsky, E., et al., *Understanding human myeloid dendritic cell subsets for the rational design of novel vaccines.* Hum Immunol, 2009. **70**(5): p. 281-8.

37. Haniffa, M., et al., *Differential rates of replacement of human dermal dendritic cells and macrophages during hematopoietic stem cell transplantation.* J Exp Med, 2009. **206**(2): p. 371-85.

38. de Gruijl, T.D., et al., *A Postmigrational Switch among Skin-Derived Dendritic Cells to a Macrophage-Like Phenotype Is Predetermined by the Intracutaneous Cytokine Balance.* The Journal of Immunology, 2006. **176**(12): p. 7232-7242.

39. Lindenberg, J.J., et al., *IL-10 conditioning of human skin affects the distribution of migratory dendritic cell subsets and functional T cell differentiation.* PLoS One, 2013. **8**(7): p. e70237.

40. Fehres, C.M., et al., *Topical rather than intradermal application of the TLR7 ligand imiquimod leads to human dermal dendritic cell maturation and CD8$^+$ T-cell cross-priming.* Eur J Immunol, 2014. **44**(8): p. 2415-24.

41. Schetters, S.T.T., et al., *Immunological dynamics after subcutaneous immunization with a squalene-based oil-in-water adjuvant.* FASEB, 2020.

42. Schetters, S.T.T., et al., *Mouse DC-SIGN/CD209a as Target for Antigen Delivery and Adaptive Immunity.* Front Immunol, 2018. **9**: p. 990.

43. Lambrecht, B.N., et al., *Mechanism of action of clinically approved adjuvants.* Curr Opin Immunol, 2009. **21**(1): p. 23-9.

44. Krausgruber, T., et al., *Structural cells are key regulators of organ-specific immune responses.* Nature, 2020. **583**(7815): p. 296-302.

45. McKee, A.S. and P. Marrack, *Old and new adjuvants.* Curr Opin Immunol, 2017. **47**: p. 44-51.

46. Yao, C., et al., *Toll-like receptor family members in skin fibroblasts are functional and have a higher expression compared to skin keratinocytes.* Int J Mol Med, 2015. **35**(5): p. 1443-50.

47. del Pilar Martin, M., et al., *Local Response to Microneedle-Based Influenza Immunization in the Skin.* mBio, 2012. **3**(2): p. e00012-12.

48. van Aalst, S., et al., *Routing dependent immune responses after experimental R848-adjuvated vaccination.* Vaccine, 2018. **36**(11): p. 1405-1413.

49. Tregoning, J.S., R.F. Russell, and E. Kinnear, *Adjuvanted influenza vaccines.* Hum Vaccin Immunother, 2018. **14**(3): p. 550-564.

50. Tregoning, J.S., R.F. Russell, and E. Kinnear, *Adjuvanted influenza vaccines.* Human Vaccines & Immunotherapeutics, 2018. **14**(3): p. 550-564.

51. Langlet, C., et al., *CD64 Expression Distinguishes Monocyte-Derived and Conventional Dendritic Cells and Reveals Their Distinct Role during Intramuscular Immunization.* The Journal of Immunology, 2012. **188**(4): p. 1751.

52. Cioncada, R., et al., *Vaccine adjuvant MF59 promotes the intranodal differentiation of antigen-loaded and activated monocyte-derived dendritic cells.* PLOS ONE, 2017. **12**(10): p. e0185843.

53. Terhorst, D., et al., *Laser-assisted intradermal delivery of adjuvant-free vaccines targeting XCR1+ dendritic cells induces potent antitumoral responses.* J Immunol, 2015. **194**(12): p. 5895-902.

54. Machado, Y., et al., *Synergistic effects of dendritic cell targeting and laser-microporation on enhancing epicutaneous skin vaccination efficacy.* J Control Release, 2017. **266**: p. 87-99.

55. Ernst, P.B. and A.R. Carvunis, *Of mice, men and immunity: a case for evolutionary systems biology.* Nat Immunol, 2018. **19**(5): p. 421-425.

56. Jameson, S.C. and D. Masopust, *What Is the Predictive Value of Animal Models for Vaccine Efficacy in Humans? Reevaluating the Potential of Mouse Models for the Human Immune System.* Cold Spring Harb Perspect Biol, 2018. **10**(4).

57. Beura, L.K., et al., *Normalizing the environment recapitulates adult human immune traits in laboratory mice.* Nature, 2016. **532**: p. 512.

58. Garcia-Vallejo, J.J. and Y. van Kooyk, *The physiological role of DC-SIGN: A tale of mice and men.* Trends in Immunology, 2013. **34**(10): p. 482-486.

59. Douam, F., et al., *Selective expansion of myeloid and NK cells in humanized mice yields human-like vaccine responses.* Nature Communications, 2018. **9**(1): p. 5031.

60. Walsh, N.C., et al., *Humanized Mouse Models of Clinical Disease.* Annual review of pathology, 2017. **12**: p. 187-215.

61. Klein, S.L. and K.L. Flanagan, *Sex differences in immune responses.* Nature Reviews Immunology, 2016. **16**: p. 626.

62. Schaefer, M., et al., *Decreased Pathology and Prolonged Survival of Human DC-SIGN Transgenic Mice during Mycobacterial Infection.* The Journal of Immunology, 2008. **180**(10): p. 6836-6845.

63. van den Broek, L.J., et al., *Progress and Future Prospectives in Skin-on-Chip Development with Emphasis on the use of Different Cell Types and Technical Challenges.* Stem Cell Rev, 2017. **13**(3): p. 418-429.

64. Ouwehand, K., et al., *Technical advance: Langerhans cells derived from a human cell line in a full-thickness skin equivalent undergo allergen-induced maturation and migration.* J Leukoc Biol, 2011. **90**(5): p. 1027-33.

65. LAN, T., et al., *Induced pluripotent stem cells can effectively differentiate into multiple functional lymphocyte lineages in vivo with negligible bias.* Stem Cells Dev. , 2016. **25**(6): p. 462-71.

66. Knorr, D.A.e.a., *Clinical-Scale Derivation of Natural Killer Cells From Human Pluripotent Stem Cells for Cancer Therapy.* Stem Cells Transl. Med, 2013. **2**: p. 274–283.

67. Gilboa, E., *The Makings of a Tumor Rejection Antigen.* Immunity, 1999. **11**: p. 263-270.

68. Fuentes-González, A.M., et al., *The modulation of apoptosis by oncogenic viruses.* Virology Journal 2013. **10**.

69. Alexandrov, L.B., et al., *Signatures of mutational processes in human cancer.* Nature, 2013. **500**(7463): p. 415-21.

70. Schiffman, M., et al., *Human papillomavirus and cervical cancer.* Lancet 2007. **370**: p. 890-907.

71. Seymour, T., A. Nowak, and F. Kakulas, *Targeting Aggressive Cancer Stem Cells in Glioblastoma.* Front Oncol, 2015. **5**: p. 159.

72. Schuster, J., et al., *A phase II, multicenter trial of rindopepimut (CDX-110) in newly diagnosed glioblastoma: the ACT III study.* Neuro Oncol, 2015. **17**(6): p. 854-61.

73. Dziurzynski, K., et al., *Consensus on the role of human cytomegalovirus in glioblastoma.* Neuro Oncol, 2012. **14**(3): p. 246-55.

74. Soroceanu, L., et al., *Cytomegalovirus Immediate-Early Proteins Promote Stemness Properties in Glioblastoma.* Cancer Res, 2015. **75**(15): p. 3065-76.

75. Mitchell, D.A., et al., *Tetanus toxoid and CCL3 improve dendritic cell vaccines in mice and glioblastoma patients.* Nature, 2015. **519**(7543): p. 366-9.

76. Buteau, C., S.N. Markovic, and E. Celis, *Challenges in the Development of Effective Peptide Vaccines for Cancer* Mayo Clin Proc, 2002. **77**: p. 339-349.

77. Chauhan, A.S., *Dendrimers for Drug Delivery.* Molecules, 2018. **23**(4).

78. Barata, T.S., et al., *From sequence to 3D structure of hyperbranched molecules: application to surface modified PAMAM dendrimers.* J Mol Model, 2011. **17**(11): p. 2741-9.

APPENDIX

NEDERLANDSE SAMENVATTING

LIST OF PUBLICATIONS

DANKWOORD

CURRICULUM VITAE

NEDERLANDSE SAMENVATTING

"Dansen met Dendritische Cellen: richten op humane huid dendritische cellen voor anti-tumor immuniteit"

Recentelijk komt het onderwerp vaccineren vaak in het nieuws en vooral ook voorbij op sociale media, en helaas niet altijd in een goed daglicht. Maar wat is vaccineren nou eigenlijk, wat houdt het werkelijk in en hoe kunnen we het vandaag de dag ook gebruiken voor anti-kanker therapie, zoals beschreven in dit proefschrift?

Van oudsher wordt vaccineren gebruikt voor het aanzetten van het immuunsysteem om ziekteverwekkers, zoals virussen, af te kunnen weren zonder hier ernstig ziek van te worden. Hiertoe worden onderdelen van het virus in het vaccin gestopt welke niet zullen leiden tot infectie, maar wel specifiek worden herkent door het immuunsysteem om de afweer op te bouwen. In het geval van infectieziekten kan dit vooraf, ofwel profylactisch, zodat het immuunsysteem op moment van infectie snel kan reageren en voorkomen dat we ziek worden. Voor kanker kunnen we enkel profylactisch vaccineren wanneer deze viraal geïnduceerd is, zoals bij baarmoederhalskanker, om het verschijnen van dit type kanker te voorkomen.

De meeste tumoren ontstaan echter door een opbouw van mutaties in de cel onder invloed van bijvoorbeeld UV-straling, met als gevolg ongeremde groei. Een anti-kanker vaccin zal alleen werken als het herkenning van deze mutaties door het immuunsysteem aanzet. Aangezien het lastig is vooraf te bepalen welke mutaties zullen opdoemen, kunnen vaccins tegen dit type kanker enkel achteraf, ofwel therapeutisch, gegeven worden. In dit proefschrift beschrijven we de ontwikkeling van een therapeutisch anti-kanker vaccin, waarvoor we melanoom ter illustratie hebben gebruikt.

Om inzicht te geven hoe een vaccin precies werkt en hoe hier gebruik gemaakt van kan worden, is het belangrijk de werking van het immuun systeem te begrijpen. In ons lichaam zitten dendritische cellen (DC) die constant de omgeving aftasten. Komen ze iets tegen wat er niet hoort te zijn, dan nemen ze dit op om te verwerken tot kleine peptiden. Tussen de vele peptiden die gegenereerd worden zitten specifieke sequenties, de antigenen, die geladen kunnen worden op zogenaamde MHC moleculen. DC migreren vervolgens naar de lymfeklieren waar T cellen het peptide gepresenteerd in MHC op het celmembraan van de DC zullen herkennen

voor activatie. Grofweg kunnen de T cellen opgedeeld worden in twee groepen: de (CD4+) helper en de (CD8+) cytotoxische T cellen. Zoals de naam al zegt, zullen helper T cellen helpen bij initiëren van gerichte immuun responsen door andere immuun cellen aan te sturen, terwijl cytotoxische T cellen zelf direct kunnen doden. Met anti-kanker vaccinatie willen we dan ook met name de cytotoxische T cellen activeren.

Voor het activeren van de helper of cytotoxische T cellen gebruikt de DC twee klassieke routes om de antigenen te presenteren. De eerste is voor componenten die van buiten de cel komen (bijvoorbeeld bacteriën) en de tweede voor componenten die aanwezig zijn in de cel (bijvoorbeeld virussen). Componenten van buiten de cel worden verwerkt tot peptiden die geladen en gepresenteerd worden op MHC type II moleculen voor helper T cel activatie, terwijl die van binnen in de cel op MHC type I moleculen worden gepresenteerd voor cytotoxische T cel activatie. Echter, de peptiden afkomstig van componenten buiten de cel kunnen door de DC ook op MHC type I moleculen geladen worden, beter bekend als cross-presentatie. Deze derde route van antigeen presentatie is met name belangrijk voor anti-kanker vaccins, aangezien het vaccin van buitenaf door de DC opgenomen zal worden.

Naast herkenning van peptide-MHC complexen hebben T cellen nog extra stimulatie van de DC nodig, gegeven via co-stimulatoire moleculen. Als deze stimulatie niet aanwezig is zullen de T cellen niet geactiveerd worden en in anergie gaan. De DC brengt co-stimulatoire moleculen tot expressie na het herkennen van een "gevaar" signaal via "patroon herkennende receptoren" (PRR). Er zijn ook PRR die opname faciliteren door het binden van suikers, de C-type lectine receptoren (CLR). Daarnaast kan opname via CLR cross-presentatie verhogen doordat peptiden beschikbaar komen voor belading van MHC type I moleculen. Een anti-kanker vaccin moet dus uit twee componenten bestaan: de tumor specifieke antigenen en een gevaar signaal.

Een belangrijk aspect van vaccineren is de plek van toedienen, omdat het vaccin bij de DC terecht moet komen om immuniteit op te kunnen bouwen. In onze huid zitten meerdere typen DC, namelijk Langerhans cellen (LC) in de epidermis (opperhuid) en drie verschillende DC in de dermis (lederhuid). De verschillende DC zijn elk gespecialiseerd in het induceren van op maat gemaakte immuun responsen. Dit maakt de huid een zeer geschikte plek voor het toedienen van een vaccin.

Appendix

In dit proefschrift hebben we de mogelijkheden onderzocht om een anti-kanker vaccin te ontwikkelen dat in de huid geïnjecteerd kan worden voor het opwekken van anti-kanker immuun responsen. Hiervoor hebben we gebruik gemaakt van het melanoom specifieke eiwit gp100, waarvan de peptide (of antigeen) sequenties bekend zijn. Deze kunnen we chemisch synthetiseren om aan het eerste benodigde component van een vaccin te voldoen. Daarnaast hebben we onderzocht of we verhoogde cross-presentatie kunnen induceren door de gesynthetiseerde gp100 peptiden te koppelen aan suikers welke CLR kunnen binden die aanwezig zijn op de verschillende huid DC. Verder hebben we onderzocht of en hoe we met behulp van het tweede vaccin component, het gevaar signaal, de cytotoxische T cel activatie kunnen verhogen.

In **hoofdstuk 2** hebben we laten zien dat peptide opname via de CLR Langerin in combinatie met het gevaar signaal Poly I:C resulteert in verhoogde cytotoxische T cel activatie. Verder hebben we laten zien dat Langerin efficiënter is voor cytotoxische T cel activatie dan een andere CLR welke ook aanwezig is op LC, Dectin-1. Dit komt doordat de synthetische peptiden opgenomen via Langerin langer intact blijven dan via Dectin-1, wat ervoor zorgt dat ze langer beschikbaar zijn om in de cross-presentatie route terecht te komen.

In **hoofdstuk 3** bestuderen we de route die antigenen nemen na opname via DC-SIGN. Ook peptide opname via deze receptor kan cytotoxische T cel activatie induceren wat we wederom konden verhogen door een gevaar signaal erbij te geven. In dit hoofdstuk laten we zien dat dit specifieke gevaar signaal, LPS, ervoor zorgt dat peptiden opgenomen via DC-SIGN vrij komen in het cytosol van de cel en daarmee beschikbaar voor cross-presentatie en cytotoxische T cel activatie.

Naar aanleiding van de bevindingen in hoofdstuk 2 en 3, waarin vaccin opname via zowel Langerin als DC-SIGN individueel versterkte cytotoxische T cel activatie gaven, was onze vraag of een verdere versterking mogelijk was door een vaccin te ontwikkelen dat simultaan gericht kan worden aan Langerin en DC-SIGN. Op die manier kunnen meerdere huid DC geactiveerd worden voor het instrueren van anti-kanker immuun responsen. Hiervoor hebben we gebruik gemaakt van een suikerstructuur welke door zowel Langerin als DC-SIGN herkend wordt. Echter heeft Langerin voorkeur voor kleine suiker-gecoate peptide-structuren, terwijl DC-SIGN beter grote opneemt. Daarom hebben we in **hoofdstuk 4** een geraamte

gebruikt waar meerdere peptiden aan gekoppeld kunnen worden. Dit gaf meerdere groottes, multivalente peptide-structuren, waaraan we de suiker Lewis Y (Le^y) hebben gekoppeld om uit te zoeken welke door beide receptoren herkent en verwerkt wordt voor cytotoxische T cel activatie. Daarbij hebben we de gevaar signalen Poly I:C en MPLA (een LPS afgeleide) gebruikt, zoals in hoofdstuk 2 en 3. Dit heeft geresulteerd in een enkel melanoom specifiek vaccin dat in één keer meerdere humane huid DC kan bereiken voor instructie van anti-kanker immuun responsen.

We hebben in **hoofdstuk 2, 3** en **4** laten zien dat het activeren van PRR op DC met behulp van de gevaar signalen Poly I:C en LPS/MPLA van belang is om betere cytotoxische T cel activatie te krijgen. In **hoofdstuk 5** hebben we onderzocht of het veel gebruikte gevaar signaal 'MDP', afkomstig van bacteriën, ook gebruikt kan worden voor activatie van humane huid DC en cytotoxische T cellen. MDP wordt herkent door een PRR welke zich in het cytosol van de DC bevindt, NOD2, en zal dus pas na opname het gevaar signaal kunnen afgeven. Daarom hebben we onze unieke multivalente peptide-structuur gebruikt, en hier chemisch MDP aan gekoppeld. We laten zien dat dit een efficiënte manier is om MDP in de huid DC te krijgen en hiermee verhoogde cytotoxische T cel activatie te genereren.

Het toedienen van intradermale vaccins geschiedt gewoonlijk via injectie, echter, zijn er nieuwe technieken in ontwikkeling die dit kunnen vergemakkelijken. Een van die technieken is het gebruik van een laser welke kleine gaatjes in de huid maakt, waarna het vaccin erop toegediend wordt. Behalve het toegenomen gemak, zijn er ook studies die laten zien dat via de laser gevaar signalen afgegeven worden, wat het apart toevoegen van gevaar moleculen aan een vaccin overbodig maakt. In **hoofdstuk 6** hebben we gekeken of onze anti-kanker vaccins ook na laser behandeling toegediend kunnen worden en of dit een toegevoegde waarde heeft ten opzichte van injecteren voor het induceren van anti-kanker immuun responsen. Hiervoor hebben we gebruik gemaakt van een humaan huid model, waarin we laten zien dat injecteren beter werkt voor het toedienen van onze anti-kanker vaccins door verhoogde opname en T cel activatie vergeleken met toediening na laser behandeling.

In conclusie, in dit proefschrift hebben we een anti-kanker vaccin ontwikkeld bestaande uit een melanoom specifiek, synthetisch multivalente peptide-structuur met daaraan suikers, en een gevaar signaal. Dit heeft geresulteerd in specifieke opname door meerdere huid DC via Langerin en DC-SIGN , na intradermale injectie.

De gerichte levering naar deze CLRs in combinatie met gevaar signalen heeft geresulteerd in verhoogde cytotoxische T cel activatie, welke de capaciteit hebben om specifiek kanker cellen te doden en daarmee kanker op te ruimen. Kortom, ons synthetische vaccin bied de mogelijkheid voor inclusie van meerdere kanker specifieke antigenen en heeft potentie voor klinisch onderzoek om kanker in de toekomst te genezen.

PUBLICATION LIST

Stolk DA, de Haas A, Vree J, **Duinkerken S**, Lübbers J, van de Ven R, Ambrosini M, Kalay H, Bruijns S, van der Vliet HJ, de Gruijl TD, van Kooyk Y. *Lipo-Based Vaccines as an approach to Target Dendritic Cells for Induction of T- and iNKT Cell Responses.* Front. Immunol. 2020 May 27.
doi: https://doi.org/10.3389/fimmu.2020.00990

Duinkerken S, Lübbers J, Stolk DA, Vree J, Ambrosini M, Kalay H, van Kooyk Y. *Comparison of intradermal injection and epicutaneous laser microporation for antitumor vaccine delivery in a human skin explant model.* bioRxiv 861930 2019 Dec 05.
doi: https://doi.org/10.1101/861930

Duinkerken S, Li RE, van Haften FJ, de Gruijl TD, Chiodo F, Schetters STT, van Kooyk Y. *Chemically engineered glycan-modified cancer vaccines to mobilize skin dendritic cells.* Curr Opin Chem Biol. 2019 Dec;53:167-172.
 doi: 10.1016/j.cbpa.2019.10.001. Epub 2019 Oct 31.

Duinkerken S, Horrevorts SK, Kalay H, Ambrosini M, Rutte L, de Gruijl TD, Garcia-Vallejo JJ, van Kooyk Y. *Glyco-Dendrimers as Intradermal Anti-Tumor Vaccine Targeting Multiple Skin DC Subsets.* Theranostics. 2019 Aug 12;9(20):5797-5809.
doi: 10.7150/thno.35059.

Horrevorts SK, Stolk DA, van de Ven R, Hulst M, van Het Hof B, **Duinkerken S**, Heineke MH, Ma W, Dusoswa SA, Nieuwland R, Garcia-Vallejo JJ, van de Loosdrecht AA, de Gruijl TD, van Vliet SJ, van Kooyk Y. *Glycan-Modified Apoptotic Melanoma- Derived Extracellular Vesicles as Antigen Source for Anti-Tumor Vaccination.* Cancers (Basel). 2019 Aug 28;11(9):1266.
doi: 10.3390/cancers11091266.

Horrevorts SK, **Duinkerken S**, Bloem K, Secades P, Kalay H, Musters RJ, van Vliet SJ, García-Vallejo JJ, van Kooyk Y. *Toll-Like Receptor 4 Triggering Promotes Cytosolic Routing of DC-SIGN-Targeted Antigens for Presentation on MHC Class I.* Front Immunol. 2018 Jun 14;9:1231.
doi: 10.3389/fimmu.2018.01231.

Machado Y, **Duinkerken S**, Hoepflinger V, Mayr M, Korotchenko E, Kurtaj A, Pablos I, Steiner M, Stoecklinger A, Lübbers J, Schmid M, Ritter U, Scheiblhofer S, Ablinger M, Wally V, Hochmann S, Raninger AM, Strunk D, van Kooyk Y, Thalhamer J, Weiss R. *Synergistic effects of dendritic cell targeting and laser-microporation on enhancing epicutaneous skin vaccination efficacy.* J Control Release. 2017 Nov 28;266:87-99. doi: 10.1016/j.jconrel.2017.09.020. Epub 2017 Sep 14.

Duinkerken S, van Kooyk Y, Garcia-Vallejo JJ. *Human cytomegalovirus-based immunotherapy to treat glioblastoma: Into the future.* Oncoimmunology. 2016 Jul 25;5(9):e1214791.
doi: 10.1080/2162402X.2016.1214791.

Fehres CM, **Duinkerken S**, Bruijns SC, Kalay H, van Vliet SJ, Ambrosini M, de Gruijl TD, Unger WW, Garcia-Vallejo JJ, van Kooyk Y. *Langerin-mediated internalization of a modified peptide routes antigens to early endosomes and enhances cross-presentation by human Langerhans cells.* Cell Mol Immunol. 2017 Apr;14(4):360-370. doi: 10.1038/cmi.2015.87. Epub 2015 Oct 12.

Appendix

DANKWOORD

Oktober 2014 begon het grote avontuur. Waar we toen de grap maakten dat 2020 ons jaar zou worden, konden we klaarblijkelijk de toekomst voorspellen. Na zinderende hitte, watervallen op de trap, pierenbadjes in de gang en de grote migratie overleefd te hebben, is nu ook ein-de-lijk mijn thesis af! Wat een bevalling, alhoewel… vergeleken daarmee valt het eigenlijk allemaal reuze mee, het duurt alleen wat langer. Het tot stand komen van dit "boekje" is uiteraard niet vanzelf gegaan en ook zeker niet zonder de hulp van velen.

Allereerst mijn promotor **Yvette**. Wat vond ik het spannend om te komen solliciteren. Bij thuiskomst op mijn nagels zitten bijten terwijl je me ongeveer 10 minuten nadat ik naar buiten was gelopen al had gemaild dat ik de positie mocht komen vervullen.. kwam ik 3 uur later pas achter. Ik ben heel erg blij dat ik mijn PhD in jou groep en onder jou supervisie heb mogen doen. Niet alleen op wetenschappelijk vlak heb ik veel van je geleerd, maar door je grote mensen kennis heb ik mezelf ook op persoonlijk vlak kunnen ontwikkelen. Je zag dingen voor ik het zelf doorhad, maar gaf ook tijd en ruimte om dit zelf te ontdekken en ervan te leren. Heel veel dank voor alle tijd en energie die je in me heb gestoken en het vertrouwen dat je me geeft om mijn carrière te vervolgen in het onderwijs onder jouw hoede!

Dan natuurlijk mijn co-promotoren. **Juan**, we met when I was a 1st year master student and supervised me during my 2nd year for my master thesis. Then I already learned that you have a very creative mind and are a great writer, and was very pleased to hear you would be there at my site during my PhD as well. You are always up-to-date with the latest technical developments and guided me to use these to up the game of my experiments and analysis. I want to thank you for your time and input during the course of my PhD. It is special that you are now here as co-promotor, who would have thought the first time I walked through your office door.

Tanja, in het begin vond ik jou best intimiderend met je ongelofelijke hoeveelheid kennis en directe aanpak. Maar gedurende de vele huid meetings heb ik je ook leren kennen als een ontzettend leuk persoon, want er werd naast goed gediscussieerd ook zeker veel gelachen. Je input is ontzettend waardevol geweest voor mijn PhD en daar wil ik je ontzettend voor bedanken. Het gezellige borrelen in Aken tijdens de DC2018 zal me altijd bijblijven.

Ook wil ik hier graag de **leescommissie** bedanken voor de tijd die ze gestoken hebben in het kritisch lezen van mijn thesis en het aanwezig zijn tijdens mijn verdediging.

Nu mijn spetterende, fantastische, niet te missen paranimfen; **Lenneke** en **Eveline**.

Lennieee, mijn absolute tegenpool, maar we hadden direct een klik toen ik me bij groep Yvette mocht voegen. Met jou heb ik zoveel gedaan dat ik het hier niet eens allemaal op kan sommen, zelfs de high-lights wordt een te lange lijst. Ik heb altijd enorm veel gehad aan je steun en frisse blik op mijn project. Ik bewonder je doorzettingsvermogen, kritische blik en de manier waarop je dingen aanpakt zonder aarzeling. We zijn geen directe collega's meer, maar ik ben heel blij om je nu echt een goede vriendin te kunnen noemen. Lang leve de "koffiemomentjes" over de telefoon!

Liliiii, onze gekke, lieve hello-kitty-china girl. Tijdens ons eerste congres in de Efteling hebben we gezellig in een stapelbedje gelegen, mijn hello-kitty pyjama broek was een directe klik. Maar ons echte grote avontuur was natuurlijk DC2016 in Shanghai!! Dumplinggsss, shoppen, zoektocht naar de perfecte zwarte schoen met rode zool, rondlopen, manicure/pedicures en owja natuurlijk onze fan-tas-tische presentaties op het congres… iets met panda's en tussen gerenommeerde onderzoekers staan… heerlijkheid! Je onverschrokkenheid, openheid, zorgzaamheid en sociale kameleon-kunde vind ik eeuwig genieten. Gelukkig zullen we elkaar nog gewoon zien, want we blijven nog "ff" hangen op de MCBI, FEEST!! En er is een klein mannetje die zo'n fantastisch mens als oppas wel kan waarderen (als mama college moet geven bijvoorbeeld).

Dan natuurlijk **Hakan** en **Martino**, de chemical magicians! Zonder jullie zou dit proefschrift er niet eens liggen. Martino, thanks for the synthesis of all those peptides! Hakan, niets van wat ik vroeg was te gek voor jou en je input hoe we het beste construct konden verkrijgen is onmisbaar geweest. Heel veel dank daarvoor!

De zoete kern: **Sophie H, Sjoerd, Sophie D**. We zijn allemaal rond dezelfde tijd begonnen en ik heb dan ook veel steun en gezelligheid aan jullie gehad. **Sophie H**, jij nam me gelijk onder je vleugels om me wegwijs te maken in het huidmodel en alle bijkomende assays. Je hebt een enorm doorzettingsvermogen en ik wil je bedanken voor de fijne samenwerking die we hebben gehad. Een samenwerking die voor mij ook erg leerzaam is geweest en heeft geresulteerd in een paar mooie hoofdstukken!

Sjoerd (Stuaaaart) **& Sophie D** (Dusosieee), dank voor alle gezellige, hylarische (iets met prinsessen inpak papier) en zeker ook wetenschappelijke momenten. **Sjoerd**, ik moest even wennen aan jou onuitputtelijke discussie modus, maar ik kan het nu heel erg waarderen. Jou kennis van de literatuur is ongekend en stiekem ook heel handig, want je stuurde alles al door voor ik überhaupt aan zoeken toe was gekomen, thanks a bunch. **Sophie D'tje**, ik heb van de zijlijn kunnen zien hoe jij kliniek en wetenschap een stukje dichter bij elkaar heb gebracht. Wat een boel positieve energie heb jij met je meegebracht en ik ben blij dat ik daar tijdens mijn PhD van heb mogen meegenieten.

Mijn O2 roomies **Dieke** en **Ernesto**! **Diek**, voor de grote verhuizing kende ik je eigenlijk helemaal niet zo goed en had ik vooral het beeld dat je een pittige tante bent die niet schroomt om te zeggen wat ze denkt. Nu is dat zeker ook iets wat ik ontzettend aan jou waardeer, je bent altijd eerlijk en zal niet om de hete brij heen draaien. Maar ik heb je als roomie ook leren kennen als een ontzettend lief en zorgzaam iemand. Ik wil je dan ook enorm bedanken voor alle koffie-momentjes en fijne gesprekken die we hebben gehad als roomies en mama's, en hoop dat we contact zullen blijven houden!

Ernie, our morning-misery-mister. You came into the room a bit later, but it was (and is ;)) so much fun! You are one of those silent forces with so much knowledge and great suggestions. Thanks for being you.

Eetclub & koffiepauze team: Kath, Lau, Do, Leo, Kel, Man, Ri, Pau (het is bijna een liedje). Zonder had ik het niet overleefd. **Kathathaaa**, "neem 3 bananen, CHUTTENEEEEY, kieeep, hink-stap-sprong…". Lachen, gieren, brullen, ik heb ervan genoten en geniet er nog steeds van. Graag gedaan en vooral beeedankt. **Laura**, de stille kracht van glycotreat. Helaas ben je een muis affeccionado, maar dat neemt niet weg dat je ook voor mijn (bijna) muisloze PhD ontzettend waardevol bent geweest. Altijd behulpzaam en in voor een afleidingspraatje, dank daarvoor! **Do'tje**, onze altijd positieve brokkenpiloot. Als student hoorde je er al direct helemaal bij en ik ben blij dat je ook je PhD in de groep bent komen doen. Het zit je niet allemaal mee, maar toch weet jij er alles uit te halen. Samen hebben we heel wat huid assays gedaan en ook kort het lab van CCA onveilig gemaakt om door te kunnen blijven stomen tijdens de verhuizing. Dank voor je positiviteit, onuitputtelijke creativiteit en gezelligheid. **Leoni** (Lehooo), wij kennen elkaar al sinds de master en ik ben blij dat we ook een

tijd op de MCBI als collega's hebben kunnen werken! Helaas moest je ons ook weer verlaten, maar we komen elkaar nog wel tegen. Je reactie op mijn zwangerschap zal ik nooit vergeten. Dankje voor alle gezelligheid! **Kelly** (vergeet niet regelmatig een dansje te doen!), **Mandy**, **Richard** en **Paula**, vooral richting het einde van mijn PhD heb ik jullie vaak lastig kunnen vallen met mijn afleidings-hyperactiviteit, suiker toevoer en lekker kunnen koffieleuten. Dank, dank, dank.

Uiteraard wil ik iedereen van **groep Yvette** (subgroep Joke, Sandra, Juan, Jan) bedanken voor behulpzame meetings, gezellige Sinterkerstvieringen en het zijn van steun en toeverlaat gedurende een PhD. **Joyce**, je voegde je bij het skin(ny) ladies team om experimenten met de huid te doen en er lekker op los te laseren. Bedankt voor al je hulp en het samen bij elkaar pipetteren van een van de hoofdstukken! **Migueltje**, we connected during one of the MCBI retreats and I had so much fun with you. Thank you for the Disney nights (dealing with a hangry me) and coffee breaks. I was very sad to see you leave and hope we can keep in touch!

Natuurlijk ook een mega dank naar alle PhDs en andere collega's van de MCBI!!! Het voelt als thuis met jullie!

Ook de studenten die onder mijn bewind hebben moeten werken wil ik bedanken voor hun input. **Jesper** en **Floor**, jullie master thesis hebben me zeer geholpen voor de introductie en discussie van dit proefschrift waarvoor dank! **Marlies**, mijn eerste studente, dank voor je inzet en vrolijke noot. **Lisa**, je staat toch maar mooi als auteur op een van de gepubliceerde hoofdstukken! Dit geeft wel aan dat je je enorm goed heb ingezet tijdens je stage, waar ik je voor wil bedanken.

Een zeer belangrijk onderdeel voor mijn thesis is de toevoer van huid geweest. Hiervoor wil ik **Lianne Meij** van de Bergman Clinics bedanken. Ook veel dank aan **Peter Puts** van SDX, die altijd met een vrolijke lach en een gezellig praatje de emmer(tje)s kwam brengen.

Mijn lieve vrienden die weinig van mijn onderzoek meekregen, maar des te meer van mijn persoonlijkheid. **Merel**, er waren eens twee jonge dames die een introweek samen doorliepen. Dit werd gevold door vele Disney relax avondjes, altijd lekker eten (EEND!), onze magische Disney-Parijs trip en de heerlijke charcuterie-wijn avondjes die onmisbaar zijn geweest om enigszins (mentaal) gezond te blijven. Merci

beaucoup! De ouwe lullen; **Wendy, Marit, Geerte, Margriet, Terry, Britt**; ik ben heel blij met jullie als vriendinnen! Eten, kletsen, zeuren, irritante grapjes maken, het kon allemaal altijd om even stoom af te kunnen blazen, duizendmaal dank! Ook **Nicole, Lieke, Sofie, Baukje** dank voor de gezellige etentjes, feestjes en kletsmomenten. Misschien niet met regelmaat, maar wel altijd heel fijn en zeer gewaardeerd! **Cor, Pep, Jep** (epic weekend Stockholm!), fijn om jullie (via manlief) nog regelmatig gezien en gesproken te hebben en te stampen op feestjes om even te ontspannen van de PhD, dank! **Balleto's**, sinds jongs af aan alles gedeeld, zo ook mijn PhD traject, misschien meer vanaf de zijlijn, maar altijd geïnteresseerd, dank.

Om al het intellectuele geweld van een PhD aan te kunnen is het net zo belangrijk om fysiek even helemaal los te gaan en ook het lijf moe te maken. Hiervoor kon ik terecht bij de beste personal trainer die er is. **Adriaan**, al vanaf mijn 15^e heb jij grote indruk op mij gemaakt. Je bent een ontzettend gedreven, slim en eerlijk mens. Waar onze relatie eerst die van student en leraar was, ben ik enorm blij dat deze is gegroeid tot een zeer dierbare relatie die ik moeilijk in een woord kan omschrijven. Je bent eigenlijk ook een coach geweest die me fysiek uitdaagde, maar waar ik ook mijn ei kwijt kon als het allemaal wat veel werd. Heel veel dank dat ik altijd bij jou terecht kon (en kan)!

Uiteraard is een dankje voor de ouders en grote zus ook op zijn plaats. **Paps, mams** en **Ellebel**, dank voor, tja, alles eigenlijk. De uitwaaiweekendjes op Texel, de altijd open deur, het vertrouwen en nog zoveel meer. Ik ben niet zo van de openbare familiaire klefheid, maar zonder jullie was dit proefschrift er zeker niet gekomen.

Timo en **Abel**, de twee belangrijkste mannen in mijn leven (*pap, jij ook nog steeds hoor*). **Timo**, mijn steun en toeverlaat, ik weet niet wat ik zonder jou zou beginnen. **Abel**, ons mooie, vrolijke, energieke kerelmansie. Kleine topper. Jij maakt elke dag een feestje.

CURRICULUM VITAE

Sanne Duinkerken was born on November 28, 1988 in Swifterbant, The Netherlands. From the age of 10 she was a student at the National Ballet Academy, later combined with the VWO (pre-univeristy) at the Gerrit van der Veen College in Amsterdam. After receiving her diploma for both the NBA and VWO in 2007, she dedicated a year of her life to Cinevox Junior Company in Neuhausen, Switzerland as professional dancer. After that she decided to turn the page and start university in 2008, where she did both the bachelor and master of Biomedical Sciences at the VU in Amsterdam. Prior to starting her master she took one year off from studying to join the board of the student association *RSVU Okeanos*. In 2012 she started her master with specialization in Cardiovascular Diseases (1st year) and Immunology (2nd year). During the first year she did a 6-month internship in the group of Hans Niessen at the Pathology department of the Amsterdam UMC. In her second year she wrote her literature thesis on the immune system and its influence on the tumor microenvironment under supervision of Juan J. Garcia-Vallejo, followed by a 5-month internship in the group of Marjolein van Egmond studying a newly developed antibody to activate neutrophils in immunotherapeutic strategies against cancer, both at the MCBI, Amsterdam UMC. She received her masters with honors (cum laude) in 2014 and continued for a PhD position in the group and under supervision of Yvette van Kooyk at the MCBI, Amsterdam UMC. The results of this work are presented in this thesis.

Now Sanne will stay put at the MCBI, Amsterdam UMC, in the group of Yvette van Kooyk as postdoc with a main emphasis on education at the university.

Appendix

193